

**Development of malignant melanoma is dependent
on a switch in Embryonic Transcription Factors
orchestrated by the BRAF-MAPK pathway**

Thesis submitted for the degree of

Doctor of Philosophy

at the University of Leicester

by

Eftychios Papadogeorgakis BSc (Hons), MSc (Hons)

Department of Cancer Studies and Molecular Medicine

University of Leicester

2013

Abstract

Reactivation of master regulators of epithelial to mesenchymal transition (MR-EMT) represents the molecular basis for tumour cell plasticity, malignant transformation and metastases. However, the current evidence on the specific role of MR-EMT in melanomagenesis has not been fully addressed. The purpose of this investigation was to assess the expression and regulation of these factors in malignant melanoma and to evaluate their prognostic and clinical significance.

In vitro experiments indicated that a switch in MR-EMT protein expression ZEB2/SNAI2 to ZEB1/TWIST1 is RAS-RAF-MAPK signalling dependent. In addition, evidence supported a MR-EMT interactome, in which transcriptional repression of ZEB2 by Fra-1 resulted in upregulation of ZEB1, independently of miR-200 family. Further *in vitro* and immunohistochemical (IHC-P) analyses showed that E-cadherin and VDR protein levels were significantly reduced by the presence of ZEB1 in melanoma cells and archive tissues. Motility assays demonstrated that ZEB1 but not ZEB2 enhances cell migration.

IHC-P analyses of ZEB2/SNAI2 (n=142/28) showed a statistically significant gradient of stronger staining at superficial sites compared to the deep sites in a select cohort of independent and matched melanoma tumour samples. In contrast, ZEB1 (n=142) and TWIST1 (n=133) showed higher staining in deep sites of primary melanomas and metastases. Trend analyses showed a significant MR-EMT switch in this progression series from high levels of ZEB2/SNAI2 in naevi towards high ZEB1/TWIST1 expression in melanomas. In primary melanomas these factors were also significant in Kaplan Meier survival curves and after two step cluster analysis the combined profile of ZEB1^{high}/TWIST1^{high}/ZEB2^{low} predicted the worse prognosis (P=0.001). Multivariate Cox regression analyses of IHC-P staining indicated that only the gain of ZEB1 (P<0.002, n=98) and superficial TWIST1 (P=0.012) were associated with poor metastasis-free survival and independent of breslow depth.

In conclusion, the reversible switch between ZEB1/TWIST1 and ZEB2/SNAI2 is controlled by RAS-RAF-MAPK pathway activity and constitutes an independent factor of poor prognosis in patients with malignant melanoma.

Acknowledgements

I am indebted to my supervisors Dr. JH Pringle and Dr. PE Hutchinson. Thank you for giving me the opportunity to undertake this project in the first place and for your continued support and encouragement over the last four years.

Dr. E Tulchinsky, thank you for pointing me into the fascinating world of EMT and your scientific passion has always been a true inspiration to me.

I am greatly honoured and feel very fortunate to meet and collaborate with passionate scientists. Thank you Gareth and Emre for giving me this opportunity and for all lengthy discussions even very late in the evenings and weekends.... I will also like to thank Karen who many times gave up her time to help me on immunohistochemical experiments and for cheering me up in periods of intense stress.

A very special thanks goes out to our technicians, Linda, Lindsay, Angie and Janine for helping me optimise immunohistochemical and PCR experiments. Thanks also to Shona, Karen, Kevin and Ali for your support and encouragement when lack of sun was driving me insane and for sharing with me cups of coffee and tea along the way.

To my friends Theresa, Eleanor and Ellie thank you for your continued friendship and support.

Eleni, my dear love, there is no enough space here to express my gratitude for your unlimited affection and for always being there for me.

And finally, mum, dad and Vasili, I have finally managed to get a "real" job now...

Contents

1	GENERAL INTRODUCTION	1
1.1	INTRODUCTION	1
1.2	MALIGNANT MELANOMA	1
1.2.1	<i>Incidence, Mortality and Survival Rates</i>	<i>1</i>
1.2.2	<i>Different Types of MM and multi-step progression of the disease.....</i>	<i>3</i>
1.2.3	<i>Malignant melanoma susceptibility genes and deregulated signalling pathways.....</i>	<i>7</i>
1.2.4	<i>Therapy of melanoma</i>	<i>14</i>
1.3	MELANOCYTIC CELL ORIGIN AND DIFFERENTIATION	17
1.3.1	<i>Location and function of melanocytes.....</i>	<i>17</i>
1.3.2	<i>Differentiation of melanocytic precursor cells into melanocytes</i>	<i>19</i>
1.4	EMT IN DISEASE AND EMBRYONIC DEVELOPMENT AND ITS TRANSCRIPTIONAL CONTROL	21
1.4.1	<i>EMT in embryogenesis.....</i>	<i>21</i>
1.4.2	<i>EMT in disease.....</i>	<i>28</i>
1.4.2.1	Definition of EMT in melanoma	30
1.4.2.2	Developmental regulators determine tumour progression	31
1.4.2.3	Master regulators of EMT (MR-EMT) in tumourigenesis	33
1.4.2.4	MicroRNAs in EMT and metastasis	37
1.5	AIMS AND OBJECTIVES.....	39
2	MATERIALS AND METHODS	41
2.1	MATERIALS.....	41
2.1.1	<i>Patients and melanoma tissues.....</i>	<i>41</i>
2.1.2	<i>Chemicals and reagents.....</i>	<i>41</i>
2.1.3	<i>Eukaryotic cell lines.....</i>	<i>42</i>
2.1.4	<i>Cell culture reagents and supplements.....</i>	<i>43</i>
2.1.5	<i>Manipulation of melanoma cell lines</i>	<i>44</i>
2.1.6	<i>RNA extraction kit.....</i>	<i>44</i>
2.1.7	<i>Total RNA quality control analysis.....</i>	<i>45</i>
2.1.8	<i>Quantitative and conventional PCR reagents and materials.....</i>	<i>45</i>
2.1.9	<i>Human Endogenous Control Array</i>	<i>45</i>
2.1.10	<i>Preparation of cytoblocks</i>	<i>45</i>
2.1.11	<i>Immunohistochemical materials</i>	<i>46</i>
2.1.12	<i>Immunoblotting materials.....</i>	<i>46</i>
2.2	METHODS	47
2.2.1	<i>RNA Isolation and manipulation.....</i>	<i>47</i>
2.2.1.1	Preparation of total RNA.....	47
2.2.1.2	Quantification of RNA	48
2.2.1.3	Converting total RNA to cDNA	48
2.2.1.4	Oligonucleotide primers and probes	48
2.2.1.5	Primer and probe design.....	49
2.2.1.6	Quantitative PCR (qRT-PCR).....	50
2.2.1.7	Standard curves	51
2.2.2	<i>miR expression by real-time qRT-PCR.....</i>	<i>52</i>
2.2.2.1	miR extraction from melanoma specimens and cell lines.....	52
2.2.2.2	Reverse transcription and pre-amplification	52
2.2.2.3	Quantitative real-time PCR	52
2.2.2.4	Short tandem repeat (STR) profiling for melanoma cell lines	53
2.2.2.5	Extraction of genomic DNA from frozen A375 pellets	53
2.2.2.6	Polymerase chain reaction (PCR) for STR profiling	54
2.2.3	<i>TaqMan[®] Human Endogenous Control Array</i>	<i>55</i>
2.2.3.1	RNA analysis and cDNA preparation	55
2.2.3.2	Array run and analysis of data	56
2.2.4	<i>Immunohistochemistry-Paraffin (IHC-P).....</i>	<i>57</i>
2.2.4.1	Haematoxylin and Eosin staining for morphology	57
2.2.4.2	Dewax and rehydration of the sections under investigation	57
2.2.4.3	Heat-induced antigen retrieval for melanoma tissues.....	57
2.2.4.4	Application of primary antibodies	58

2.2.4.4.1	Human melanoma tissues	58
2.2.4.4.2	Mouse melanoma model sections.....	58
2.2.4.5	Application of the secondary antibody and the Novolink Polymer Detection System	60
2.2.4.6	Application of the secondary antibody and the ABC-AP Detection System.....	60
2.2.4.7	Semiquantitative immunohistochemical evaluation for MR-EMT, VDR and E-cadherin	61
2.2.5	<i>Cell culture of normal melanocytes and melanoma cell lines</i>	62
2.2.5.1	Recovery of cells from frozen storage	62
2.2.5.2	Passaging of normal melanocytes and melanoma cells.....	63
2.2.5.3	Long term storage of cell cultures	63
2.2.5.4	Treatment of HEMN with 1a, 25-Dihydroxyvitamin D3	63
2.2.5.5	Treatment of melanoma cell lines with pharmacological inhibitors.....	64
2.2.5.6	RNA interference experiments for A375 melanoma cells.....	64
2.2.5.7	Luciferase reporter assays	66
2.2.5.8	Cell motility assays.....	67
2.2.5.9	Sample preparation for Western blotting.....	67
2.2.6	<i>Western blotting</i>	68
2.2.6.1	Protein extraction from melanoma and HEM cell lines	68
2.2.6.2	Protein quantification	68
2.2.6.3	Sodium dodecyl sulphate polyacrylamide gel electrophoresis (SDS-PAGE).....	69
2.2.6.4	Protein transfer and immunological detection of PVDF immobilised proteins	70
2.2.7	<i>Statistical analysis</i>	72
3	REGULATION OF MR-EMT BY THE RAS-RAF MAPK PATHWAY.....	73
3.1	INTRODUCTION	73
3.2	AIMS AND OBJECTIVES.....	75
3.3	RESULTS.....	76
3.3.1	<i>MR-EMT expression in melanoma cell lines and melanocytes</i>	76
3.3.2	<i>The effect of BRAF^{V600E} and MEK inhibitors on the expression of MR-EMT in melanoma cells</i>	77
3.3.3	<i>The effect of p38 / JNK and PI3K inhibitors on the expression of MR-EMT in melanoma cells</i>	79
3.3.4	<i>The kinetics of MR-EMT modulation in melanoma cells treated with U0126</i>	83
3.3.5	<i>Does MEK signalling influence MR-EMT protein stability?</i>	87
3.3.6	<i>ZEB1 expression is repressed by ZEB2</i>	89
3.3.7	<i>Fra-1 links the BRAF pathway with the MR-EMT network in A375 cells</i>	92
3.3.8	<i>Is regulation of ZEB1 and ZEB2 genes dependent on miRs in BRAF^{V600E} melanoma cells?</i> 94	
3.4	DISCUSSION.....	100
3.4.1	<i>Regulation of MR-EMT by the BRAF-MEK MAPK signalling pathway in melanoma cells</i>	100
3.4.2	<i>Is there any effect of PI3K, JNK and p38 signalling pathways on MR-EMT?</i>	101
3.4.3	<i>Posttranslational modifications of MR-EMT in BRAF^{V600E} melanoma cells</i>	103
3.4.4	<i>Establishment of an EMT interactome in BRAF mutated melanoma cells</i>	105
3.4.5	<i>Fra-1 perturbs the expression of MR-EMT in melanoma cells</i>	106
3.4.6	<i>Posttranscriptional regulation of MR-EMT: miRs</i>	109
3.4.7	<i>Conclusions</i>	113
4	FUNCTIONAL EFFECTS OF ZEB PROTEINS IN MELANOMA.....	114
4.1	INTRODUCTION	114
4.2	AIMS AND OBJECTIVES.....	116
4.3	RESULTS.....	117
4.3.1	<i>The effect of ZEB proteins on the expression of E-cadherin in melanoma tissues</i>	117
4.3.2	<i>The effect of MR-EMT on the expression of E-cadherin in melanoma cultures</i>	126
4.3.3	<i>The effect of ZEB1 on VDR expression in melanoma cell lines and tissues</i>	128
4.3.4	<i>Expression of miR-125b in melanocytic tumours</i>	133
4.3.5	<i>The effect of ZEB1 and ZEB2 on the migration of melanoma cells</i>	134
4.4	DISCUSSION.....	139
4.4.1	<i>E-cadherin - ZEB1/2 relationships in melanocytic tumours and cell lines</i>	139
4.4.2	<i>ZEB1 regulates VDR expression in MM</i>	142
4.4.3	<i>ZEB proteins affect migration in BRAF mutated melanoma cell lines</i>	146

4.4.4	Conclusions	148
5	DISTRIBUTION OF MR-EMT IN MELANOMA TISSUES AND MOUSE MELANOMA MODEL	149
5.1	INTRODUCTION	149
5.2	AIMS AND OBJECTIVES	150
5.3	RESULTS.....	151
5.3.1	<i>Patient demographics and melanocytic tissues.....</i>	<i>151</i>
5.3.2	<i>MR-EMT immunoreactivity control examples</i>	<i>153</i>
5.3.3	<i>Immunohistochemical evaluation examples</i>	<i>157</i>
5.3.4	<i>Expression of ZEB1 and ZEB2 in a mouse BRAF^{V600E} melanoma model.....</i>	<i>160</i>
5.3.5	<i>Expression of MR-EMT proteins in benign and MM tumours.....</i>	<i>162</i>
5.3.5.1	MR-EMT immunostaining patterns.....	162
5.3.5.2	Expression of EMT modulators during melanoma progression	163
5.3.5.2.1	ZEB1	163
5.3.5.2.2	ZEB2	164
5.3.5.2.3	TWIST1.....	165
5.3.5.2.4	SNAI2	166
5.3.6	<i>Correlation of MR-EMT expression with clinical parameters</i>	<i>184</i>
5.4	DISCUSSION.....	187
5.4.1	<i>A subset of MR-EMT has distinct protein expression patterns in melanocytic lesions ...</i>	<i>187</i>
5.4.1.1	ZEB1	188
5.4.1.2	ZEB2	189
5.4.1.3	ZEB1 and ZEB2 expression patterns in paired samples.....	191
5.4.1.4	TWIST1.....	192
5.4.1.5	SNAI2	194
5.4.2	<i>Expression of ZEB proteins in a mouse BRAF^{V600E} model.....</i>	<i>196</i>
5.4.3	<i>MR-EMT expression and clinical outcome</i>	<i>197</i>
5.4.4	<i>Conclusions</i>	<i>199</i>
6	FINAL DISCUSSION	201
6.1	A NETWORK OF MR-EMT CONTRIBUTES TO THE NEOPLASTIC TRANSFORMATION OF MELANOCYTES.....	201
6.2	FRA-1: AN APPEALING TARGET FOR THERAPY	203
6.3	LIMITATIONS OF THE STUDY	205
6.4	FINAL CONCLUSIONS.....	209
6.5	FUTURE WORK	210
6.5.1	<i>ZEB2/SNAI2 - miR-200/E-cadherin co-expression paradox.....</i>	<i>210</i>
6.5.2	<i>MR-EMT expression by BRAF activation</i>	<i>211</i>
6.5.3	<i>Role of Fra-1 in malignant melanoma</i>	<i>211</i>
6.5.4	<i>Clinical aspects</i>	<i>212</i>
6.5.5	<i>Migration and invasion of melanoma cells.....</i>	<i>213</i>
7	APPENDIX	214
7.1	I-ETHICS-LETTER OF APPROVAL	214
7.2	II-TABLE S1-SUMMARY OF PRIMARY MMS USED IN THIS STUDY	216
7.3	III - STR PROFILING FOR A375 MELANOMA CELLS	219
7.4	IV-POST-ENDOGENOUS CONTROL ARRAY ANALYSIS / EXPRESSION STABILITY OF CANDIDATE ENDOGENOUS GENES 223	
7.5	V-DISTRIBUTION OF THE MR-EMT/VDR/E-CADHERIN STAINING INTENSITY AND PATTERN (TOTAL H-SCORE) 226	
7.6	VI-CELL LINES AND VDR LIGAND TREATMENTS	228
	PUBLICATIONS.....	229
	REFERENCES.....	230

Index of Figures

Figure 1.1 - The 20 most common causes of death from cancer in the UK (2010)	3
Figure 1.2 - Progression models of malignant melanoma	6
Figure 1.3 - Selected targeted genes and molecular pathways in cutaneous neoplasias	12
Figure 1.4 - The central melanoma axis and key therapeutic targets in malignant melanoma.....	16
Figure 1.5 - Human epidermal melanocytes are confined to the basal layer of the epidermis	18
Figure 1.6 - EMT-associated transcription factors control trunk neural crest induction, survival and delamination during embryogenesis	26
Figure 1.7 - Schematic representation showing the main regulatory interactions controlling melanoblast specification	27
Figure 2.1 - Thermal cycling conditions for qRT-PCR using TaqMan probes	51
Figure 3.1 - Protein analysis of MR-EMT in different melanoma cell lines, HEMN and keratinocytes ...	73
Figure 3.2 - Pharmaceutical agents inhibiting MAPK-signalling pathways used in this study	74
Figure 3.3 - Western blot analysis of the expression of MR-EMT proteins in a panel of melanoma cell lines	77
Figure 3.4 - The effect of BRAF and MEK inhibitions on the expression of MR-EMT in A375P and IPC-298 cells.	78
Figure 3.5 - The effect of SB203580 inhibitor on MR-EMT in A375P and A375M melanoma cell lines .	80
Figure 3.6 - The effect of SP600125 inhibitor on MR-EMT in A375P and A375M melanoma cell lines..	81
Figure 3.7 - The effect of the PI3K inhibitor wortmannin on MR-EMT factors in melanoma cell lines ..	82
Figure 3.8 - The kinetics of MR-EMT modulation in A375P treated with U012	85
Figure 3.9 - The kinetics of MR-EMT modulation in A375M treated with U012	86
Figure 3.10 - Regulation of MR-EMT on the level of protein stability in melanoma cells	88
Figure 3.11 - Post-transfection efficiency analysis of MR-EMT by western blottin	90
Figure 3.12 - siRNA-mediated depletion of SNAI2 and TWIST1 in A375M melanoma cells	91
Figure 3.13 - The effect of siRNA-mediated depletion and MEK inhibition of ZEB proteins in A375M melanoma cells	92
Figure 3.14 – The effect of Fra-1 siRNA mediated depletion and U0126 on ZEB proteins in A375 melanoma cells	93
Figure 3.15 - The effect of luciferase miRNA expression reporter vectors containing <i>ZEB1</i> or <i>ZEB2</i> 3'UTRs in bladder cancer cell lines.....	95
Figure 3.16 - The effect of miRNA expression reporter vectors in melanoma cancer cell lines	96
Figure 3.17 - miR-200 family expression in A375 melanoma cell lines by qRT-PCR	99
Figure 4.1 - Immunohistochemical staining of serial sections of paired metastasis specimens for the expression of E-cadherin, ZEB1 and ZEB2	119

Figure 4.2 - Immunohistochemical staining of serial sections of a metastatic primary melanoma specimen for the expression of E-cadherin, ZEB1 and ZEB2.....	120
Figure 4.3 - Immunohistochemical staining of serial sections of a matched lymph node metastasis specimen for the expression of E-cadherin, ZEB1 and ZEB2.....	121
Figure 4.4 - Immunohistochemical staining of serial sections of a metastatic primary melanoma specimen for the expression of E-cadherin, ZEB1 and ZEB2.....	122
Figure 4.5 - Immunohistochemical staining of serial sections of a matched lymph node metastasis specimen for the expression of E-cadherin, ZEB1 and ZEB2.....	123
Figure 4.6 - Immunohistochemical staining of serial sections of a metastatic primary melanoma specimen for the expression of E-cadherin, ZEB1 and ZEB2.....	124
Figure 4.7 - Immunohistochemical staining of serial sections of a matched lymph node metastasis specimen for the expression of E-cadherin, ZEB1 and ZEB2.....	125
Figure 4.8 - The effect of siRNA-mediated depletion of ZEB1 and ZEB2 on E-cadherin protein expression in A375P and A375M cells.	127
Figure 4.9 - The effect of siRNA-mediated depletion of ZEB1 on VDR expression in A375P and A375M cells..	129
Figure 4.10 - Immunohistochemical staining of primary metastatic melanomas for VDR and ZEB1. ..	130
Figure 4.11 - Immunohistochemical staining of lymph node metastasis for VDR and ZEB1	131
Figure 4.12 - Consecutive immunostainings for VDR and ZEB1 of a matched metastatic case.....	132
Figure 4.13 - Differential expression of miR-125b (Δ Ct) in melanocytic lesions by qRT-PCR	133
Figure 4.14 - The effects of ZEB1 and ZEB2 knockdown on tumour cell migration in A375P melanoma cells	136
Figure 4.15 - The effects of ZEB1 and ZEB2 knockdown on tumour cell migration in A375M melanoma cells.	138
Figure 5.1 - Immunohistochemical and western blot analyses of ZEB1 and ZEB2 expression in control cell lines.....	154
Figure 5.2 - Immunohistochemical and western blot analyses of TWIST1 and SNAI2 expression in control cell lines	155
Figure 5.3 - Immunohistochemical and western blot analyses of SNAI1, E-cadherin and VDR expression in control cell lines and tissues.	156
Figure 5.4 - Staining intensity examples for ZEB1.....	157
Figure 5.5 - Staining intensity examples for ZEB2.....	158
Figure 5.6 - Staining intensity examples for TWIST1	159
Figure 5.7 - Immunohistochemical analysis of the expression of ZEB1 and ZEB2 in the mouse BRAF ^{V600E} model of malignant melanoma.....	161
Figure 5.8 - Representative photomicrographs of ZEB1, ZEB2 and TWIST1 expression in common acquired melanocytic naevi	167
Figure 5.9 - ZEB1, ZEB2 and TWIST1 immunoreactivity in epidermal melanocytes	168

Figure 5.10 - Representative photomicrographs of SNAI2 expression in common acquired melanocytic naevi.....	169
Figure 5.11 - Representative sections of benign naevi showing loss of SNAI2 expression throughout the depth of the tumour	170
Figure 5.12 - Box and whisker plot showing nuclear ZEB1 and ZEB2 immunostaining in melanocytic naevi.....	171
Figure 5.13 - Progression related ZEB1 and TWIST1 expression in independent primary MMs and lymph node metastases.	172
Figure 5.14 - Representative sections of progression related ZEB2 expression in MM	173
Figure 5.15 - Representative serial sections of progression related ZEB1, ZEB2 and TWIST1 expression in a paired nodal metastasis	174
Figure 5.16 - Representative photomicrographs of SNAI2 expression in a paired nodal metastasis....	175
Figure 5.17 - ZEB1 and ZEB2 immunohistochemical staining of serial sections of a primary MM	176
Figure 5.18 - Immunostaining for ZEB1 and ZEB2 in serial sections of a nodal metastasis (1 st example)..	177
Figure 5.19 - Immunoreactivity for ZEB1 and ZEB2 in serial sections of a lymph node metastasis (2 nd example)	178
Figure 5.20 - Box and whisker plots of ZEB1 IHC staining (H-Score) for a melanoma independent progression series including naevi, primary melanoma and metastasis	179
Figure 5.21 - Box and whisker plots of ZEB2 IHC staining (H-Score) for a melanoma independent progression series including naevi, primary melanoma and metastasis	180
Figure 5.22 - Box and whisker plots of TWIST1 IHC staining (H-Score) for a melanoma independent progression series including naevi, primary melanoma and metastasis	181
Figure 5.23 - MR-EMT expression in paired melanoma samples.....	183
Figure 5.24 - Kaplan Meier survival curves comparing disease free survival in patients with primary cutaneous MM with or without metastases.....	185
 Figure 6.1 - Proposed model illustrating RAS-RAF-MEK dependent regulation of MR-EMT in melanoma cells	207
Figure 6.2 - Schematic representation of molecular signalling pathways linking MEK-Fra-1 with MR-EMT in carcinoma and melanoma cells.	208

Index of Tables

Table 1.1 - Main characteristics of different types of melanoma.....	4
Table 1.2 - Synopsis of familial and somatic mutations in malignant melanoma.....	9
Table 1.3 - Summary of genetic alterations in cutaneous melanomas from body sites with different levels of sun exposure.....	13
Table 1.4 - Location and functions of extracutaneous melanocytes and melanocyte imitators.....	19
Table 1.5 - EMT-related changes in cell properties	21
Table 2.1 - BRAF and NRAS mutation status in human melanoma cell lines used in this study.....	43
Table 2.2 - Primers and TaqMan® gene expression assays for quantitative PCR experiments.....	50
Table 2.3 - Reaction conditions for qRT-PCR using TaqMan probes.....	51
Table 2.4 - TaqMan® MicroRNA Assays used in this study.....	53
Table 2.5 - Thermal cycling conditions for STR profiling.....	55
Table 2.6 - List of primary antibodies used for immunohistochemistry	59
Table 2.7 - List of siRNAs used for transient transfections	65
Table 2.8 - Required volumes for 10% resolving and 5% stacking gels	69
Table 2.9 - List of primary and secondary antibodies used for immunoblotting.....	71
Table 4.1 - Distribution of ZEB1/ZEB2 and E-cadherin staining intensity and pattern in matched melanoma cases.....	118
Table 5.1 - Clinicopathological characteristics in a subset of MM patients.....	152
Table 5.2 - Univariate and multivariate Cox proportional hazard analysis for clinical prognostic factors, age, gender, tumour Breslow depth, ulceration, stage and MR-EMT expression (H-Score).	186

List of abbreviations

ABC	Avidin-Biotin Complex
AKT	v-akt murine thymoma viral oncogene homolog 3
ALM	Acral Lentigous
ANCI	American National Cancer Institute
AP	Alkaline phosphatase
APC	Adenomatous polyposis coli gene
ARF	Alternative open reading frame
AR	Androgen receptor
ASIP	Agouti signaling protein
ATCC	American Type Culture Collection
ATF2	Activating transcription factor 2
BAX	BCL2-associated X protein
BCA	Bicinchoninic acid
BCL2	B-cell lymphoma 2
bHLH	Basic helix-loop-helix transcription factor
BMP	Bone morphogenic protein
Bp	Base pair
BRAF	V-raf murine sarcoma viral oncogene homolog B1
BSA	Bovine serum albumin
CAN	Common acquired naevi
CCND1	Cyclin D1
CDH	Cadherin
CDK4	Cyclin dependent kinase 4
Cdk1	Cyclin dependent kinase inhibitor
CDKN2A	Cyclin-dependent kinase inhibitor 2A
cDNA	Complimentary DNA
c-FOS	FBJ murine osteosarcoma viral oncogene homolog
CHCl ₃	Chloroform
ChiP	Chromatin-immunoprecipitation assay
c-Jun	Jun proto-oncogene
cKIT	V-kit Hardy-Zuckerman 4 feline sarcoma viral oncogene homolog
CMM	Cutaneous Malignant Melanoma
c-Myc	v-myc myelocytomatosis viral oncogene homolog
COSMIC	Catalogue of Somatic Mutations in Cancer
CREB	cAMP responsive element binding protein
CRUK	Cancer Research UK
CSD	Chronic sun-induced damage
Ct	Cycle threshold
CtBP	C-terminal-binding protein
DAB	3, 3'-diaminobenzidine
Dct	Dopachrome tautomerase
DHT	5 α -dihydrotestosterone
DiIC ₁₂ (3)	1,1'-Didodecyl-3,3,3',3'-tetramethylindocarbocyanine perchlorate
DMEM	Dulbecco's Modified Eagles Medium
DMSO	Dimethyl sulphoxide

DNA	Deoxyribonucleic acid
DRIP	Vitamin D receptor interacting protein
DUSP5	Cysteine-dependent dual-specificity protein phosphatase 5
ECL	Enhanced chemiluminescence
ECM	Extracellular matrix
ECS	Endometrial carcinosarcoma
EDTA	Ethylenediaminetetra-acetic acid
EGF	Epidermal growth factor
ELK1	Member of ETS oncogene family
EMEM	Eagle Minimum Essential Medium
EMT	Epithelial-Mesenchymal Transition
ERK1/2	Extracellular signal-related kinase 1/2
ESCC	Oesophageal squamous cell carcinoma
ETS1	v-ets erythroblastosis virus E26 oncogene homolog 1
FGF	Fibroblast growth factor
FGFR3	Fibroblast growth factor receptor 3
FBS	Foetal bovine serum
FCS	Foetal calf serum
FLT3	FMS-related tyrosine kinase 3
FoxD3	Forkhead box D3
Fra	Fos-related antigen
FSP1	Fibroblast-specific protein 1
GAPDH	Glyceraldehyde-3-phosphate dehydrogenase
GEM	Genes, Environment and Melanoma
GSK3 β	Glycogen synthase kinase-3 β
GWAS	Genome-wide associated studies
HCC	Hepatocellular carcinomas
HDAC1	Histone deacetylase 1
HEMN	Epidermal Melanocytes-Neonatal
HNSCC	Head and neck squamous cell carcinomas
HOXD10	Homeobox D10 protein
HPRT1	Hypoxanthine phosphoribosyltransferase 1
HRP	Horseradish peroxidase
IHC	Immunohistochemistry
IMS	Industrial methylated spirits
LEF/TCF4	Lymphoid-enhancer binding factor/T-cell factor-4
LMM	Lentigo maligna melanoma
LOH	Loss of heterozygosity
MAPK	Mitogen-activated protein kinase
MAPKAPK	Mitogen-activated protein kinase-activated protein kinase
MC1R	Melanocortin 1 receptor
MDCK	Madin-Darby canine kidney
MET	Mesenchymal-epithelial transition

miR	microRNA
MITF	Microphthalmia-associated transcription factor
MM	Malignant melanoma
MMP	Matrix metalloproteinase
MNK	MAP kinase interacting serine/threonine kinase 1
mRNA	Messenger ribonucleic acid
MSA	Migration staging area
MSI	Microsatellite instability
mTOR	mammalian target of rapamycin
NaP	Sodium pyruvate
NC	Neural crest
NCCs	Neural crest cells
NEAA	Non essential amino acids
NF- κ B1	Nuclear factor kappa B1
NM	Nodular melanoma
NANOG	Nanog homeobox
NPA	Non primary antibody
NRAS	Neuroblastoma RAS viral oncogene homolog
NSCLC	Non-small-cell lung cancer
OCT4	POU domain transcription factor OCT4
PBS	Phosphate buffered saline
PCAF	P300/CBP-Associated Factor
PCR	Polymerase chain reaction
PET	Polyethylene terephthalate
PI3K	Phosphatidylinositol 3-kinase
Ppa	Partner of paired
PPIA	Peptidylprolyl isomerase A
PTEN	Phosphatase and tensin homolog
PTH	Parathyroid hormone
PVDF	Polyvinylidene fluoride
qRT-PCR	Quantitative real-time PCR
RB	Retinoblastoma
RGP	Radial growth phase of primary melanoma
RIN	RNA integrity number
RNA	Ribonucleic acid
RPLP0	Ribosomal protein large P0
RPE	Retinal pigment epithelium
rRNA	Ribosomal RNA
RT	Reverse transcription
RTK	Receptor tyrosine kinase
RT-PCR	Reverse transcriptase polymerase chain reaction
RXR	Retinoid X receptor
SDS	Sodium dodecyl sulphate

SEER-CSR	Surveillance, Epidemiology and End Results Cancer Statistics Review
SIP	Smad-interacting protein
siRNA	Short-interfering RNA
SKIP	Ski-interacting protein
SNP	Single nucleotide polymorphism
SOX2	SRX (sex determining region Y)-box 2
SpCC	Spindle cell carcinoma
SRC	Steroid receptor co-activator
SS	Synovial sarcomas
SSM	Superficial spreading melanoma
STAT3	Signal transducer and activator of transcription 3 (acute-phase response factor)
STR	Short tandem repeat
TAE	Tris acetic acid EDTA
<i>Taq</i>	<i>Thermus aquaticus</i>
TBS	Tris buffered saline
TE	Trypsin / EDTA
TEMED	N, N, N, N'-tetramethylethylenediamine
TGF- β	Transforming growth factor beta
T _m	Melting temperature
TNF- α	Tumour necrosis factor- α
TP53	Tumour protein 53
TRPS1	Tricho-rhino-phalangeal syndrome type 1
TSG	Tumour suppressor gene
TYR	Tyrosinase
TYRP1	Tyrosinase-related protein 1
UBC	Ubiquitin C
U0126	1, 4-diamino-2,3-dicyano-1,4-bis [2-aminophenylthio] butadiene
UPS	Ubiquitin-proteasome system
UV	Ultraviolet
VAB	Veronal acetate buffer
VDR	Vitamin D Receptor
VDRE	Vitamin D response element
VGP	Vertical growth phase
ZEB	Zinc finger E-box binding homeobox
3'-UTR	3'- untranslated region
5'-UTR	5'- untranslated region

1 General Introduction

1.1 Introduction

Awareness of skin melanoma as a disease entity is not recent, having possibly first been described in the 5th century B.C by the Greek physician Hippocrates who referred to "black cancer" and "fatal black tumours with metastases". Despite recent treatment strategies and therapeutic agents, metastatic melanoma remains one of the cancers most resistant to treatment and there is therefore imperative to determine new diagnostic markers of disease progression and targets for the treatment of aggressive melanocytic neoplasias. This chapter provides an overview of the key aspects of melanoma disease, such as epidemiology, driver mutations and important signalling pathways followed by a literature review in regards to the origin of skin melanocytes and the role of Epithelial to Mesenchymal Transition (EMT) and associated key transcription factors in both embryonic development and disease.

1.2 Malignant melanoma

1.2.1 Incidence, Mortality and Survival Rates

It is fitting that the largest organ in the human body, the skin, has the likelihood to become affected with such a life-threatening disease as melanoma. The incidence and mortality of malignant melanoma (MM), which is the least common but the most life threatening form of skin cancer, has continued to increase steeply worldwide over the last decades with the highest incidence rate in Australia, with New Zealand ranking a close second, and the lowest in Asian populations (Coory et al., 2006, Jones et al., 1999, Godar, 2011). According to GLOBOCAN, a worldwide database of cancer incidence

and mortality rates, an estimated 200,000 (1.6 %) new melanoma cases and 46,372 deaths (0.6 %) occurred in 2008 (Bray et al., 2012, Ferlay et al., 2010).

The American National Cancer Institute (ANCI) has recently published an update on the Surveillance, Epidemiology and End Results Cancer Statistics Review (SEER-CSR) based on cases diagnosed for cancer between 1975 and 2009 in the United States (US) (Howlader N, 2011). It is estimated that the lifetime risk of both sexes for developing MM was approximately 2%, and the age-adjusted incidence and death rate was 21.0 and 2.7 per 100,000 people per year respectively (Howlader N, 2011). For 2012, the American Cancer Society predicted that there will be more than 76,000 new cases of melanoma (*in situ* and invasive) and approximately 9,180 deaths from the disease (Howlader N, 2011). It is notable that melanoma incidence has grown alarmingly in younger age groups during the past quarter century and more specifically is the most common form of cancer among young adults, in the 25- to 29-year-age group, and the second most common type of cancer in individuals 15- to 29-years of age, when gender was not taken into account (Bleyer et al., 2006).

According to the Cancer Research UK (CRUK), the incidence rate for melanoma in the UK has almost quadrupled since early 1970s and more than 12,000 new cases diagnosed with the disease in 2010 (CRUK, 2010a). The most recent UK skin cancer age-standardised mortality statistics showed that male mortality rate increased significantly in the last four decades from 1.2 to 3.1 per 100,000 compared with the female rate, which was only changed from 1.4 to 2.2 per 100,000 for the same period of time (CRUK, 2010b). The current lifetime risk of MM in the UK is relatively low in relation to other types of cancer and about 1.65% for both genders (CRUK, 2010a).

Nevertheless, MM remains one of the least common causes of death in the UK compared to other types of malignancies Figure 1.1.

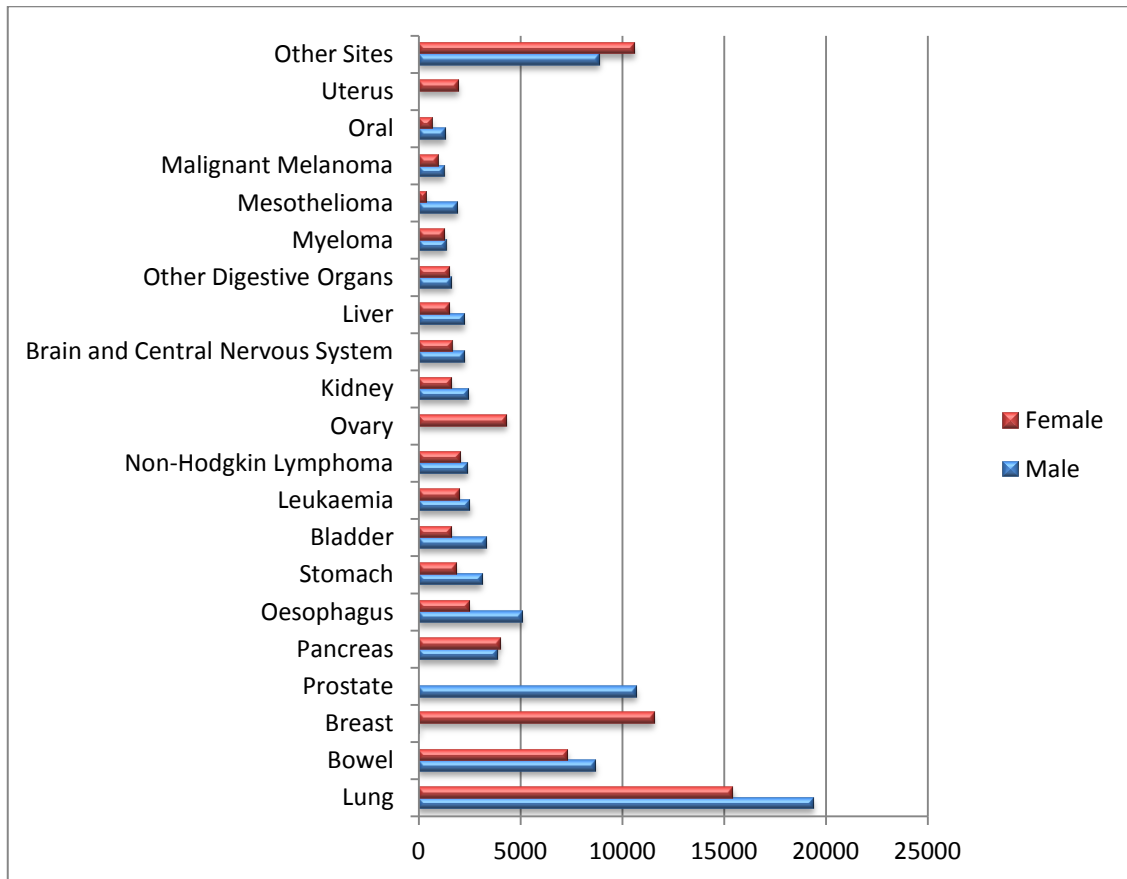


Figure 1.1 - The 20 most common causes of death from cancer in the UK (2010). The malignant neoplasm is the 18th cause of death from cancer (Chart redrawn from CRUK - mortality statistics for common cancers, CRUK, 2010c).

1.2.2 Different Types of MM and multi-step progression of the disease

There are four main histologic types of cutaneous melanoma that have distinctive pathological features and are summarized in Table 1.1. Superficial spreading, nodular and lentigo maligna or "Hutchinson's melanotic freckle" melanomas make up about 90-95% of all diagnosed melanoma cases (MacKie, 2000, Porras and Cockerell, 1997).

On the other hand, acral lentiginous melanoma and other infrequent types of melanoma, such as ocular, vaginal or rectal account for the rest 5-10% (MacKie, 2000, Phan et al., 2006, Porras and Cockerell, 1997).

Table 1.1 - Main characteristics of different types of melanoma. Note that the main prognostic indicators of MM include depth of invasion (Clark level) and thickness of the primary tumour (Breslow).

Melanoma Sub-types	Location	Lesion Characteristics	Incidence [all diagnosed melanomas]	Prognosis
Superficial spreading (SSM)	Trunk, upper arms, and thighs	Flat, dark macules, asymmetric with irregular borders and colour variations, outward spread	~70%	Slow growth (long flat phase) Good prognosis
Nodular (NM)	Anywhere on the body	Dome-shaped, dark brownish black, or black, in colour, downward growth, may also appear in an area without any previous lesion, lack of radial growth phase	~10-15%	Rapid growth Very poor prognosis
Lentigo maligna (LMM)	Most common on the face and other chronically sun-exposed areas	Large, flat, with irregular borders, mainly tan, brown, black coloured lesions, outward growth, may form dark nodules	~10%	Slow growth Good prognosis
Acral Lentiginous (ALM)	Hands, feet, under the fingernails and toenails, mucous membranes e.g. mouth and nose	Large, brown, black, or multi-coloured, streaked appearance, flat or nodular	~5%*	Poor prognosis

*[Up to 46 and 73% in Asian and black skinned populations, respectively - Reviewed in Kabigting et al., 2009]

The development of MM is characterised by a sequence of genetic alterations from normal melanocytes to life threatening invasive melanoma. Ackerman's group was the first to propose a multi-step process of melanoma tumourigenesis (linear progression) encompassing five distinct stages of progression (Ackerman, 1980). According to this model, schematically outlined in Figure 1.2, oncogenic stimulus can lead to an initial aberrant proliferation of melanocytes at the junction of epidermal and dermal layers of the skin in order to establish a melanocytic non tumourigenic lesion. There are two types of early benign lesions, common acquired and congenital naevi without any dysplastic

phenotype and dysplastic naevi with nuclear atypia. The third stage is defined as the radial growth phase of primary melanoma (RGP), and refers to the spread of a small subset of relatively stable naevi to *in situ* melanomas, which grow laterally and in proximity to the epidermis, but cells do not have the ability to metastasise. As the lesion progresses, radial growth phase is followed by a vertical growth phase (VGP) in which neoplastic melanocytes penetrate the basal layer and invade into the underlying dermis and subcutaneous fat, having the potential for metastasis. In the last step, melanoma cells invade out and disseminate through the blood stream or lymphatic vessels to distant sites in the body (Chin, 2003, Gaggioli and Sahai, 2007, Ibrahim and Haluska, 2009).

Contrary to the prevailing dogma of linear model of tumour progression, increasing evidence revealed divergent gene expression profiles between primary tumours and corresponding lymph node metastases (Bissig et al., 1999, Torres et al., 2007). In addition, recent reports focusing on the analysis of disseminated tumour cells by employing PCR-based whole genome amplification and comparative genomic hybridization techniques supported the notion that early transformed cells are capable of dissemination (Husemann et al., 2008, Klein et al., 2002). However, the obvious caveat of these studies is that the survival of disseminated tumourigenic clones or single cells at distant sites does not necessarily translate to initiation of a secondary tumour.

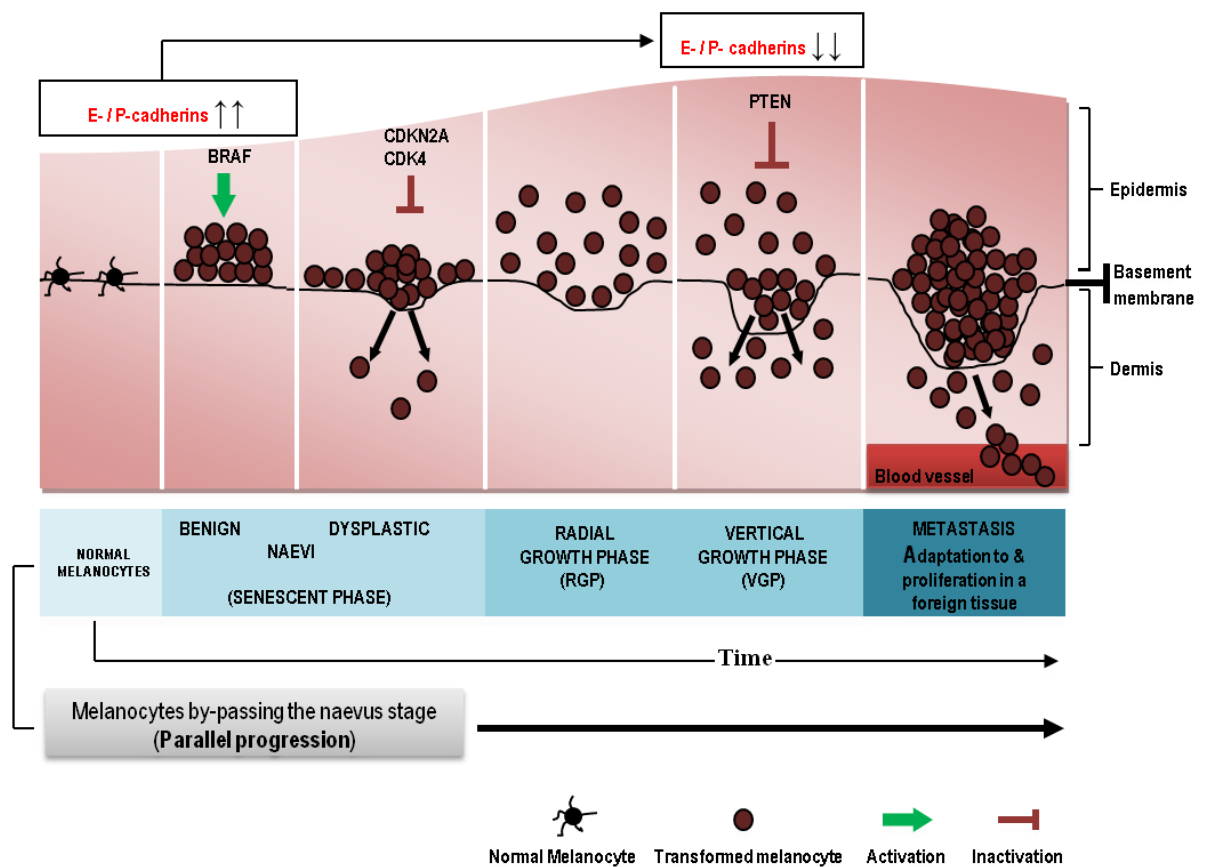


Figure 1.2 - Progression models of malignant melanoma. According to the linear progression model, transformation of normal melanocytes to malignant neoplastic cells is a multistep process with associated genetic alterations in specific genes. The initiation process involves cell proliferation with constitutive activation of v-raf murine sarcoma viral oncogene homolog B1 (*BRAF*), which induces an irreversible growth arrest (senescence) response. At this stage naevi can remain quiescent for many years and rarely develop into melanomas. Additional genetic events such as inactivation of cyclin-dependent kinase inhibitor 2A cyclin-p16^{INK4a}/dependent kinase 4 (*CDKN2A-p16^{INK4a}/CDK4*) genes are necessary for melanocytes to bypass senescence and enter the radial growth phase (RGP), which is considered as the first step towards the invasive melanocytic phenotype. Therefore, bypassing oncogene-induced senescence is a prerequisite for malignant transformation. Late processes in melanoma development, which include the vertical growth phase (VGP) and metastasis, are accompanied by loss of phosphatase and tensin homolog (*PTEN*) and reduced expression of E-/P-cadherins. Other genes, like microphthalmia-associated transcription factor (*MITF*) and tumour protein 53 (*TP53*), are implicated during melanomagenesis, however their pathogenic significance is controversial and the need for more studies is evident. According to the parallel progression model, a significant subgroup of metastatic melanomas does not involve oncogene-induced senescence and formation of naevi. These tumours could possibly derive from dermal stem cell populations (both models reviewed in Klein, 2009). Figure redrawn from (Ibrahim and Haluska, 2009). Red T-shaped arrow indicates inactivation; green arrow indicates activation; black and brown circles indicate normal and transformed melanocytes respectively.

Over the past two decades major advances in molecular biology have allowed identification and characterisation of genetic changes involved in the multi-step melanoma oncogenesis, which include alterations of tumour suppressor genes (TSGs), oncogenes, extracellular matrix proteins, loss of heterozygosity (LOH) and microsatellite instability (MSI).

1.2.3 Malignant melanoma susceptibility genes and deregulated signalling pathways

The process of melanomagenesis is thought to include one or more mutations, which can be sporadic or inherited (familial). Sporadic melanomas represent almost 90% of all melanoma cases and arise from somatic mutations of genes (Table 1.2). On the other hand, familial melanomas account for the rest 10% of all melanoma cases and they are characterised by germline (transmitted from one generation to the next) mutations in cancer-susceptibility genes, which differ in their degree of penetrance (Meyle and Guldberg, 2009, Ward et al., 2012). Despite advances in genome analysis using a number of high-throughput technologies, like microarrays and quantitative real-time PCR (qRT-PCR), there is a small number of low, moderate and high-penetrance susceptibility genes found to date in familial melanomas (Table 1.2) (Gudbjartsson et al., 2008, Ward et al., 2012).

The major signalling pathways involved in melanocytic tumours have been described in-depth in several review articles, but three have been identified to be nearly invariably deregulated in melanomas (Dahl and Guldberg, 2007, Hocker et al., 2008, Sekulic et al., 2008). These are, the receptor tyrosine kinase (RTK)-RAS signalling pathway (Figure 1.3), through mutations of *NRAS* (up to 42% frequency in primaries and metastases) or *BRAF* (up to 70% in melanomas), the ARF-p53 cascade, through mutations of *p14^{ARF}*

(up to 70% in sporadic melanomas) or *TP53* (up to 32% in primary melanomas), and the p16^{INK4a}/CDK4/RB pathway, with mutations of *INK4A* (up to 70% in nonfamilial melanomas) or *CDK4* (in 2-3% of all familial melanomas) (Table 1.2). Less frequently dysregulated pathways in melanoma malignancies include the Wnt / β -catenin pathway with mutations in adenomatous polyposis coli gene (*APC*) (in ~15% of cell lines and biopsy samples) (Worm et al., 2004) or *β -catenin* (higher frequency *in vitro*, 23%, than *in vivo*, <5%) (Omholt et al., 2001, Reifemberger et al., 2002, Rubinfeld et al., 1997) and the PI3K-AKT cascade (Figure 1.3), with mutations of *PTEN* (up to 38% in primary melanomas), *AKT* (in <5% of melanomas, *AKT3* isoform is activated in about 43% of nonfamilial melanomas and in 4% of benign naevi) (Stahl et al., 2004, Vredeveld et al., 2012) or *PI3K* (in ~1% of primary melanomas) (Curtin et al., 2006a).

Interestingly, recent population-based studies in MM support the existence of a unique relationship between distinct genetic alterations and different levels of sun exposure, reinforcing the hypothesis that divergent pathways may lead to cutaneous melanoma at different sites (Table 1.3) (Curtin et al., 2005). In addition, the frequency distribution of melanocytic lesions by anatomic site is different between Caucasians and other ethnic minority populations. While Caucasians have a predilection to develop melanomas on sun-exposed sites, such as face and neck, African-Americans and Asians develop melanomas of rare entity which are predominantly located on sun-protected mucosal and acral sites (Bellows et al., 2001, Byrd et al., 2004, Cress and Holly, 1997, Ishihara et al., 2001).

Table 1.2 - Synopsis of familial and somatic mutations in malignant melanoma

MM Mutation type	Penetrance (risk alleles)	Gene	Loci	Change	Frequency	References
FAMILIAL¹ (Germline)	High	<i>CDKN2A-p16^{INK4a}</i>	9p21	Inactivation by: mutation, deletion or promoter methylation	-Mutations in <i>CDKN2A</i> account for 35-40% of familial melanomas -In an Italian study, 3.2% of families had <i>p14^{ARF}</i> mutation -GenoMEL study <ul style="list-style-type: none"> • Overall alterations: 40% of familial melanomas • ~40% of mutations were specific to <i>p16^{INK4a}</i> • 64% of high risk families carried such mutations • Highest proportion of mutations in Europe (57%) and lowest in Australia (20%) -Genes Environment and Melanoma (GEM) study: <ul style="list-style-type: none"> • 1.2% in first primaries • 2.9% in multiple primaries • 27% of high risk families carried missense mutations in the reading frames for both <i>p16/p14</i> 	(Berwick et al., 2006, Binni et al., 2010, Goldstein et al., 2006, Meyle and Guldberg, 2009, Yeh and Bastian, 2009, Wu et al., 2007)
		<i>CDK4</i>	12q14	Mutation, amplification	-0.8% of Norwegian multiple primary melanoma patients were positive for a <i>CDK4</i> Arg24His mutation -GenoMEL study: 2-3% of mutations were specific to <i>CDK4</i>	(Helsing et al., 2008)
	Moderate/ modifier	<i>MC1R</i>	16q24.3	SNP	-All four most frequent variants were associated with increased melanoma risk -Carrying multiple variants has an additive risk [2.25 (1 variant)-to nearly 6-fold risk (2 variants) to develop melanoma] -Increased the penetrance of <i>CDKN2A</i> mutations (50-84%)	(Box et al., 2001, Demenais et al., 2010, Gudbjartsson et al., 2008, Hayward, 2003, S Raimondi et al., 2008, Stahl et al., 2004a)
	Low	<i>ASIP</i>	20q11.2-q12	SNP	GWAS in European and Australian populations showed an odd ratio between <i>ASIP</i> SNPs and CMM varied between 1.45-1.72 (significant risk)	(Brown et al., 2008, Gudbjartsson et al., 2008, Nan et al., 2009, Sulem et al., 2008)
		<i>TYR</i>	11q14-q21	SNP	GWAS showed an odd ratio between <i>TYR</i> variants and CMM varied between 1.22-1.27 (significant risk)	(Bishop et al., 2009, Chatzinasiou et al., 2011, Gudbjartsson et al., 2008)
		<i>TYRP1</i>	9p23	SNP	Few recent studies demonstrated that <i>TYRP1</i> variants decreased the risk of CMM (odd ratio < 1)	(Chatzinasiou et al., 2011, Gudbjartsson et al., 2008, Nan et al., 2009)

¹Genome-wide associated studies (GWAS) for familial melanoma susceptible genes were conducted by the Melanoma Genetics Consortium (GenoMEL). Abbreviations: *CDKN2A*, cyclin-dependent kinase inhibitor 2A; *CDK4*, cyclin-dependent kinase 4; *MC1R*, melanocortin 1 receptor; *ASIP*, agouti signaling protein; *TYR*, tyrosinase; *TYRP1*, tyrosinase-related protein 1; SNP, single-nucleotide polymorphisms

Table 1.2 (Continued)

MM Mutation type	Gene	Loci	Change	Frequency	References
SPORADIC²	<i>BRAF</i>	7q34	Constitutive activation; most common V600E	40% in congenital naevi 80% in CAN 50-70% in primary melanomas and metastases, of which 90% are V600E mutated	(Dessars et al., 2009, Edlundh-Rose et al., 2006, Goydos et al., 2005, Hodis et al., 2012, Omholt et al., 2003, Pollock et al., 2003, Poynter et al., 2006, Saldanha et al., 2004, Ugurel et al., 2007a, Wu et al., 2007)
	<i>CDKN2A</i> <i>p16^{INK4a}</i> / <i>p14^{ARF}</i>	9p21	Inactivation by mutation, deletion or promoter methylation	20-70% loss in primary melanomas >50% loss in melanoma metastases	(Casorzo et al., 2005, Curtin et al., 2005, Hodis et al., 2012, Pollock et al., 2001, Rakosy et al., 2008, Sini et al., 2008)
	<i>NRAS</i>	1p13.2	Activating mutation; most common Q61R	55% in congenital naevi 6-18 % in CAN 4-42% in primary melanomas and metastases	(Colombino et al., 2012, Demunter et al., 2001, Dessars et al., 2009, Gorden et al., 2003, Papp et al., 2003, Papp et al., 1999, Poynter et al., 2006, Saldanha et al., 2004, Ugurel et al., 2007a)
	<i>TP53</i>	17p13.1	Mutation or deletion	18-32% in primaries 9% in metastasis	(Zerp et al., 1999, Ragnarsson-Olding et al., 2002)
	<i>PTEN</i>	10q23.3	Inactivation by deletion, mutation	0-8% loss in melanocytic naevi Up to 38% in primary cutaneous melanomas Up to 65% in metastases	(Birck et al., 2000, Goel et al., 2006, Slipicevic et al., 2005, Tsao et al., 2003, Vredevelde et al., 2012, Whiteman et al., 2002)
	<i>FGFR3</i>	4p16.3	Mutation or deletion; most common R248C	Restricted to benign lesions, 33% R248C mutation in epidermal naevi	(Hafner et al., 2006)

Table 1.2 (Continued)

SPORADIC²	<i>cKIT</i>	4q11-q12	Activating mutations, gene amplifications	<56% in primary melanomas 10-13% positivity in metastasis >43% expression in naevi	(Curtin et al., 2006b, Oba et al., 2011, Stefanou et al., 2004, Willmore-Payne et al., 2005, Woenckhaus et al., 2003)
	<i>mTOR</i>	1p36.2	Activation	73% in primary melanomas 4% in benign naevi	(Karbowniczek et al., 2008, Populo et al., 2011)
	<i>BCL-2</i>	18q21.3	Gene amplification	>85% expression in naevi >88% in primary melanomas 35-52% expression in metastases	(Nazarian et al., 2010a, Zhuang et al., 2007)
	<i>MITF</i>	3p14.2-p14.1	Gene amplification	Absent in naevi 11% in primaries 15-23% in metastases	(Garraway et al., 2005, Ugurel et al., 2007b)

²Data for genetic changes in human sporadic melanoma are from the Catalogue of Somatic Mutations in Cancer (COSMIC) database (Forbes et al., 2008, Forbes et al., 2010). The top six genes for sporadic melanoma are ranked by reported frequency (COSMIC database, tissue overview for benign and malignant melanomas [≥ 198 human tissue samples] excluding spitz, blue naevi, mucosal, acral, ocular and melanomas of genital origin). Numerous genes are deregulated in sporadic cancers, but not mentioned here. Cell line data was excluded. Abbreviations: *ARF*, alternative open reading frame; *BRAF*, v-raf murine sarcoma viral oncogene homolog B1; *NRAS*, neuroblastoma RAS viral oncogene homolog; *mTOR*, mammalian target of rapamycin; *FGFR3*, fibroblast growth factor receptor 3; *PTEN*, phosphatase and tensin homolog; *cKIT*, v-kit Hardy-Zuckerman 4 feline sarcoma viral oncogene homolog; *TP53*, tumour protein 53; *BCL2*, B-cell lymphoma 2; *MITF*, microphthalmia-associated transcription factor; CSD, melanomas on skin with chronic sun-induced damage

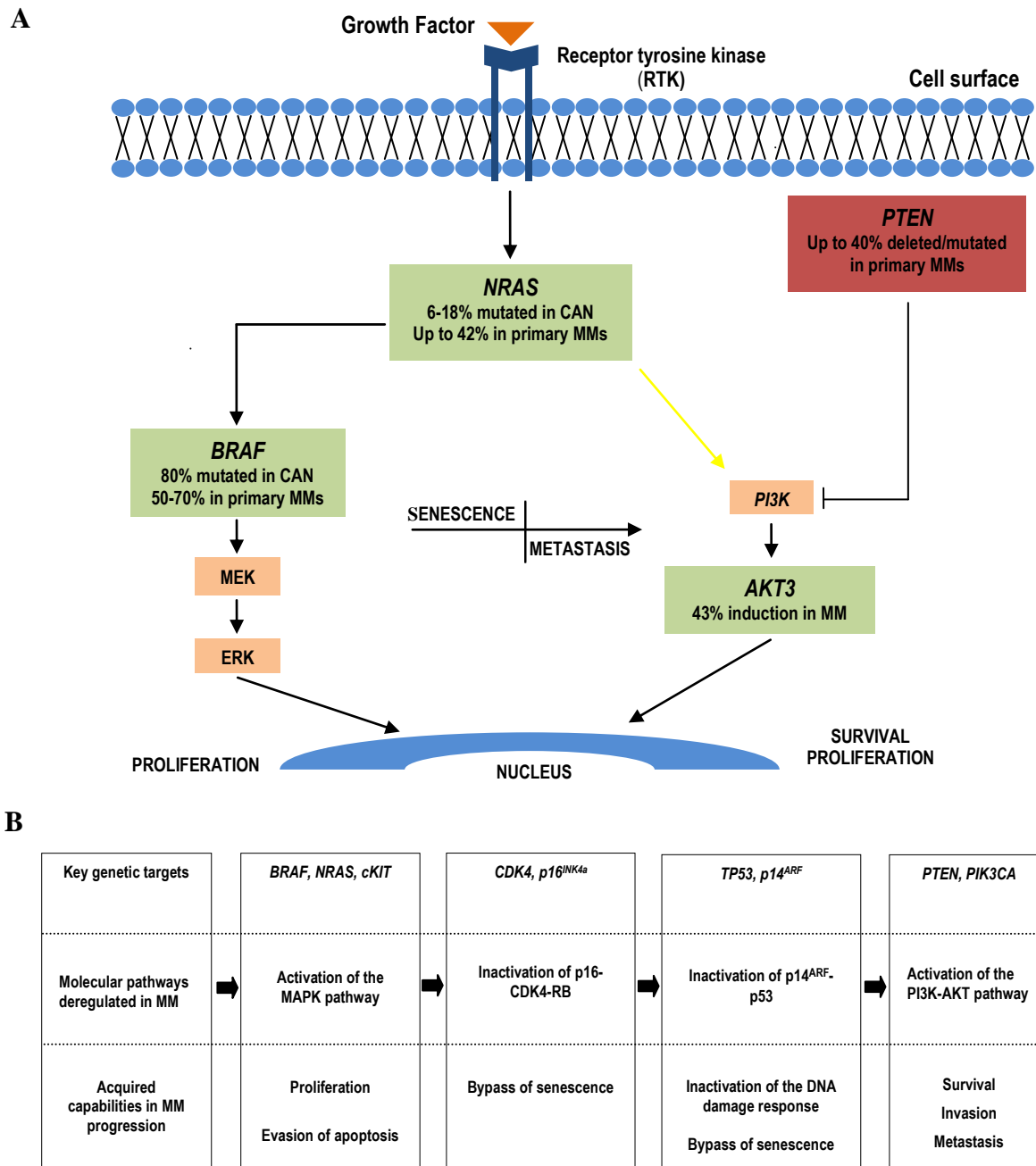


Figure 1.3 - Selected targeted genes and molecular pathways in cutaneous neoplasias. (A) Simplified diagram showing the mitogen-activated protein kinase (MAPK, left branch) and phosphatidylinositol 3-kinase (PI3K/AKT, right branch) pathways of the NRAS signalling network in melanomagenesis. Cell surface RTKs upon binding of various growth factors trigger NRAS activation, which initiates a series of phosphorylation events and ultimately results in activation of ERK. Then, phosphorylated ERK translocates to the nucleus and targets a broad range of proteins affecting cell proliferation and growth (Fecher et al., 2008). In the MAPK pathway the most common mutation (missense) is in the *BRAF* oncogene (V600E, substitution of glutamic acid for valine at amino acid 600) and its activation result to a senescent-non replicative state. However, progression to melanoma requires additional hits, including silencing of TSGs, like *PTEN* and *TP53*, but other unidentified genes may also contribute to full malignant conversion. Activation of *PI3K* by RTKs results in activation of v-akt murine thymoma viral oncogene homolog 3 (*AKT3*), which controls many cellular events, such as cell proliferation and survival. *PTEN* acts as a negative regulator in the PI3K pathway and if altered *AKT3* is constitutively active favouring a highly tumorigenic phenotype (Stahl et al., 2004a). Recent data demonstrated cooperative interaction between *PTEN* loss and activation of *BRAF* oncogene in MM (Dankort et al., 2009). Loss and gain of function is shown in red and green boxes respectively. (B) Hypothetical model associating key altered genes and different pathways that these genes operate during melanoma initiation and progression. Figure-B redrawn from Dahl and Guldberg, 2007.

Table 1.3 - Summary of genetic alterations in cutaneous melanomas from body sites with different levels of sun exposure

SITE	GENES					
	<i>BRAF</i>	<i>NRAS</i>	<i>KIT</i>	<i>Cyclin D1</i>	<i>CDK4</i>	<i>β-catenin</i>
CSD¹	Infrequent mutations	Infrequent mutations	Frequent mutations / amplifications	Increased number of copies, inversely correlated with mutations in <i>BRAF</i>	Amplification, less frequent in primaries compared to mucosal and acral melanomas	Infrequent mutations
	6-11% in melanomas	14-19% in melanomas	28% in primaries			22% in primaries
Mucosal²	Infrequent mutations	Infrequent mutations	Frequent mutations	Same as CSD	Amplification, more frequent in mucosal melanomas compared to CSD and non-CSD	More studies needed to confirm frequency
	Up to 11% in melanomas	5-6% in melanomas	39% in primaries from mucosa		Same specimens were negative for <i>BRAF</i> mutations and <i>cyclin D1</i> amplifications	
Acral³	Infrequent mutations	Infrequent mutations	Frequent amplification	Frequent amplification	Frequent amplification	Same as mucosal
	15-23% in melanomas	up to 10% in melanomas	36% in primaries from acral skin	45% in melanomas, inversely correlated with mutations in <i>BRAF</i>	More frequent in acral melanomas compared to CSD and non-CSD	
Non-CSD⁴	Frequent mutations	Highest mutation frequency	Infrequent mutations	Same as CSD	Same as CSD	Frequent mutations
	54-59% in melanomas	21%-30% in primaries	0% in primaries			52% in primaries
References: Bastian et al., 2000, Cohen et al., 2004, Curtin et al., 2006b, Curtin et al., 2005, Demirkan et al., 2007, Edwards et al., 2004, Maldonado et al., 2003, Platz et al., 2008, Sauter et al., 2002, Takata et al., 2005						
¹ CSD, melanomas on skin with chronic sun-induced damage; ² mucosal, melanomas on sun protected mucosal membrane; ³ acral, melanomas on the soles, palms, or sublingual sites; ⁴ Non-CSD, melanomas on skin without chronic sun-induced damage						

1.2.4 Therapy of melanoma

Despite progress in understanding the molecular biology of melanoma, major clinical problems remain. Firstly, disseminated melanoma is not currently curable and often leads to death in less than one year (Barth et al., 1995). Secondly, it is not possible to predict which melanocytic lesions will metastasise. This justifies the search for new prognostic biomarkers and potentially drugable pathways.

Until recently, none of the few approved for clinical use therapies showed promising beneficial effects on patient survival in advanced melanocytic lesions. The discovery of activating serine/threonine protein kinase *BRAF* or *NRAS* mutations in cutaneous melanomas has stimulated the development of targeted therapies aimed at blocking their deleterious effects on disease progression (Figure 1.4). As previously mentioned (Table 1.2) *BRAF*^{V600E} is the most prevalent mutation in cutaneous melanoma and that makes BRAF the most veritable target in the therapeutic landscape. Despite impressive initial antitumour activity of recently approved BRAF selective inhibitor PLX4032 (also known as Vemurafenib) in metastatic melanoma patients, the clinical response was proved to be limited (the majority of patients relapsed in <1 year) by emergence of acquired resistance (Heidorn et al., 2010, Nazarian et al., 2010b, Su et al., 2012).

Molecular analysis of clinical specimens and cell lines has identified multiple mechanisms of resistance to single agent BRAF inhibitors that led to the paradoxical activation of CRAF and HRAS mutation driven secondary cutaneous squamous-cell carcinomas. These mechanisms involve recovery of ERK phosphorylation (Paraiso et al., 2010), development of *de novo* *NRAS* or *MEK* mutations (Emery et al., 2009, Nazarian et al., 2010b), activation of the kinase MAP3K8 (COT) (Johannessen et al., 2010), a serine/threonine kinase that activates ERK through RAF-independent but MEK-dependent mechanisms, and MAPK

independent signalling through receptor tyrosine kinases such as insulin-like growth factor 1 receptor (Villanueva et al., 2010) and platelet-derived growth factor receptor β (Nazarian et al., 2010b). In turn, these findings have suggested that biomarkers for drug resistance and combination therapies are urgently needed.

Recent phase 1 and 2 clinical trials testing the combination of a MEK inhibitor (trametinib) with a BRAF inhibitor (dabrafenib) showed an improved progression-free survival and decreased toxicity in patients with *BRAF* V600E and V600K mutations compared with dabrafenib monotherapy (Flaherty et al., 2012). In addition, skin squamous-cell carcinomas, which are commonly observed with dabrafenib alone, were less frequently seen with trametinib-dabrafenib combination therapy. Apart from inhibiting the same molecular pathway at two different levels, *in vitro* experiments showed that concurrent RAS-RAF MAPK and PI3K-AKT pathway inhibition in tumours with activating *BRAF* mutations resulted in reduction of growth and survival of melanoma cells (Smalley et al., 2006, Jaiswal et al., 2009). These preliminary results suggested that simultaneous targeting of several pathways may overcome resistance to BRAF inhibitors in *BRAF*-mutant melanomas, but require validation in larger patient populations and randomised trials.

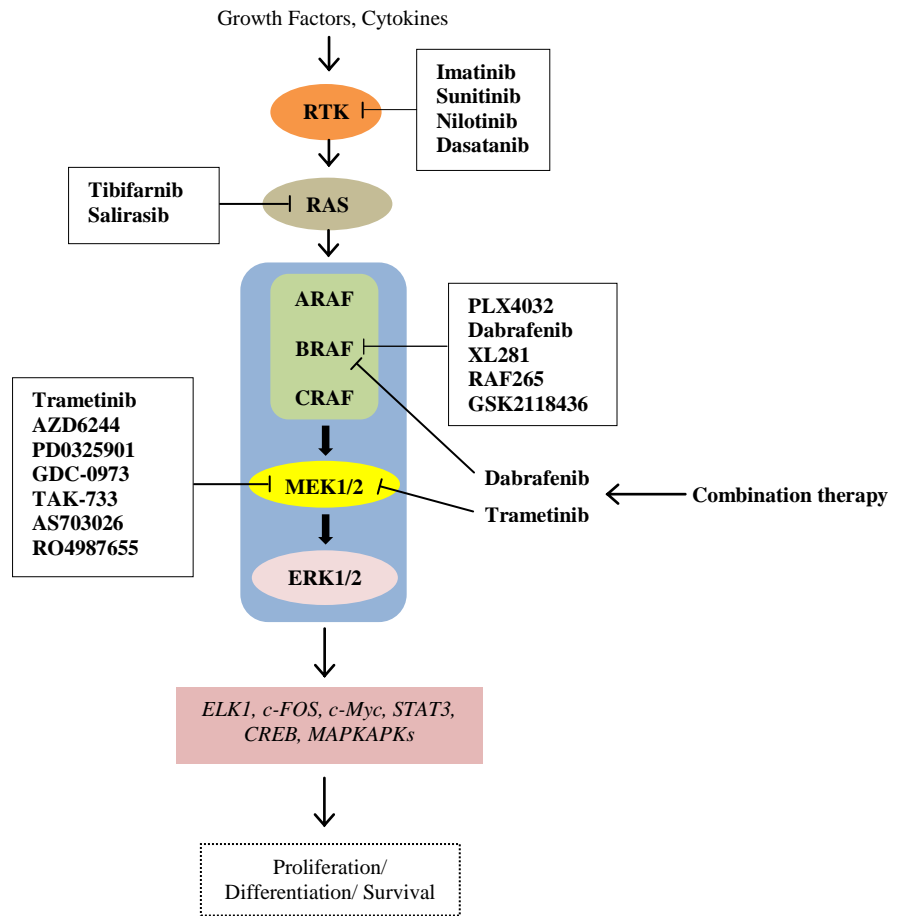


Figure 1.4 - The central melanoma axis and key therapeutic targets in malignant melanoma. Stimulation of the RTK/NRAS/BRAF/MEK/ERK signalling stream is central in the majority of melanomas. *BRAF* and *NRAS* are the most commonly activated oncogenes in cutaneous melanomas. Pharmaceutical agents known to inhibit various components of the RTK/NRAS/BRAF/MEK/ERK axis and currently in clinical trials are listed in the white boxes. Upon stimulation, ERK1/2 phosphorylates a large number of transcription factors (selected factors are shown in pink boxes). Abbreviations: *ELK1*, member of ETS oncogene family; *c-FOS*, FBJ murine osteosarcoma viral oncogene homolog; *c-Myc*, v-myc myelocytomatosis viral oncogene homolog; *STAT3*, signal transducer and activator of transcription 3 (acute-phase response factor); *CREB*, cAMP responsive element binding protein; *MAPKAPK*, mitogen-activated protein kinase-activated protein kinase.

1.3 Melanocytic cell origin and differentiation

1.3.1 Location and function of melanocytes

Melanocytes are pigment-producing stellate cells residing in the basal layer of the epidermis, surrounded by keratinocytes in approximately a 1:30 ratio, and forming an association called epidermal melanin unit (Figure 1.5). The main function of melanocytes is to "shield" DNA from solar radiation-induced damage through melanin pigment production. Synthesis and storage of melanin takes place in specialized lysosome-related membrane bound organelles, termed melanosomes, and that was initially proposed more than 40 years ago by Seiji and colleagues (Seiji et al., 1963). Mature melanosomes are subsequently transferred through the elongated dendrites of melanocytes into the cytoplasm of adjacent epidermal and hair follicle keratinocytes, providing constitutive skin pigmentation and forming a so called "supranuclear" cap that protects epidermis by scattering solar radiation. In this regard, the melanin unit of the epidermis is considered as the "guardian of the skin".

However, melanocytes are not restricted to the skin suggesting functions beyond pigmentation and UV protection (Plonka et al., 2009). Recent studies have shown that melanocytes are also located in the brain (substantia nigra and locus coeruleus), heart, inner ear (stria vascularis of the cochlea) and even in the visceral adipose tissue and some of their functions are summarized in Table 1.4.

Regarding human cutaneous melanocytes other functions apart from melanin genesis are recently documented. The main non pigmentary functions of human melanocytes include production of various neurotransmitters, like acetylcholine and noradrenaline, potent anti-microbial,-fungal properties, phagocytosis and antigen presentation, suggesting an important role in the skin immune system (Elwary et al., 2006, Le Poole et al., 1993a, Le Poole et al., 1993b, Plonka et al., 2009). It is demonstrated that melanin binds to different bacterial toxins

and some pharmaceuticals, for instance the antimalarial agent quinine, act as a physical barrier against invading microorganisms (Mackintosh, 2001). Also and in context with the antifungal properties of melanocytes, the same study suggested that fair-skinned individuals are in fact more susceptible to fungal epidermal infections compared to dark skinned people.

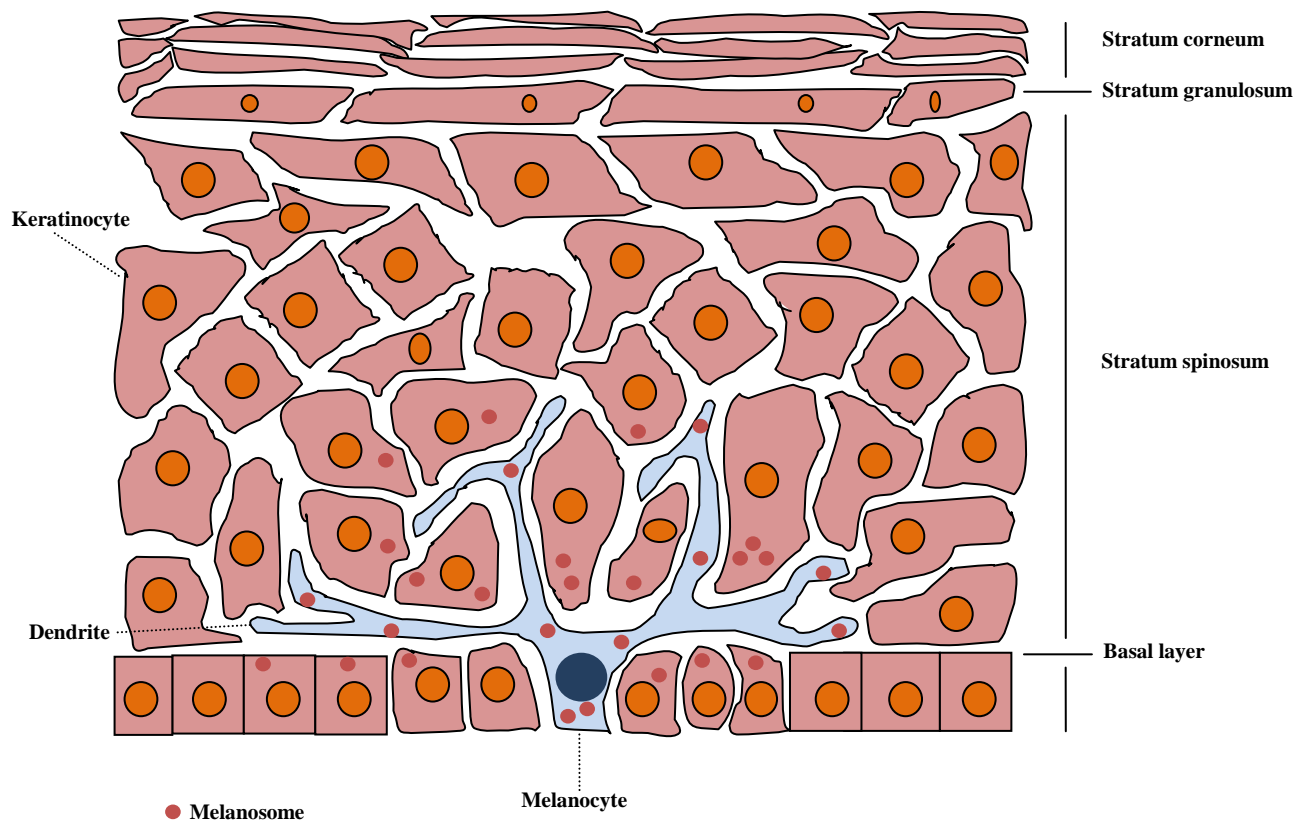


Figure 1.5 - Human epidermal melanocytes are confined to the basal layer of the epidermis. Melanosomes, which are membrane-bound cytoplasmic organelles responsible of melanin biosynthesis, are transferred to neighboring keratinocytes by a mechanism that resembles exocytosis. (Chart redrawn from the textbook *Cancer of the Skin*; Rigel D.S; Chapter 3; page 25; Rigel et al., 2011).

Table 1.4 - Location and functions of extracutaneous melanocytes and melanocyte imitators

Location	Cell type	Function	References
Eye (choroid, RPE [*])	RPE cells (neuroectoderm origin) Uveal melanocytes (NC derived cells)	Pigmentation, UV protection, vision, development of the iris and ciliary	(Bharti and Arnheiter, 2005, Hu et al., 2008)
Ear (cochlea)	Strial intermediate cells (cochlear melanocytes)	Normal development of cochlea and protective role against premature age-related and noise-induced hearing loss	(Hayashi et al., 2007, Murillo- Cuesta et al., 2010, Tachibana, 2001)
Heart (atrioventricular valves)	Cardiac melanocytes	Potential involvement in the cardiac valve development; Normal balance of oxidative species and calcium homeostasis in the myocardium	(Brito and Kos, 2008, Levin et al., 2009)
Brain (neurons of the substantia nigra and locus coeruleus)	Pigmented neurons (produce neuromelanin)	Detoxification e.g. chelate and accumulate environmentally toxic metals like mercury	(Takeda et al., 2007, Zecca et al., 2008)
Visceral adipose tissue (morbidly obese patients)	Adipocytes	Consumption by melanin of singlet oxygen and hydroxyl radicals (to neutralise excess ROS)	(Randhawa et al., 2009)

* Retinal pigment epithelium

1.3.2 Differentiation of melanocytic precursor cells into melanocytes

All vertebrate skin pigment cells or melanocytes, apart from the retinal pigment epithelium of the eye (RPE), which originates from the ectoderm, are emerged from the primitive neural crest (NC). The NC is a multipotent transient population of cells that migrate from the neural tube to sites elsewhere in the body of the embryo during vertebrate development and terminally differentiate into at least four derivatives, sensory neurons, glia, adrenal cells and pigmented melanocytes (Bronner-Fraser and Fraser, 1988, Dupin and Le Douarin, 2003). Several lines of evidence indicate that there is a gradual lineage restriction toward the melanoblast fate from multipotent neural crest stem cells to bipotent glial-melanocyte lineage progenitors, which then becomes further restricted to unpigmented melanocytes, also called melanoblasts (Dupin et al., 2000). These melanocyte lineage cells emigrate from the

primitive NC along the dorsolateral pathway to the newly developing hair follicles or distribute the entire epidermis.

Melanoblasts once in the hair follicles are segregated into two populations (Nishimura et al., 2002). One population consists of melanocyte stem cells, resides in the lower permanent portion of the hair follicle (the bulge region) and serves as a melanocyte reservoir for hair pigmentation. The other population locates in the hair matrix where melanocytic progenitors are differentiated into mature melanocytes to replenish new pigmented hairs. In addition, few studies demonstrated that bulge melanoblasts in human follicles represent a supplemental reservoir for the pigmentation of postnatal epidermis (Horikawa et al., 1996, Narisawa et al., 1997).

Based on recent studies it is likely that there is a niche of melanocyte stem cells located in the dermal layer of the skin to replace epidermal melanocytes during repair and skin regeneration. The most compelling data comes from isolation of human pluripotent precursor cells from the dermis of human foreskins lacking hair follicles, which were immunohistochemically strongly positive for the neural crest cell markers NGFRp75 and nestin and capable of self-renewing. When these intradermal stem cells were placed in three-dimensional human skin reconstructs they migrated to the basal epidermis and successfully differentiated into melanocytes (Li et al., 2010). Terminally differentiated melanocytes residing the epidermis will provide pigment to the skin and protect the body from UV radiation. In a similar manner, but upon a different gene expression profile precursors of neurons and glia cells invade through the ventral migratory pathway and acquire their terminal differentiated characteristics.

1.4 EMT in disease and embryonic development and its transcriptional control

1.4.1 EMT in embryogenesis

Precursor melanogenic and neurogenic cells in the epithelium of NC migrate from the neural tube and undergo transition into a mesenchymal phenotype through a complex and tightly regulated biological program, highly conserved between multicellular organisms, named Epithelial-Mesenchymal Transition (EMT).

Many recent studies have showed that the EMT model involves a series of dramatic changes in the cytoskeleton and cell adhesion-junctions, which their primary role is to facilitate interactions between different cell types (Table 1.5) (Sauka-Spengler and Bronner-Fraser, 2008, Thiery and Sleeman, 2006, Yang and Weinberg, 2008). The induced phenotypical changes that occur during EMT activation are regulated by a number of distinct signalling networks, such as the transforming growth factor- β (TGF- β), Wnt (Wint) and tyrosine kinase receptor (RTK) pathway (Correia et al., 2007, Darken and Wilson, 2001, Zohn et al., 2006). Activation of different receptors by a diverse set of extracellular stimuli, for instance epidermal and fibroblast growth factors (EGF/FGF), triggers the expression of downstream transcriptional regulators that "respond" to these cues (Monsoro-Burq et al., 2003).

Table 1.5 - EMT-related changes in cell properties

Epithelial markers	Mesenchymal markers
Immotile Non invasive Polarised	Elongated Motile Invasive Non polarised
E-cadherin Cytokeratins Desmoplakins Claudins Occludins Mucin-1	N cadherin Vimentin Fibronectin CDH7

Upon stimulation of different signalling cues, multipotent neural cells can undergo EMT dissociating from the neuroepithelium of dorsal neural tube and migrating either dorsolaterally (melanogenic fate) or ventrally (neurogenic fate) (Figure 1.6). It has been shown in chicken and zebrafish embryo models that early emigrating neural crest cells (NCCs) are neurogenic and invade ventrally towards the sites, where they will form neurons and ganglia. At a later stage and when ventral migration gradually stops, upregulation of specific transcription factors and pigment markers permit to a subpopulation of neural cells to migrate into the space between the ectoderm and somite ("classic" melanoblast migration route), where they will differentiate into melanocytes. More recently, a study showed that a proportion of melanocytes emerge from neural precursors (Schwann cells) that migrate ventrally indicating developmental plasticity (Ernfors, 2010). However, recent evidence demonstrated that in mouse embryos both routes are invaded simultaneously (reviewed in Theveneau and Mayor, 2012).

The main EMT transcriptional mediators with considerable importance in the neural crest development, specification and survival of the neural crest cells in chick, *Xenopus* and mouse embryos are the members of *SNAI* homologues 1 and 2 (LaBonne and Bronner-Fraser, 2000, Linker et al., 2000), also known as *SNAIL* and *SLUG* respectively, the members of the zinc finger E-box binding homeoboxes 1 and 2, known as *ZEB1* (*δEF1*) and *ZEB2* (*SIP1*) (Miyoshi et al., 2006, Postigo et al., 2003, Takagi et al., 1998, Van de Putte et al., 2003, van Grunsven et al., 2000, Vandewalle et al., 2009), and the members of *TWIST* homologues 1 and 2, known as *TWIST1* and *TWIST2* (formerly *Dermo-1*) (O'Rourke and Tam, 2002, Soo et al., 2002, Susic et al., 2003).

Loss-of-function experiments in these genes by using morpholino antisense oligonucleotides resulted in apoptotic elimination of neural crest progenitors, delamination arrest of NCCs and failure in neural tube closure, suggesting their essential role during embryonic EMT (Carl et al., 1999, Chen and Behringer, 1995, Soo et al., 2002, Tribulo et al., 2004, Van de Putte et al., 2003, Vega et al., 2004). A central role of these transcription factors is the downregulation of key "gatekeeper" genes that stabilise the epithelial phenotype.

It is now well established from a variety of studies, that a number of genes involved in cell adhesion, migration and invasion are transcriptionally deregulated and one of the best studied is the *E-cadherin* (*CDH1*), a single transmembrane glycoprotein that mediates stable epithelial cell-cell adhesions that are termed adherens junctions. Analysis of the human *E-cadherin* promoter have revealed repeated motifs containing a core of six bases CAGGTG, called E-box elements, which are target sites by specific zinc-fingers transcription factors in many EMT processes during embryogenesis (Pla et al., 2001, Taneyhill, 2008).

The main transcription factors that have been found to bind with high affinity and directly to the E-box elements and suppressing E-cadherin expression are the members of *SNAI* homologues 1 and 2, ZEB1 and ZEB2 (Bolos et al., 2003, Cano et al., 2000, Comijn et al., 2001, Grooteclaes and Frisch, 2000, Kataoka et al., 2000, Nieto, 2002, van Grunsven et al., 2003). In addition, the embryonic helix-loop-helix (bHLH) transcription factors TWIST1/2 also downregulate E-cadherin, but in contrast to *SNAI* and *ZEB* genes are more likely to act via an indirect mechanism, for instance through enhanced expression of transcriptional repressor(s) of the *E-cadherin* gene or by allowing the binding of a transcriptional repressor(s) to the *E-cadherin* promoter (Peinado et al., 2007, Yang and Weinberg, 2008).

Apart from the transcriptional regulators contribution to the EMT program, another mechanism of E-cadherin silencing involves the β -catenin pathway. Several lines of evidence indicate that functional repression of E-cadherin is associated with disruption of intercellular contacts, and dissociation of one of its binding partners, β -catenin, from a complex containing α -, β -catenin and p120. This complex is associated with the intracellular domain (tail) of E-cadherin and its primary role is to establish links with the actin cytoskeleton. Then the released β -catenin translocates to the nucleus and interacts with the lymphoid-enhancer binding factor/T-cell factor-4 (LEF/TCF4) enhancing the expression of target genes (Behrens et al., 1996, Schmalhofer et al., 2009) (Figure 1.7). Recent reports demonstrated that two genes upregulated by the Wnt β -catenin dependent signals were *SNAI2* and *TWIST1*, which in their turn suppress E-cadherin expression (Conacci-Sorrell et al., 2003, Onder et al., 2008). Therefore, it is now more evident that acquisition of the mesenchymal phenotype can partially emerge from E-cadherin loss, mediated by several transcription factors and β -catenin release.

To date, a limited number of transcription factors have been identified to regulate genes required for melanoblast specification, and the most important is the *MITF*, also known as the master regulator of melanogenesis (Thomas and Erickson, 2008). MITF plays a key role in melanoblast survival and melanocyte lineage commitment during embryogenesis, and regulates the expression of enzymes involved in melanin biosynthetic pathway, such as TYRP-1, TYR and Dopachrome tautomerase (Dct) (reviewed in Goding 2000, Widlund and Fisher, 2003).

Mounting evidence also suggests a functional link between T-box genes, which are transcription factors characterised by a highly conserved DNA-binding domain (T-domain), and developmental processes, such as determination of cell fate during organogenesis

(Lamolet et al., 2001, Szeto et al., 2002). Recently, ChIP analysis and cell-based reporter assays demonstrated that Tbx2 and Tbx3 directly repress the expression of E-cadherin (Rodriguez et al., 2008, Wang et al., 2012). In addition, it has been shown that the *Tbx2* promoter contains a MITF binding site indicating that activation of MITF upon commitment to the melanocyte lineage is likely to modulate Tbx2 expression (Carreira et al., 1998).

Finally, apart from the NC development during embryogenesis, which requires large-scale cell movements, other best studied embryogenic EMT events include the formation of mesoderm (an embryonic layer generated during gastrulation), placenta, somites, cardiac valve development and male Müllerian duct regression (in male reproductive tracts) (Gros et al., 2005, Kokkinos et al., 2010, Nakaya and Sheng, 2008, Person et al., 2005, Zhan et al., 2006).

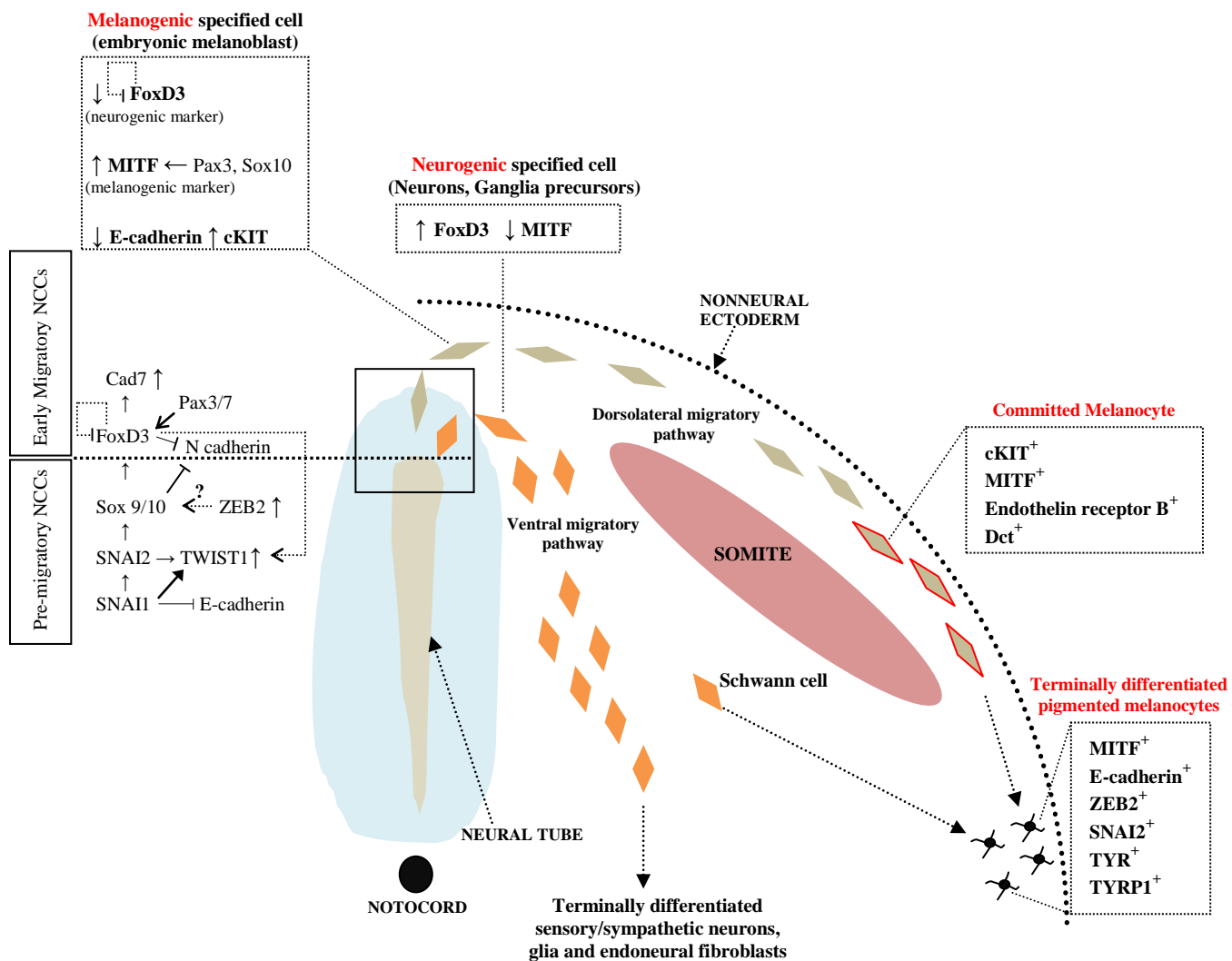


Figure 1.6 - EMT-associated transcription factors control trunk neural crest induction, survival and delamination during embryogenesis. Strong evidence from gain- and loss-of-function analyses in *Xenopus laevis* (frog) embryos indicated that activation of several transcription factors [including but not restricted to SRY (sex determining region Y)-box 9, 10 (*Sox 9/10*), paired-domain box 3, 7 (*Pax3/7*), forkhead box D3 (*FoxD3*), *SNAI1*, *SNAI2* and *TWIST1*] in the pre-migratory NCCs are needed not only for the specification of both neuronal and melanogenic lineages but also in modifying cell-cell adhesion properties (reviewed in Betancur et al., 2010, Steventon et al., 2005). *FoxD3* and *Sox 9/10* are directly responsible for the negative regulation of type I-cadherins, such as N-cadherin, in chicken and mouse embryos. In addition, type II-cadherins, such as Cadherin 7 (*Cad7*) and $\beta 1$ integrins, are upregulated to promote delamination (Cheung et al., 2005). *Sox10* and *Pax3* induce *MITF* expression in melanoblasts when they exit the neural tube. Furthermore, and based in *Xenopus* model system it is reported that *SNAI1* expression precedes *SNAI2* and plays an early role in neural crest development (Aybar et al., 2003). *SNAI1* directly represses *E-cadherin* expression in NCCs in mouse embryos (Cano et al., 2000). In mouse embryos, pre-migratory and migrating cranial NCCs showed high levels of *ZEB2* transcripts and a possible indirect transcriptional effect of *ZEB2* on *Sox10* (Van de Putte et al., 2003). Finally, the transcription factor *FoxD3* plays a critical role in the lineage switch from neuronal to melanoblast as repress melanogenesis by binding directly to the *MITF* promoter. Therefore, in order for the melanoblasts to migrate and enter the dorsolateral pathway *FoxD3* should be downregulated by upstream inhibitory cues. ↑ indicates activation; ↓ or T-shaped arrows indicate inactivation;> indicates possible indirect activation.

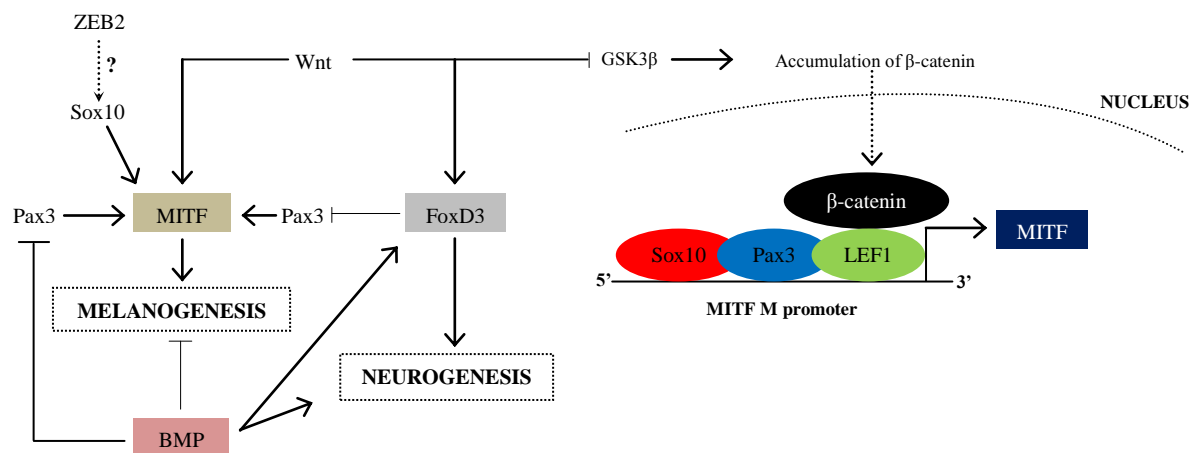


Figure 1.7 - Schematic representation showing the main regulatory interactions controlling melanoblast specification. MITF expression is regulated by the synergistic activity of Pax3 and Sox10 and also requires Wnt β -catenin-dependent signalling. Although it has been postulated an indirect transcriptional effect of ZEB2 on Sox10 in pre-migratory and migrating cranial NCCs (Van de Putte et al., 2003), it is currently unknown whether there is ZEB2 activation that could contribute to melanoblast specification through Sox10 and MITF upregulation. Upon Wnt signals (Wnt3a and Wnt1), β -catenin enters the nucleus, associates with the LEF1 and the forming complex binds to the M promoter of the MITF upregulating its expression and promoting melanoblast formation (reviewed in Dorsky et al., 1998, Saito et al., 2003). In contrast, Wnt signalling in mouse NC induced formation of sensory neurons in a β -catenin-dependent manner (Lee et al., 2004). Gain of Wnt signalling is required in combination with bone morphogenic proteins (BMP) to induce FoxD3 expression and subsequent neurogenesis (Jones and Trainor, 2005, Thomas and Erickson, 2008). A recent study demonstrated that MITF is inhibited via a FoxD3-mediated repression of Pax3 (Thomas and Erickson, 2009). Abbreviation: GSK3 β , glycogen synthase kinase-3 β .

1.4.2 EMT in disease

Historically, the epithelial to mesenchymal transitions were first described in a chick embryo by Matthias Duval in 1879, who observed emigration of neural crest cells emerged from the neural tube. However, he was not able to distinguish between epithelial and migratory mesenchymal cells (Duval, 1879). In the early 1980s Greenburg and Hay were the first to show that epithelial cells are not stationary under certain conditions and they concluded that adult and embryonic epithelial cells if suspended in type I collagen gels have the capacity to acquire EMT-like traits, such as loss of polarity and motility (Greenburg and Hay, 1982).

EMT programs are normally operative in embryonic morphogenesis, transiently activated during wound healing, but can also contribute to different diseases. The best known paradigms of EMT-dependent pathological situations are those of fibrosis and carcinogenesis. In fibrosis, tissue injury at sites of chronic inflammation, such as kidney, lung, liver and heart, leads to accumulation of fibroblasts, mainly derived from epithelial cells undergoing local EMT or bone marrow (Kalluri and Neilson, 2003). In tumours, activation of EMT by transformed cells is essential for invasion and establishment of secondary tumours at distant sites, which represents the last step of the metastatic cascade of malignancies. This cascade can be divided into two major phases, the physical dissemination of primary tumour and colonisation, also called macrometastasis (Geiger and Peeper, 2009, Lee et al., 2006a, Yang and Weinberg, 2008).

In the first phase, malignant cells with activated EMT invade locally and degrade the basement membranes by releasing protein-degrading enzymes, such as matrix metalloproteinases (MMPs). Then, invasive transformed cells can migrate either slowly in a mesenchymal form or faster acquiring an amoeboid form and translocate through vasculature (blood and/or lymph vessels) to distant anatomical sites, in a process called

intravasation. A very small proportion of transformed cells will eventually survive from cell death and extravasate from vessels into organs (micrometastasis). In the second phase of the invasion-metastasis cascade, disseminated micrometastatic tumour cells can, on rare occasions, spread to specific organs forming macroscopic tumours (colonisation/metastasis). In several cases mesenchymal micrometastatic cells revert to an epithelial state, a process analogous in the formation of epithelial organs during embryonic development, known as mesenchymal to epithelial transition (MET) (Hugo et al., 2007).

A prerequisite for disseminated malignant cells to successfully colonise to distant sites is their ability to adapt to a "foreign" microenvironment and suppress anoikis, a process in which apoptosis (programmed cell death) is triggered by loss of cell adhesions (detachment-induced apoptosis) (Frisch and Francis, 1994, Mayhew et al., 1999). Anoikis also occurs under normal physiological conditions, for instance replacement of the epithelial lining in the gastrointestinal tract, when enterocytes, the predominant cells in the intestinal epithelium generated from stem cells at the crypt base, reach the tip of the intestinal villi (do Vale et al., 2007, Grossmann et al., 2001, Hall et al., 1994). In addition, numerous studies showed that establishment of a macrometastasis is also dependent on tumour cell dormancy, a state in which extravasated transformed cells remain quiescent for a prolong period of time (Barkan et al., 2008, Luzzi et al., 1998, Morris et al., 1997, Paez et al., 2012).

1.4.2.1 Definition of EMT in melanoma

It is becoming increasingly common to read of the concept of EMT in melanocytic malignancies. In addition, a notable body of literature suggests that melanocytes perturb elements of embryonic EMT pathways during propagation of the disease. By definition, it is important to understand that "classic" EMT, like the one described in carcinomas and embryonic development, does not exist in melanomas.

To start with, EMT in melanocytic lesions refers to transformation of melanocytes rather than epithelial cells. As further described in various *in vitro* experiments a transformed melanocyte acquires a very large number of coordinated molecular changes, including loss of senescence, gradual loss of intercellular adhesions (e.g. E-cadherin), switch to other cadherins (e.g. from P- and E-cadherins to N-cadherin) and gain of stem-cells associated proteins, such as Nodal (Bosserhoff et al., 2011, Cook et al., 2003, Topczewska et al., 2006). Furthermore, transformed melanocytes are phenotypically plastic with neural crest-derived melanoblasts, the progenitors of melanocytes. *In vivo* analyses pose the question that evidence for EMT may escape histological analysis as no methods are currently available to track cells undergoing EMT in time and space. Nonetheless, development of melanoma animal models with conditional knock-in or knock-outs of EMT transcriptional mediators will aim to further define the role of EMT in melanoma. Evidence of EMT in clinical biopsies can further be supported by detection of mesenchymal biomarkers and loss of junctional cadherins in neoplastic cells (Liu and Brown, 2010, Zhang et al., 2012).

Finally, it is noteworthy to mention that melanocytes have subtle differences compared to epithelial cells, such as lack of apical-basal polarity and tight junctions. However, an apparent paradox comes from the observation that melanocytes acquire a phenotype that both E-cadherin, an epithelial cell marker, and vimentin, an intermediate filament protein

synthesized primarily by cells of mesenchymal origin, are strongly expressed (Si et al., 1993). Therefore, melanocytes are neither epithelial nor mesenchymal cells and may be best viewed as a mixed cell type displaying properties of both.

1.4.2.2 Developmental regulators determine tumour progression

As already described in Figure 1.6, in order for neural oligopotent precursor cells to migrate and further differentiate into unipotent cell types, either melanoblasts or neural precursors, need to pass through an EMT. Studies based on embryonic model systems and cell lines (normal and transformed) revealed that tumorigenic cells in order to invade and disseminate to distant sites in the body reactivate EMT processes, which share similar characteristics with those occur during the embryonic development (Kuriyama and Mayor, 2008, Nieto, 2009, Theveneau and Mayor, 2012).

A number of studies have postulated a convergence between cell lineage and tumour phenotype (lineage-dependency or addiction). In this model of cancer progression, cell of origin plays a central role in tumour morphology and behaviour as transformed cells seem to accomplish a molecular reprogramming by adapting traits of mesenchymal progenitor cells. Following this model, functional analyses showed that expression of developmental mesenchymal markers, for example nuclear β -catenin, transcriptional repressors, like SNAILs and ZEBs, and fibroblast-specific protein 1 (FSP1), also known as S100A4, and loss of lineage-markers characteristic for epithelial cells, for instance cytokeratins 8/18 and E-cadherin, associates with high-grade malignancies and poor prognosis (Barrallo-Gimeno and Nieto, 2005, Garraway and Sellers, 2006, Peinado et al., 2004, Thiery, 2002, Thiery, 2003, Thiery et al., 2009, Xue et al., 2003). It is also demonstrated an EMT correlation with the expression of S100A4 and β -catenin in different types of cancers, as their inhibition in malignant cells suppress metastasis. Moreover, thorough review of the literature identifies the MITF and the androgen receptor gene (AR) as the most typical examples of master

lineage-survival oncogenes (Berger et al., 2004, Garraway et al., 2005). Increasing experimental data suggests that few lineage-associated transcriptional repressors are also deregulated in different malignancies of the relevant lineage.

MITF, as previously mentioned in section 1.4.1, is considered as the master regulator gene of melanogenesis having an essential role in melanoblast survival, melanocytic lineage commitment and melanocyte differentiation by triggering cell cycle exit through induction of the cyclin dependent kinase inhibitor (cdki) p16^{INK4a} (reviewed in Goding 2000, Widlund and Fisher, 2003). However, emerging evidence suggests that this gene also plays an important role in melanoma pathogenesis. Gene expression profiling and genetic studies demonstrated that *MITF* gene was amplified in 15-23% of human metastatic melanomas and associated with decreased patient survival (Table 1.2, Garraway et al., 2005). A recent study by Wellbrock and colleagues demonstrated that high levels of MITF are required downstream of oncogenic *BRAF*^{V600E} to stimulate proliferation and survival in melanoma cells. In this regard, *BRAF*^{V600E} stimulates MITF transcription through upregulation of the octamer-binding transcription factor BRN2 (N-Oct-3) (Wellbrock et al., 2008).

Like MITF, other lineage-survival markers are characterised, including the androgen receptor gene, cyclin D1 oncoprotein (*CCND1*) and FMS-related tyrosine kinase 3 (*FLT3*) (Brasel et al., 1995, Garraway and Sellers, 2006, Sicinski et al., 1995, Thiede et al., 2002). The androgen receptor has a decisive role in normal prostate prenatal development promoting survival and differentiation of the associated epithelial prostate lineage. Interestingly, androgen (5 α -dihydrotestosterone (DHT) and testosterone)-dependent AR activation mediates the malignant transformation of the prostate epithelium (Berger et al., 2004). In addition, it is found that retinoblastoma (*RB*) tumour suppressor gene, an important negative regulator of cell-cycle progression, plays a dominant role in AR

transcription as its deletion or silencing in progressed prostate malignancies is associated with AR downregulation and loss of cell-cycle control (Heinlein and Chang, 2004, Sharma et al., 2010). Apart from MITF and AR role in oncogenesis, emerging data based on animal models and cell lines suggest that several distinct lineage-associated transcription repressors of E-cadherin are capable of orchestrating EMT programmes during prenatal development and in different types of cancer.

1.4.2.3 Master regulators of EMT (MR-EMT) in tumourigenesis

In recent years, transcriptional factors were uncovered as negative regulators of E-cadherin expression and have been associated with cancer aggressiveness, resistance to anoikis and chemotherapeutics. Among them, TWIST family of transcriptional repressors is increasingly considered to have an important contribution to neoplastic transformation and progression. The embryonic helix-loop-helix transcription factor TWIST1 suppresses directly *E-cadherin* when complexed with the chromatin modifier polycomb-group protein Bmi1 (Yang et al., 2010). However and in contrast to its direct *E-cadherin* repression a recent report suggested that TWIST1-induced EMT requires a direct activation of SNAI2 to repress *E-cadherin* transcription (Casas et al., 2011). Rosivatz *et al.* indicated that overexpression of TWIST1 is associated with E-cadherin loss and metastatic potential in human diffuse-type gastric carcinomas (Rosivatz et al., 2002).

Additional studies revealed that TWIST1 is associated with many types of human and murine aggressive tumours, including breast malignancies (Martin et al., 2005), prostate tumours (Kwok et al., 2005), hepatocellular carcinomas (HCC) (Lee et al., 2006b) and oesophageal squamous cell carcinomas (ESCC) (Yuen et al., 2007). In addition, a study conducted by Yang and colleagues demonstrated that TWIST1 is highly induced in late stage breast malignancies and inversely correlated with E-cadherin expression (Yang et al., 2004). The same group has also highlighted that TWIST1 silencing of expression in 4T1, a

highly invasive mouse mammary tumour cell line, markedly reduced the formation of lung metastatic nodules. In a different study, melanoma tissue microarrays showed that *TWIST1* was notably upregulated and correlated with poor survival in more than 50% of melanoma samples (Hoek et al., 2004).

Even if *TWIST2* has been studied to a lesser extent, a limited number of reports demonstrated that similarly to its sibling gene, *TWIST1*, is upregulated in different tumour-derived cancer cell lines (from melanoma, kidney, breast and lung) (Ansieau et al., 2008, Fang et al., 2011, Hui et al., 2009, Li et al., 2012) and frequently overexpressed in human head and neck squamous cell carcinomas (HNSCC) (Gasparotto et al., 2011), melanoma tumours (Ansieau et al., 2008) and cervical carcinomas (Li et al., 2012). However, an elegant recent study by Ansieau *et al* suggested that both *TWIST* genes, apart from their essential contribution as progression factors in late stage malignancies may also prevent an early stage oncogene-induced senescence (Ansieau et al., 2008). These experiments have raised the possibility that a potential mechanism for avoidance of *RAS*-induced senescence could be the cooperative oncogenic action of *RAS* and *TWIST1/2* with subsequent loss of key senescent inducers, like the tumour suppressor *p16* gene.

Work by Serrano and colleagues in 1997 addressed for the first time the phenomenon of *RAS* (oncogene)-induced cellular senescence as a protective mechanism in pre-malignant lesions against uncontrolled proliferation (Serrano et al., 1997). A characteristic example refers to melanocytic naevi (benign lesions), which remain in a stable proliferative arrest for prolonged period of time upon constitutive activation of oncogenic *BRAF*. However, transformed melanocytes require additional hits, such as loss of p53 or p16 tumour suppressor proteins, before acquisition of invasive and metastatic phenotypes (Gray-Schopfer et al., 2006, Michaloglou et al., 2005, Patton et al., 2005).

Over the past few years, studies revealed that expression of the SNAI superfamily of zinc-finger transcription factors play a crucial role in both neural crest cell migration and cancer invasiveness (Barrallo-Gimeno and Nieto, 2005, Huber et al., 2005, Nieto, 2002). The vertebrate specific *SNAI*-related genes are divided into two subfamilies, *SNAI1* and *SNAI2* and both induce EMT. The first member of the *SNAI* family, *SNAI1*, is a homologue of the *snail* gene in *Drosophila melanogaster*, where it was initially identified as a gene essential for cell migration in a developing mesoderm (Grau et al., 1984). The second member, *SNAI2*, was first characterised in chick embryos and was found to be critical for neural crest and mesoderm delamination (Nieto et al., 1994).

SNAI1 and *SNAI2* activation is now believed to favour tumour progression in a subset of carcinomas by repression of *E-cadherin* and other epithelial genes, such as *cytokeratin-18* and *desmoplakin* (Batlle et al., 2000, Cano et al., 2000, Guaita et al., 2002). Based on various *in vitro* and *in vivo* analyses, expression of these direct E-cadherin repressors have been associated with progression, lymph node metastasis and poor prognosis in a panel of clinical breast, ovarian, HNSCC and ESCC samples and cell lines (Blanco et al., 2002, Come et al., 2006, Elloul et al., 2005, Uchikado et al., 2005, Yang et al., 2007). Moreover, *SNAI1* expression was overexpressed and correlated with loss of E-cadherin and distant metastasis in most of the colon carcinoma biopsies (Roy et al., 2005), as well as with MMP-7 and MT1-MMP expressions in HCCs (Miyoshi et al., 2005). *SNAI1* expression was associated with MMP-2 increase, E-cadherin decrease and tumour invasion in squamous cell carcinomas (SCCs) (Yokoyama et al., 2003).

An interesting study conducted by Saito proposed a potential role of *SNAI1*-mediated E-cadherin inactivation as an alternative mechanism of E-cadherin downregulation in synovial sarcomas (SS) (Saito et al., 2004). In this model, a small proportion of SS cases

acquire a spindle-shaped phenotype, which resembles mesenchymal cell morphology, due to *SNAI1* mediated repression of genes involved in epithelial differentiation. Another study reported an important association between *SNAI2* expression and experimental melanoma metastasis in mice (Gupta et al., 2005). Remarkably, short-interfering RNA (siRNA)-mediated inhibition of *SNAI2* in immortalized melanocytes that have been previously transformed with oncogenic *Ras* protein (*Ras*G12V, yielding Mel-STR cells) and subcutaneously introduced into postnatal mice led to suppression of lung metastases by more than ten-fold when compared to control Mel-STR tumours.

Similarly to *SNAI* and *TWIST* genes, the *ZEB* family of transcription factors has also been reported to have a central position in malignant cancer progression. In vertebrates there are two well-characterised two-handed zinc finger / homeodomain *ZEB* proteins, *ZEB1* and *ZEB2*. *ZEB1* transcription factor was firstly identified as a post-gastrulation DNA-binding transcriptional repressor that regulates *δ-crystallin* gene in embryonic chicken lens by inhibiting its enhancer element (Funahashi et al., 1993). On the other hand, vertebrate *ZEB2* shares sequence similarities with *ZEB1* and it was characterised using the yeast two-hybrid screening system as a transcriptional repressor that specifically binds to TGF- β receptor-activated Smad-interacting proteins (SIPs) (Verschuere et al., 1999).

Nuclear accumulation of Smads and interaction with *ZEB2* mediates DNA-binding to regulatory regions, for instance E-box sequences, located in the promoters of target genes. Screening of *ZEB1* protein for different colorectal, non-small-cell lung (NSCLC) and type II endometrial cancer cell lines and tumour samples showed correlation with complete suppression of E-cadherin, dedifferentiation, increased invasion and poor prognosis (Aigner et al., 2007, Ohira et al., 2003, Singh et al., 2008). In contrast, RNA-i mediated knockdown of *ZEB1* in a poorly differentiated breast cancer cell line MDA-MB-231 was sufficient to

reverse the mesenchymal features of these cells (Eger et al., 2005). ZEB2 expression has been associated with acquisition of a mesenchymal invasive phenotype in different malignancies and particularly in oral squamous cell carcinoma, lung, kidney, breast, ovarian and gastric advanced tumours (Elloul et al., 2005, Maeda et al., 2005, Oztas et al., 2010, Rosivatz et al., 2002, Vandewalle et al., 2009). In addition, ZEB2 metastatic propensity seems to be dependent on MMP-1,-2,-MT1 upregulation in a panel of HCC cell lines (Miyoshi et al., 2004). Recent reports provided evidence that ZEB1 and ZEB2 expression is targeted by different non-coding RNAs, so-called microRNAs (miRs).

1.4.2.4 MicroRNAs in EMT and metastasis

MiRs are short (~22 nucleotides) non-protein-coding ribonucleic acids (RNAs) that have been shown to inhibit gene expression (Esquela-Kerscher and Slack, 2006). More than a decade ago, Victor Ambros and Rosalind Lee have discovered that *lin-4*, a gene responsible for the developmental timing of the ring worm *Caenorhabditis elegans* (a nematode), produces small non-coding RNA, rather than a protein-coding mRNA, repressing the expression of the mRNA *lin-14* by binding to its 3'untranslated region (3'UTR) (Lee et al., 1993). As a consequence of the *lin-7* function, the nematodes could only progress to the second stage of their development (Reinhart et al., 2000). Since then, hundreds of miRs (logged at the miRBase at Sanger Institute) have been identified in human genome, showing that miRs could be considered as one of the most important classes of regulatory genes in humans.

Further bioinformatic studies have provided evidence that a large number of the human mRNAs (approximately one-third) could be regulated by miRs (Kiriakidou et al., 2004, Lewis et al., 2003, Rajewsky, 2006). In addition, many experiments using mutations on various components of the miR pathway have demonstrated that miRs have an essential role in many biological processes, such as cell death, cell proliferation and regulation of insulin

secretion (Calin and Croce, 2006, He and Hannon, 2004). Apart from miRs physiological role as regulators of gene expression, recent findings have demonstrated that more than 50% of the miR genes are located at chromosomes associated with various human cancers (Calin et al., 2004, Zhang et al., 2007). Genetic aberrations, such as genomic deletions, amplifications, mutations, and epigenetic factors like, DNA hypermethylation, lead to human carcinogenesis by altering the expression of target proteins implicated in important biological processes (Volinia et al., 2006). Furthermore, an increasing number of publications reveal the dual role of miRs as tumour suppressors or oncoproteins during the acquisition of a malignant phenotype. Finally, advances in high-throughput techniques, such as microarrays and quantitative real-time PCR (qRT-PCR), supported the identification of differential miR expression profiles in neoplastic cells compared to their normal counterpart cells (Nelson et al., 2004).

1.5 Aims and Objectives

MR-EMT, mainly represented by the SNAI, TWIST and ZEB families, act downstream of embryonic EMT pathways *in vivo* and efficiently induce EMT upon ectopic expression in epithelial cell cultures. Elevated expression of MR-EMT is generally considered as poor prognosis marker associated with a high risk of metastatic dissemination. To date no comprehensive study on the MR-EMT network in melanoma has yet been performed. Therefore the main aim of this study was to investigate the expression and regulation of the MR-EMT network in melanoma cell lines and the clinical significance of specific MR-EMT in tumour tissues.

Hypothesis

Malignant melanomas acquire a specific MR-EMT phenotype, characteristic of neural crest melanocyte precursors, which is associated with metastasis and poor prognosis.

The specific aims and objectives for each results chapter were as follows:

Chapter 3 - Aims

- To assess which MR-EMT proteins are expressed and how these transcription factors are regulated *in vitro*.
- To test whether there is a link between the MR-EMT expression and oncogenic signalling pathways activated in malignant melanoma.

Objectives

- Gene and protein expression studies were carried out on several melanoma cell lines and assessed by real time qRT-PCR and western blotting. Experiments with siRNA-

mediated knockdowns of individual MR-EMT and addition of pharmacological inhibitors inhibiting different signalling cascades were also conducted.

Chapter 4 - Aim

- To assess which MR-EMT have a biological significance in melanoma.

Objectives

- An immunohistochemical work was carried out to compare the protein expression levels between E-box binding MR-EMT and known target genes E-cadherin and VDR.
- To further evaluate the effect of MR-EMT on VDR and E-cadherin *in vitro*, siRNA-mediated knockdowns of specific MR-EMT proteins and motility assays were conducted.

Chapter 5 - Aim

- To assess whether the expression of MR-EMT proteins has a clinical significance to melanoma progression and patient survival.

Objectives

- An immunohistochemical work was carried out to assess the expression of MR-EMT in a mouse melanoma model and human melanoma samples from a cohort of patients.
- To correlate the expression of MR-EMT with clinicopathological variables using univariate and multivariate models.

2 Materials and Methods

2.1 Materials

2.1.1 Patients and melanoma tissues

Melanocytic tissues were identified from the Histopathology and Dermatology Departments, University Hospitals of Leicester and represent patients presenting between 1996 and 2006. Local Ethics Committee approval was obtained for the tissue analysis (Appendix I, REC: 6791, UHL: 8141, LNR REC1). Histological sections and formalin-fixed paraffin embedded (FFPE) tissue blocks were retrieved from the archive. Unfortunately, access to melanoma clinical samples was limited and sequential cases were used if sufficient material was remained in the tissue blocks. Demographic information on the MM cases included age at primary excision, gender, time to last follow-up visit / clinical metastasis and stage was determined from the Breslow thickness and ulceration of the primary tumour. All pathological data was available from reports and checked by Dr. PE Hutchinson and Dr. JE Osborne (Dermatology department, Leicester Royal Infirmary, UK). Details of cases with follow-up data used in this study are summarized in Appendix II.

2.1.2 Chemicals and reagents

All general chemicals were purchased from Sigma-Aldrich Ltd (Dorset, UK) and Fischer Scientific Ltd (Loughborough, UK) unless otherwise stated.

2.1.3 *Eukaryotic cell lines*

Cell lines used in this study (SK-MEL-2, SK-MEL-5, SK-MEL-28, RPMI-7951, and WM-266-4) were from the American Type Culture Collection (ATCC, Manassas, VA, USA). SK-MEL-30 and IPC-298 were obtained from the German Collection of Microorganisms and Cell Cultures (Leibniz Institut DSMZ, Braunschweig, Germany). A375P and A375M were originally obtained from Wellcome Trust Functional Genomics Cell Bank (St. George's, University of London, UK). The Human Epidermal Melanocytes (HEM)-neonatal (HEMN) and -adult (HEMa) were from the TCS Cellworks Ltd (Buckingham, London, UK). The human urinary bladder RT-112, osteosarcoma HOS, human epithelial carcinoma A431, human embryonic kidney 293 (HEK293) and HEK293 Snail-8SA-transfected (Grotegut et al., 2006) were carcinoma cell lines obtained from Dr. E Tulchinsky (Department of Cancer Studies and Molecular Medicine, Leicester University, UK). All cell lines were maintained at low passages and stored in vials at a temperature of about 196°C, in in-house tanks of liquid nitrogen. Classification of melanoma cell lines according to *BRAF* or *NRAS* mutation status is described in Table 2.1.

Table 2.1 - *BRAF* and *NRAS* mutation status in human melanoma cell lines used in this study

Cell line	<i>BRAF</i>	<i>NRAS</i>	Notes	References
A375P	+ (V600E)	WT	A poorly metastatic human melanoma cell line derived from a 54-year-old female	(Bruggen et al., 1978, Giard et al., 1973)
A375M	+ (V600E)	WT	Derived from a metastasis of the parental A375P	(Collisson et al., 2003, Giard et al., 1973, Kozlowski et al., 1984)
IPC-298	WT	+ (Q61L)	Established from the primary tumour (right cervical) of a 64-year-old woman with cutaneous melanoma	(Aubert et al., 1993)
RPMI-7951	+ (V600E)	WT	Derived from a metastatic site of a MM (lymph node)	(Tanami et al., 2004)
SK-MEL-2	WT ¹	+ (Q61R)	Derived from a metastatic site of a MM (skin of thigh)	(Davies et al., 2002, Fogh et al., 1977)
SK-MEL-5	+ (V600E)	WT	Derived from a metastatic site of a MM (axillary node)	(Fogh et al., 1977, Tanami et al., 2004)
SK-MEL-28	+ (V600E)	WT	Derived from the primary tumour of a 51-year-old man with cutaneous melanoma	(Davies et al., 2002, Fogh et al., 1977)
SK-MEL-30	WT	+ (Q61K)	Derived from tumour tissue (subcutaneous metastasis) of a 67-year-old Caucasian man with malignant melanoma	(Carey et al., 1976)
WM-266-4	+ (V600D)	WT	Derived from a metastatic site of a MM	(Davies et al., 2002)

¹WT, wild type

2.1.4 Cell culture reagents and supplements

Epidermal melanocyte basal medium (a sterile HEPES and bicarbonate buffered medium containing essential and non-essential amino acids, organic compounds, inorganic salts, trace minerals and vitamins), growth supplement [a concentrated 100× sterile solution containing bovine insulin, hydrocortisone, heparin, phorbol 12-myristate 13-acetate (PMA), bovine transferrin, basic fibroblast growth factor, foetal bovine serum (FBS) and bovine pituitary extract (BPE)], antibiotic supplement (containing 25 mg/ml gentamicin and 50 µg/ml amphotericin B, 1000× concentrate), HEPES-Buffered Saline Rinsing Solution, Trypsin/EDTA (T/E), and Trypsin Blocking Solution were obtained from TCS Cellworks Ltd, UK. Eagle's minimum essential medium (EMEM) modified to contain Earle's balanced salt solution (BSS), non-essential amino

acids (NEAA), 2mM L-Glutamine, 1mM sodium pyruvate (NaP) and 1500 mg/L sodium bicarbonate (NaHCO₃, 1.5 g/L), without phenol red were obtained from ATCC, USA. Roswell Park Memorial Institute (RPMI 1640) medium with L-Glutamine but without phenol red, foetal bovine serum (FBS), Penicillin/Streptomycin antibiotic solution (containing 5,000 units of penicillin and 5,000 µg of streptomycin/ml) and dimethyl sulphoxide (DMSO) were from Gibco, UK. Tissue culture flasks (25, 75 and 150 cm²) and 6, 12 and 24 well plates were all supplied from BD Falcon, UK.

2.1.5 Manipulation of melanoma cell lines

U0126 (1,4-diamino-2,3-dicyano-1,4-bis [2-aminophenylthio] butadiene) and 1a, 25-Dihydroxyvitamin D₃ (calcitriol) were purchased from New England Biolabs (Hertfordshire, UK) and Sigma-Aldrich respectively. Cell Line Nucleofector[®] Kit Amaxa V was supplied by Lonza (Verviers, Belgium). PLX4720 and PD184352, selective inhibitors of BRAF^{V600E} and MEK respectively, were obtained from Prof. Catrin Pritchard (Department of Biochemistry, University of Leicester, UK). Specific inhibitors for p38 mitogen-activated protein kinase (SB203580) and c-Jun N-terminal kinase (SP600125) were from New England Biolabs and Sigma-Aldrich respectively. Specific inhibitor for PI3 kinase (Wortmannin) was purchased from New England Biolabs. The proteasome inhibitor MG132 and cycloheximide (CHX) were obtained from Merck Millipore, UK. The GSK-3β inhibitor lithium chloride (LiCl) was made in-house.

2.1.6 RNA extraction kit

TRIzol[®] and the RNeasy Mini Kit were supplied by Sigma-Aldrich and Qiagen Ltd (West Sussex, UK) respectively.

2.1.7 Total RNA quality control analysis

The RNA 6000 NanoChip and RNA 6000 Nano reagent kit (containing gel matrix, dye concentrate, marker and ladder) were all obtained from Agilent Technologies (Berkshire, UK).

2.1.8 Quantitative and conventional PCR reagents and materials

For real-time quantitative PCR, microAMP 96-well plates, adhesive films, custom designed and inventoried FAM-labelled TaqMan probes, Fast SYBR[®] Green and 2×TaqMan[®] Fast PCR Universal Master mixes were from Applied Biosystems (Foster City, CA). Custom designed oligonucleotide primers were synthesized by Sigma-Genosys, UK. The Taqman[®] MicroRNA assay (Applied Biosystems, Foster City, CA) was used to analyse the expression of miRs. The short tandem repeat (STR) PCR was performed by using the AmpFlSTR[®] SGM Plus[®] PCR Amplification Kit (Applied Biosystems, Foster City, CA).

2.1.9 Human Endogenous Control Array

The TaqMan[®] Endogenous Control Array cards and the TaqMan[®] Gene Expression Master Mix were purchased from Applied Biosystems.

2.1.10 Preparation of cytoblocks

All human melanoma tissue and cell blocks were paraffin-embedded by Ms. AK Gillies using the Shandon Cytoblock[®] cell block preparations system (Thermo Scientific).

2.1.11 Immunohistochemical materials

Detection of human melanoma tissue-bound primary antibodies was performed using the NovolinkTM Polymer System and supplied by Leica Microsystems (Milton Keynes, UK). Tris-HCl buffers saline (TBS, wash buffer containing 500 mM Tris base, 1.5 M NaCl, pH 9.0), Tris-EDTA antigen retrieval buffers (10 mM Tris base, 1 mM EDTA, pH 8.0) and veronal acetate buffer (VAB, pH 9.2) were from in-house stocks.

2.1.12 Immunoblotting materials

The supersignal western extended duration and enhanced chemiluminescence (ECL) substrates for HRP, bicinchoninic (BCA) protein assay reagent, protein standard bovine serum albumin (BSA) and the restore plus western blot stripping buffer, were all from Thermo Scientific. The precision plus dual colour protein size marker and 30% acrylamide / bis-acrylamide electrophoresis solution were from Bio-Rad Laboratories (Hertfordshire, UK). N, N, N, N'-tetramethylethylenediamine (TEMED), ammonium persulphate (APS) and Tween-20 were from Sigma-Aldrich. Polyvinylidene fluoride (PVDF) membranes were purchased from Millipore (Durham, UK). Reagents including Laemmli lysis buffer, TBS-T, loading buffer, transfer buffer, wash buffer, resolving gel buffer and stacking buffer were made from in-house stocks.

2.2 Methods

2.2.1 *RNA Isolation and manipulation*

2.2.1.1 Preparation of total RNA

Total RNA was extracted from cells by combining the TRIzol[®] extraction method with Qiagen RNeasy mini kit (Qiagen, UK). This method is designed for the extraction and purification of up to 100 µg of total RNA from 1 to 10×10^6 cells. All mammalian eukaryotic cells were seeded in 25 or 75 cm² flasks. Total RNA from cell lines was extracted at the exponential growing phase (around $1-2 \times 10^6$ cells) and then the cells were trypsinised and centrifuged at 1000 rpm for 5 min. The resulting pellet was resuspended in 1 ml of TRIzol[®] reagent (Sigma, UK) and either incubated at room temperature for 5 min for immediate RNA extraction or stored at -20°C for later handling.

Two hundred µl of chloroform (CHCl₃) was then added to the lysed with TRIzol[®] cells and left to stand for 3 minutes at ambient temperature. To precipitate total cellular RNA the samples were centrifuged at 13,000 rpm for 15 min at 4°C (cold room). After the centrifugation, upper aqueous layer containing RNA, was removed and transferred to clean labelled sterile bijoux, where the volume was measured by pipetting. To provide ideal binding conditions, not only for RNA species >200 nucleotides, but also for low-molecular-weight RNAs, like miRs, 1.25× of absolute ethanol was added to the lysates. Samples were then applied to a silica-base spin column and after a series of washes, in order to remove all potential contaminants, pure and concentrated RNA was eluted in 30-50 µl of RNase-free water and stored at -20°C until required.

2.2.1.2 Quantification of RNA

The concentration of RNA was determined by either the NanoDrop Spectrophotometer ND-1000 (NanoDrop Technologies, USA) or ND-8000 8-Sample UV-Vis Spectrophotometer (Thermo Scientific, Wilmington, USA). In order to measure the RNA concentration, 1 µl of total RNA, previously prepared using the TRIzol[®] extraction combined with the Qiagen RNeasy mini kit, was resuspended in RNase-free water and loaded onto the pedestal. The purity of the RNA sample was verified by comparing the absorbance values at 260 and 280 nm. Pure RNA has an A₂₆₀/280 ratio of around 2 (1.9-2.1).

2.2.1.3 Converting total RNA to cDNA

Prior to the utilisation of the quantitative real-time PCR (qRT-PCR), it is essential to convert RNA to cDNA due to the fact that Taq polymerase could not use RNA as a template. Reverse transcription (RT) was conducted on all individual RNA samples using a High Capacity RNA-to-cDNA kit (Applied Biosystems) and 100 ng of total RNA was reverse transcribed with 20×RT Enzyme Mix according to the manufacturer's protocol. The 20 µl reactions were then incubated in a GeneAmp 9700 96-well thermal cycler (Applied Biosystems) for 60 min at 37°C, 5 min at 95°C (to inactivate enzymes) and stored at -20°C until required for RT-PCR analysis. The minus RT reactions were used as control reactions for DNA contamination.

2.2.1.4 Oligonucleotide primers and probes

Oligonucleotide primers for this study were synthesised from Sigma-Genosys and the most suitable for this project are listed in Table 2.2. The primers were supplied as lyophilised pellets and before use were briefly centrifuged at 13,000 rpm at room temperature. The primers were then diluted in sterile water to a final concentration of 200 pmoles/µl and aliquots were taken and further diluted (1:20) to a working

concentration of 10 pmoles/ μ l, transferred into fresh eppendorf tubes and stored at -20°C. TaqMan[®] FAM-labelled MGB probes (working concentration of 200 nM / 10 μ l total volume reactions) were obtained from Applied Biosystems and stored at -20°C (Table 2.2).

2.2.1.5 Primer and probe design

All custom primers for conventional PCR and qRT-PCR were designed using two web-based programs, a program from MIT (U.S) called Primer3 version 0.4.0 (<http://frodo.wi.mit.edu/>) and the Primer Express version 3.0 from Applied Biosystems. For quantitative real-time PCR assays, custom TaqMan[®] FAM-labelled MGB probes were designed using the Primer Express program software (version 3.0) from Applied Biosystems. The same software was also used to check for eventual self and cross-complementarities between the forward and reverse primers and hairpin loops formation. Furthermore, certain criteria were taken into consideration during the primer design and were in accordance with recommendations outlined by Applied Biosystems. To begin with, the primers were designed to have a melting temperature (T_m) with a range from 58-60°C, a primer length between 18-26 nucleotides, a GC content range from 30-80% and a maximum of two G and C residues in the last five 3'-end nucleotides. Also for optimum PCR efficiency, the amplified PCR products were expected to be 60-120 base pairs (bp) in length. Primer sequence specificity was cross-checked with the NCBI Nucleotide Basic Local Alignment Search Tool (BLAST) (<http://blast.ncbi.nlm.nih.gov/Blast.cgi>). All primers were specifically designed close to the 3'-end and sequence variability among different samples was avoided by selecting sequence regions free of known single nucleotide polymorphisms (SNPs) (<http://www.ncbi.nlm.nih.gov/projects/SNP/>). Similarly, custom and TaqMan[®] FAM-

labelled MGB probes were designed following recommendations outlined from Applied Biosystems and their sequences were checked with the BLAST search tool.

Table 2.2 - Primers and TaqMan[®] gene expression assays for quantitative PCR experiments

Primer	Sequence (5' → 3')	Length(nt)	Entrez Accession Number	Genomic Position (Exon)	Amplicon Length(bp)
<u>PPIA</u>					
F	GGT TCC TTC TGC GTG AAT TAC CA	23	NM_021130.3	5	75
R	GGA ATA CGT AAC CAG ACA ACA CAC A	25			
Probe	CCA CTT GTG CAT CTC AG	17			
<u>RPLP0</u>					
F	GGC TAC CCA ACT GTT GCA TCA	21	NM_001002.3	7	69
R	GAC AAG GCC AGG ACT CGT T	19			
Probe	CCC GTT GAT GAT AGA ATG	18			
<u>UBC</u>					
F	CTT AGA GGT GGG ATG CAG ATC TTC	24	NM_021009	2	71
R	TCG GCT CCA CTT CGA GAG T	19			
Probe	ACC AGT CAG GGT CTT CA	17			
ZEB1	Applied Biosystems (Hs00232783_m1)	N/A	NM_001128128.2	4 → 5	63
ZEB2	Applied Biosystems (Hs00207691_m1)	N/A	NM_001171653.1	5 → 6	67
SNAI2	Applied Biosystems (Hs00950344_m1)	N/A	NM_003068.4	2 → 3	86
TWIST1	Applied Biosystems (Hs01675818_s1)	N/A	NM_000474.3	1	85

F - forward primer; R - reverse primer; PPIA - peptidylprolyl isomerase A; RPLP0 - ribosomal protein, large, P0; UBC - ubiquitin C

2.2.1.6 Quantitative PCR (qRT-PCR)

Real-time PCR was performed using a standard TaqMan[®] PCR kit protocol on a StepOnePlus™ thermal cycler (Applied Biosystems). The relative amount of gene transcripts was normalized to UBC. Thermal cycling and reaction conditions are shown in Figure 2.1 and Table 2.3 respectively. Data were analysed according to the $\Delta\Delta C_t$ method (Livak and Schmittgen, 2001).

Table 2.3 - Reaction conditions for qRT-PCR using TaqMan probes

Reaction component	µl/reaction [custom]	µl/reaction [inventoried]
2× TaqMan Fast Universal Master Mix	5	5
Forward primer (F)	0.6	–
Reverse primer (R)	0.6	–
c-DNA sample *	3.6	4.5
FAM-MGB probe	0.2	0.5 (+F/R)
Total per reaction	10	10

* Different dilutions

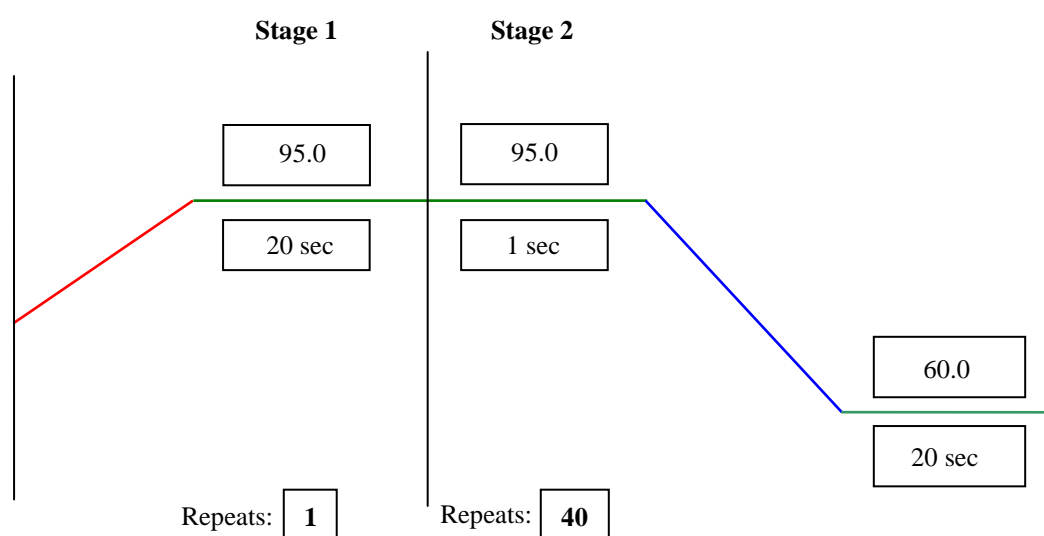


Figure 2.1 - Thermal cycling conditions for qRT-PCR using TaqMan probes. At holding stage 1 the denaturation program was 20 sec at 95°C. The amplification and quantification program (stage 2) was repeated for 40 cycles (1 sec at 95°C and 20 sec at 60°C). Detection of the PCR products were performed with TaqMan® FAM-labelled MGB probes.

2.2.1.7 Standard curves

Standard curves were generated for each primer / probe set using suitable cDNA templates. To optimise efficiency for each custom probe set, different dilution series (1:2 to 1:10) of cDNAs were set up. Efficiency was calculated from the gradient of the slope.

2.2.2 *miR expression by real-time qRT-PCR*

2.2.2.1 miR extraction from melanoma specimens and cell lines

RNA was extracted manually from micro-dissected FFPE melanoma and naevus sections using the Qiagen miRNeasy isolation kit (Qiagen) according to the manufacturer's instructions. MicroRNA isolation from melanoma cell lines was achieved by combining the TRIzol[®] extraction method with Qiagen RNeasy mini kit (section 2.2.1.1). Quantity and purity of RNA samples were determined using the NanoDrop Spectrophotometer ND-1000 (section 2.2.1.2).

2.2.2.2 Reverse transcription and pre-amplification

To produce cDNA Taqman[®] MicroRNA RT kit (Applied Biosystems) was used in accordance with the manufacturer's instructions. MiR-200 family members (-a, -b, -c, -141, -429), miR-125b and endogenous control miR-191 specific cDNAs were generated from total RNA, previously extracted from melanoma cell lines or FFPE tissues, using the TaqMan[®] MicroRNA Reverse Transcription Kit with RNA-specific RT primers (TaqMan[®] MicroRNA Assay, Applied Biosystems).

2.2.2.3 Quantitative real-time PCR

Quantitative real-time PCR Taqman[®] MicroRNA assays (Applied Biosystems) were used to analyse the expression of miRs that showed the most significant differential expression in melanoma tissue microarray experiments performed by Dr. SR Elshaw (Department of Cancer Studies and Molecular Medicine, Leicester University, UK). All reactions, including no-template controls and -RT controls were performed in triplicate on the 96-well StepOnePlus[™] Fast Real Time PCR system (Applied Biosystems). Selection of the most stable miR expressed across multiple melanoma samples was carried out using geNorm algorithm-based software (section 2.2.3.2) and miR-191 emerged as the most stable. Data were analyzed according to the $\Delta\Delta C_t$ method

(Livak and Schmittgen, 2001). Details of miR assays used for quantitative PCR experiments are shown in Table 2.4.

Table 2.4 - TaqMan® MicroRNA Assays used in this study

miR	Mature miRNA Sequence	miRBase Accession Number*
hsa-miR-125b	UCCCUGAGACCCUAAACUUGUGA	MIMAT0000423
hsa-miR-200a	UAACACUGUCUGGUAAACGAUGU	MIMAT0000682
hsa-miR-200b	UAAUACUGCCUGGUAAUGAUGA	MI0000342
hsa-miR-200c	UAAUACUGCCGGGUAAUGAUGGA	MIMAT0000617
hsa-miR-141	UAACACUGUCUGGUAAAGAUGG	MIMAT0000432
hsa-miR-429	UAAUACUGUCUGGUAAAACCGU	MIMAT0001536
hsa-miR-191	CAACGGAAUCCCAAAAGCAGCUG	MIMAT0000440

*miRBase: the miR database (<http://www.mirbase.org/>)

2.2.2.4 Short tandem repeat (STR) profiling for melanoma cell lines

To check whether there was any cross-contamination between human cell lines, STR profiling was performed in two different batches of A375P and A375M cells by Ms. E Socratous (East Midlands Forensic Pathology Unit, University of Leicester, UK).

2.2.2.5 Extraction of genomic DNA from frozen A375 pellets

Removal of proteins from genomic DNA was achieved by extraction with phenol:chloroform:isoamyl alcohol (25:24:1) solutions according to manufacturer's instructions (Sigma-Aldrich). Melanoma cells were initially ruptured using a lysis solution (0.5 mL, 0.05 M Tris, pH 8.0 / 0.1% SDS) and 25 µl of proteinase K (10 mg/mL) and incubated for 1 hr at 37°C. An equal volume of phenol:chloroform:isoamyl alcohol (25:24:1) was added to the samples and then centrifuged at 13,000 rpm for 2 min at ambient temperature. Immediately after centrifugation, the upper aqueous layer containing DNA was removed and transferred into new microcentrifuge tubes, where the volume was measured by pipetting. An equal

volume of chloroform:isoamyl alcohol (24:1) was added to the samples and further centrifuged at 13,000 rpm for 2 min at room temperature. Aqueous phase was discarded and the final volume of the DNA samples was measured by pipetting. Precipitation of DNA was achieved by adding one-tenth volume of 1 M NaCl and three volumes of ice cold absolute ethanol. Resultant solutions were then mixed by pipetting and placed at -20°C overnight. Samples were then centrifuged for 10 min at 4°C and after carefully removing the supernatant pellets were washed with 70% ethanol. Finally, the DNA pellets were centrifuged, air-dried for 5 min, resuspended in 50 µl of 1×TE and stored at 4°C until required. The concentration of DNA in aqueous solution was determined using the NanoDrop Spectrophotometer ND-1000. One µl of DNA was loaded onto the pedestal and the absorbance was measured. The purity of the DNA sample was verified by comparing the absorbance values at 260 and 280 nm. Pure DNA has an A₂₆₀/A₂₈₀ ratio of around 1.8.

2.2.2.6 Polymerase chain reaction (PCR) for STR profiling

Polymerase chain reaction was first developed by Kary Mullis in 1986 and became one of the most powerful techniques with many applications in gene diagnosis, forensics and molecular evolution (Mullis et al., 1986). Briefly, this technique permits the amplification of specific DNA sequences by the design of oligonucleotide primers complementary to DNA strands (with a known base sequence) in a region of interest (Powledge, 2004). The STR amplification reaction was performed by using the AmpFlSTR® SGM Plus® PCR Amplification Kit according to manufacturer's instructions (Applied Biosystems). The PCR reactions were performed on GeneAmp 9700 96-well thermal cycler and the thermal cycling conditions are shown in Table 2.5.

Table 2.5 – Thermal cycling conditions for STR profiling

	Initial incubation step	Melt	Anneal	Extend	Final extension	Final hold
	HOLD	CYCLE (28)			HOLD	HOLD
Temperature	95°C	94°C	59°C	72°C	60°C	4°C
Time (min)	11:00	1:00	1:00	1:00	45:00	hold

PCR products were detected by capillary electrophoresis on a ABI Prism 3130 Genetic Analyser (Applied Biosystems), data was collected using 3130 Data Collection v3.0 software and analysed using Genemapper[®] ID software v3.2. The STR profiles generated for A375P and A375M cell lines are shown in Appendix III.

2.2.3 TaqMan[®] Human Endogenous Control Array

2.2.3.1 RNA analysis and cDNA preparation

Total RNA was extracted from melanoma cell lines and cultured normal melanocytes (section 2.2.1.1) and the concentration of RNA was quantified with a NanoDrop ND-8000 8-Sample UV-Vis Spectrophotometer (Thermo Scientific, USA) at 260 nm wavelength (section 2.2.1.2). Integrity of total RNA fraction was assessed using the Agilent 2100 Bioanalyser and associated RNA NanoChip reagents according to manufacturer's instructions (Agilent Technologies, UK). An RNA integrity number (RIN) was generated for each sample based on the ratio of ribosomal (28 and 18S) bands. The RIN algorithm assigns a score from 10 to 1, where maximum score represents a high quality intact RNA and minimum score represents a highly degraded RNA. A threshold value of $RIN \geq 8$ was applied. Reverse transcription was conducted as previously described (Section 2.2.1.3).

2.2.3.2 Array run and analysis of data

A commercially available pre-formatted and inventoried 384-well TaqMan[®] Human Endogenous Control Array, containing 16 assays for commonly used housekeeping genes, was selected and real time qRT-PCR was performed using an ABI 7900HT Fast Real-Time PCR system (Applied Biosystems, Foster City, CA). Reactions were prepared in a total volume of 100 µl containing 2 µl (100 ng/µl) of cDNA, 48 µl of nuclease free water and 50 µl of Gene Expression Master Mix (Applied Biosystems), loaded into each sample-loading port and briefly centrifuged (Heraeus Multifuge 3S Centrifuge, Thermo Scientific) for 1 min at 1200 rpm twice. Following the centrifugation step the interconnecting channels were closed using a Sealing Device, the loading ports were removed and the array was loaded into the ABI 7900HT Fast Real-Time PCR system. Thermal cycling conditions, baseline and threshold values were automatically set for all plates using the ABI SDS (vs. 2.3) software. The array data was analysed using two freely-available programs, the geNorm (vs. 3.5) (Vandesompele et al., 2002) and NormFinder (Andersen et al., 2004), in order to obtain stability comparisons of candidate reference genes. Both validation programs are Microsoft Excel add-ins and ranked all tested genes according to their expression stability across samples. Best combination of two endogenous genes was also calculated (Appendix IV).

2.2.4 Immunohistochemistry-Paraffin (IHC-P)

2.2.4.1 Haematoxylin and Eosin staining for morphology

Tissue sections were deparaffinised by immersion in 100% xylene twice (3 min each time), rehydrated for 1 min in 99% and 95% industrial methylated spirits (IMS) and rinsed in tap water for 1 min. The slides were then stained in Haematoxylin for 5 min and Eosin for 1 min and rinsed in tap water for 3 min. Sections were dehydrated in 95% and 99% industrial methylated spirits (IMS) for 1 min, immersed in 100% xylene twice (3 min each time) and mounted using a DPX aqueous mounting agent (2 drops per slide).

2.2.4.2 Dewax and rehydration of the sections under investigation

Consecutive sections from FFPE benign naevi, primary and metastatic melanoma archival tissue specimens were cut (3µm) and mounted onto Vectabond (VectorLabs, UK) treated slides. The purpose of using vectabond coated slides was to avoid loss of tissue from the slide surface following the use of heat-induced epitope retrieval methods. Next, the slides were dried for 5 min at 65°C in an air incubator. Sections were then dewaxed (a major limiting step) by immersion in 100% xylene for 5 min once, rehydrated for 10-15 sec in 99% and 95% industrial methylated spirits (IMS) and washed in tap water for 3 min.

2.2.4.3 Heat-induced antigen retrieval for melanoma tissues

In this study, the rehydrated slides were placed in a plastic rack and immersed in 1× TE buffer (Tris at pH 9.0, EDTA) in order to inactivate nucleases which degrade DNA or RNA. The slides were then microwaved in TE for 20 min on full power setting at 750 W. For E-cadherin, staining sections were pressure cooked in 1× citrate buffer (at pH 6.0) for 30 sec at 120°C. After the epitope recovery procedure was complete, the slides were allowed to cool down for 15 min at room temperature. For mouse

melanoma sections, ZEB1 and ZEB2 antigen retrieval was performed in 1× citrate buffer (at pH 6.0).

2.2.4.4 Application of primary antibodies

2.2.4.4.1 Human melanoma tissues

Following the antigen retrieval, the human melanoma slides were removed from the rack, washed in TBS (Tris-buffered saline, pH 7.6, twice for 5 min) and placed in an incubation tray where a peroxidase blocking solution was applied onto the slides for 5 min to neutralise endogenous peroxidase, followed by TBS washing (2×5 min). The next step was to add a minimum amount of 100 µl protein block solution (Leica Microsystems) onto each section for 5 min in order to reduce non-specific binding of primary antibody and polymer, followed by TBS washing (2×5 min). After the critical step of protein blocking, the primary antibodies were diluted in TBS. One hundred µl of the diluted primary antibodies was then applied to serial tissue sections from each specimen (Table 2.6). Non primary antibody (NPA) slides were kept in TBS and used as negative controls for each run. Finally, the slides were incubated in an incubation tray overnight at 4°C.

2.2.4.4.2 Mouse melanoma model sections

Following protein unmasking, the mouse melanoma tissue sections were removed from the rack, washed in TBS (Tris-buffered saline, pH 7.6, twice for 5 min) and placed in an incubation tray where 100 µl of the avidin solution was applied onto the slides for 10 min, followed by TBS washing (2×5 min). The next step was to add a minimum amount of 100 µl biotin solution onto each section for 10 min and then sections were washed again in TBS (2×5 min). After the critical step of biotin blocking, 100 µl of normal swine serum (Dako, UK), diluted (1:5) in blocking solution (BS), which was prepared

by mixing 50 ml of TBS, 1.5 g of 3% Bovine serum albumin (BSA) (Biomedicals, Germany), and 50 µl of 0.1% Triton X-100, (Fisons, UK), was applied to each tissue section for 10 min at room temperature. Serum blocking solution was then drained off and optimally diluted primary antibodies were applied to cover mouse sections (Table 2.6). Non primary antibody (NPA) slides were kept in TBS and used as negative controls for each run. Finally, the slides were incubated in an incubation tray overnight at 4°C.

Table 2.6 - List of primary antibodies used for immunohistochemistry

Primary antibody	Dilution	Antigen retrieval & Incubation duration	Detection system & Chromogen	Vendor	References*
ZEB1 (H-102 / rabbit-polyclonal)	1:1000	20 min, 1×TE buffer, microwave (750W), 4°C overnight	Novolink Polymer, DAB	Santa Cruz Biotechnology (Heidelberg, Germany)	(Sayan et al., 2009)
For mouse sections:	1:400	20 min, 1×Citrate buffer, microwave (750W), 4°C overnight	ABC-AP, Fast Red		
ZEB2 (CUK2 / rabbit-polyclonal)	1:5000	20 min, 1×TE buffer, microwave (750W), 4°C overnight	Novolink Polymer, DAB	Donated by Dr. AE Sayan, University of Southampton, UK	(Sayan et al., 2009)
For mouse sections:	1:5000	20 min, 1×Citrate buffer, microwave (750W), 4°C overnight	ABC-AP, Fast Red		
SNAI1 (clone EC3 / mouse)	1:50	20 min, 1×TE buffer, microwave (750W), 4°C overnight	Novolink Polymer, DAB	Donated by Dr. AG De Herreros, University of Pompeu Fabra, Barcelona, Spain	(Franci et al., 2006)
SNAI2 (clone C19G7 / rabbit)	1:50	20 min, 1×TE buffer, microwave (750W), 4°C overnight	Novolink Polymer, DAB	New England Biolabs (Ipswich, UK)	(Shirley et al., 2012)
TWIST1 (clone 2C1a / mouse)	1:100	20 min, 1×TE buffer, microwave (750W), 4°C overnight	Novolink Polymer, DAB	Abcam (Cambridge, UK)	(Ansieau et al., 2008)
E-cadherin (clone 36 / mouse)	1:2000	30 sec, 1×Citrate buffer, pressure cooker (120°C), 4°C overnight	Novolink Polymer, DAB	BD Transduction Laboratories™ (Oxford, UK)	(Do et al., 2004)
VDR (clone D-6 / mouse)	1:200	20 min, 1×TE buffer, microwave (750W), 4°C overnight	Novolink Polymer, DAB	Santa Cruz Biotechnology	(Wang et al., 2010)

*References to previous validation of primary antibodies used for IHC-P

2.2.4.5 Application of the secondary antibody and the Novolink Polymer Detection System

After treatment of slides with the relevant primary antibody, human melanoma tissue sections were firstly washed in TBS (2×5 min), covered with the post primary blocking solution for 30 min and followed by washing in TBS (2×5 min). The slides were then incubated with the Novolink polymer, which recognises only mouse and rabbit immunoglobulins, for 30 min, and further washed in TBS (2×5 min). For visualization of the antigen-antibody interactions the slides were treated with 3, 3'-diaminobenzidine (DAB) working solution, by adding 50 µl of DAB chromogen to 1 mL of Novolink DAB substrate buffer, for 5 min. Finally, the slides were washed in tap water for 5 min, counterstained in Mayer's Haematoxylin for 30 sec, washed again in running tap water and mounted using an Aquatex aqueous mounting agent (2 drops per slide).

2.2.4.6 Application of the secondary antibody and the ABC-AP Detection System

After treatment of slides with either ZEB1 or ZEB2 primary antibodies, mouse tissue sections were removed from the tray and washed in TBS (2×5 min). Then, the slides were placed in the incubation tray where 100 µl of the polyclonal secondary biotinylated swine anti-rabbit antibody (Bt'd SaR, Dako), previously diluted 1:800 in BS, was added to each slide for 30 min.

Detection of ZEB1 and ZEB2 was performed by the avidin-biotin complex method (ABC). After incubation with the primary and the biotinylated secondary antibodies, the slides were washed in TBS (2×5 min), covered by 100 µl of avidin-biotin complex alkaline phosphatase-AP conjugated [ABC-AP, containing 492 µl of BS, 4 µl of Streptavidin (Dako) and 4 µl of biotinylated alkaline phosphatase (Dako)], which had been previously mixed and then left to stand at room temperature for 30 min before use. The slides were then incubated for 30 min at room temperature. All treated slides were

transferred into a Coplin or Hallendahl jar, washed firstly in TBS (2×5 min) followed by washing in distilled water (5 min) and VAB for another 5 min.

For visualization of the antigen-antibody interactions the slides were treated with Fast Red solution. This solution was prepared by combining 50 ml of VAB with 12 mg of levamisole and 25 mg of fast red TR salt and then by adding with gentle mixing 25 mg of naphthol AS-BI phosphate disodium salt, previously dissolved in 20 µl of dimethylformamide. After filtration, 50 µl of the Fast Red solution was poured onto the slides for 1 hr. Finally, the slides were washed in tap water for 5 min, counterstained in Mayer's Haematoxylin for 10 sec, washed again in running tap water for 5 min and mounted using an Aquatex aqueous mounting agent (2 drops per slide).

2.2.4.7 Semiquantitative immunohistochemical evaluation for MR-EMT, VDR and E-cadherin

In this study staining of MR-EMT was graded as positive only when nuclear staining was detectable. H-Score which measures the percentage of stained tumour cells and the intensity of the staining was used to evaluate MR-EMT staining. To each section was given a score on a scale of 0 to 3 for the intensity of the nuclear staining, with a maximum immunoreactivity of 300 and minimum of 0. Positive staining was scored via the H-Score (Kinsel et al., 1989) and calculated as follows:

$$\text{H-Score} = 1 \times (\% \text{ weak staining}) + 2 \times (\% \text{ moderate staining}) + 3 \times (\% \text{ strong staining})$$

Three observers agreed the criteria for levels of positive staining (Dr. JH Pringle, Dr. PE Hutchinson and Mr. E Papadogeorgakis). Four representative dermal fields were assessed; two from the superficial tumour close to the epidermal basal lamina in the papillary dermis and two from the deepest tumour sites within the reticular dermis and H-Scores were calculated separately for superficial and deep sites. Inter-observer

agreement was measured using 20 randomly selected cases and an intra-class correlation coefficient (ICC) indicated high agreement (ICC = 0.92).

For ZEB1 and TWIST1, scores of 0 (H-Score = 0) were considered negative and immunoreactivity of 1 (H-Score = 1-100), 2 (H-Score = 100-200) and 3 (H-Score = 200-300) was scored as positive. For ZEB2, SNAI2 and E-cadherin, scores of 0 and 1 (H-Score = 1-100) were considered negative and immunoreactivity of 2 (H-Score = 100-200) and 3 (H-Score = 200-300) was scored as positive. For VDR, all melanoma tumours presenting either a cytoplasmic or nuclear immunostaining in at least 25% of the neoplastic cells were scored as positive (1+).

2.2.5 Cell culture of normal melanocytes and melanoma cell lines

2.2.5.1 Recovery of cells from frozen storage

All melanoma cell lines and human epidermal melanocytes were retrieved from liquid nitrogen and immediately transferred to a 37°C water bath, until fully thawed by agitation. Then the cells were rapidly removed from ampoules in a class II safety cabinet and re-suspended in 10 ml of a relevant to each cell line pre-warmed media (described in section 2.1.4) supplemented with 10% FCS and Penicillin / Streptomycin antibiotic solution. SK-MEL-2, SK-MEL-5, RPMI-7951 and WM-266-4 were further supplemented with 1% NEAA and 1% NaP, and SK-MEL-28 with 1% NEAA. Epidermal melanocytes were resuspended in a bicarbonate buffered medium containing a mix of vitamins, minerals, inorganic salts, essential and non-essential amino acids, supplemented with antibiotics and growth supplements (described in section 2.1.4). The cells were centrifuged at 1000 rpm for 5min at room temperature and the pellets were resuspended in 5-10 ml of complete media. Finally, an appropriate number of cells was

seeded in 25 / 75 cm² flasks or 6 / 12 well plates and incubated at 37°C under 5% CO₂ in a humidified atmosphere, until passaging.

2.2.5.2 Passaging of normal melanocytes and melanoma cells

Both normal and melanoma cells were grown until reached 80-90% confluency and then passaged every 72 hr. To passage the cells, the appropriate culture medium was removed and each flask was washed with PBS and 3-5 ml of fresh sterile 1× Trypsin / EDTA (TE) solution was added. The flasks were then incubated at 37°C for 1-2 min until complete detachment of cells. Trypsin activity was terminated by addition of 5-10 ml pre-warmed complete media, and cells were transferred to a fresh 15 ml Falcon tube and centrifuged at 1000 rpm for 5 min. After centrifugation of cells, 2 ml of a cell suspension was used to seed a 75 cm² flask containing 10 ml of complete media.

2.2.5.3 Long term storage of cell cultures

Cells at the exponential growing phase (around $1-2 \times 10^6$ cells) were washed, trypsinised and centrifuged at 1000 rpm for 5 min. The resulting pellet was resuspended in 10% DMSO and FCS solution, and approximately 1×10^6 cells were transferred to a cryotube and stored initially at -80°C overnight (under isopropanol) and then to liquid nitrogen for later handling.

2.2.5.4 Treatment of HEMN with 1a, 25-Dihydroxyvitamin D3

For induction of VDR expression 1a, 25-Dihydroxyvitamin D3 (calcitriol, from Sigma-Aldrich) was used. Normal melanocytes were cultivated in Melanocyte Growth Medium in either 25 cm² flasks or 6 / 12-well plates. Semi-confluent cells were then incubated with calcitriol and culture medium at different concentrations (10^{-8} and 10^{-9} M) for 24, 48 and 72 hrs, without replacing the medium. Normal melanocytes incubated with culture medium and absolute ethanol served as controls

(untreated cells). Calcitriol stock solutions of 10 μM in absolute ethanol were stored at -20°C in the dark until needed for use.

2.2.5.5 Treatment of melanoma cell lines with pharmacological inhibitors

For inhibition of the ERK/MAPK signalling pathway, the U0126 was used. To make 10 mM stock solutions, 5 mg of U0126 (supplied as a lyophilized white powder) dissolved in 1.31 ml DMSO, aliquoted to avoid multiple freeze / thaw cycles and subsequent degradation of the inhibitor, and stored at -20°C until required. Melanoma cells were grown in appropriate complete medium in 75 cm^2 flasks until reached 60-70% confluency, at 37°C in a humidified atmosphere of 5% CO_2 . U0126 inhibitor was added at a dose of 10 μM directly to the culture complete medium of melanoma cells at different time points. Melanoma cells incubated with culture medium and DMSO served as controls (untreated cells). Similarly, a final concentration of 10 μM for PLX4720 and PD184352 was used for all treatments of melanoma cells. SB203580 and wortmannin were used at final concentrations of 10 μM and 1 μM respectively. For inhibition of JNK activation cells were treated with 10 μM of SP600125.

2.2.5.6 RNA interference experiments for A375 melanoma cells

When melanoma cultured cells, grown in 150 cm^2 flasks, had reached optimal density (70-80% confluency) were harvested using trypsin, transferred to a 1.5 ml fresh eppendorf tube and centrifuged at 3000 rpm for 2 min. The resulting supernatant was discarded and the cell pellet was resuspended in 1 ml PBS. Ten μl of cell suspension was then transferred to Coulter Counter vials and mixed with 10 ml of Isoton. Cell concentration was determined by using the Z2 Coulter counter (Beckman Coulter, UK). Six cm^2 dishes were pre-incubated in a humidified incubator (37°C , under 5% CO_2 in a humidified atmosphere) by filling the appropriate number of the dishes with 3 ml of RPMI 1640. The required number of cells (1×10^6 cells per sample) was centrifuged at

1000 rpm for 5 min at room temperature. The resulting supernatant was removed completely and cell pellets were carefully resuspended in 100 µl room temperature Amaxa Nucleofector[®] Solution V / sample, and combined with 100 nM / sample siRNAs or 2 µg pmaxGFP[®] Vector (Lonza, UK) or negative scramble (non-targeting) siRNA (Thermo Scientific, UK). Resulting cell suspensions were transferred to certified cuvettes, closed with the cap and inserted into Amaxa's Nucleofector[®] Cuvette Holder (Lonza, UK) applying program X-001. After transfection, cell suspensions were added immediately to approximately 500 µl of pre-equilibrated RPMI 1640 complete media, gently mixed and finally transferred into the pre-equilibrated 6 cm² dishes (final volume 3.5 ml media per dish). Cells were then incubated at 37°C under 5% CO₂ in a humidified atmosphere until required for assaying. Western blots were used to confirm siRNA-mediated gene knockdown. Details of siRNAs used for transient transfections of melanoma cells are shown in Table 2.7.

Table 2.7 - List of siRNAs used for transient transfections

Target name	siRNA sequence (sense strand)	Vendor	Reference
SNAI2 (#1)	5'- GGACCACAGUGGCUCAGAA(UU) - 3'	Sigma-Genosys	(Park et al., 2008b)
SNAI2 (#2)	5'- GCAUUUGCAGACAGGUCAA(UU) - 3'	Sigma-Genosys	(Tripathi et al., 2005)
ZEB1	5'- GGACUCAAGACAUCUCAGU(dTdG) - 3'	Donated by Dr. E Tulchinsky*	–
ZEB2	5'- GAACAGACAGGCUUACUUA(dTdT) - 3'	Donated by Dr. E Tulchinsky	–
TWIST1	ON-TARGET plus SMARTpool	Thermo Scientific	–
Fra-1 (#1)	5'- CACCAUGAGUGGCAGUCAG(dTdT) - 3'	Donated by Dr. E Tulchinsky	–
Fra-1 (#2)	ON-TARGET plus SMARTpool	Thermo Scientific	–

*Department of Cancer Studies and Molecular Medicine, Leicester University, UK

2.2.5.7 Luciferase reporter assays

For luciferase assays, 5×10^5 cells were seeded in 6 cm² dishes one day prior to transfections. A375P and A375M cells were transfected with 1 µg of either wild type pmiR luciferase reporter vectors (pMIR-REPORT, Invitrogen, UK) or with the vector containing 3'UTR of human *ZEB1* or *ZEB2* (a kind gift from Dr. E Tulchinsky) using Lipofectamine[®] 2000 (Invitrogen, UK) for 24 hrs. The efficiency of each transfection was monitored using 1 µg co-transfected β-galactosidase expression vector, pCMVβ-gal (Invitrogen, UK). Transfected A375 cells were treated with U0126 or MOCK-treated for further 24 hrs. Forty-eight hrs post transfection, cells were harvested, lysed and the luciferase activity was measured according to the manufacturer's instructions (Promega, Southampton, UK) with Sirius single tube luminometer (Titertek-Berthold, Pforzheim, Germany). All experiments were performed in triplicate and normalized to the activity of β-galactosidase.

2.2.5.8 Cell motility assays

Transfected A375 cells with siRNAs against ZEB1 and ZEB2 (section 2.2.5.6) were cultured for 48 hrs. Cells were fluorescently labelled with the lipophilic tracer 1,1'-Didodecyl-3,3,3',3'-tetramethylindocarbocyanine perchlorate [DiIC₁₂(3)] at a concentration of 10 µg/ml in phenol-free RPMI 1640 containing 1% FCS at 37°C (under 5% CO₂ in a humidified atmosphere) for 1 hr. Melanoma cells were then washed three times in PBS and phenol-free RPMI 1640 / 1% FCS was added for a further 1 hr. Finally, cells were harvested and counted in preparation for assaying.

The required number of FluoroBlokTM cell culture inserts with 8 µm fluorescence blocking polyethylene terephthalate (PET) membranes (BD Biosciences, UK) was placed into each well of a 24-well companion plate. Melanoma cells were resuspended in 200 µl of phenol-free RPMI 1640 / 1% FCS and added to the upper chambers at a density of 5×10^4 cells/insert. Seven hundred µl of RPMI 1640 / 10% FCS was used as a chemoattractant in the lower wells, while 2×10^4 cells were added to the control wells (no insert, 700 µl RPMI 1640 / 10% FCS). The migration assay was run for up to 72 hrs at 37°C under 5% CO₂ in a humidified atmosphere, and migrating cells were detected by a bottom-reading fluorescent plate reader (FLUOstar OPTIMA plate reader, BMG Labtech, UK) using excitation/emission wavelengths of 530/590 nm, with measurements taken every 2 hrs.

2.2.5.9 Sample preparation for Western blotting

For cell pellets, cells were harvested and centrifuged at 1000 rpm for 5 min. The supernatant was then removed and the cell pellet resuspended in appropriate pre-warmed complete medium, transferred to 1.5 ml fresh eppendorf tubes and centrifuged for 13,000 rpm for 2 min. The resulting supernatant was discarded and cell pellets were stored at -20°C until required.

2.2.6 Western blotting

2.2.6.1 Protein extraction from melanoma and HEM cell lines

200-500 µl of 1×Laemmli lysis buffer (100 mM Tris-HCl, pH 6.8, 20% glycerol and 2% SDS) were added to each sample according to size pellet. Samples were then denatured by heating at 95°C for 5 min, cooled down for 2 min, sonicated for approximately 10 seconds (Amplitude did not exceed 10 microns) and centrifuged for 13,000 rpm for 1 min. The resulting solutions were then stored at -20°C until required.

2.2.6.2 Protein quantification

Protein quantification in each sample was carried out using the BCA protein assay Kit (Thermo Scientific-Pierce, Rockford, USA). Briefly, a working solution, with an apple green colour, was prepared by mixing 50 parts of reagent A (carbonate buffer containing BCA) with 1 part of BCA reagent B (cupric sulphate solution) (50:1, reagent A:B), for example 5 ml of reagent A with 100 µl of reagent B. Then, 5 µl of a protein solution containing 1×Laemmli lysis buffer was added to 500 µl of the BCA working solution and the resulting solution was briefly vortexed and incubated either for 5 min at 37°C incubator (5% CO₂ in a humidified atmosphere) or left at room temperature for 10 min. The absorbance at 562 nm was measured after the zero had been set against 500 µl of BCA reagent containing 5 µl of the same buffer (1×Laemmli) as the protein solution. The protein concentration of samples was finally calculated by reference to a standard curve constructed from absorbance against known protein concentrations for a series of BSA standards (2 µg/µl) (Thermo Scientific-Pierce, Rockford, USA).

2.2.6.3 Sodium dodecyl sulphate polyacrylamide gel electrophoresis (SDS-PAGE)

Slab minigels (10 cm × 7 cm × 0.75 cm) were poured between glass plates of 1.5 mm thickness. An example of the required volumes of each solution to achieve 10% resolving and 5% stacking gels is shown in Table 2.8. Polymerisation was initiated by addition of 10% APS and 0.1% TEMED to each gel. The forming solution was mixed gently, poured into a Bio-Rad cassette and 150 µl of 99% IMS was layered over the top of the acrylamide solution to prevent evaporation and the gel was left for 30-45 min to polymerise. After the gel had set the IMS was removed and washed briefly in water before the stacking gel was poured. The stacking gel was loaded and left for further 30-45 min to set. Finally, a gel comb inserted and left to set at room temperature.

10-25 µg of total protein per sample was mixed in a ratio of 1:10 with 5× loading buffer, containing fresh 2 mM β-mercaptoethanol, 0.125 % w/v bromophenol blue and 5× Laemmli buffer. Samples were then denatured at 95°C for 5 min and loaded into each well. Five µl of a protein weight marker (Precision Plus dual Colour, BioRad, UK) was also loaded into a separate well. Electrophoresis was performed in running buffer containing 25 mM Tris-HCl, 190 mM glycine and 0.1% w/v SDS, at 120 Volts and once the bromophenol blue dye front had run the required distance, the gel was used for immunoblotting.

Table 2.8 - Required volumes for 10% resolving and 5% stacking gels

Solution	10% resolving gel (mL, 2 gels)	5% stacking gel (mL, 2 gels)
30% acrylamide / bis acrylamide solution	5	1.7
Gel buffer (1.5 Tris-HCl, pH 8.8 for resolving and 6.8 for stacking gels)	3.8	1.25
10% w/v SDS	0.15	0.1
10% APS	0.15	0.1
TEMED	0.006	0.01
Sterile H ₂ O	5.9	6.8

2.2.6.4 Protein transfer and immunological detection of PVDF immobilised proteins

Transfer of polypeptides on either PVDF or nitrocellulose membranes was performed as previously described (Towbin et al., 1979). Protein fractionated on an SDS-PAGE gel was initially removed and washed by immersing the gel in transfer buffer (25 mM Tris-HCl, 190 mM glycine and 20% (v/v) methanol) for 2 minutes. Then the gel was placed onto a PVDF membrane, previously wetted with methanol for few seconds, and soaked in transfer buffer for 1 minute. The SDS-PAGE gel and PVDF membrane were then sandwiched between two pieces of pre-wetted in transfer buffer Whatmann 3MM filter papers and fiber pads (equally in size to the gel), assembled into a BioRad gel holder cassette, with the gel facing the cathode and the membrane the anode, before transferred in a Trans-Blot wet electrophoresis transfer tank (BioRad, UK). Protein electrophoresis was performed in transfer buffer at 25 V overnight at RT or at 100 V for 1 hr at 4°C. PVDF membranes containing immobilised proteins were removed from the cassette and blocked by incubation in blocking solution [5% Marvel milk powder in TBS-T (0.1% v/v Tween-20, 1×TBS (150 mM NaCl, 10 mM Tris-HCl, pH 7.5))] for 1 hr at RT. Membranes were then probed with the indicated primary antibodies (Table 2.9) in TBS-T-Milk blocking solution for 1 hour at room temperature with shaking. The blots were washed 4 times in TBS-T at RT for 4 min and the antibody binding was detected by using the appropriate horseradish peroxidase (HRP)-conjugated secondary antibodies (Dako, UK) in blocking solution for 1 hr at RT (Table 2.9). The blots were further washed 4 times for 4 minutes with TBS-T and peroxidase activity was detected by incubating the membranes either for 1 min, when using enhanced chemiluminescent substrates, or 5 min with extended duration substrates (Pierce, UK). Finally, light emission was visualised using X-ray film (General Electric, UK) at different exposure time periods.

Table 2.9 - List of primary and secondary antibodies used for immunoblotting

Primary antibody	Dilution	Target MW (kDa)	Vendor	References
ZEB1 (H-102/rabbit polyclonal)	1:2000	~200	Santa Cruz Biotechnology	(Sayan et al., 2009)
ZEB2 (clone 1C6/mouse)	1:5 (Hybridoma supernatant)	~190	Donated by Dr. AE Sayan	(Oztas et al., 2010, Sayan et al., 2009)
SNAI1 (clone EC3/mouse)	1:100	~30	Donated by Dr. A García De Herreros	(Franci et al., 2006)
SNAI2 (clone C19G7/rabbit)	1:200	~30	New England Biolabs	(Joost et al., 2012)
TWIST1 (clone 2C1a/mouse)	1:100	~21	Abcam	(Ansieau et al., 2008)
E-cadherin (clone 36/mouse)	1:2000	~120	BD Transduction Laboratories™	(Gross et al., 2009)
VDR (clone D-6/mouse)	1:2000	~50	Santa Cruz Biotechnology	(Wang et al., 2010)
p-JNK (Thr183/Tyr185, clone 81E11/rabbit)	1:1000	~46, 54	New England Biolabs	(Biton and Ashkenazi, 2011)
p-c-Jun (Ser63, clone 54B3/rabbit)	1:1000	~48	New England Biolabs	(Lan et al., 2012)
pAKT (Thr308, clone C31E5/rabbit)	1:1000	~60	New England Biolabs	(Guertin et al., 2009)
pFra-1 (Ser265/rabbit polyclonal)	1:1000	~40	New England Biolabs	(Sayan et al., 2012)
p-p38 (Thr180/Tyr182, clone 12F8/rabbit)	1:1000	~43	New England Biolabs	(Miyaji et al., 2009)
pERK1/2 (Thr202/Tyr204, clone 197G2/ rabbit)	1:1000	~42, 44	New England Biolabs	(Fehrenbacher et al., 2008)
p-MAPKAPK2 (Thr334, clone 27B7 / rabbit)	1:1000	~49	New England Biolabs	(Carrozzino et al., 2009)
Cyclin D1 (H-295 / rabbit polyclonal)	1:500	~37	Santa Cruz Biotechnology	(Mejlvang et al., 2007)
α -Tubulin (clone B-5-1-2 / mouse)	1:10000	~50	Sigma-Aldrich	(Vergara et al., 2011)
Secondary antibody				
Goat Anti-Rabbit	1:2500	–	Dako	–
Rabbit Anti-Mouse	1:2500	–	Dako	–

2.2.7 Statistical analysis

For statistical analysis of the IHC results, the effect of tumour type (e.g. metastasising and no-metastasising primary tumours) was investigated by the Kruskal-Wallis one-way analysis of variance (ANOVA) (independent samples) or Friedman test (matched samples). The effect of tumour site within individuals was investigated by the Wilcoxon Signed Rank Test (Unistat Statistical Package, version 5.0, Unistat, UK). Trend analysis for independent and matched samples was investigated by the Jonckheere-Terpstra and Page's L tests respectively using the Statistical Package for the Social Sciences (SPSS), version 20.0, (IBM, USA). Correlations were investigated by Spearman's rho test and inter-relationships by linear regression analysis (Stata software package, version 7.0, Stata Corporation, Texas, USA). Effects on metastasis were investigated by Kaplan-Meier analysis of H-Scores (SPSS), which were compared by the log-rank test and by univariate and multivariate Cox regression (SPSS). To identify patient groups distinguished by patterns of MR-EMT immunostaining a two-step cluster analysis was performed (SPSS). In regards to the *in vitro* assays, results were analyzed by repeated-measures two-way ANOVA followed by Bonferroni's post- tests (GraphPad Prism Software Inc., version 5, San Diego, CA). All experiments were representative of at least three individual experiments, unless otherwise stated. P values of <0.05 were considered statistically significant.

3 Regulation of MR-EMT by the RAS-RAF MAPK pathway

3.1 Introduction

Stimulation of the RTK/NRAS/BRAF/MEK/ERK signalling stream is central in the majority of melanomas. However, increasing evidence suggests that other MAPK signalling cascades play an important role as well in at least a subset of melanomas (section 1.2.3 , Figures 1.3 and 3.2).

Initial preliminary unpublished data obtained from Dr. E Tulchinsky (Department of Cancer Studies and Molecular Medicine, Leicester University, UK) (Figure 3.1) has indicated that a small number of *BRAF* and *NRAS* mutated melanoma cell lines express both the embryonic transcription factors ZEB1 and ZEB2, which are responsible for the execution of EMT embryonic genetic programs. EMT has been implicated in metastatic dissemination of different carcinoma types and also in the progression of melanoma. In addition, ZEB1 was correlated with loss of E-cadherin expression (Figure 3.1).

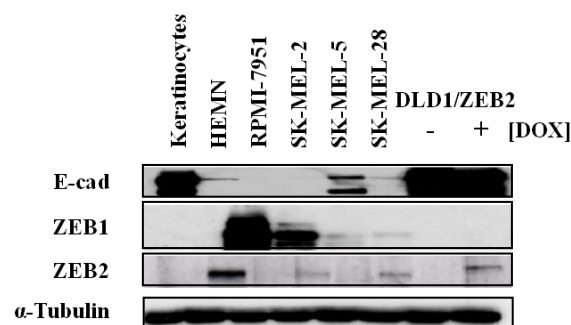


Figure 3.1 - Protein analysis of MR-EMT in different melanoma cell lines, HEMN and keratinocytes. The colon cancer cell line DLD1 with Tet-on DOX-regulated ZEB2 expression was constructed. Cells were cultured with or without DOX for 48 hrs.

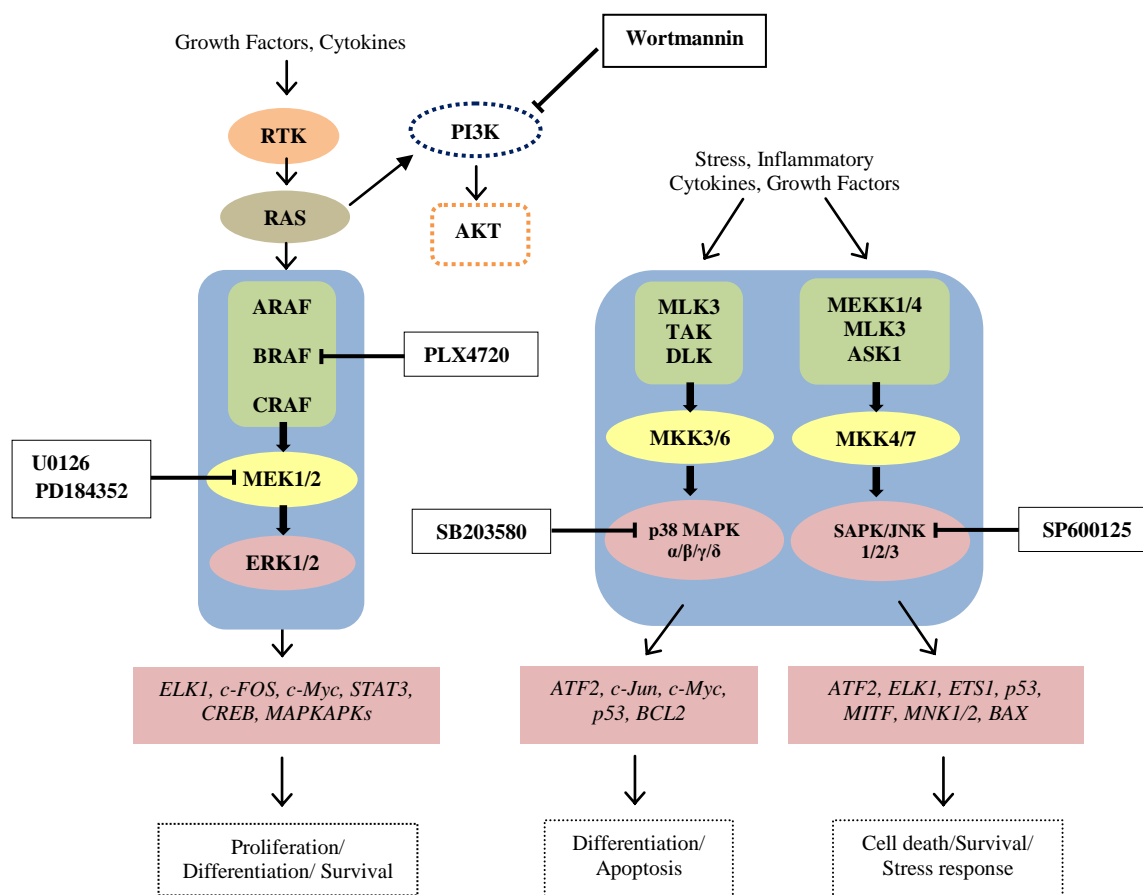


Figure 3.2 - Pharmaceutical agents inhibiting MAPK-signalling pathways used in this study.

Pharmaceutical agents known to inhibit various components of MAPK signalling pathways and used in this study are listed in the white boxes. Concomitant activation of both Ras and PI3K/AKT pathways is commonly seen in MMs. Upon stimulation, ERK1/2, p38 and JNK phosphorylate a large number of transcription factors (shown in pink boxes). Other MAPK pathways (p38, PI3K and JNK) are also depicted. Figure redrawn from Lopez-Bergami, 2011. Abbreviations: *ELK1*, member of ETS oncogene family; *c-FOS*, FBJ murine osteosarcoma viral oncogene homolog; *c-Myc*, v-myc myelocytomatosis viral oncogene homolog; *STAT3*, signal transducer and activator of transcription 3 (acute-phase response factor); *CREB*, cAMP responsive element binding protein; *MAPKAPK*, mitogen-activated protein kinase-activated protein kinase; *ATF2*, activating transcription factor 2; *c-Jun*, jun proto-oncogene; *ETS1*, v-ets erythroblastosis virus E26 oncogene homolog 1; *MNK*, MAP kinase interacting serine/threonine kinase 1; *BAX*, BCL2-associated X protein.

3.2 Aims and Objectives

The main aim of this chapter was to determine which MR-EMT proteins are expressed in melanoma and how they are regulated in cultured melanoma cells.

The specific objectives for this chapter were as follows:

- Is there a link between the oncogenic NRAS/BRAF MAPK pathway and expression of MR-EMT proteins in melanoma cells? Are other MAPK signalling cascades (p38, PI3K and JNK) important in regulating MR-EMT expression in melanoma cells? To address these questions, potent kinase and oncogene inhibitors were applied to melanoma cultures.
- To investigate at which level (transcriptional or posttranslational) the effect of BRAF and MEK inhibition regulates the MR-EMT by qRT-PCR assays and western blotting after addition of U0126.
- To test whether MEK signalling influences the protein stability of MR-EMT. For this purpose, cycloheximide, MG132 and LiCl treatments of melanoma cells were carried out.
- To assess interactions between MR-EMT by siRNA mediated knockdowns and treatment of melanoma cells with the MEK inhibitor U0126.
- To test whether Fra-1 links BRAF-MAPK signalling with ZEB1 and ZEB2 proteins by siRNA experiments and western blotting.
- To assess the effect of miR on MR-EMT in melanoma cultures by siRNA-mediated knockdowns of MR-EMT and qRT-PCR assays.

3.3 Results

3.3.1 *MR-EMT expression in melanoma cell lines and melanocytes*

Protein expression levels of MR-EMT in a panel of established malignant melanoma cell lines, with either *BRAF* or *NRAS* mutations as well as in human epidermal melanocytes, were measured by western blotting (Figure 3.3). RT-112 urinary bladder carcinoma cell line was used as a negative control for MR-EMT proteins apart from SNAI2. Osteosarcoma cells (HOS) were used as a positive control as it has been shown to express ZEB1/2, SNAI1/2 and TWIST1 (Sayan et al., 2009). Expression of constitutive-active Snail-8SA was induced in HEK293-FlpInTRex-Snail-8SA cells, HEK-293 cells expressing Snail under the control of the tetracycline-inducible system, by adding 1 µg/ml DOX to the culture medium and was used as a positive control for SNAI1 expression (Grotegut et al., 2006). Cell cultures of human primary neonatal melanocytes were positive for ZEB2 and SNAI2, but negative for ZEB1 and TWIST1. Whereas *BRAF* mutated melanoma cell lines expressed either ZEB2 or both ZEB proteins, TWIST1 expression was correlated with ZEB1. By contrast, ZEB2 protein expression was detected only in one mutant *NRAS* cell line (IPC-298). All melanoma cell lines expressed different levels of SNAI2, and SNAI1 was expressed only in a small proportion of the cell lines (WM-266-4, A375P and A375M). Of note, the expression level of SNAI1 was higher in the metastatic A375M cell line in comparison with the parental non invasive A375P (Figure 3.3).

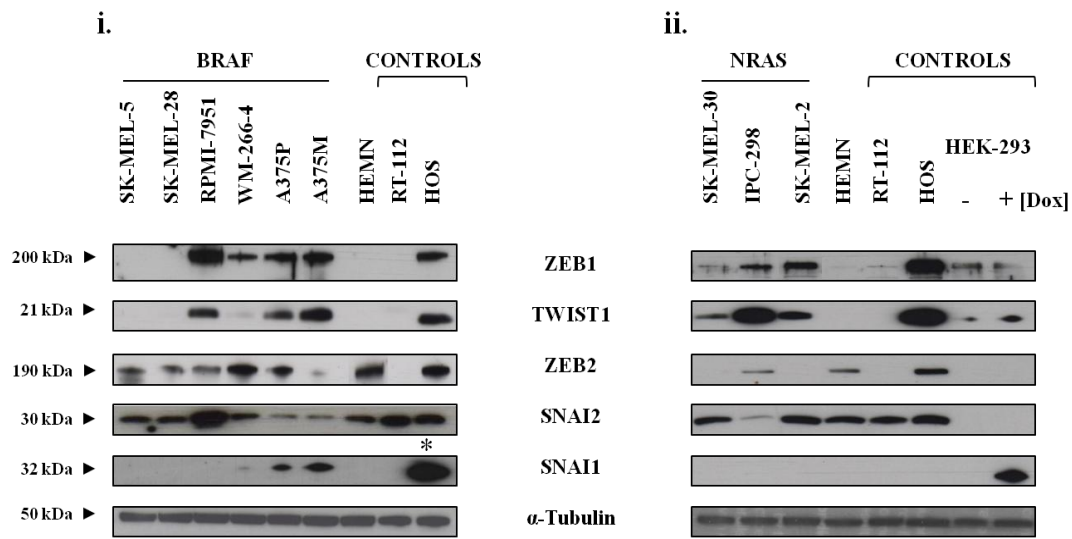


Figure 3.3 - Western blot analysis of the expression of MR-EMT proteins in a panel of melanoma cell lines. (i) *BRAF* and (ii) *NRAS* mutated melanoma cell lines and HEMN. HEK-293 cells were used as a negative control for SNAI2. To control for equal loading blots were probed with anti- α -Tubulin antibody. (*) HEK-293 cells expressing Snail.

3.3.2 The effect of *BRAF*^{V600E} and MEK inhibitors on the expression of MR-EMT in melanoma cells

Treatment of A375P cells with PLX4720, a potent and selective mutant *BRAF* inhibitor, and MEK inhibitors, PD184352 and U0126, effectively inhibited pERK1/2 signalling (Figure 3.4). By contrast, PLX4720 treatment of mutant *NRAS*^{Q61L} IPC-298 cell line was found to increase ERK1/2 phosphorylation after 24 hours. This observation confirmed that inhibition of *BRAF*^{WT} in *RAS* mutant cancer cells enhances MEK-ERK hyperactivation (Heidorn et al., 2010). In addition, treatment of A375P cells with PLX4720 or MEK inhibitors PD184352 and U0126 downregulated ZEB1 and TWIST1, but upregulated ZEB2 and SNAI2. Likewise, in *NRAS* mutated IPC-298 cells expression levels of ZEB1/TWIST1 or ZEB2/SNAI2 were down- or upregulated respectively, when MEK was inhibited. However, it was noted that rebound pERK1/2 activity after PLX4720 treatment in IPC-298 cells led to increased expression of ZEB1

and TWIST1 and downregulation of ZEB2 and SNAI2. Thus, inhibition of RAS-RAF signalling showed a clear tendency of bringing MR-EMT expression to a pattern observed in normal melanocytes ($\text{ZEB2}^{\text{high}}\text{SNAI2}^{\text{high}}/\text{ZEB1}^{\text{low}}\text{TWIST1}^{\text{low}}$).

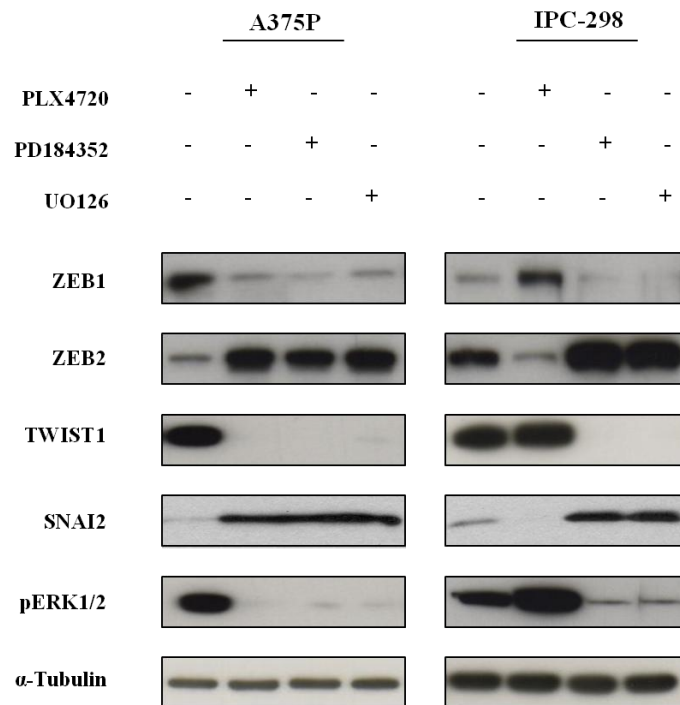


Figure 3.4 - The effect of BRAF and MEK inhibitions on the expression of MR-EMT in A375P and IPC-298 cells. Melanoma cells were treated with DMSO (-), 10 μM PLX4720, 10 μM PD184352 and 10 μM UO126 for 24 hours. The efficacy of the inhibitors was monitored by pERK1/2 detection.

3.3.3 The effect of p38 / JNK and PI3K inhibitors on the expression of MR-EMT in melanoma cells

To test whether key constitutive active signal transduction pathways in melanoma other than the MAPK-ERK contributed to the regulation of MR-EMT, melanoma cells were treated with a panel of pharmacological inhibitors. The efficacy of the p38-MAPK pathway inhibitor SB203580, the c-Jun N-terminal kinase (JNK) SP600125 inhibitor and the PI3K inhibitor Wortmannin, in inhibiting their target pathways, was validated by western blotting analyses for total and phosphorylated MAPKAPK-2 (a direct target of p38 MAPK), c-Jun (regulated by phosphorylation at Ser63 and Ser73 through SAPK-JNK) and AKT respectively (Figures 3.5-3.7).

As previously documented (Estrada et al., 2009), simultaneous activation of both ERK and p38 pathways is unique to melanomas. A375P and A375M cells had not only high ERK activity but also elevated p38 kinase activity (Figure 3.5). Inhibition of melanoma cell lines with SB203580 alone for 24 hours yielded similar expression of EMT regulators following treatment with the specific MEK inhibitors U0126 and PD184352 ($\text{ZEB1}^{\text{low}}/\text{TWIST1}^{\text{low}}/\text{ZEB2}^{\text{high}}/\text{SNAI2}^{\text{high}}$) (Figure 3.4).

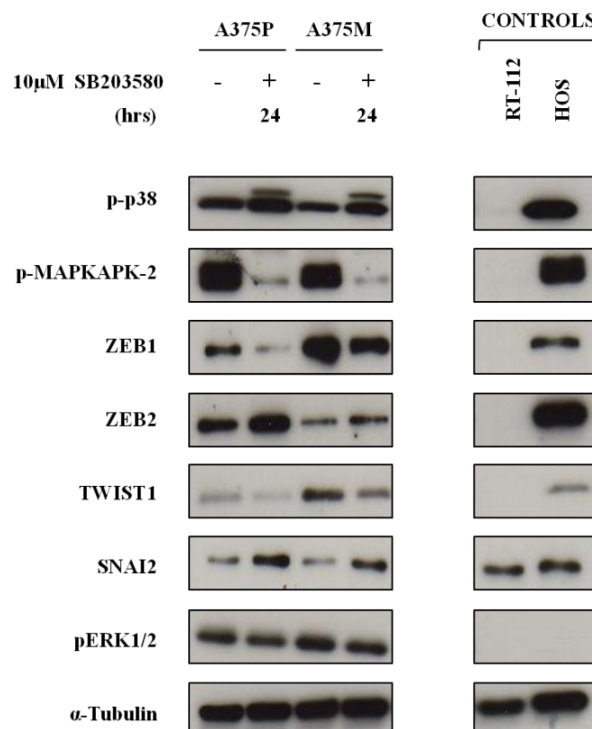


Figure 3.5 - The effect of SB203580 inhibitor on MR-EMT in A375P and A375M melanoma cell lines. Melanoma cells were treated with 10 µM SB203580 (p38 inhibitor) for 24 hrs and their efficacy was monitored by p-MAPKAPK-2 detection.

To determine the implication of JNK signalling pathway in EMT repressors in melanoma, A375P and A375M cells were treated with the JNK inhibitor SP600125 (10 µM) for 24 hours (Figure 3.6). Inhibition of either A375P or A375M cells resulted in a minor augment of p-JNK and ZEB1 protein expression, however SP600125 efficacy could not be assessed with certainty due to undetectable protein levels of p-c-Jun (Ser63) in these cells. As shown in Figure 3.6 there was no effect of JNK inhibition on the expression levels of ZEB2, SNAI2 and TWIST1.

Finally, potential contribution of PI3K pathway in MR-EMT in melanoma was assessed with the PI3K inhibitor wortmannin (1 µM) (Figure 3.7). MR-EMT proteins did not appear to be affected by pAKT depletion in melanoma cell lines tested. Of note, wortmannin efficacy could not be assessed with certainty in IPC-298 and A375M cells due to undetectable basal levels of pAKT (Thr308) in these cells. In addition,

combination of PI3K (wortmannin, 1 μ M) and MEK (U0126, 10 μ M) inhibitors significantly induced ZEB2 and decreased ZEB1 protein levels in melanoma cells, suggesting that MR-EMT expression was affected only after ERK-MAPK pathway inhibition.

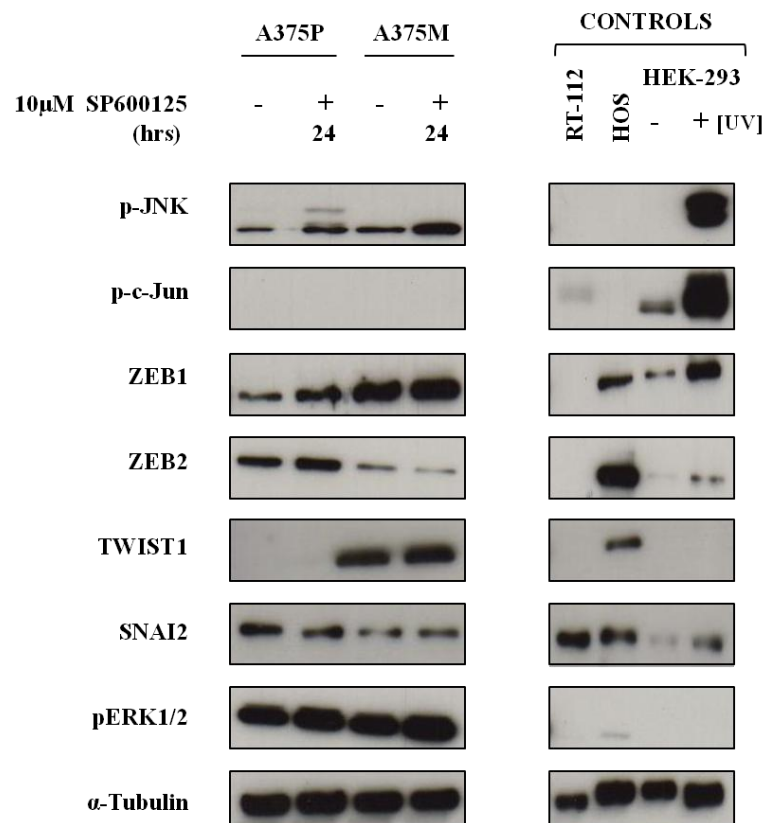
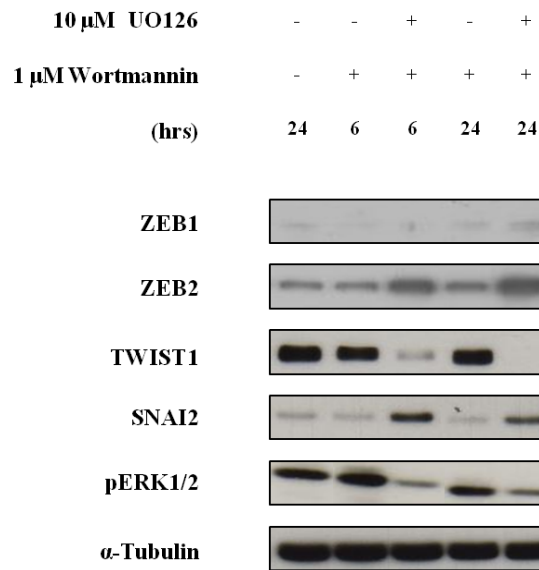
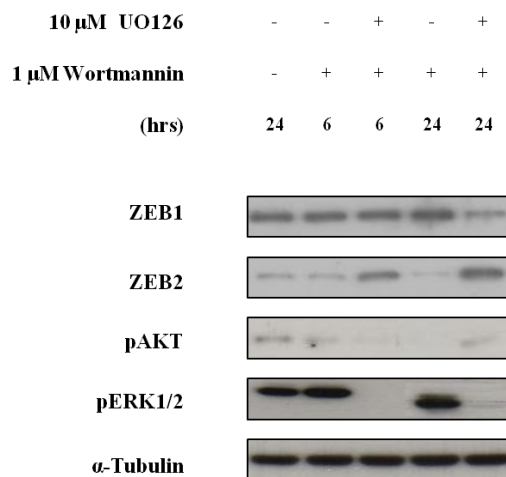


Figure 3.6 - The effect of SP600125 inhibitor on MR-EMT in A375P and A375M melanoma cell lines. Melanoma cells were treated with 10 μ M SP600125 (JNK inhibitor) for 24 hrs and their efficacy was monitored by p-c-Jun detection. Total cell extracts from HEK-293 cells, prepared without treatment, served as a negative control. HEK-293 cells treated with UV light served as a positive control.

i. IPC-298



ii. A375P



iii. A375M

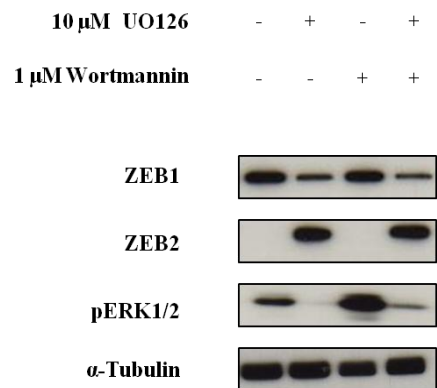


Figure 3.7 - The effect of the PI3K inhibitor wortmannin on MR-EMT factors in melanoma cell lines. (i) IPC-298, (ii) A375P and (iii) A375M cells were cultured with wortmannin (1 μ M) for different times and also treated with U0126 (10 μ M). A375M cells were treated with U0126 and wortmannin for 24 hrs. Protein lysates were analysed by western blotting with the indicated antibodies. To control U0126 treatments pERK1/2 antibody was used.

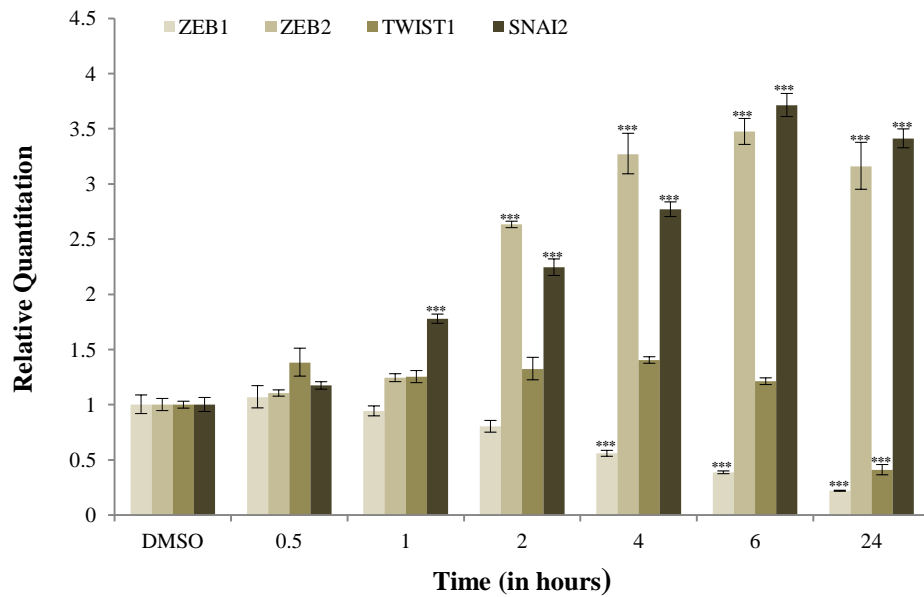
3.3.4 The kinetics of MR-EMT modulation in melanoma cells treated with U0126

To further investigate the contribution of the BRAF-MEK pathway to the regulation of MR-EMT in melanoma, A375P and A375M cells were treated for different time periods (0.5 to 24 hours) with 10 μ M U0126 (Figures 3.8 and 3.9). Transcript levels of ZEB1, ZEB2, SNAI2 and TWIST1 were determined by real time qRT-PCR using the TaqMan system with specific gene expression assays (Chapter 2, Table 2.2). Real time qRT-PCR analysis showed that the UBC Ct values obtained for A375P and A375M remained unchanged before and after U0126 treatment (Ct average \sim 17). Relative expression of MR-EMT was normalized to endogenous control gene UBC. Untreated A375P and A375M cells (average Ct values after 0.5 and 24 hours) were used as calibrators for each separate run. The fold-change of MR-EMT compared to UBC for each sample was measured against the expression level of the calibrator (RQ=1).

The kinetics of upregulation of SNAI2 and ZEB2 after U0126 treatment in A375P cells showed a maximum fold change by 3.7 and 3.4 respectively after 6 hours compared to the untreated melanoma cells (Figure 3.8-i). Increased expression levels of SNAI2 and ZEB2 were observed as early as 1 and 2 hours respectively after exposure to U0126 ($P<0.001$ in both, two-way ANOVA / Bonferroni post-test). In contrast, ZEB1 and TWIST1 mRNA expression levels were significantly decreased after 4 and at 24 hours respectively after U0126 addition ($P<0.001$ in both, two-way ANOVA / Bonferroni post-test). Furthermore, downregulation of ZEB1 and TWIST1 after U0126 treatment indicated a maximum fold change by 0.2 and 0.4 respectively after 24 hours compared to the untreated melanoma cells (Figure 3.8-i).

In A375M cells, U0126 suppressed ZEB1 and TWIST1 expression by 0.28 and 0.3-fold respectively after 24 hours (Figure 3.9-i). On the contrary, MEK1/2 depletion has induced SNAI2 and ZEB2 expression by 3 and 4-fold respectively after 6 hours. In addition, kinetic analysis showed that U0126 treatment significantly inhibited ZEB1 and TWIST1 after 4 ($P<0.05$, two-way ANOVA / Bonferroni post-test) and 24 hours ($P<0.01$) respectively, but induced SNAI2 and ZEB2 mRNA expression after 4 ($P<0.01$) and 2 hours ($P<0.05$) respectively. Of note, activation of ZEB2 and SNAI2 in both cell lines preceded the downregulation of ZEB1 and TWIST1. Similar kinetics was observed when protein expression of MR-EMT was analysed by immunoblotting (Figures 3.8-ii and 3.9-ii). However, transcriptional effects of U0126 on SNAI2 and TWIST1 were not as substantial as the effects on protein levels.

i.



ii.

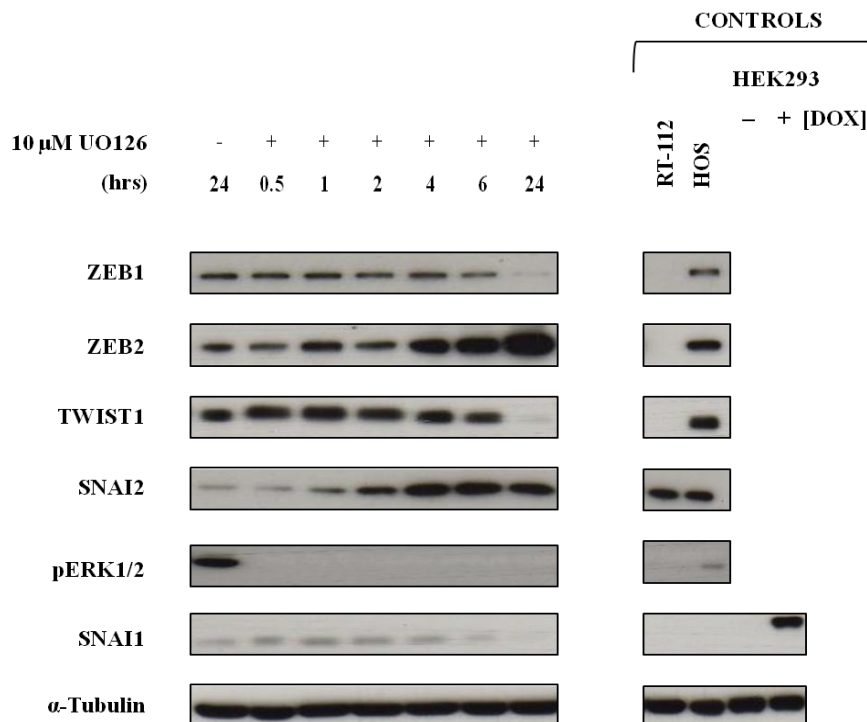
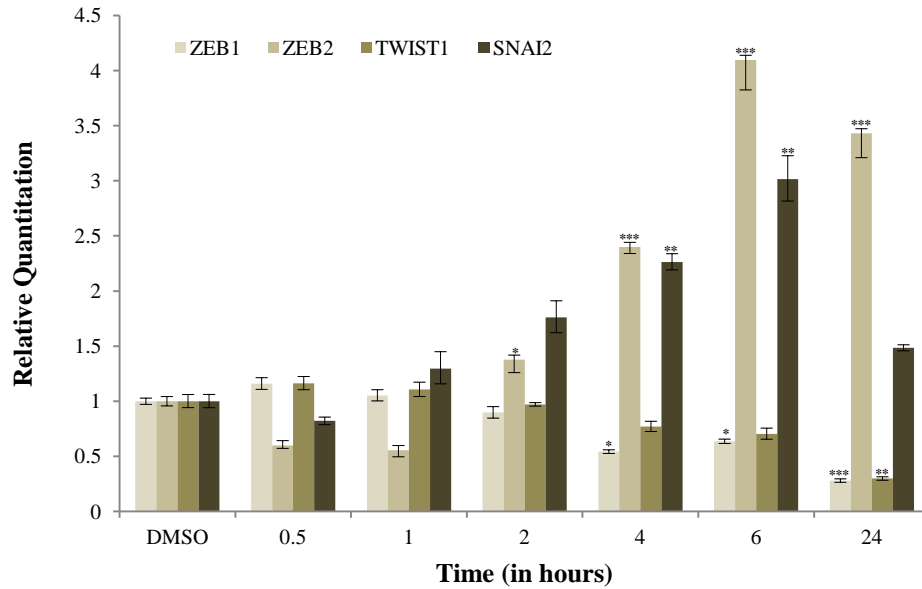


Figure 3.8 - The kinetics of MR-EMT modulation in A375P treated with U0126. Melanoma cells were treated with U0126 (10 μM) for indicated intervals and the expression of MR-EMT was analysed by (i) qRT-PCR with gene specific primers and (ii) western blotting. Real time qRT-PCR assays were performed in triplicate wells. Graphs represent the mean values of the relative transcript levels and error bars represent the standard error of the mean (mean ± SD) from three independent assays. Data was analysed by two-way ANOVA with Bonferroni post-tests. *** denote significant difference between untreated (DMSO) and treated with U0126 A375P cells (P<0.001). For all western blotting experiments melanoma cells incubated with DMSO served as controls (untreated cells). Inhibition of ERK1/2 phosphorylation by U0126 was confirmed by using an anti-pERK1/2 antibody. Equal loading was confirmed by α-Tubulin.

i.



ii.

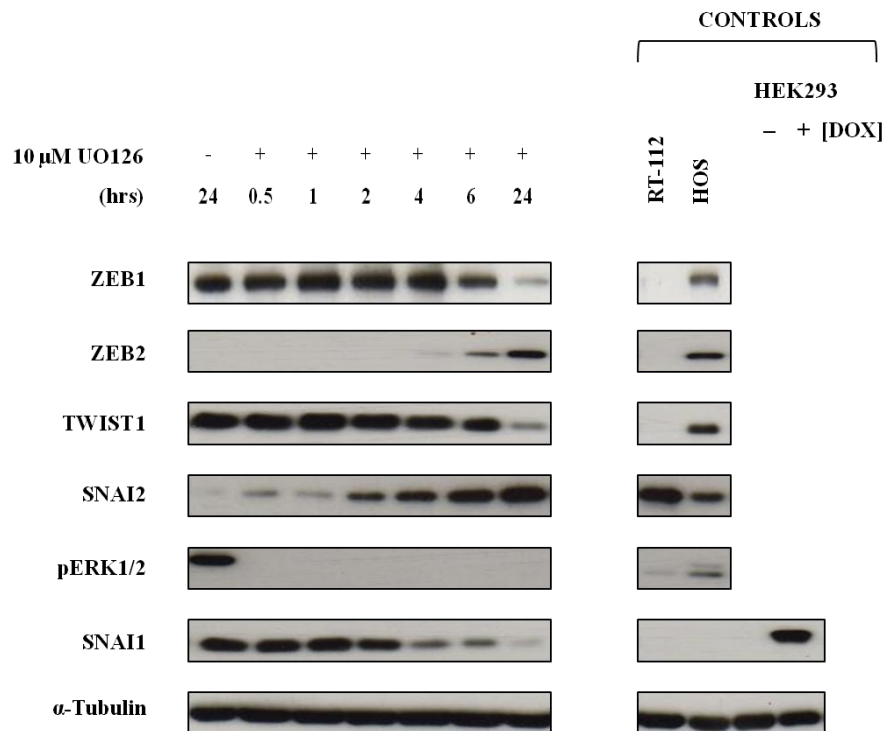


Figure 3.9 - The kinetics of MR-EMT modulation in A375M treated with U0126. Melanoma cells were treated with U0126 (10 μM) for indicated intervals and the expression of MR-EMT was analysed by (i) qRT-PCR with gene specific primers and (ii) western blotting. qRT-PCR assays were performed in triplicate wells. Graphs represent the mean values of the relative transcript levels and error bars represent the mean ± SD from three independent assays. Significant difference compared to untreated A375M cells was determined by two-way ANOVA followed by Bonferroni post-tests (*P<0.05; **P<0.01; ***P<0.001). For all western blotting experiments melanoma cells incubated with DMSO served as controls (untreated cells). Inhibition of ERK1/2 phosphorylation by U0126 was confirmed by using an anti-pERK1/2 antibody. Equal loading was confirmed by α-Tubulin.

3.3.5 Does MEK signalling influence MR-EMT protein stability?

Regulation of TWIST1 and SNAI2, but not ZEB1 or ZEB2, occurred also on the level of protein stability. The effect of cycloheximide (CHX), a translational inhibitor, on the MR-EMT stability was examined using the metastatic A375 melanoma cell line. ZEB1 and ZEB2 appeared to be stable and their stability was unaffected by MEK inhibition (Figure 3.10-i). On the contrary, treatment of the A375M cells with both CHX and U0126 led to increased SNAI2 protein stability, but TWIST1 was markedly destabilised. Consistently, ZEB1 and ZEB2 proteins were insensitive to the proteasomal inhibitor MG132, whereas SNAI2 and TWIST1 were degraded via a proteasome pathway (Figure 3.10-ii). The amount of TWIST1 was clearly increased in melanoma cells pre-treated with LiCl (a potent GSK-3 β inhibitor) indicating that GSK-3 β may promote TWIST1 degradation in melanoma cells. Treatment of melanoma cells with both LiCl and MG132 stabilised SNAI2, as well as SNAI1, indicating that proteasomal degradation and GSK-3 β -dependent phosphorylation were involved in the regulation of SNAI1 and SNAI2 (Figure 3.10-ii). Finally, decreased expression of ZEB1 and ZEB2 proteins after combined addition of LiCl and MG132 (24 hrs, +/- U0126) may be explained, at least in part, by low viability of melanoma cells.

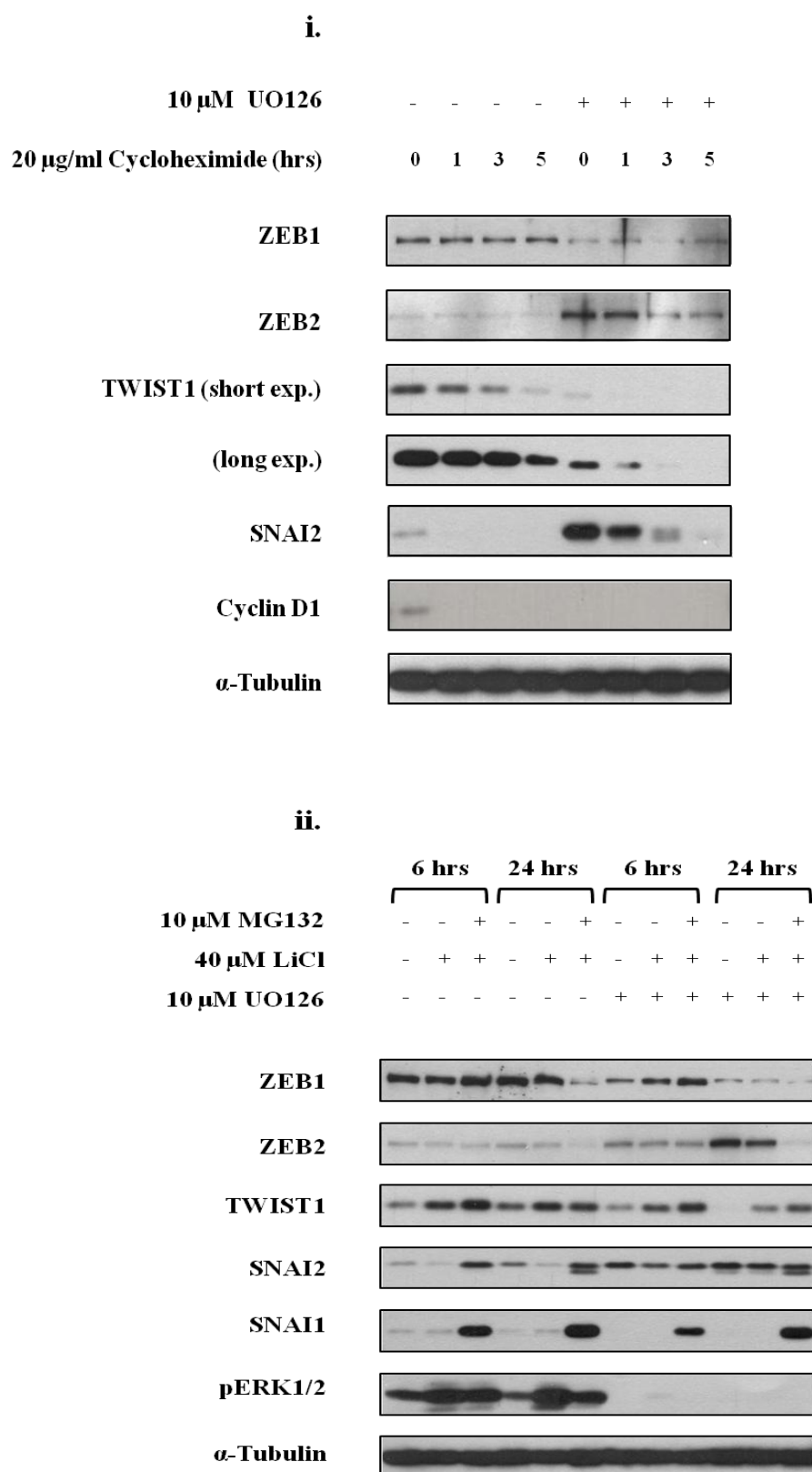


Figure 3.10 - Regulation of MR-EMT on the level of protein stability in melanoma cells.
 (i) A375M cells were cultured with or without UO126 for 24 hours and then treated with cycloheximide for different times. To control cycloheximide treatment a short-lived protein (cyclin D1) was used. (ii) A375M cells were treated with UO126, the proteosomal inhibitor MG132, GSK-3 β inhibitor LiCl or left untreated for 6 and 24 hours. Protein lysates were analysed by western blotting with the indicated antibodies. All blots were kindly provided by Dr. GJ Browne (Department of Cancer Studies and Molecular Medicine, University of Leicester, UK).

3.3.6 *ZEB1 expression is repressed by ZEB2*

To further investigate the functional relevance of MEK-dependent alterations in MR-EMT expression pattern to melanoma progression ZEB1, ZEB2, SNAI2 and TWIST1 were specifically and individually depleted in A375M cells by transfection with short-interfering RNAs. The efficacy of each knockdown was verified in A375P and A375M cell lines by western blotting 72 (for SNAI2 and TWIST1) and 96 hours (for ZEB1 and ZEB2) after transfection (Figure 3.11). SNAI2 knockdown was tested with two different siRNAs. SNAI2-2 and combined siRNAs had the greatest effect (Figure 3.11).

In A375M cells, siRNA mediated knockdown of either SNAI2 or TWIST1 had no effect on ZEB1, ZEB2 and E-cadherin protein expression levels (Figure 3.12-i/ii). In contrast, coexposure of melanoma cells to TWIST1 siRNA and MEK inhibitor U0126 increased ZEB2 and SNAI2, but reduced ZEB1 protein level (Figure 3.12-ii). Knockdown of SNAI2 combined with U0126 showed no difference in the expression of TWIST1, ZEB1 and ZEB2 (Figure 3.12-i). Finally, ZEB2 depletion reproducibly augmented ZEB1 protein levels (Figure 3.13-i) and markedly attenuated downregulation of ZEB1 by MEK inhibition (Figure 3.13-ii). ZEB1 and ZEB2 knockdowns did not affect SNAI2 and TWIST1 levels in metastatic melanoma A375M cells (Figure 3.13-i).

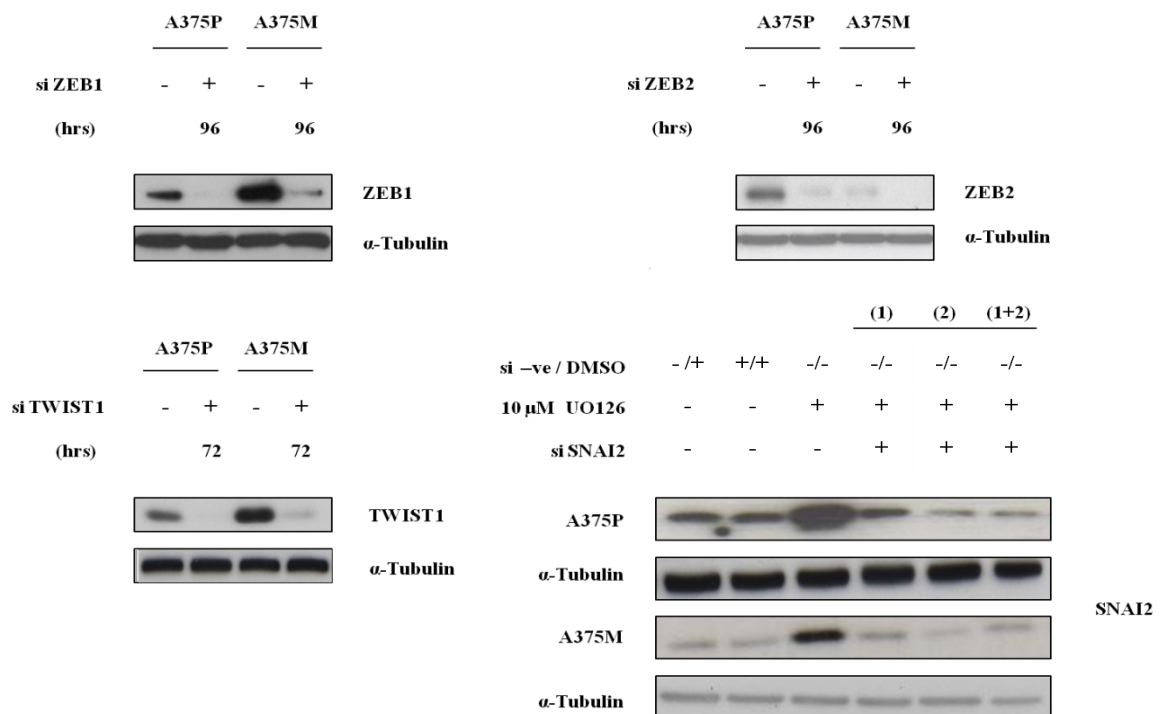


Figure 3.11 - Post-transfection efficiency analysis of MR-EMT by western blotting. To enhance target specificity for TWIST1 a mixture of four siRNAs (SMARTpool) was used. Melanoma cells were transfected for 72 hours with different siRNAs to SNAI2. To further assess transfection efficiency for SNAI2 knockdown, 10 μ M U0126 was added for 24 hours. (1): si SNAI2-1, (2): si SNAI2-2, (1+2): si SNAI2-1+2 and si -ve: negative control siRNA (with a scrambled sequence).

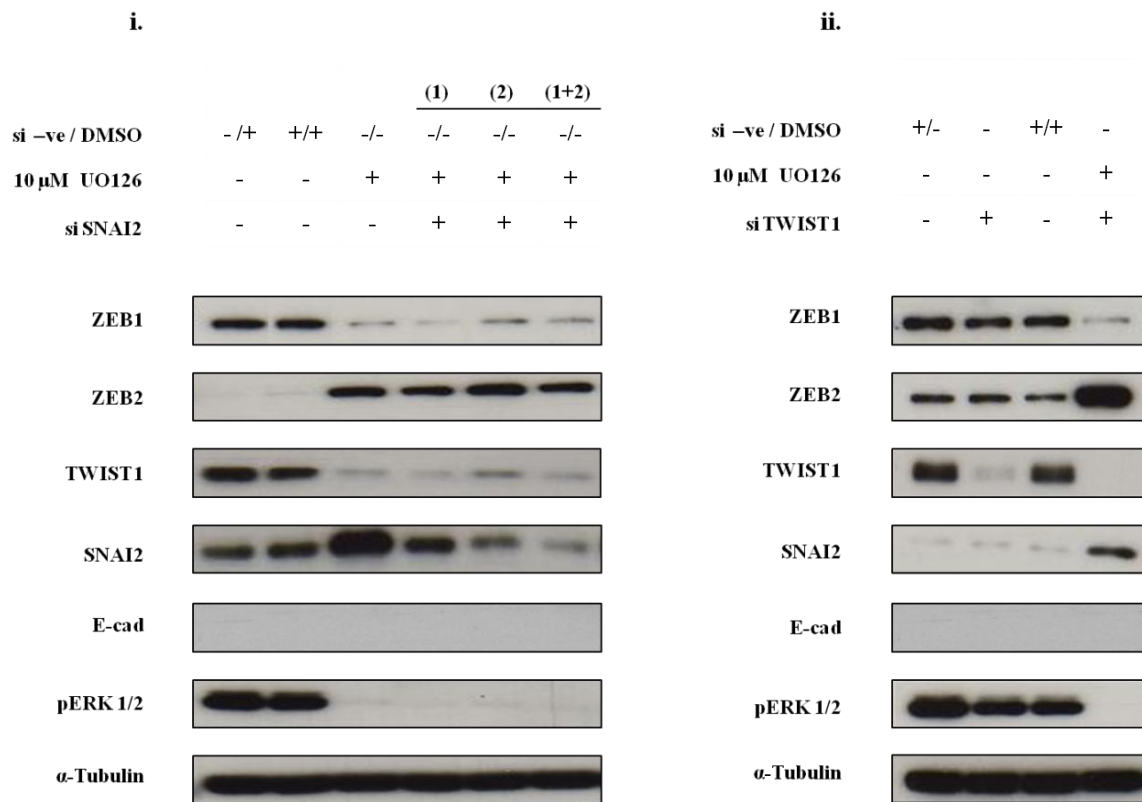


Figure 3.12 - siRNA-mediated depletion of SNAI2 and TWIST1 in A375M melanoma cells. A375M cells were transfected with (i) SNAI2 and (ii) TWIST1 or control siRNAs for 72 hours, treated with DMSO or UO126 for 24 hours and the immunoblotting was performed with the indicated antibodies. (1): si SNAI2-1, (2): si SNAI2-2, (1+2): si SNAI2-1/2 and si -ve: negative control siRNA (with a scrambled sequence). Note that knockdowns of SNAI2 and TWIST1 produced no effect on E-cadherin expression.

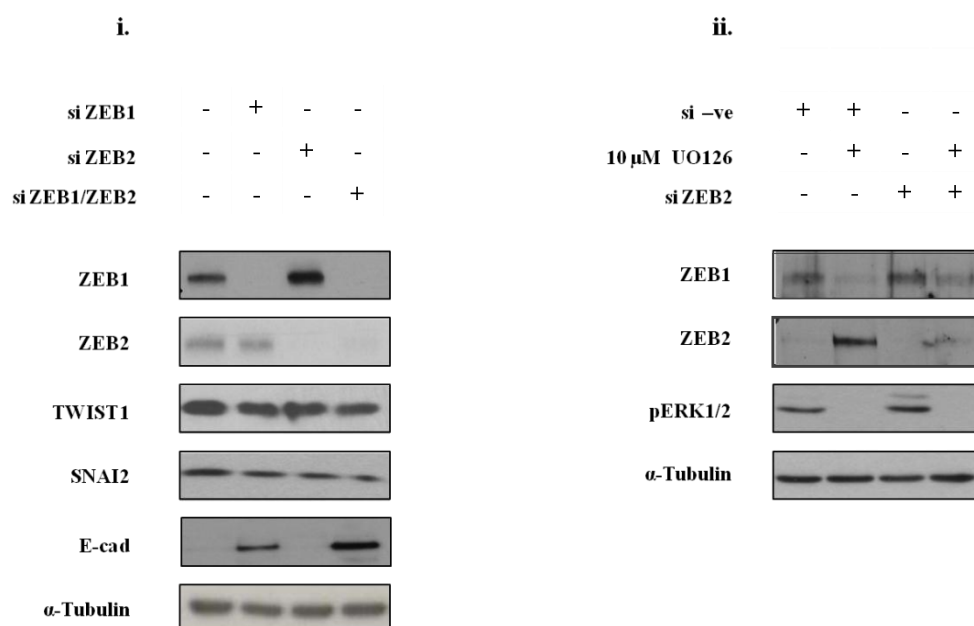


Figure 3.13 - The effect of siRNA-mediated depletion and MEK inhibition of ZEB proteins in A375M melanoma cells. (i) A375M cells were transfected with ZEB1, ZEB2 or control siRNAs for 96 hours. (ii) A375M cells were transfected with ZEB2 siRNA for 96 hours and treated with UO126 for 24 hours. The expression of MR-EMT proteins was analysed in western blotting as indicated.

3.3.7 *Fra-1 links the BRAF pathway with the MR-EMT network in A375 cells*

Given that the RAS-RAF-MEK-ERK pathway plays a key role in melanoma, it has been anticipated accumulation of Fra-1, which requires ERK-dependent stabilising phosphorylation events, in melanoma cell lines (Casalino et al., 2003). Indeed, preliminary *in vitro* experiments showed that phosphorylated Fra-1 (active form) was highly expressed in the majority of melanoma cell lines, but not in normal primary melanocytes (Figure 3.14-i). In order to determine whether Fra-1 is necessary for ZEB1 and ZEB2 regulation, melanoma cells were transfected with two different small interfering RNAs - Fra-1 specific (Chapter 2, Table 2.7) and compared with a scrambled siRNA control. As shown in Figure 3.14-ii, effective silencing of Fra-1 in A375P and A375M cells resulted in strong activation of ZEB2, but downregulation of ZEB1. Finally, combined Fra-1 transient depletion and MEK inhibition by UO126 in

A375P cells resulted in augmented ZEB2 expression, but decreased ZEB1 protein levels, compared to siFra-1 or MEK inhibition alone (Figure 3.14-iii).

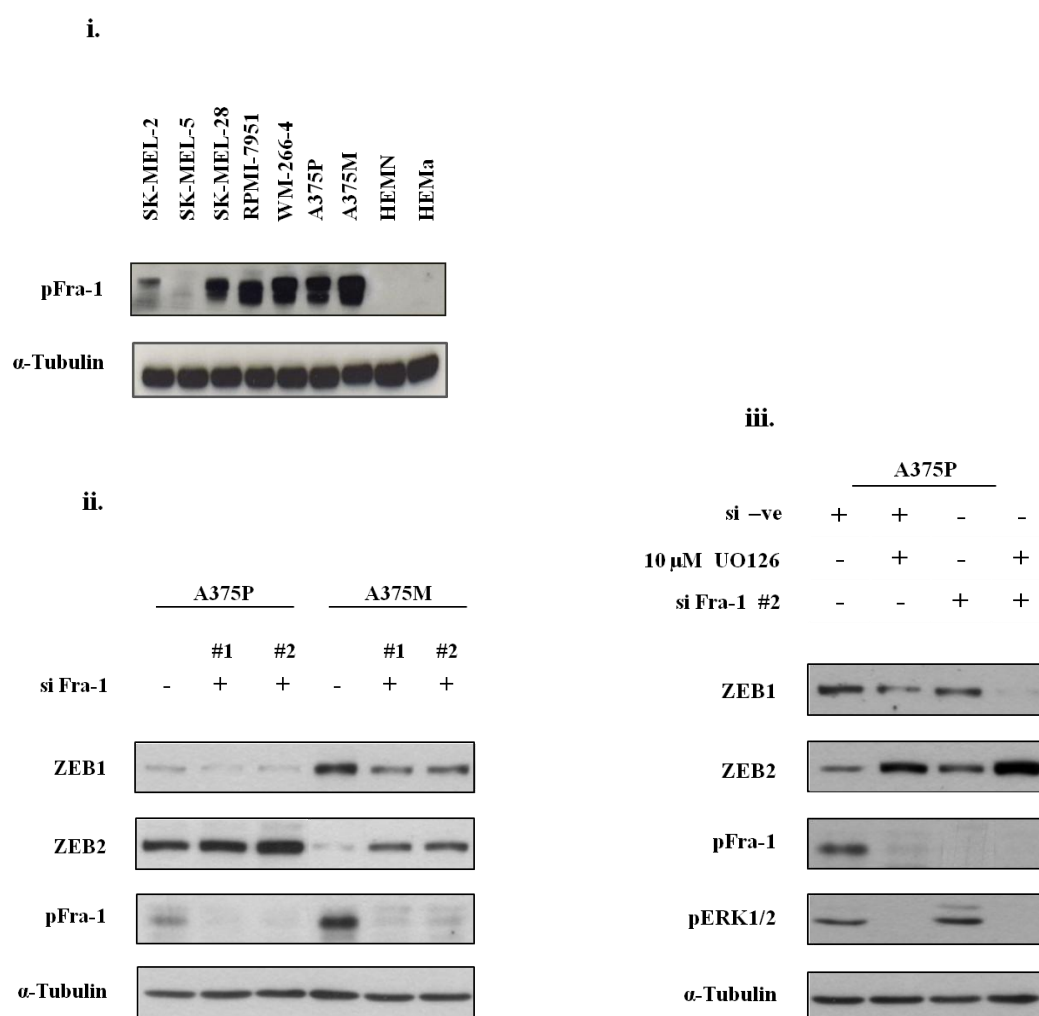


Figure 3.14 - The effect of Fra-1 siRNA mediated depletion and U0126 on ZEB proteins in A375 melanoma cells. (i) Western blot analysis of the expression of Fra-1 protein (upper bands indicate phosphorylation at Ser265) in a panel of human melanoma cell lines and normal neonatal (HEMN) and adult (HEMa) melanocytes. (ii) Fra-1 knockdown with siRNA #1 and #2 (SMARTpool) in A375P and A375M cell lines. (iii) Combined Fra1 knockdown with siRNA #2 and U0126 in A375P cells. Expression of phosphorylated (p) Fra-1 at Ser265, pERK1/2 and ZEB proteins was analysed 72 hours post-transfection by western blotting.

3.3.8 *Is regulation of ZEB1 and ZEB2 genes dependent on miRs in BRAF^{V600E} melanoma cells?*

To address the effect of MEK1/2 inhibition on the expression levels of miR-200 family members and whether the BRAF-MAPK pathway regulates ZEB1 and ZEB2 via these miRs, *ZEB1* and *ZEB2* 3' UTR luciferase reporters, previously validated on bladder cancer cell lines by Dr. E Tulchinsky (Department of Cancer Studies and Molecular Medicine, Leicester University, UK), were used. Adjunction of miR-200-targeted 3'UTR sequences of *ZEB1* or *ZEB2* to a luciferase reporter strongly repressed *ZEB1* ($P<0.05$, two-way ANOVA / Bonferroni post-test) or *ZEB2* expression ($P<0.05$) in RT-112 cells (epithelial phenotype), but had no significant effect in UMUC-3 cells (mesenchymal phenotype) compared to the empty pMIR-REPORT vectors (no *ZEB1* or *ZEB2* 3'UTRs) (Figure 3.15).

In *BRAF^{V600E}* melanoma cell lines A375P and A375M, the highest relative luciferase activity was observed in DMSO treated cells transfected with luciferase reporters containing *ZEB1* or *ZEB2* 3' UTRs (Figure 3.16). In addition, the luciferase activities were significantly reduced after addition of U0126 ($P<0.05$, two-way ANOVA / Bonferroni post-test) compared to DMSO treated vectors containing *ZEB2* or *ZEB1/ZEB2* 3'UTRs in A375P and A375M cells respectively. Thus, these results suggest that both *ZEB1* and *ZEB2* are regulated at the transcriptional level, but independently of miRs (Figure 3.16).

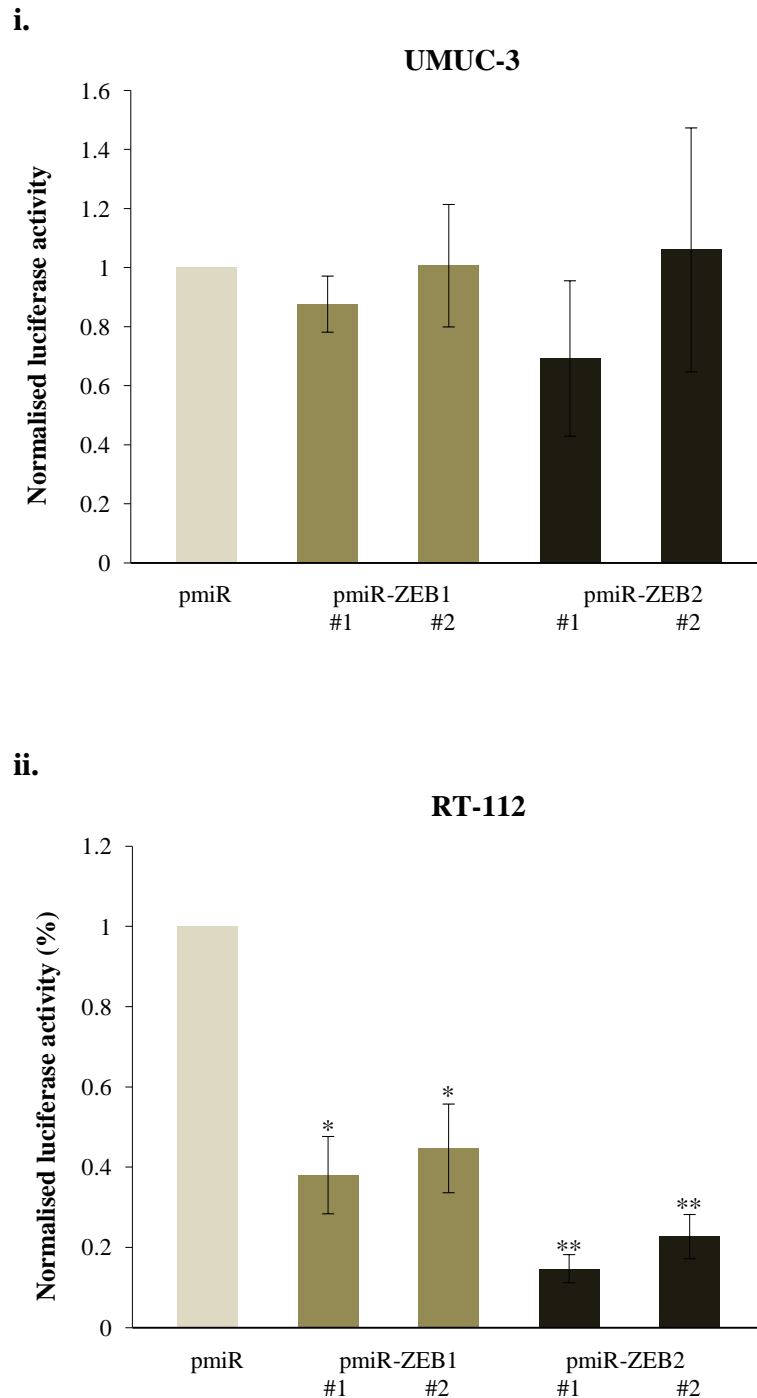


Figure 3.15 - The effect of luciferase miRNA expression reporter vectors containing *ZEB1* or *ZEB2* 3'UTRs in bladder cancer cell lines. An epithelial *ZEB1*/*ZEB2*-negative (RT-112) cell line (i) and a *ZEB1*-positive (UMUC-3) mesenchymal cell line (ii) were transiently transfected with the wild type pMIR-REPORT vector or with vectors containing *ZEB1* or *ZEB2* 3'UTRs (clones #1 and #2). The activity of the wild type pmiR reporter was taken as 1. pCMV β -gal was co-transfected in each experiment to normalise for transfection efficiency. Relative luciferase activity is expressed as means \pm SD from three individual experiments and analyzed by two-way ANOVA with Bonferroni post-tests (* $P < 0.05$; ** $P < 0.01$).

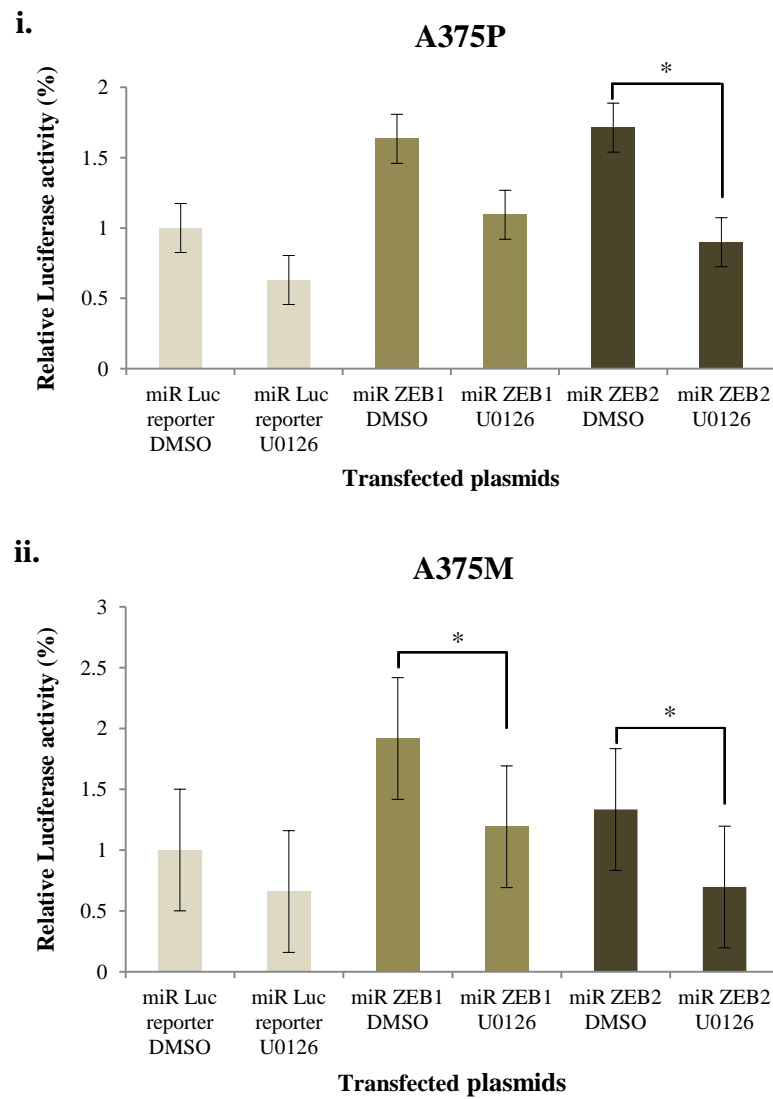
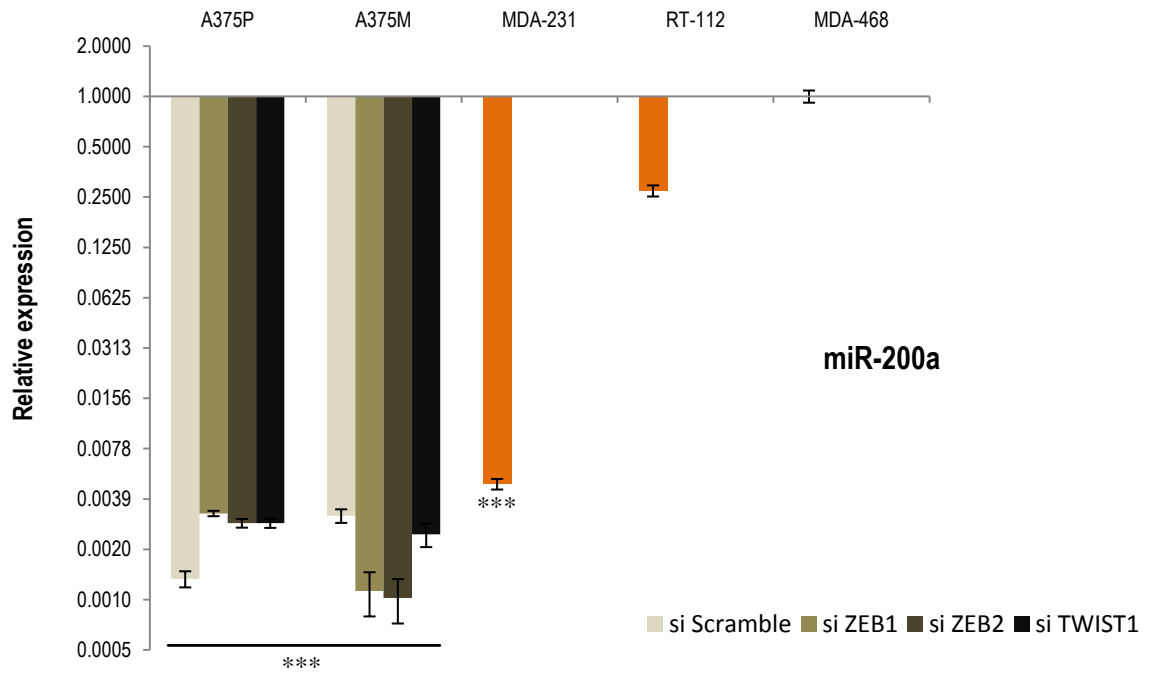
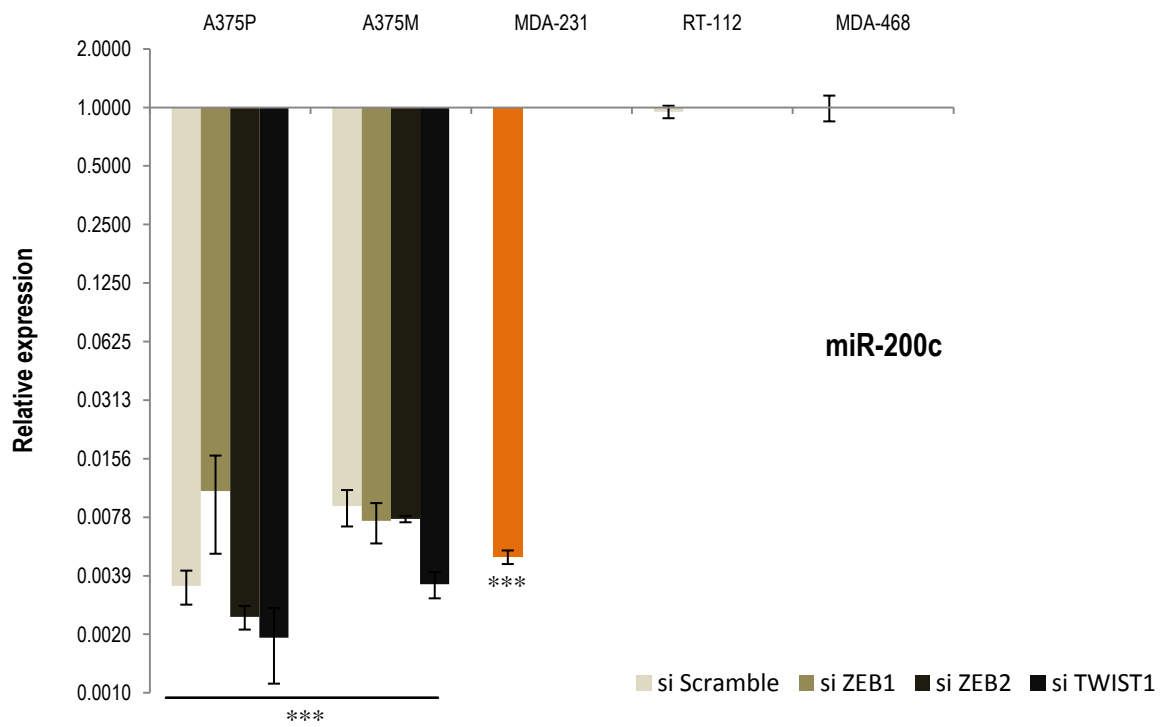


Figure 3.16 - The effect of miRNA expression reporter vectors in melanoma cancer cell lines. Melanoma cell lines A375P (i) and A375M (ii) were transiently transfected with the wild type pMIR-REPORT vector or with vectors containing *ZEB1* or *ZEB2* 3'UTRs (clone #1). Transfected melanoma cells were treated with U0126 or MOCK-treated for 24 hrs. The activity of the wild type pmiR vector / DMSO was taken as 1. pCMV β -gal was co-transfected in each experiment to normalise for transfection efficiency. Relative luciferase activity is expressed as means \pm SD from three individual experiments and analyzed by two-way ANOVA with Bonferroni post-tests (* $P < 0.05$; ** $P < 0.01$).

As the basal expression levels of miR-200 family members in melanoma cell lines A375P (high ZEB2 and low ZEB1/TWIST1 protein expression) and A375M (high ZEB1/TWIST1 and low ZEB2 protein expression) were low to undetectable, it was worth investigating whether siRNA-mediated depletion of ZEB1, ZEB2 or TWIST1 would have any effect on miR-200 family expression levels. Untransfected cell lines with known miR-200 levels (MDA-468, miR-200 high-expressing cells / MDA-231, miR-200 low-expressing malignant cells) and double negative for ZEB1/ZEB2 protein expression RT-112 cells were also used to control the experiments. Although the ZEB1/ZEB2 and TWIST1 siRNA-mediated knockdowns were efficient (Figure 3.11), qRT-PCR analyses of miR-200a,-c,-141 and -429 showed a similar expression level compared to the scrambled siRNA controls in A375P and A375M cell lines ($P>0.05$, two-way ANOVA / Bonferroni post-test) (Figure 3.17-A-D). Similarly, no significant differences were observed in miR-200 family expression levels between MDA-231 and A375 melanoma cells and between cancer cells with an epithelial phenotype (RT-112 and MDA-468) ($P>0.05$, two-way ANOVA / Bonferroni post-test). However, the miR-200 family expression levels in MDA-231 (mesenchymal phenotype) and melanoma cells was significantly lower compared to cancer cells with epithelial phenotypic characteristics (RT-112 and MDA-468) ($P<0.001$, two-way ANOVA / Bonferroni post-test).

A**B**

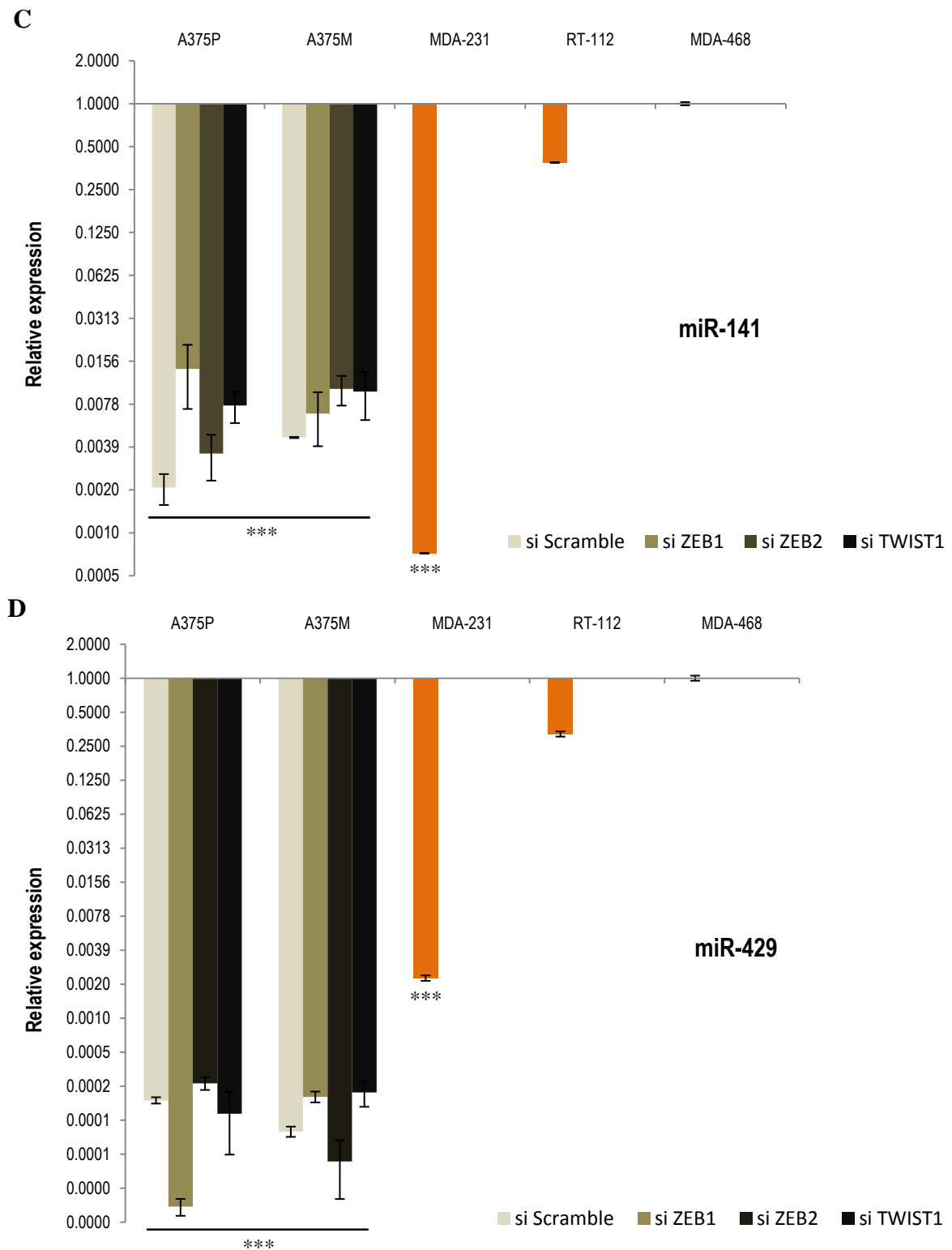


Figure 3.17 - miR-200 family expression in A375 melanoma cell lines by qRT-PCR. Relative expression of miR-200a (A), miR-200c (B), miR-141(C) and miR-429 (D) was calculated based on the $\Delta\Delta C_t$ method and normalised with miR-191. The y axis is a log scale. Changes in miR expression in melanoma cell lines A375P and A375M were analysed 48 and 72 hours after siRNA transfections to TWIST1 and ZEB1/ZEB2 respectively. MDA-231 (mesenchymal phenotype) and RT-112/MDA-468 (epithelial phenotype) cell lines were untransfected (orange coloured bars). MDA-468 benign breast cells were used as calibrators for each separate run. Data are representative of triplicate experiments. Each value shown is the mean \pm SD of three replicate measurements. Data was analysed by two-way ANOVA with Bonferroni post-tests. *** denote significant difference between A375 or MDA-231 cells (mesenchymal phenotype) and cancer cells with an epithelial phenotype (RT-112 and MDA-468) ($P < 0.001$). Note that miR-200b was excluded from analysis as Ct values were higher than the cut-off of 35.

3.4 Discussion

3.4.1 Regulation of MR-EMT by the BRAF-MEK MAPK signalling pathway in melanoma cells

The cell-based findings from this study indicated that MR-EMT, which are essential for normal embryogenesis, are reactivated in melanoma cultures. Moreover, the MAPK pathway seems to play an important role by regulating a network of MR-EMT in melanomas. Comparing the protein expression levels of MR-EMT, ZEB1 and TWIST1 were co-expressed at higher levels in poorly differentiated cell lines (Figure 3.3). In contrast to ZEB1 and TWIST1, SNAI2 and ZEB2 were expressed in all tested human melanoma cell lines harboring a *BRAF* mutation. Interestingly, it has been observed a switch from $\text{SNAI1-ZEB1-TWIST1}^{\text{low}}/\text{SNAI2-ZEB2}^{\text{high}}$ to $\text{SNAI1-ZEB1-TWIST1}^{\text{high}}/\text{SNAI2-ZEB2}^{\text{low}}$ protein expression patterns between low (P) and high metastatic (M) A375 cells respectively (Figure 3.3). Compared to highly metastatic A375 cells, melanocytes expressed higher protein levels of ZEB2 and SNAI2, but not ZEB1, TWIST1 and SNAI1, indicating that these transcription factors may be key determinants in regulating neural crest cell precursor differentiation into melanocytes.

In accordance with previous work, SNAI1 has been associated with the mobility and invasive properties in various carcinoma cell lines. In this study, SNAI1 protein expression was only detectable in three *BRAF* mutated melanoma cell lines and this may be attributed to its unstable nature (half-life ~25 min) (Mikesh et al., 2010, Zhou et al., 2004). Therefore it is plausible to suggest that the biological role of a subset of MR-EMT in melanoma cells may include maintenance of a phenotype characteristic of neural crest precursor cells after transient activation of other EMT regulators, for example SNAI1.

Pharmacological inhibition of the BRAF-MEK pathway and assessment of ZEB1, ZEB2, TWIST1 and SNAI2 mRNA expressions by real time qRT-PCR revealed that this pathway regulates these factors at the transcriptional level (Figures 3.8 and 3.9). In addition, it has been provided evidence that reactivation of ZEB2 and SNAI2 preceded the inhibition of ZEB1 and TWIST1, suggesting a potential regulatory hierarchy between these genes in the course of melanoma progression.

Taken together, the findings from this work indicated that BRAF-MEK activation in transformed melanocytes drives a rapid reprogramming of MR-EMT, an event that contributes to malignant transformation. Moreover, a transient inactivation of the BRAF-MEK MAPK pathway restitutes the original pattern of expression of these transcription factors, highlighting the reversibility of melanoma transformation.

3.4.2 Is there any effect of PI3K, JNK and p38 signalling pathways on MR-EMT?

The RAS/RAF/MEK/ERK signalling cascade is the major tumorigenic subgroup of the MAPK pathway in melanoma. Multiple lines of evidence indicated that hyperactivation of this pathway represent a hallmark of cutaneous malignant melanoma as direct cell proliferation, metastasis and survival programs (reviewed in Lopez-Bergami, 2011). Although the ERK pathway has been extendedly studied in melanomas recent publications documented that other MAPK signalling subgroups, namely the JNK, p38 and the PI3K-AKT, play an essential role in melanoma development. Therefore, while this study demonstrated a reprogramming of embryonic MR-EMT, initiated in response to BRAF-MEK activation, it has been queried the relationship between MR-EMT and other MAPK signalling pathways.

Several recent evidences revealed a growth-promoting role of the stress-activated protein kinases or JNK proteins (reviewed in Lopez-Bergami, 2011). In melanomas, JNK activation supports survival by controlling cycle arrest and apoptosis. Phospho-JNK activation showed a markedly increased ZEB1 protein expression levels in A375 melanoma cells (Figure 3.6). However, SP600125 efficacy could not be assessed with certainty in these cells as basal levels of p-c-Jun were not detectable.

A recent report demonstrated that the PI3K-PTEN pathway downregulates E-cadherin via transcriptional upregulation of SNAIL and TWIST1 in melanoma cells (Hao et al., 2012). Additionally, attenuation of ZEB2 mRNA was shown to promote melanomagenesis by regulating PTEN expression in a miR dependent manner (Karreth et al., 2011). Herein, effective inhibition of AKT activity by wortmannin treatment in A375P cells did not induce any significant changes in the protein expression levels of ZEB1 and ZEB2 (Figure 3.7-ii). Protein expression of ZEB1 and ZEB2 was only altered upon combination of U0126 and wortmannin inhibitors indicating a MEK-dependent modulation of these transcription factors.

The p38 MAPK pathway is activated upon external stress signals and often engages a tumour suppression function by negatively regulating cell survival and proliferation. In melanomas a number of studies indicated p38 MAPK involvement in melanogenic differentiation and apoptosis (reviewed in Lopez-Bergami, 2011). Remarkably, constitutive active ERK has been found to be linked with activation of JNK and p38 in human melanoma indicating interplay among these cascades (Lopez-Bergami et al., 2007). Concurrent activation of p38 and ERK seems to be unique to melanomas, as in carcinomas p38 inhibition predictably resulted in enhanced ERK activity preventing tumourigenesis.

A375 cell lines showed high pERK1/2 and p-p38 ratio reinforcing the perception of their simultaneous activation and lack of negative feedback from p38 to ERK in melanomas (Figure 3.5). In addition, p-MAPKAPK2 downregulation showed a similar MR-EMT expression profile following treatment with MEK inhibitors (Figures 3.4 and 3.5). However, SB203580 treatments did not change the levels of ERK compared to the untreated control suggesting that p38 MAPK may be linked to an ERK-independent regulation of MR-EMT in melanoma.

3.4.3 Posttranslational modifications of MR-EMT in *BRAF*^{V600E} melanoma cells

Posttranslational modification by ubiquitin is a common mechanism for targeting proteins for proteasomal degradation by the proteasome (Hershko and Ciechanover, 1998). Recently, a common regulatory pathway for SNAI1, SNAI2, TWIST1 and ZEB2 has been characterised in *Xenopus* embryos (Lander et al., 2011). The stability of these EMT-induced transcription factors was found to be tightly controlled by the ubiquitin-proteasome system (UPS) and a single ubiquitin E3 ligase Ppa (Partner of paired; human homologue FBXL14) that targets their proteasomal degradation. This mechanism may also exist during tumour progression and herein it was addressed whether MR-EMT are regulated at a posttranslational level in melanoma cells.

According to this study, regulation of SNAI2 and TWIST1, but not ZEB1 or ZEB2 occurred also on the level of protein stability (Figure 3.10). Notably, while MEK inhibition stabilised SNAI2, it destabilised TWIST1, suggesting that RAS-BRAF MAPK pathway plays a key role in the stability of these proteins (Figure 3.10). Consistently, experiments with the inhibitor MG132 demonstrated that in A375 cells both SNAIs and TWIST1 proteins are degraded via a proteasomal pathway. However,

the underlying mechanisms seem to be different. Firstly, while proteasomal degradation of SNAIL and TWIST1 was stimulated, degradation of SNAIL2 was attenuated by a MEK1/2 inhibitor. Secondly, treatment of melanoma cultures with a GSK-3 β inhibitor (LiCl) augmented the protein expression of TWIST1. This suggests that active GSK-3 β may counteract TWIST1 transcriptional repressor activity by promoting its proteasomal degradation in melanoma cells.

A study by Lopez-Bergami and colleagues demonstrated that in A375 melanoma cells constitutively active ERK mediates inactivation of GSK-3 β via its phosphorylation at Ser9/Ser21 (Lopez-Bergami et al., 2007). Therefore, it can be proposed a mechanism in which inactivation of ERK leads to phosphorylation and nuclear export of TWIST1 by GSK-3 β with subsequent ubiquitylation and degradation of TWIST1. A recent report indicated that a small C-terminal domain phosphatase dephosphorylates and suppresses the ubiquitylation of SNAIL (Wu et al., 2009). It has also been suggested an antagonistic function of the phosphatase to active GSK-3 β that stabilises SNAIL. Similarly, an upstream active MAPK signalling may also induce TWIST1 protein stability by upregulating an as yet unidentified phosphatase.

The pattern of the response of SNAIL2 to LiCl is similar to that of SNAIL, a known GSK-3 β target. The concentration of SNAIL and SNAIL2 was increased in melanoma cells only in the presence of combined LiCl and MG132. The same effect of both inhibitors on SNAIL protein expression was observed in MCF7 cells (SNAIL-MCF7 stable clones) where GSK-3 β -mediated phosphorylation and proteasomal degradation was first described (Zhou et al., 2004). Additionally, it was evident that ZEB1 and ZEB2 proteins were stable and resistant against proteasomal degradation in A375 cells independently of MAPK signalling.

3.4.4 Establishment of an EMT interactome in BRAF mutated melanoma cells

Increasing evidence suggest that the EMT-induced transcriptional repressors are rarely expressed on their own during tumour development. Indeed, few reports revealed that in different subset of cancers, cross-talk among these factors may act cooperatively by inducing each other expression to program EMTs, thereby establishing an "EMT interactome" (Taube et al., 2010). Initial studies in colorectal cell lines showed that ectopic overexpression of SNAIL was able to enhance ZEB1, but not ZEB2, expression, and repress different epithelial promoters (*E-cadherin* and *cytokeratin 18*) (Guaita et al., 2002). Another study demonstrated that SNAIL acts rather as an early marker of EMT, followed by SNAIL2 upregulation which seems to be more implicated in the late stages of invasive colorectal tumours (Shioiri et al., 2006).

Similarly, a recent report using two mouse skin carcinoma cell lines, CarB and HaCa4, revealed that SNAIL and SNAIL2 collaboration reflects a different invasion potential (Olmeda et al., 2008). As such, SNAIL favours local invasion, but SNAIL2 expression further contributes to acquisition of a more aggressive phenotype, associated with distant site-specific metastasis in the lung and liver. Based on IHC-P, Western blot and mRNA analyses, a study by Yoshida *et al* in ovarian clinical samples and cell lines reported that a set of transcription regulators, SNAIL, SNAIL2, ZEB2 and TWIST1 were upregulated in progressed carcinoma rather than benign neoplasms (Yoshida et al., 2009). However, only SNAIL showed an inverse correlation with E-cadherin in aggressive ovarian cancers. Additive function of EMT regulators was also demonstrated in HCCs. In this type of cancer, co-expression of SNAIL and TWIST1, but not SNAIL2, promotes invasion and metastasis (Yang et al., 2009). Recent data analyses using qRT-PCR and ICH-P in a cohort of gastric carcinoma formalin-fixed, paraffin-embedded tissues have presented evidence that SNAIL2 upregulation, in 58% of samples, correlates

significantly with E-cadherin loss and may act synergistically with ZEB2 in intestinal-type and SNAIL in diffuse-type gastric malignancies (Alves et al., 2007).

ZEB2^{-/-} mouse embryos express significantly high ZEB1 in paraxial mesoderm and in neural folds than their wild-type counterparts indicating that interplay between ZEB proteins may exist (Miyoshi et al., 2006). Herein, using RNA interference technology silencing of ZEB2 led to a markedly upregulation of ZEB1 (Figure 3.13). Transient depletion of ZEB2 and MEK inhibition further reduced downregulation of ZEB1 underlying a MEK-dependent switch from ZEB2 to ZEB1 in melanoma cultures. Thus, the biological role of MEK-repressed ZEB2 might be to stabilise a melanoblast-like phenotype by activating ZEB1. Elimination of ZEB1 did not markedly affect ZEB2 protein levels indicating a hierarchical but not a mutual dependence between these factors. For effective repression of target genes, ZEB2 binds DNA as a monomer to bipartite CACCT sequences located in close proximity to each other (separated by at least 44 bp) (Remacle et al., 1999). As TF search program (TFSEARCH: Searching Transcription Factor Binding Sites) predicted three putative ZEB2-binding bipartite DNA elements localised within 1.3 kb upstream the *ZEB1* transcription start site, it is plausible to assume involvement of these sites in the silencing of ZEB1.

3.4.5 Fra-1 perturbs the expression of MR-EMT in melanoma cells

Activator protein (AP1) transcription factor complexes represent heterodimers between basic region-leucine zipper transcription factors of Fos (c-Fos, FosB, Fra-1 and Fra-2) and Jun (c-Jun, JunB and JunD) families or homodimers of Jun-Jun (Young and Colburn, 2006). Despite the fact that deregulated activation of AP-1 is linked to oncogenesis, increasing evidence suggests that detection of Fra-1 protein, encoded by

the *fosl1* gene, may be more predictive for oncogenic activity. Moreover, several lines of evidence have demonstrated that Fra-1 plays a crucial role in tumour cell motility, cell cycle progression and survival and regulated in an ERK-dependent manner in different types of tumour cell lines and human malignancies either at earlier or late stages of their development (Ramos-Nino et al., 2002, Tulchinsky, 2000).

Few studies have documented that Fra-1 links EMT with RAS-ERK signalling pathways in carcinoma cells. A recent report has indicated that activation of ERK2 and the late response gene *Fra-1* by RAS induces an EMT phenotype via a downstream upregulation of ZEB1 and ZEB2 expression in MCF-10A cells, a transformed human mammary epithelial cell line with constitutively active *ERK2* or *Ras-V12* (Shin et al., 2010a). Induction of ZEB1 and ZEB2 subsequently contributed to loss of E-cadherin. Likewise, a study has also reported a Fra-1 dependent stimulation of SNAI2 expression in response to MEK1 signalling in intestinal cells (Lemieux et al., 2009). In parallel to this study, another group has confirmed SNAI2 association with ERK-Fra-1 axis in breast cancer cell lines (Chen et al., 2009). The same group has also demonstrated that Fra-1-dependent SNAI2 activation is required for *in vitro* cell invasiveness.

In melanoma cells the RAS-RAF-MEK-ERK pathway is constitutively active and there is a growing body of evidence suggesting its role in the oncogenic behaviour of melanoma (Fecher et al., 2008). More recent evidence from Massoumi and colleagues revealed a direct link between ERK activation and SNAI1 expression in malignant melanoma cells (Massoumi et al., 2009). However, activation of SNAI1 by ERK1/2 was Fra-1 independent. A microarray analysis (Dr. E Tulchinsky, personal communication) showed that in Fra-1 silenced bladder cultures the expression of SNAI2 was decreased more than 3-fold in comparison with the control (scramble

siRNA transfected cells). Notably, none of other EMT transcription factors expression was changed compared to control bladder cells.

This study demonstrated that phosphorylated Fra-1 was elevated in all melanoma cell lines but not in SK-MEL-5 and cultured human epidermal melanocytes. SK-MEL-2, an *NRAS* mutant, also exhibited low Fra-1 activity but less in comparison with the *BRAF* mutated cell lines (Figure 3.14-i). Effective transient knockdown of Fra-1 in A375 melanoma cells largely mimicked the effect of MEK inhibitors on ZEB1 and ZEB2 expression, suggesting that Fra-1 links the BRAF pathway with the MR-EMT network, may act as a direct repressor of ZEB2 and ZEB2 is in turn a repressor of ZEB1 in MM (Figures 3.4 and 3.14-ii). This shift has functional implications because ZEB1 is considered as the *bona fide* repressor for E-cadherin in tumours of epithelial origin. Interestingly, simultaneous Fra-1 depletion and MEK inhibition by U0126 in A375P cells resulted in stronger activation of ZEB2 protein expression, but downregulation of ZEB1, compared to single treatments with siFra1 or U0126 indicating that Fra-1 is necessary for ERK1/2-mediated regulation of ZEB1 and ZEB2 protein expression (Figure 3.14-iii).

Unpublished data from ChIP analyses and a conventional 5'-RACE in *BRAF* mutated melanoma cell lines further suggested that Fra-1 acts as a MEK-induced factor, which directly represses *ZEB2* transcription via a repressor element located 2.7 kb upstream of the transcription site (Dr. E Tulchinsky and Dr. GJ Browne, personal communication). Thus, these observations support the notion that the RAS-MEK-Fra-1-MR-EMT axis not only exists but also Fra-1 could act as a transcriptional repressor, rather than an activator of *ZEB2*, in melanocytic tumours. However, additional studies are required to address the relevance of Fra-1 to melanoma spread and regulation of MR-EMT network

in vivo and examine the mechanisms of transcriptional repression of *ZEB2* mediated by Fra-1.

3.4.6 Posttranscriptional regulation of MR-EMT: miRs

A large body of evidence has postulated the correlation of modified miR expressions with the EMT-induced switch between cell phenotypes and metastasis (reviewed in Korpál et al., 2008). Screening of 60 human cancer cell lines (NCI60), divided according to the ratio of E-cadherin/Vimentin expression, and ovarian cancer specimens for endogenous miR targets revealed that miR-200 family (miR-200a,-b,-c,-141 and -429) is a powerful marker of epithelial phenotype and repress the expression of *ZEB1* and *ZEB2* transcription factors. In that model authors proposed a novel mechanism in which miR-200 family contributes to suppression of cancer metastasis by targeting directly *ZEB1* and *ZEB2*. So, upregulation of miR-200 family members suppress *ZEB1* and *ZEB2* functions and allow cells to maintain an epithelial phenotype (high E-cadherin expression). Inversely, inhibition of endogenous miR-200 family members can induce a mesenchymal phenotype and tumour progression (loss of E-cadherin, high vimentin expression) (Park et al., 2008a).

In a parallel study, Gregory and colleagues demonstrated a cooperative repression of *ZEB1* and *ZEB2* by miR-200 family and miR-205 in a mesenchymal group of Madin-Darby canine kidney (MDCK) cells following TGF- β induction in FIGO (International Federation of Gynecology and Obstetrics) stage III-IV advanced ovarian tumour samples (Gregory et al., 2008). Subsequent studies supported the role of miR-200 family and miR-205 on *ZEB1* and *ZEB2* in multiple human tumour types, including spindle cell carcinoma (SpCC) (Zidar et al., 2011), breast cancer (Tryndyak et al., 2010) and endometrial carcinosarcomas (ECSs) (Castilla et al., 2011). In addition to the

repressive effect of miR-200 on ZEB1 and ZEB2, it has been reported a ZEB/miR-200 double-negative feedback loop, suggesting that miR-200 family members are transcriptional targets of ZEB1 and ZEB2 (Brabletz and Brabletz, 2010, Burk et al., 2008). Similar to *ZEB* family genes, qRT-PCR analyses revealed that TWIST1 may act as a transcriptional activator for miR-200 and miR-205 in invasive bladder tumours (Wiklund et al., 2011).

To date, there are few data in the literature to demonstrate a possible effect of miRs on other MR-EMT. A report by Ma et al. showed that miR-10b has an important role in the metastasis of breast cancer cells (Ma et al., 2007). This particular miR, induced by TWIST1, was found to exert its regulatory function by silencing the expression of the HOXD10 (Homeobox D10) protein, previously characterised as an important gene progressively lost in high-grade breast malignancies (Carrio et al., 2005). In both metastatic melanoma clinical samples and cell lines, decreased expression of miR-9 indicated a nuclear factor kappa B1 (NF- κ B1)-dependent upregulation of SNAI1 (Liu et al., 2012a). In addition, the direct interaction of miR-203 with the SNAI2 3'UTR could influence tumourigenicity in breast tumours (Zhang et al., 2011).

As previously described, miR-200 family and miR-205 are key regulators of ZEB1 and ZEB2 in carcinoma cells and are frequently silenced in advanced malignancies. In A375 cultures, activities of luciferase reporters containing 3'UTR of *ZEB1* and *ZEB2* were not diminished as compared with the empty pmiR vectors (Figure 3.16). In agreement with these data, luciferase reporters were also insensitive to MEK inhibition (Figure 3.16). Moreover, siRNA-mediated transfections of ZEB1, ZEB2 and TWIST1 showed minute changes in the expression of miR-a,-c,-141 and -429 members of the miR-200 family compared to scrambled siRNA controls (Figure 3.17). Hence, transient

knockdown of ZEB1, ZEB2 and TWIST1 did not result to an increase in the expression of miR-200 family members, supporting an independent regulation of these transcription factors by miR-200 family. This conclusion is consistent with previous data showing lack of miR-200 family expression even in E-cadherin-positive melanoma cells, such as SK-MEL-28 (Park et al., 2008c).

These observations were further supported by unpublished results in our lab that showed a significant downregulation of miR-200 family and miR-205 in primary MMs and nodal metastases when compared with naevi, suggesting a tumour suppressor role in this disease (Dr JH Pringle, personal communication). In contrast to our results, Mueller *et al* reported distinct miR expression profiles in melanomas and found miR-200-a,-c,-141 to be significantly upregulated in primary tumour melanoma cell lines relative to normal cultured melanocytes, indicating their possible role in early progression of the disease (Mueller et al., 2009). However, these miRs have not been tested *in vivo* suggesting that their upregulation might be due to an artefact of long-term cultures and cell culture conditions. Nevertheless, loss or reduced expression of miR-200 family and miR-205 was recently found to be reproducibly reduced with melanoma progression in patient samples (Liu et al., 2012b, Philippidou et al., 2010, Xu et al., 2012).

Since miR levels in A375 cultures were not significantly upregulated by knockdown of the MR-EMT, it is clear that these genes are not key regulatory factors controlling EMT and are possibly regulated by a different mechanism in melanocytes and melanoma transformed cells. A number of mechanisms may help control miR-200 activity, such as the epigenetic inactivation by CpG island hypermethylation and associated retention of E-cadherin expression. Indeed, a recent study indicated that repression of miR-200

family is linked to an aberrantly methylated CpG island in the promoter region of these miRs in a panel of human tumour cell lines (colon, lung and breast) (Davalos et al., 2012). As a result, each of these carcinoma cell lines acquired a mesenchymal phenotype displaying higher levels of expression of ZEB1 and ZEB2, and lack of E-cadherin. In this context, epigenetic silencing of miR-200 family members is highly plausible and could be advantageous for dissemination of melanoma cells.

3.4.7 Conclusions

- *BRAF* and *NRAS* mutated melanoma cell lines showed two patterns of expression with high ZEB2 and SNAI2 or high ZEB1, SNAI1 and TWIST1. Interestingly, metastatic A375M cells showed increased protein levels of ZEB1, TWIST1 and SNAI1, but decreased ZEB2 and SNAI2, compared to the less metastatic parental (A375P) cells.
- Cultured human melanocytes expressed ZEB2 and SNAI2, but not ZEB1, TWIST1 or SNAI1.
- Evidence from *in vitro* experiments indicated that a switch in MR-EMT expression ($\text{ZEB1}^{\text{low}}/\text{TWIST1}^{\text{low}} / \text{ZEB2}^{\text{high}}/\text{SNAI2}^{\text{high}}$ to $\text{ZEB1}^{\text{high}}/\text{TWIST1}^{\text{high}} / \text{ZEB2}^{\text{low}}/\text{SNAI2}^{\text{low}}$) is RAS-RAF-MEK MAPK-dependent.
- P38 MAPK signalling pathway may be linked to an ERK-independent regulation of MR-EMT in melanoma.
- Pharmacological inhibition of MEK1/2 repressed two MR-EMT, ZEB2 at a transcriptional level, and SNAI2 on two levels, transcriptional and posttranslational, by promoting its proteasomal degradation.
- The effect on ZEB1 and ZEB2 expression was transcriptional and independent of miR-200 family.
- Further experiments demonstrated that Fra-1 may act as a MEK-induced factor which downregulates *ZEB2* transcription and enhances ZEB1 expression.

4 Functional effects of ZEB proteins in melanoma

4.1 Introduction

In the past two decades various studies demonstrated that EMT repressor genes are upregulated in advanced stages of cancer and suppress E-cadherin expression. Melanoma progression involves transition from a radial to vertical growth, characterised by invasion into the dermis and subcutaneous tissue. The underlying mechanism involves loss of E-cadherin in concert with upregulation of N-cadherin. This switch permits melanoma cells to interact with N-cadherin-expressing cells in the dermis, dermal fibroblasts and with the vascular endothelium, which stimulates metastasis (reviewed in Bonitsis et al., 2006). However, apart from E-cadherin other target genes essential to cancer development were found to be inhibited by these repressors. One of the most important identified targets in high-grade tumours is the Vitamin D Receptor (VDR) gene.

Vitamin D receptor was first discovered in chicken intestine, belongs to the superfamily of nuclear receptors for steroid hormones, and can be considered as a ligand-activated transcription factor (Haussler and Norman, 1969). Binding of the active hormone 1 α ,25-dihydroxyvitamin D₃ to its nuclear receptor (VDR) causes a conformational change and recruitment of its dimerization partner retinoid X receptor (RXR). The effect of the activated heterodimer VDR-RXR is to interact with vitamin D response elements (VDREs) in the promoter region of target genes. Subsequent recruitment into the transcriptional pre-initiation complex (VDR-RXR-VDRE) of several distinct nuclear proteins, such as steroid receptor co-activators (SRCs), vitamin D receptor interacting protein (DRIP) and Ski-interacting protein (SKIP), regulates gene expression (Brown et al., 1999, Haussler et al., 1997, Plum and DeLuca, 2010). Since

VDR discovery in 1969, a plethora of studies illustrated that VDR mediates most, if not all, of the biological effects of 1 α ,25-dihydroxyvitamin D₃, also called calcitriol or designated as 1,25(OH)₂D₃, the most active metabolite of vitamin D.

As yet, more than two hundred genes have been reported to exhibit functional VDREs (Ramagopalan et al., 2010). A subset of vitamin D responsive genes are associated with the classical actions of vitamin D hormone, which include bone mineralization, attainment of calcium homeostasis, and regulation of cell proliferation, apoptosis and differentiation (Holick, 2007). Functional VDREs related to bone homeostasis include several bone-related genes, like osteopontin, osteocalcin, parathyroid hormone (PTH) and bone sialoprotein (Farach-Carson and Ridall, 1998). On the other hand, VDREs associated with anti-proliferative and pro-differentiation functions include the cell cycle regulating protein p21, transforming growth factor (TGF- β), fibronectin and β 3-integrin (reviewed in Haussler et al., 1997). Furthermore, diversity of scientific literature suggests that alterations in vitamin D levels and polymorphisms of the VDR gene are implicated in many diseases, such as hypertension (Wang et al., 2008), diabetes (Zipitis and Akobeng, 2008) and diverse tumour types (Hendrickson et al., 2011, Lopes et al., 2010, Thill et al., 2010).

The data obtained in recent years indicate that E-cadherin repressors interact with VDR and contribute to the progression of cancer. Experiments by Cano and Palmer were the first to indicate that E-cadherin expression is activated by 1,25(OH)₂D₃, but repressed from SNAIL in colon carcinoma cells (Cano et al., 2000, Palmer et al., 2001). Preliminary unpublished data from our lab demonstrated that downregulation of the VDR protein levels is associated with malignant transformation and local invasion in melanoma tissue samples.

4.2 Aims and Objectives

The primary aim of this chapter was to test whether ZEB1 and ZEB2 modulates the expression of known E-box binding targets, E-cadherin and VDR, in melanoma.

The specific objectives of this chapter were as follows:

- To assess the protein expression pattern of ZEB1, ZEB2 and E-cadherin in a small subset of paired primary and secondary melanoma tissues by IHC-P.
- To test the expression of VDR in selected ZEB1 immunopositive melanocytic lesions by IHC-P.
- To investigate the effect of ZEB1 and ZEB2 on VDR and E-cadherin protein expressions in melanoma cells by transient siRNA-mediated assays.
- To assess the expression of miR-125b, known to target VDR, in naevi, primary melanomas and nodal metastases.
- To test the effect of transient siRNA-mediated depletion of ZEB1 and ZEB2 on the motility of melanoma cells by migration assays.

4.3 Results

4.3.1 *The effect of ZEB proteins on the expression of E-cadherin in melanoma tissues*

To evaluate the expression of ZEB1 and ZEB2 with E-cadherin status, a small cohort of ten matched pairs of primary tumours and their corresponding metastases was assessed by immunohistochemistry. Validation of antibody specificity using IHC-P and western blotting is shown in Chapter 5 (Figures 5.1 and 5.3-B). E-cadherin was localized to the cell membrane, while ZEB1 and ZEB2 staining was nuclear. E-cadherin, ZEB1 and ZEB2 were scored based on overall intensity and extent of immunoreactivity (see section 2.2.4.7). E-cadherin immunoreactivity revealed a homogeneous staining in metastatic primary MMs and a gradient of staining with stronger peripheral staining compared to the intratumoural sites in nodal metastases, where in some cases there were areas of negative staining. Out of ten primary tumours with strong membrane-bound E-cadherin immunoreactivity, eight (80%) showed reduced expression in the corresponding metastases (Figures 4.1-4.7-A, Table 4.1). This result was in line with previous publications indicating that E-cadherin loss is associated with melanoma invasiveness (Haass et al., 2004, Shirley et al., 2012).

ZEB1 was detected in 20% (2/10) of primary melanomas and in 40% (4/10) of paired metastases and interestingly its immunoreactivity was confined in small areas at deep / intratumoural sites of primary MMs and matched metastases (Figures 4.1, 4.3 and 4.5-B, Table 4.1). In addition, ZEB1-positive tumour areas showed lack of E-cadherin expression (Figures 4.3-A/B and 4.5-A/B). This near mutually exclusive pattern of ZEB1 and E-cadherin expression may indicate a critical role of ZEB1 in EMT in melanocytic lesions.

Expression of ZEB2 was detected in 100% (10/10) of primary melanomas and in 60% (6/10) of corresponding metastases (Figures 4.1-4.7-C). Comparing expression of ZEB2 in primary melanomas in the superficial and deep sites, there was decreased expression in the deep sites in 90% (9/10) of primary melanomas (Figure 4.2-C-i, Table 4.1). Furthermore, out of six matched lymph nodes with positive ZEB2 immunoreactivity at peripheral sites, all cases revealed very low reactivity in the intratumoural sites (Figures 4.3, 4.5 and 4.7-C, Table 4.1). ZEB1-positive tumours with absent E-cadherin showed negative ZEB2 protein expression (Figures 4.3 and 4.5), but interestingly in ZEB1-negative melanomas E-cadherin and ZEB2 were co-expressed (Figures 4.1, 4.2, 4.4, 4.6, and 4.7). Unfortunately, due to the small sample size of melanomas and the low number of ZEB1-positive tumours it was not feasible to evaluate statistically the reciprocal staining pattern between ZEB1 and ZEB2 / E-cadherin.

Table 4.1 - Distribution of ZEB1/ZEB2 and E-cadherin staining intensity and pattern in matched melanoma cases

	PAIRED SAMPLES			
	Tumour area	Measure (positive)	Primary MMs	Nodal Metastases
E-cadherin (membrane staining)	Superficial	(2+, 3+)	10/10 (100%)	2/10 (20%)
	Deep	H-Score>100	5/10 (50%)	2/10 (20%)
ZEB1 (nuclear staining)	Superficial	(1+, 2+, 3+)	0	0
	Deep	H-Score >0	2/10 (20%)	4/10 (40%)
ZEB2 (nuclear staining)	Superficial	(2+, 3+)	10/10 (100%)	6/10 (60%)
	Deep	H-Score>100	1/10 (10%)	1/10 (10%)

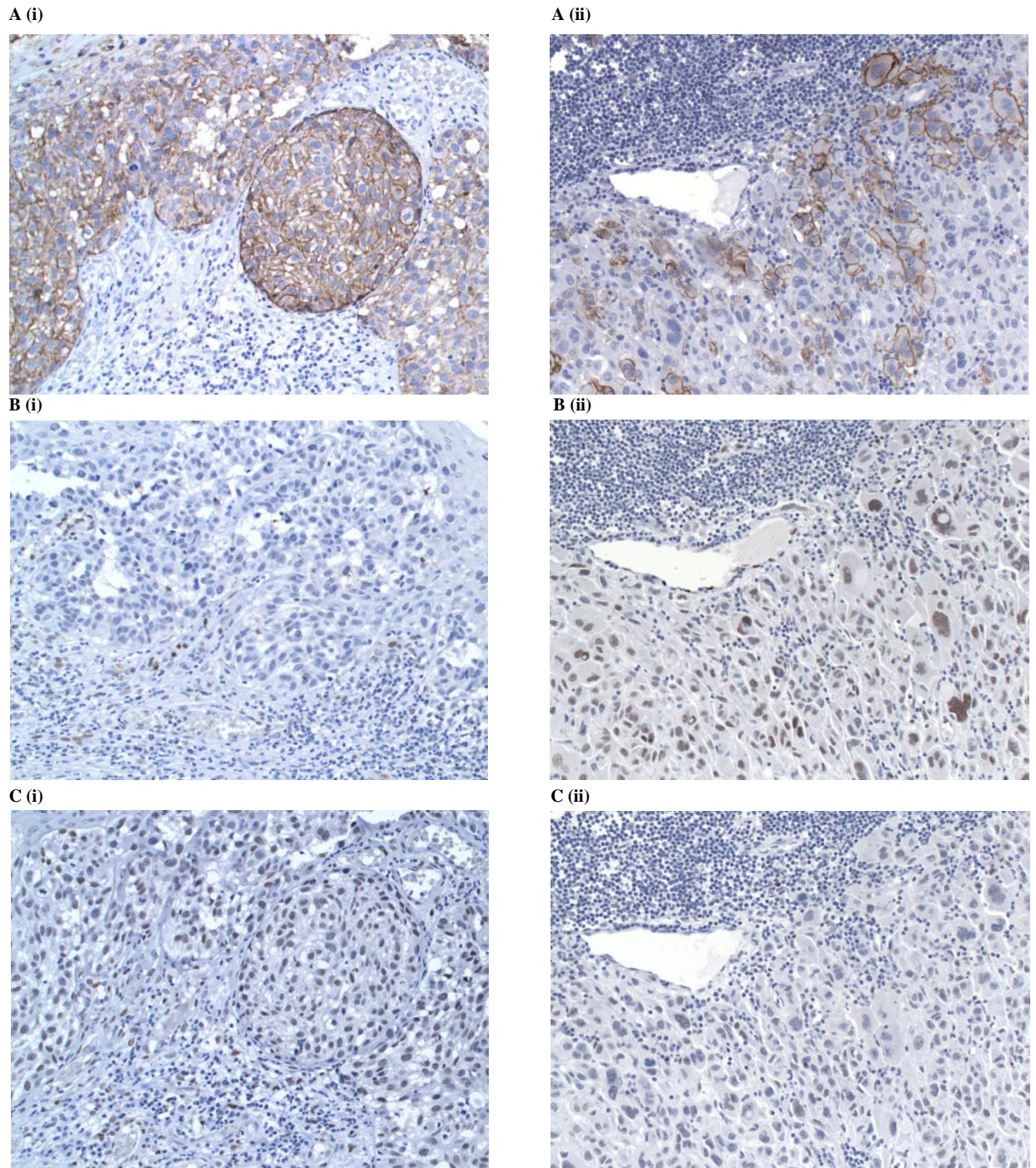


Figure 4.1 - Immunohistochemical staining of serial sections of paired metastasis specimens for the expression of E-cadherin, ZEB1 and ZEB2. Low power view ($\times 20$) of the primary MM shows strong cell membrane reactivity for E-cadherin (A-i), complete absence of staining for nuclear ZEB1 (B-i) and positive nuclear ZEB2 immunostaining (C-i) of tumour cells in superficial sites of MM. Low power magnification ($\times 20$) of the matched lymph node metastasis reveals weak cell membrane staining for E-cadherin (A-ii), positive nuclear ZEB1 reactivity (B-ii) and negative ZEB2 staining (C-ii) of tumour cells in the intratumoural area of the node.

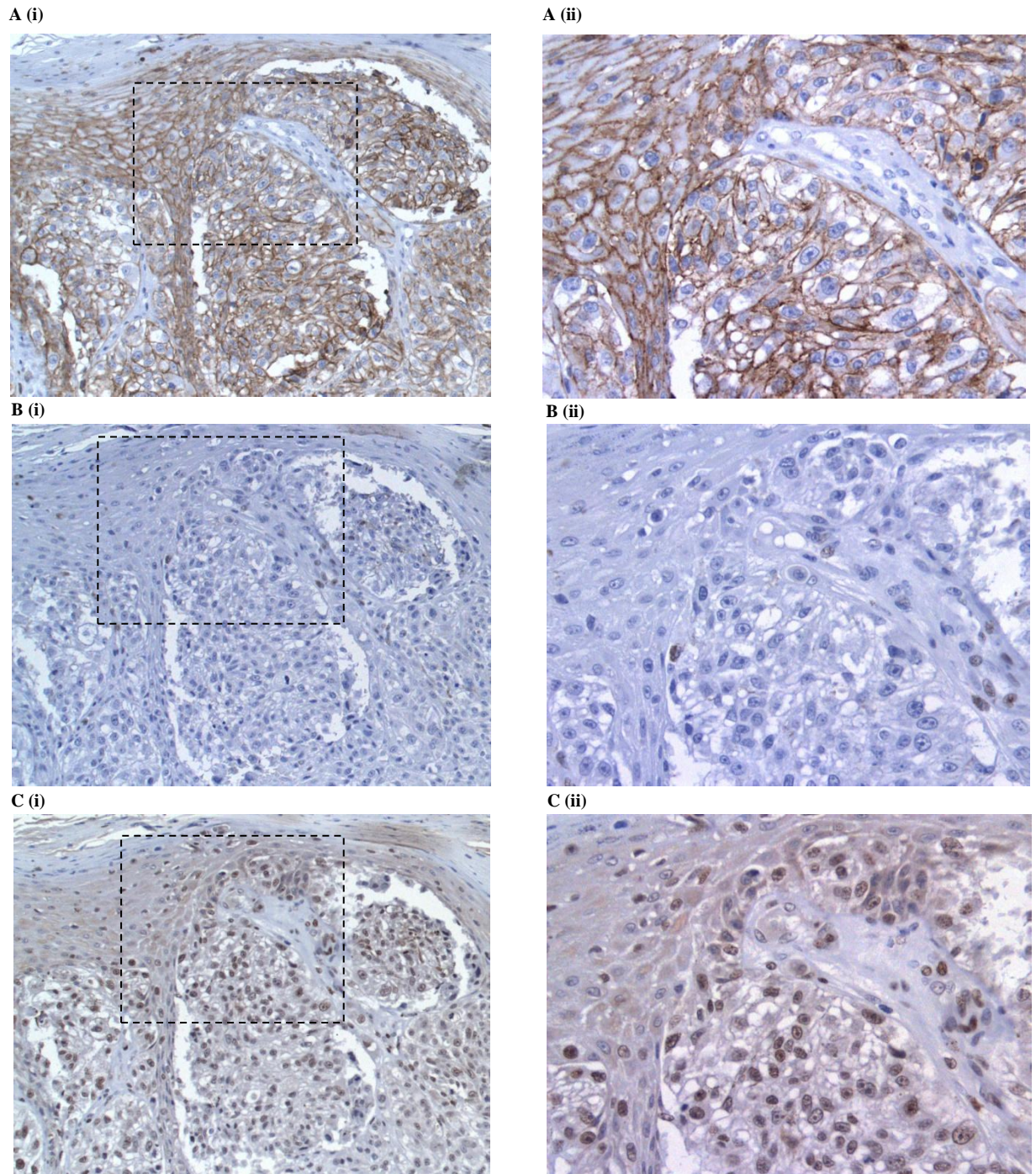


Figure 4.2 – Immunohistochemical staining of serial sections of a metastatic primary melanoma specimen for the expression of E-cadherin, ZEB1 and ZEB2. Low power view (×20) of the primary metastatic melanoma exhibits strong cell membrane E-cadherin reactivity (A-i), complete absence of staining for nuclear ZEB1 (B-i) and strong nuclear ZEB2 immunoreactivity (C-i) of tumour cells in superficial sites of MM. (A-C-ii) High power magnifications (×40) of A-C-i (rectangles). Staining of the paired lymph node metastasis is shown in Figure 4.3.

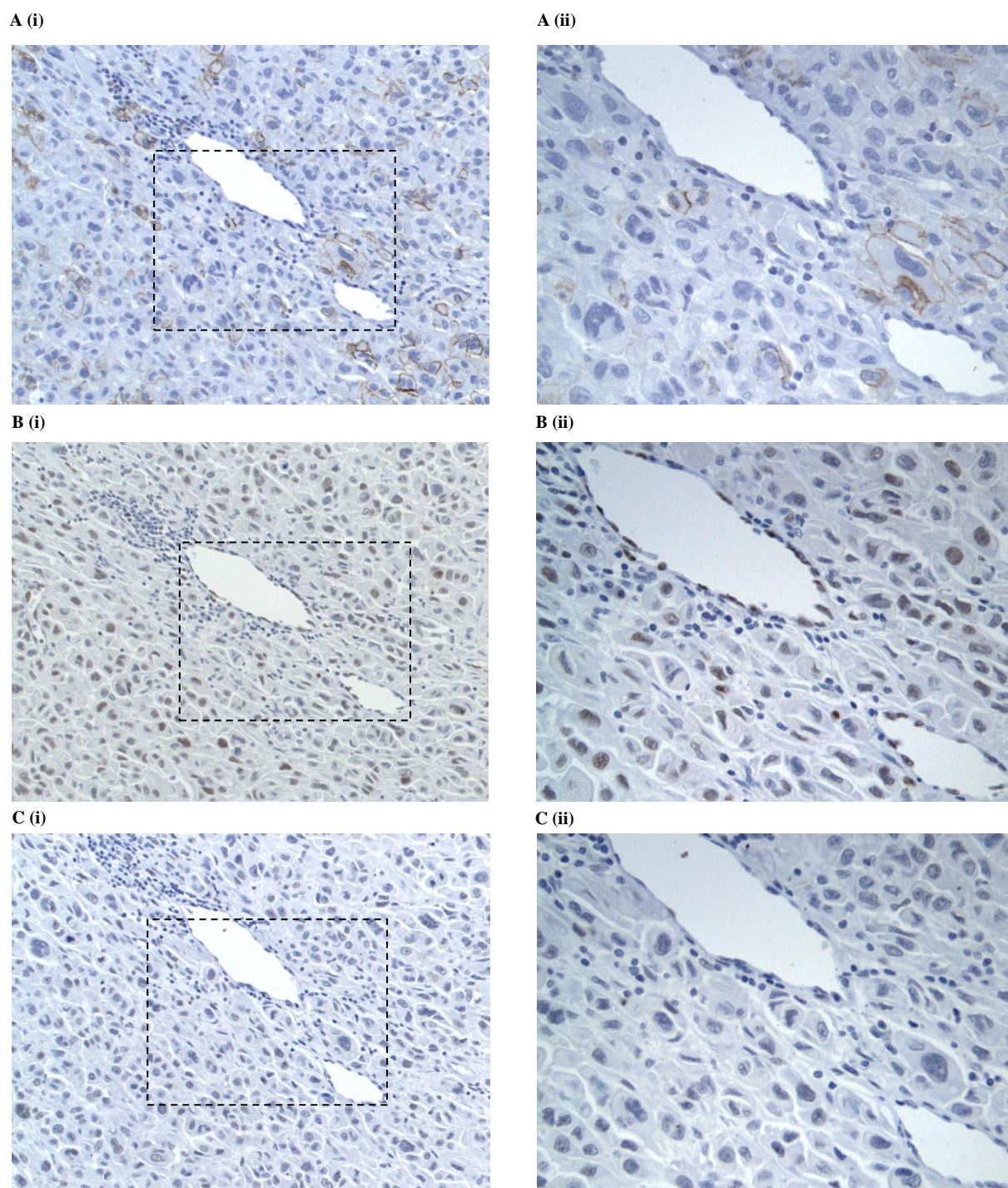


Figure 4.3 - Immunohistochemical staining of serial sections of a matched lymph node metastasis specimen for the expression of E-cadherin, ZEB1 and ZEB2. Low power view ($\times 20$) of nodal matched metastasis exhibiting weak cell membrane positivity for E-cadherin (A-i), strong nuclear ZEB1 immunoreactivity (B-i) and complete loss of ZEB2 nuclear staining (C-i) of tumour cells in the intratumoural area of the node. A-C-ii: higher power magnifications ($\times 40$) of A-C-i (rectangles).

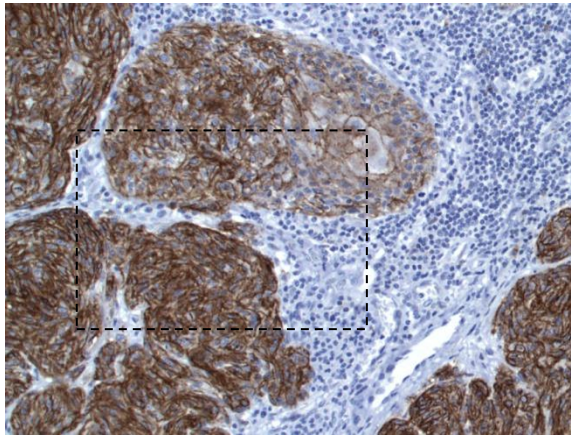
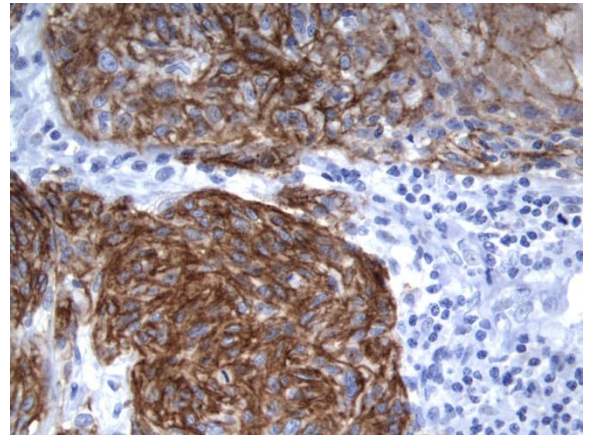
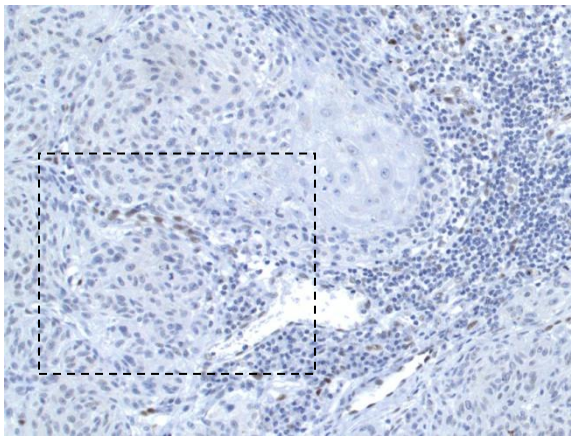
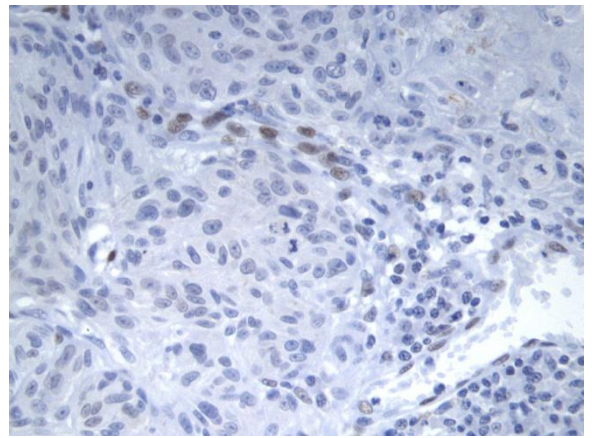
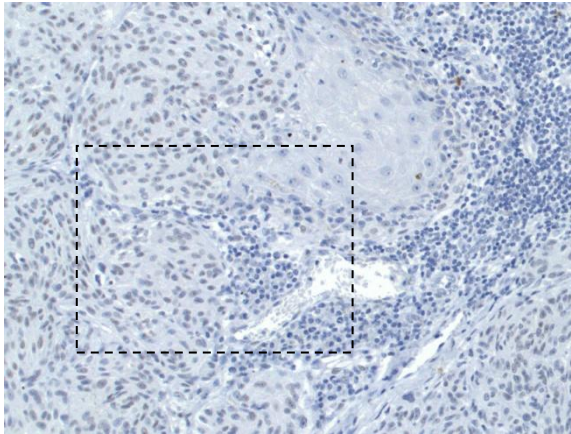
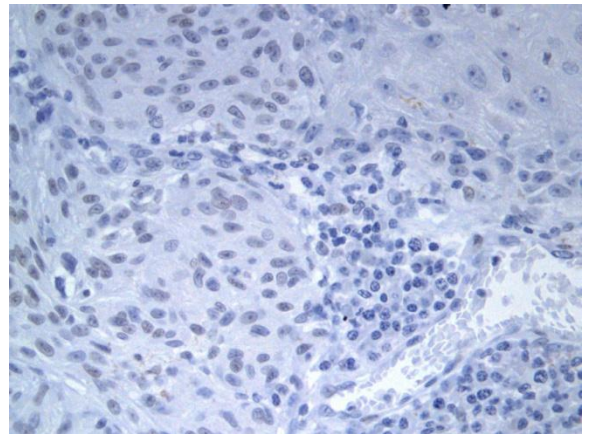
A (i)**A (ii)****B (i)****B (ii)****C (i)****C (ii)**

Figure 4.4 - Immunohistochemical staining of serial sections of a metastatic primary melanoma specimen for the expression of E-cadherin, ZEB1 and ZEB2. Low power view ($\times 20$) of the primary metastatic melanoma revealed strong cell membrane E-cadherin reactivity (A-i), complete absence of staining for nuclear ZEB1 (B-i) and weak nuclear ZEB2 immunoreactivity (C-i) of tumour cells in the deep sites of MM. (B-ii) High power magnification ($\times 40$) of B-i (rectangle) shows few positive stromal cells for ZEB1 in contrast with adjacent negative-tumour cells. A-C-ii: higher magnifications ($\times 40$) of A-C-i (rectangles). Staining of the paired nodal metastases is shown in Figure 4.5.

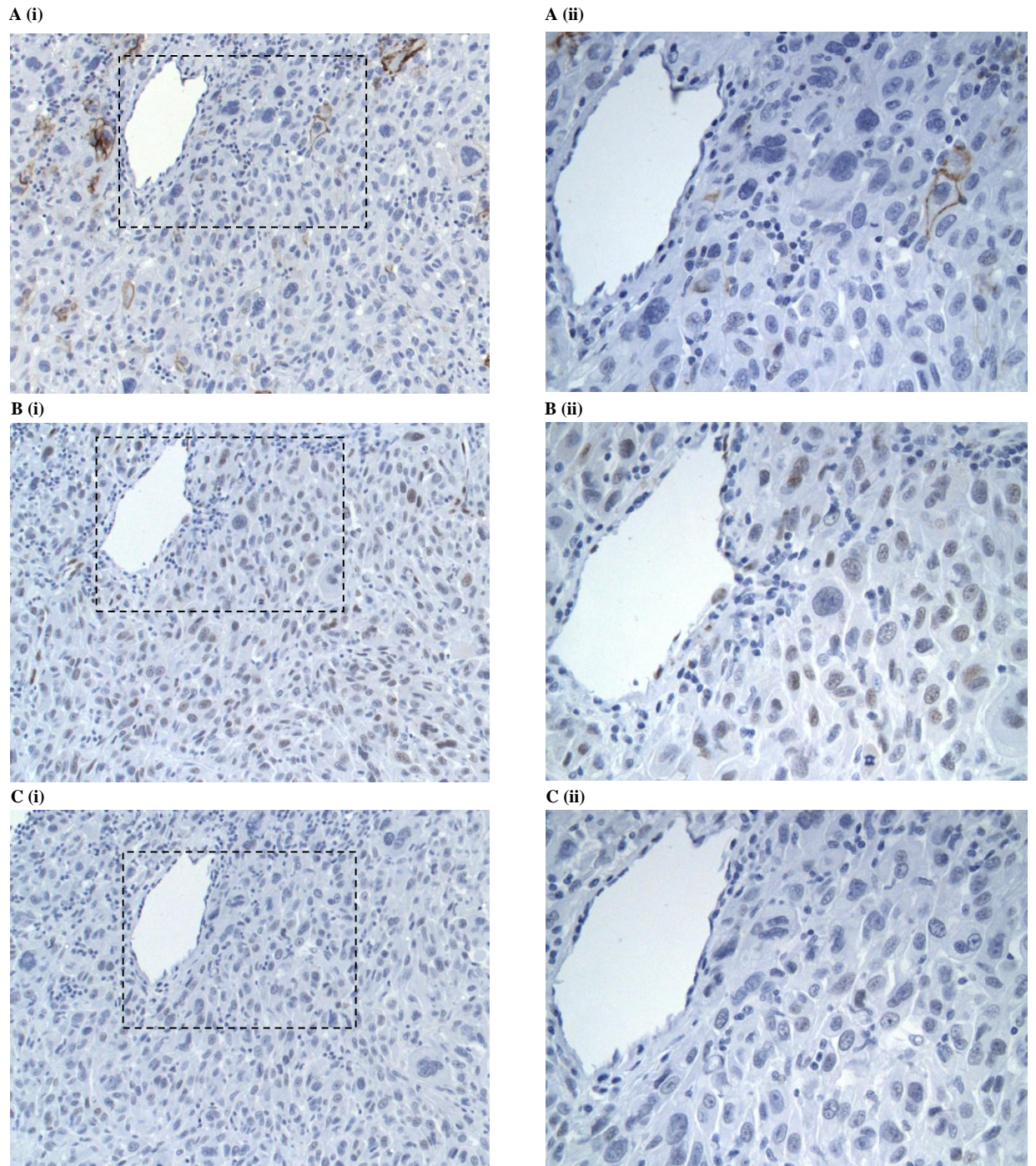


Figure 4.5 - Immunohistochemical staining of serial sections of a matched lymph node metastasis specimen for the expression of E-cadherin, ZEB1 and ZEB2. Low power view (×20) of a nodal metastasis demonstrating complete absence of reactivity for E-cadherin (A-i), strong nuclear ZEB1 immunoreactivity (B-i) and complete loss of ZEB2 nuclear staining (C-i) of tumour cells in the central part of the node. A-C-ii: higher magnifications (×40) of A-C-i (rectangles).

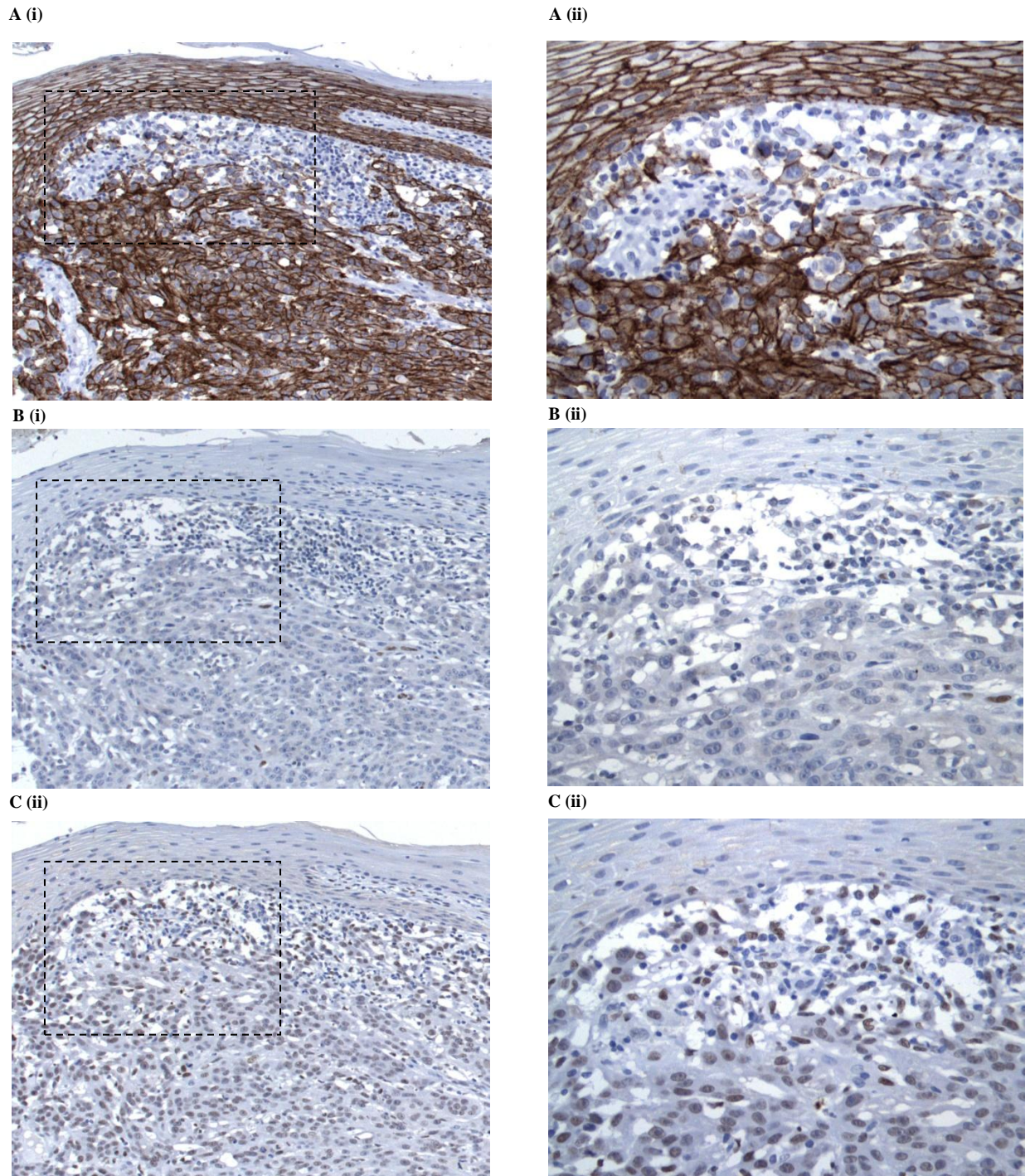


Figure 4.6 - Immunohistochemical staining of serial sections of a metastatic primary melanoma specimen for the expression of E-cadherin, ZEB1 and ZEB2. Low power view ($\times 20$) of the primary metastatic melanoma shows strong cell membrane E-cadherin reactivity (A-i), complete absence of staining for ZEB1 (B-i) and strong nuclear ZEB2 immunoreactivity (C-i) of tumour cells in the superficial sites of MM. (B-ii) High power magnification ($\times 40$) of B-i (rectangle) shows few positive stromal cells for ZEB1 in contrast with adjacent negative-tumour cells. A/B/C-ii: higher power magnifications ($\times 40$) of A/B/C-i (rectangles). Staining of the matched nodal metastasis is shown in Figure 4.7.

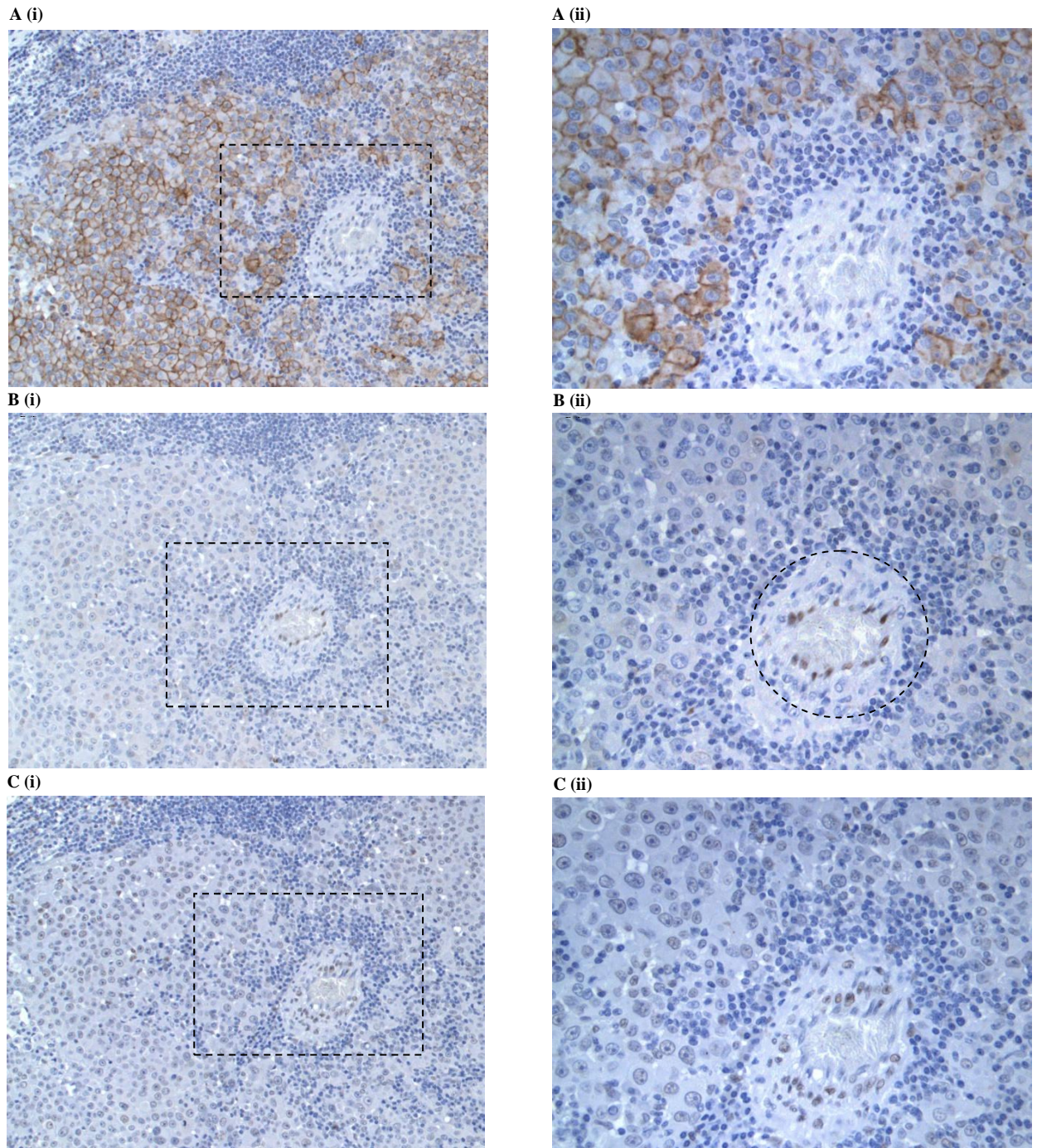


Figure 4.7 - Immunohistochemical staining of serial sections of a matched lymph node metastasis specimen for the expression of E-cadherin, ZEB1 and ZEB2. Low power view ($\times 20$) of a nodal matched metastasis exhibiting moderate reactivity for E-cadherin (A-i), complete loss of nuclear ZEB1 immunoreactivity (B-i) and weak nuclear ZEB2 staining (C-i) of tumour cells in the intratumoural area of the node. High power magnification ($\times 40$) of A-i (rectangle) shows positive cells for E-cadherin in contrast with adjacent negative-inflammatory and endothelial cells. A-C-ii: higher magnifications ($\times 40$) of A-C-i (rectangles). Note that endothelial cells (circle) were positive for ZEB1 (B-ii).

4.3.2 The effect of MR-EMT on the expression of E-cadherin in melanoma cultures

A poorly metastatic (A375P) cell line and a highly metastatic melanoma cell line (A375M), derived from a metastasis of the parental A375P, were used to determine alterations in E-cadherin protein profile *in vitro*. Melanoma cells were transiently transfected with either individual to ZEB1, ZEB2, SNAI2 and TWIST1 or combined siRNAs to ZEB1 and ZEB2 (Figures 3.12, 3.13-i and 4.8). In A375M cells, western blot analysis demonstrated that ZEB1 depletion led to an upregulation of E-cadherin protein expression after 96 hours (Figures 3.13-i and 4.8). In contrast, A375P cells showed reactivation of E-cadherin only after simultaneous silencing of ZEB1 and ZEB2 genes (Figure 4.8). ZEB2 knockout alone in both A375P and A375M cell lines and transient depletion of SNAI2 and TWIST1 in A375M cells by siRNAs produced no effect on E-cadherin protein levels (Figures 3.12, 3.13-i and 4.8). Interestingly, double knockdown of ZEB1 and ZEB2 proteins resulted in augmented re-activation of E-cadherin compared to siZEB1 alone, indicating an additive effect of ZEB2 on ZEB1 in metastatic melanoma cells (Figures 3.13-i and 4.8).

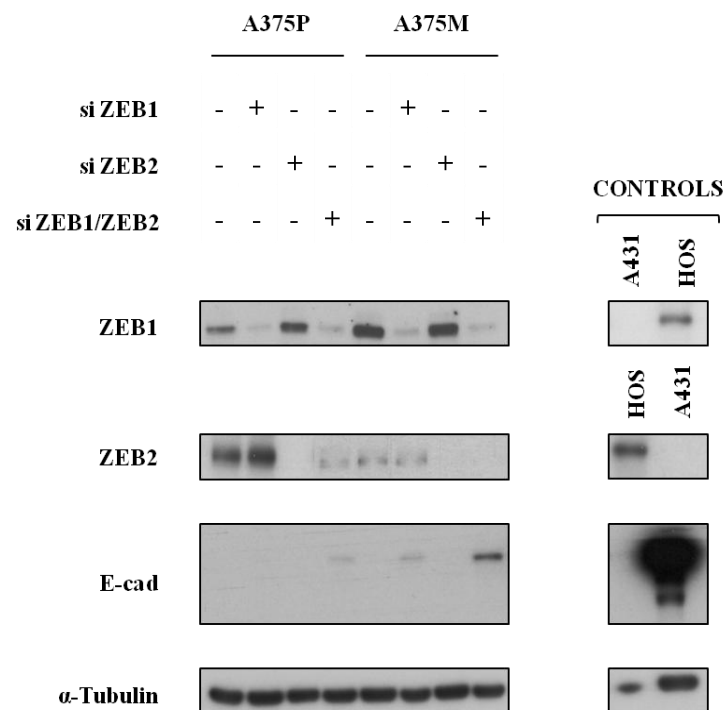


Figure 4.8 - The effect of siRNA-mediated depletion of ZEB1 and ZEB2 on E-cadherin protein expression in A375P and A375M cells. Melanoma cells were transfected with ZEB1, ZEB2 or co-transfected with ZEB1 and ZEB2 or control (-) siRNAs for 96 hours. A431 and HOS cells were used as a positive and negative control for E-cadherin (E-cad) respectively. Immunoblotting was performed with the indicated antibodies. Equal loading was confirmed by α -Tubulin. The blots shown are representative of four individual experiments.

4.3.3 The effect of ZEB1 on VDR expression in melanoma cell lines and tissues

To investigate the possibility that ZEB1 upregulation in MMs may also cause VDR downregulation, two melanoma cell lines (A375P and A375M) were examined by western blotting. The protein expression level of VDR was less in high ZEB1-expressing A375M metastatic melanoma cells compared to low ZEB1-A375P cells. Transient transfection of melanoma cells with ZEB1 siRNA led to increased VDR protein levels (Figure 4.9). In A375P cells, ZEB1 knockdown also showed an insignificant increase in ZEB2 protein levels.

The inhibitory effect of ZEB1 on VDR expression was next examined by immunohistochemistry in a small cohort of thirty specimens of melanomas, of which ten primary MMs, ten lymph node metastases and ten matched pairs of primary tumours and their corresponding metastases. Validation of antibody specificity using IHC-P and western blotting is shown in Chapter 5 (Figures 5.1 and 5.3-C). The results of immunohistochemistry staining of the VDR and ZEB1 are shown in Figures 4.10-4.12 and Appendix V-e. Both nuclear and cytoplasmic VDR staining was seen in the superficial and deeper sites of the primary MM cases (matched / independent). These cases (n=20) showed a distinct gradient of staining with stronger superficial nuclear staining compared to the deep sites, where the staining was mainly cytoplasmic (Figures 4.10-A/B-i and 4.12-A-i). VDR protein expression in lymph node metastases (matched / independent, n=20) showed cytoplasmic staining only (Figures 4.11-A-i, 4.12-B/C-i and Appendix V-e). Nuclear immunoreactivity of ZEB1 was detected in 20% (2/10) of primary tumours and 40% (4/10) of the corresponding matched metastases. Similar results were obtained in independent primary melanomas and metastases (n=20).

Consistent with previous results (section 4.3.1), ZEB1 staining was confined in small areas at deep / intratumoural sites of primary MMs and nodal metastases (Figure 4.12-A/B-ii). When VDR and ZEB1 were co-expressed in the deeper sites of the primary MMs and in the intratumoural areas of lymph nodes, VDR was localised to the cytoplasm of malignant cells (Figures 4.11 and 4.12).

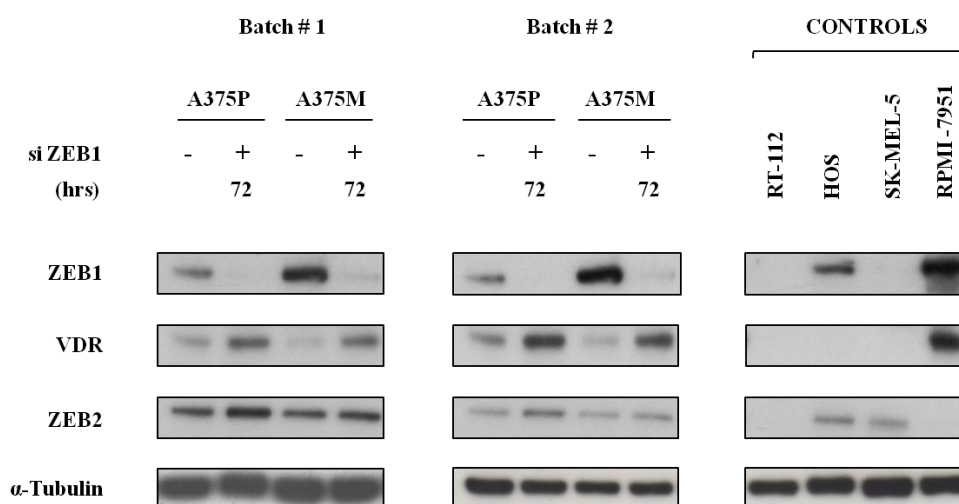
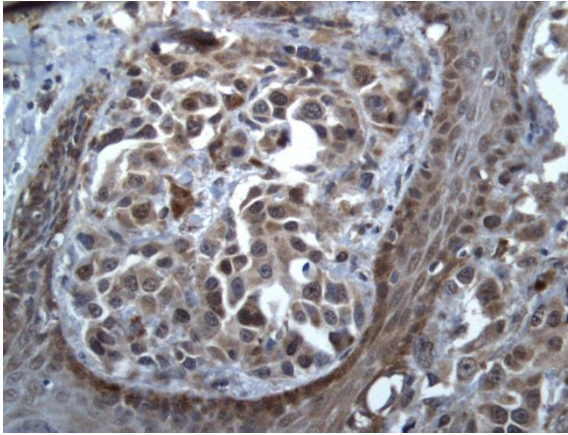
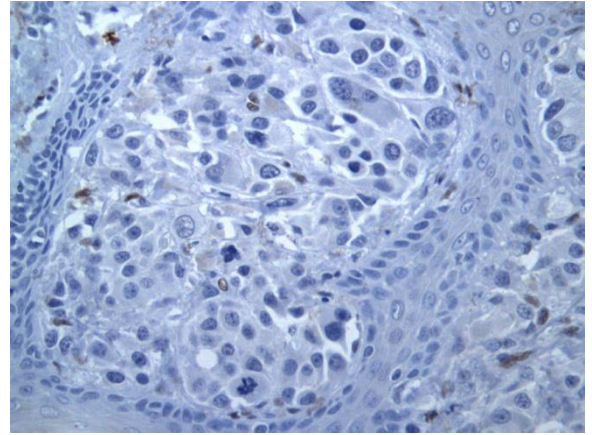


Figure 4.9 - The effect of siRNA-mediated depletion of ZEB1 on VDR expression in A375P and A375M cells. Melanoma cells were transfected with ZEB1 or control siRNA for 72 hours and the expression of ZEB1, ZEB2 and VDR proteins was analysed in western blotting as indicated. RPMI-7951 and SK-MEL-5 melanoma cells were used as a positive and negative control for VDR respectively. HOS and RT-112 cells were used as positive and negative controls for ZEB1 and ZEB2 respectively. Note that two different batches of melanoma cells were tested (#1 and #2). Equal loading was confirmed by α -Tubulin. The blots shown are representative of three individual experiments per batch of melanoma cells.

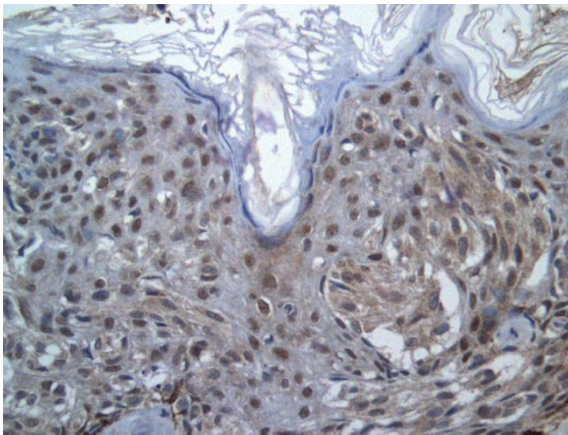
A (i)



A (ii)



B (i)



B (ii)

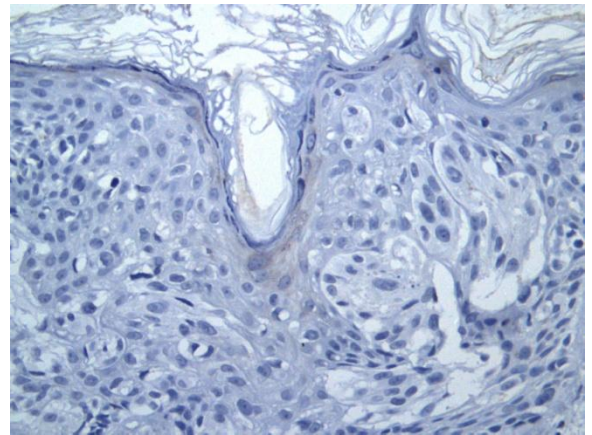
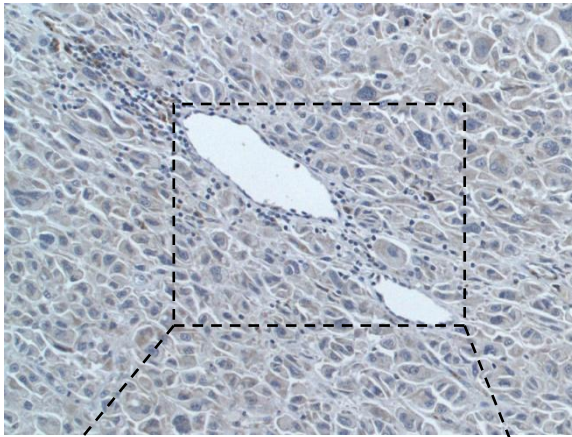
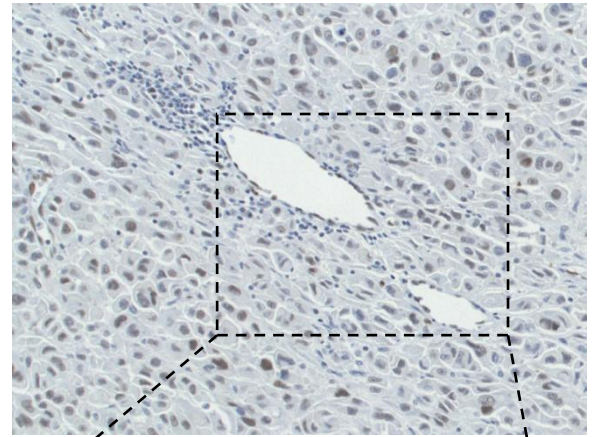


Figure 4.10 - Immunohistochemical staining of primary metastatic melanomas for VDR and ZEB1. Low power view (×20) of the same area of two primary melanomas showing superficial positive nuclear VDR staining (A/B-i) and ZEB1 negative staining (A/B-ii) in tumour cells.

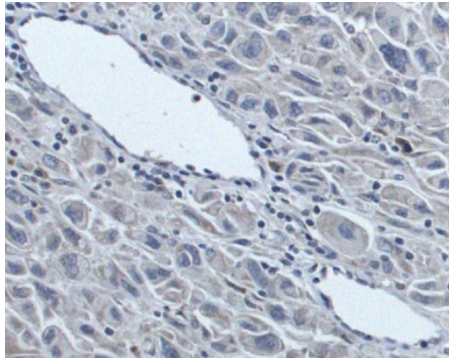
A (i)



A (ii)



B (i)



B (ii)

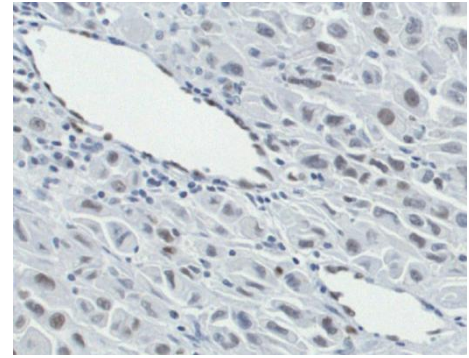


Figure 4.11 - Immunohistochemical staining of lymph node metastasis for VDR and ZEB1. Low power view ($\times 20$) of a metastatic case in lymph nodes shows positive cytoplasmic VDR staining (A-i) and positive nuclear ZEB1 staining (A-ii) of tumour cells in the central part of the node (rectangle). (B-i/ii) High power view ($\times 40$) of A-i/ii (rectangles).

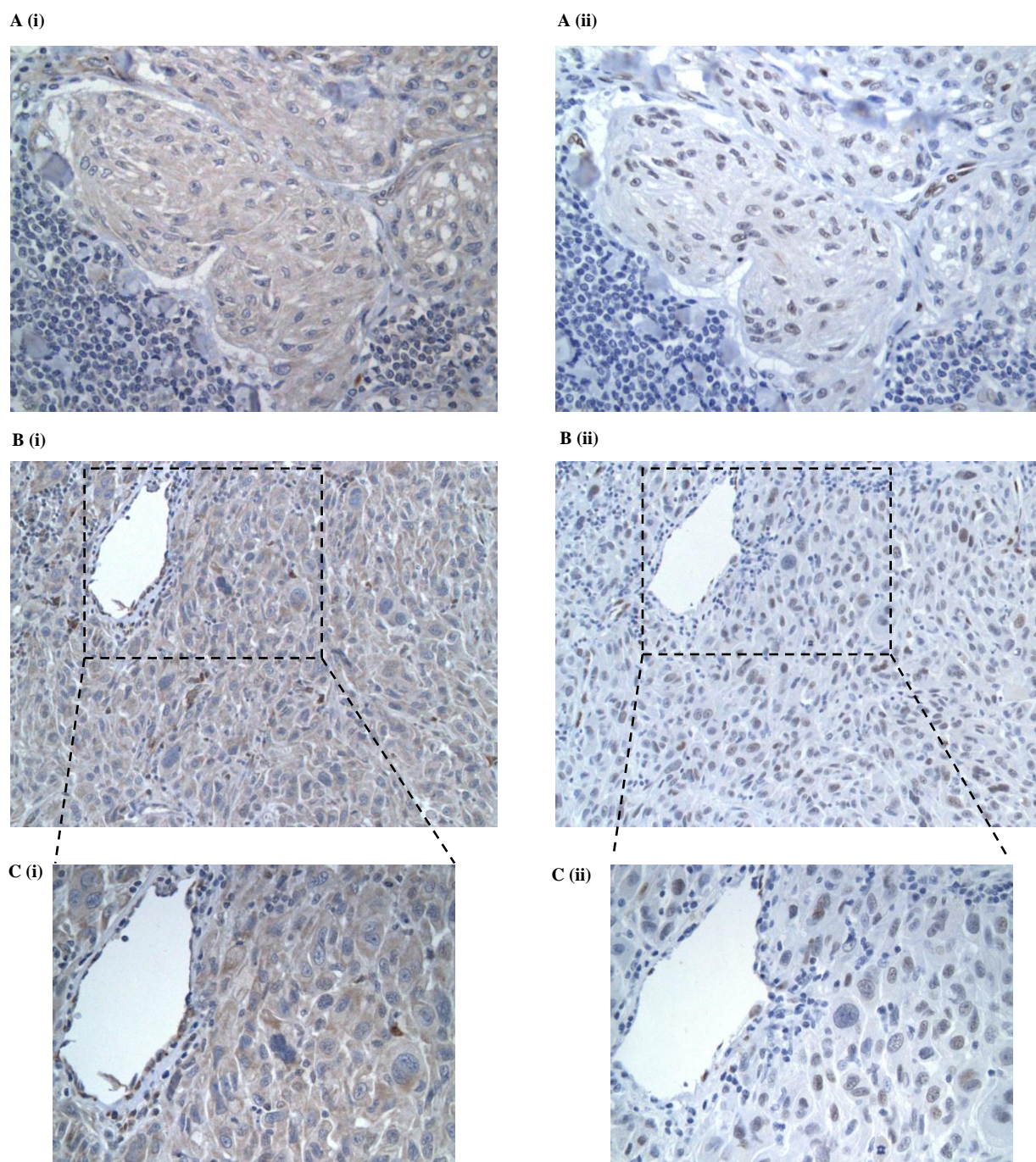


Figure 4.12 - Consecutive immunostainings for VDR and ZEB1 of a matched metastatic case. Low power magnification ($\times 20$) reveals positive cytoplasmic VDR (A-i) and positive nuclear ZEB1 staining (A-ii) of tumour cells in the deeper sites of a primary melanoma. Low power view ($\times 20$) of the corresponding metastasis in the inner core part of the lymph node shows cytoplasmic VDR immunoreactivity (B-i) and occasional nuclear staining for ZEB1 in cancer cells (B-ii). (C-i/ii) High power view ($\times 40$) of B-i/ii (rectangles).

4.3.4 Expression of miR-125b in melanocytic tumours

The expression of miR-125b in 55 melanomas was compared to 15 common acquired naevi (Figure 4.13). Unpaired t-tests revealed that there was a significant difference between common acquired naevi and primary melanomas / nodal metastases ($P < 0.0001$). A significant trend was found between common acquired naevi, primary melanomas with or without metastases and nodal metastases ($P < 0.001$, one-way ANOVA, post-test for a linear trend). These data suggest that loss of miR-125b may be involved in an early progression of cutaneous MM.

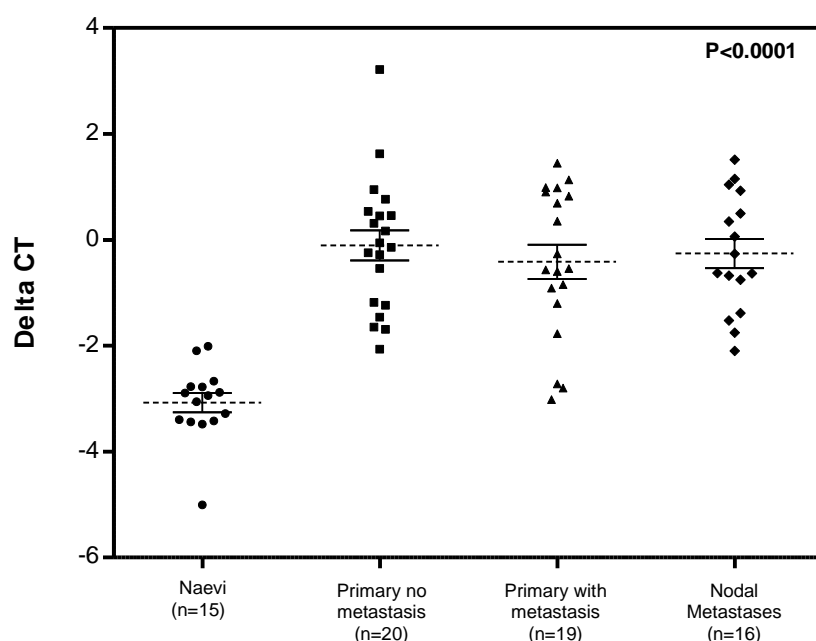
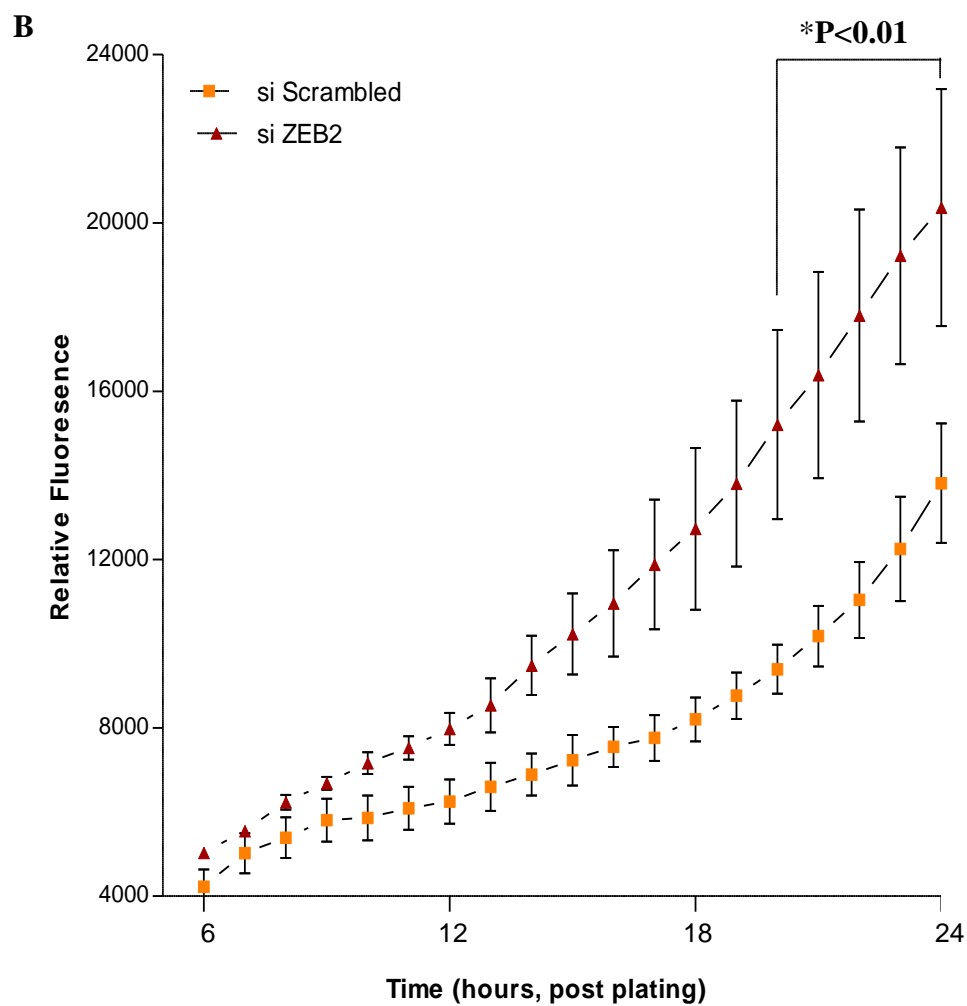
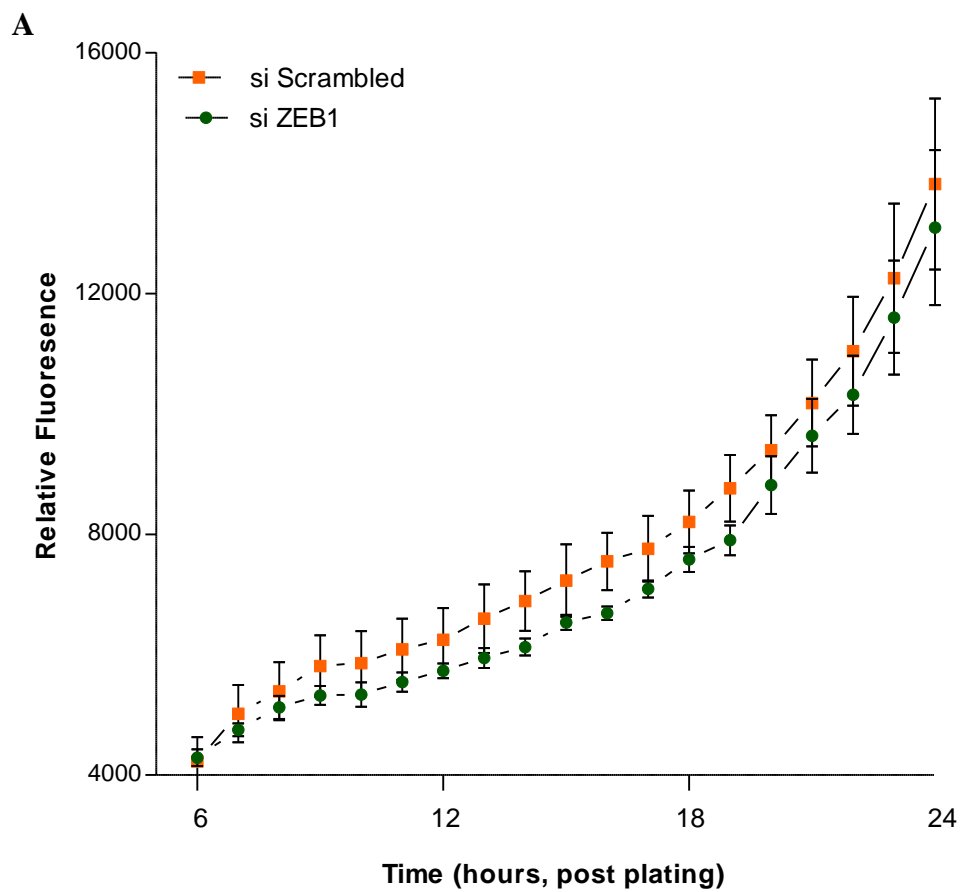


Figure 4.13 - Differential expression of miR-125b (ΔCt) in melanocytic lesions by qRT-PCR. RNA was extracted from CAN, primary MMs and nodal metastases. All measurements were performed in triplicates and normalized to endogenous levels of miR-191. Linear trend analysis showed a significant loss of miR-125b expression with tumour progression ($P < 0.0001$, one-way ANOVA, post-test for a linear trend). Mean \pm standard error of the means is included for each group.

4.3.5 The effect of ZEB1 and ZEB2 on the migration of melanoma cells

Transient knockdown with siRNAs was used to determine the effects of ZEB1, ZEB2 and combined siZEB1 / ZEB2 on migration in two melanoma cell lines (A375P and A375M) (Figures 4.14 and 4.15). Melanoma cells were efficiently transfected as shown in Figures 3.11, 3.13-i and 4.8. A375P cell line transfected with siZEB1 and siZEB1 / ZEB2 showed no significant decrease in motility compared with scramble siRNA controls (Figure 4.14-A/C). In contrast, siZEB2-transfected A375P cells showed enhanced migration over scramble siRNA control and became significant with increasing time ($P < 0.01$, two-way ANOVA / Bonferroni post-test) (Figure 4.14-B). No significant increase in migration was evident in the siZEB2-transfected A375M cells over scramble siRNA control with time (Figure 4.15-B). siZEB1 and siZEB1 / ZEB2 decreased tumour cell motility compared to scrambled siRNA in A375M cells, however significance appeared at later time points ($P < 0.05$ in both, two-way ANOVA / Bonferroni post-test) (Figure 4.15-A/C).



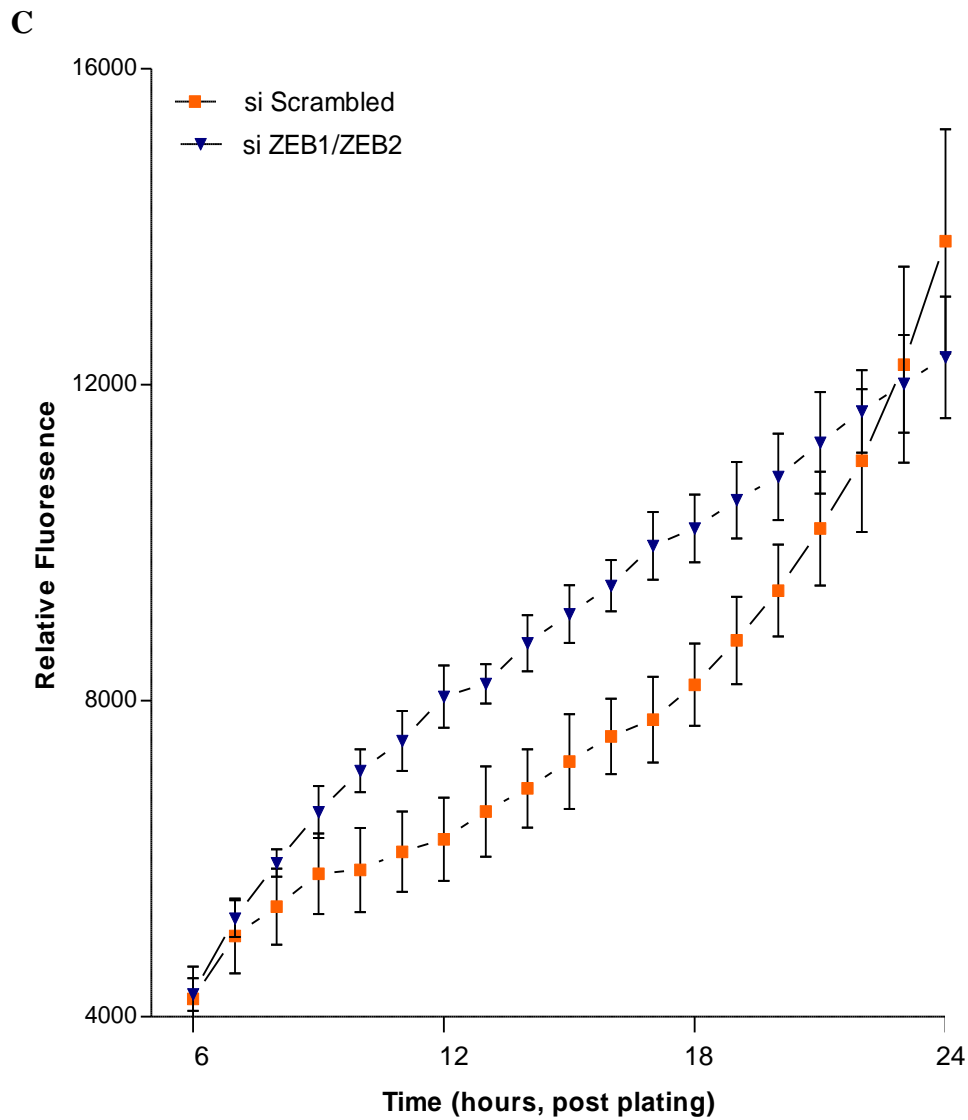
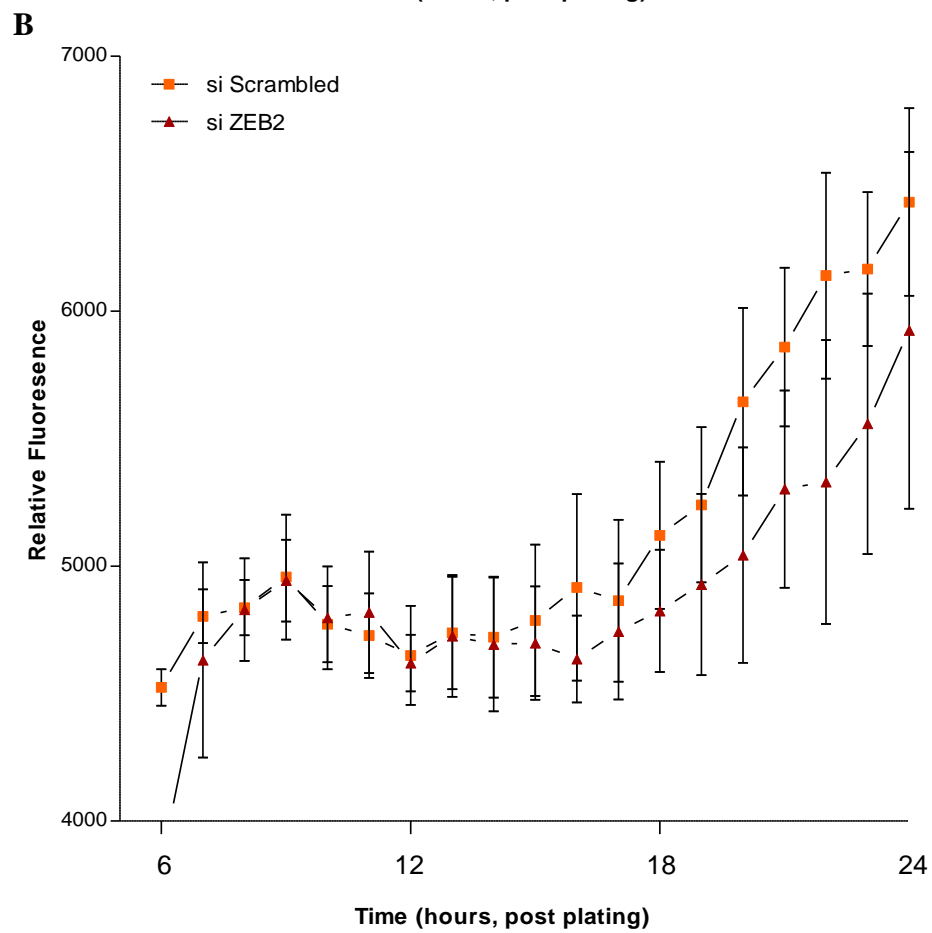
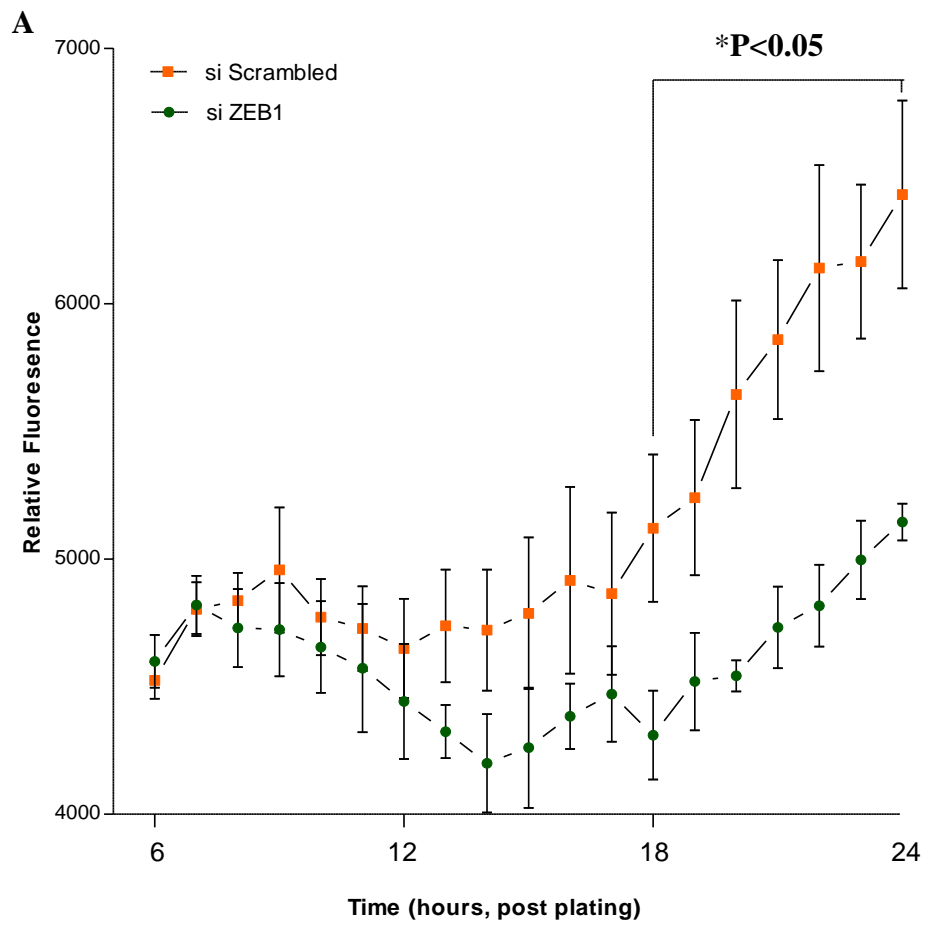


Figure 4.14 - The effects of ZEB1 and ZEB2 knockdown on tumour cell migration in A375P melanoma cells. Monitoring tumour cell migration in real time using a modified Boyden chamber assay in A375P cells transfected with siRNAs to ZEB1 (A), ZEB1 (B) and ZEB1/ZEB2 (C). Monitoring of motility assays started 48 hrs post-transfection with the relevant siRNA. In all cases, data points represent the mean of two replicates representing two separate transfections. Standard error of the mean is included for each data point. *P<0.01 compared to scrambled siRNA.



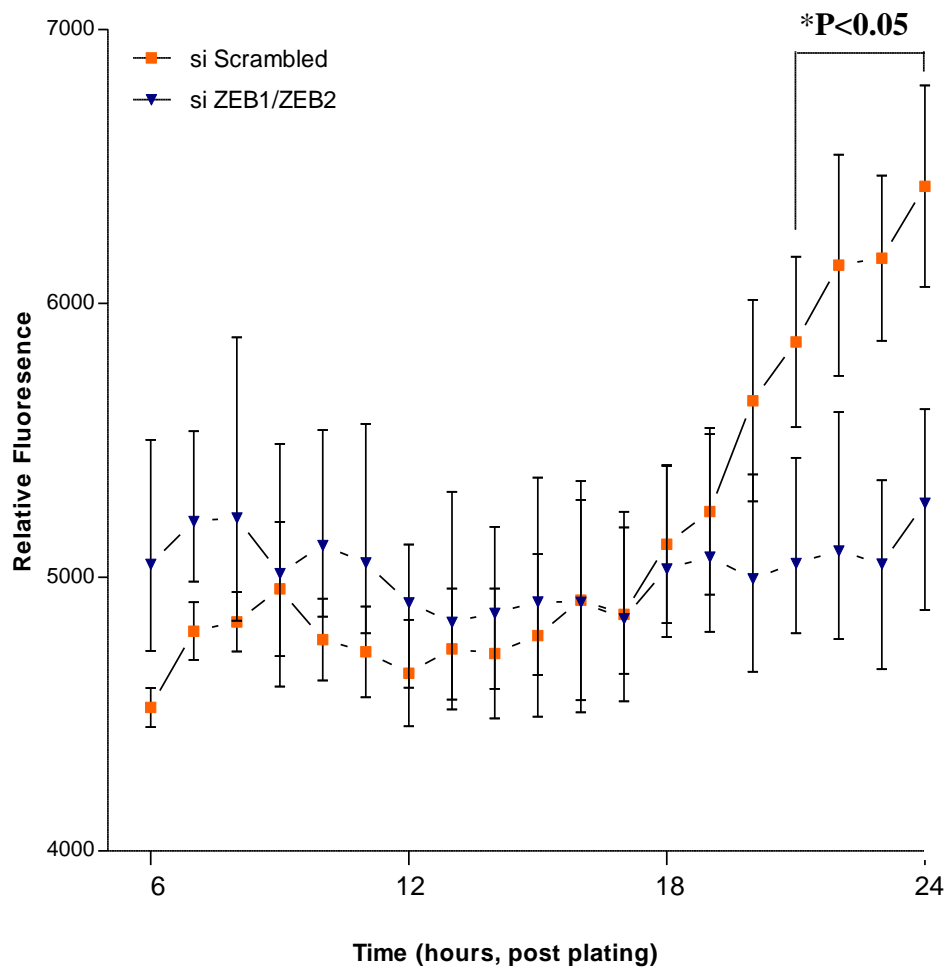
C

Figure 4.15 - The effects of ZEB1 and ZEB2 knockdown on tumour cell migration in A375M melanoma cells. Monitoring tumour cell migration in real time using a modified Boyden chamber assay in A375M cells transfected with siRNAs to ZEB1 (A), ZEB1 (B) and ZEB1/ZEB2 (C). Monitoring of motility assays started 48 hrs post-transfection with the relevant siRNA. In all cases, data points represent the mean of two replicates representing two separate transfections. Standard error of the mean is included for each data point.*P<0.05 compared to scrambled siRNA.

4.4 Discussion

4.4.1 *E-cadherin - ZEB1/2 relationships in melanocytic tumours and cell lines*

Loss of E-cadherin is a hallmark of EMT that is implicated in the transition from horizontal to vertical growth in MM (Hsu et al., 2000). Its silencing could be mediated by various epigenetic mechanisms, including transcriptional repression by MR-EMT and promoter hypermethylation. In siRNA mediated knockdown experiments of individual MR-EMT, ZEB1, but not ZEB2, SNAI2 or TWIST1, restored expression of E-cadherin in melanoma cells which is consistent with previous results (Figures 3.12, 3.13-i and 4.8) (Wels et al., 2011). This observation was confirmed in other BRAF mutated melanoma cell lines, including WM-266-4 and RPMI-7951 (Dr. E Tulchinsky, personal communication). These findings may imply that transient activation of ZEB1 is sufficient to maintain repression of E-cadherin without requiring additional epigenetic mechanisms in malignant melanomas, such as DNA methylation.

It has been recently documented that both ZEB1 and SNAI2 cooperatively repressed E-cadherin expression (Wels et al., 2011). Co-expression of these transcription factors was essential in enhancing migration of metastatic melanoma cells and suggested a regulatory feedback during EMT. Herein, simultaneous inhibition of ZEB1 and ZEB2 showed the most significant effect on E-cadherin upregulation and further enhanced the effect of ZEB1 individual gene silencing in A375M cells, indicating that ZEB2 does not repress E-cadherin on its own.

The *in vitro* findings were consistent with IHC-P analyses that showed reduced E-cadherin and increased ZEB1 protein levels in a subset of metastatic primary melanomas and lymph node metastases. Several recent reports provided supporting evidence for a reciprocal expression of ZEB1 and E-cadherin in the progression of

different malignancies (section 1.4.2.3). In addition, a study by Browne *et al* documented that even if ZEB1 was infrequently expressed in muscle invasive bladder carcinomas, its expression was perfectly correlated with the lack of E-cadherin (Browne *et al.*, 2010). In the present study, the near mutually exclusive pattern of ZEB1 and E-cadherin expression in metastatic melanoma tissues indicated that ZEB1 may act as a potent repressor of E-cadherin in human melanocytic tumours.

Less published data is available concerning the expression of ZEB2 in tumour tissues. Recently, new ZEB2 antibodies were tested showing high specificity and this has opened the possibility of exploring the expression pattern of ZEB2 in patient tissues and human tumour cell lines (Oztas *et al.*, 2010). Whereas ZEB1 protein was expressed in a range of E-cadherin negative carcinoma cell lines, ZEB2 was hardly ever detectable in transformed malignant cells *in vitro* (Sayan *et al.*, 2009). In contrast, this study demonstrated a variable expression of ZEB2 protein in all melanoma cultures tested (Figure 3.3).

Increased ZEB2 expression correlated inversely with E-cadherin in advanced stages of different types of carcinomas (Dai *et al.*, 2012, Imamichi *et al.*, 2007, Sayan *et al.*, 2009). Interestingly, in this work immunohistochemical staining of serial sections in a small series of paired melanoma specimens showed that the majority of tumour areas co-expressed ZEB2 and E-cadherin. This result coincides with a limited number of previous findings, which indicated a positive correlation between ZEB2 and E-cadherin expression in a subset of aggressive carcinomas, including malignant mesotheliomas (Sivertsen *et al.*, 2006).

More recently, Browne *et al* demonstrated muscle invasive bladder tumour cases in which E-cadherin and ZEB2 were co-expressed (Browne et al., 2010). Multiple tissue arrays suggested that in most of the analysed normal tissues, such as colon surface epithelium and kidney tubules, ZEB2 and E-cadherin were co-existent (Oztas et al., 2010). Therefore and unlike ZEB1, E-cadherin and ZEB2 expression is not necessarily mutually exclusive. In accordance with this observation other MR-EMT showed the same pattern of expression. SNAI2 was found to be co-expressed with E-cadherin in invasive ductal carcinomas of the human breast, in patients with ESCC and during cutaneous wound re-epithelialisation of migrating adult keratinocytes in mice (Come et al., 2004, Savagner et al., 2005, Uchikado et al., 2005). Furthermore, the overall survival rate was worse in a subset of ESCC patients with preserved E-cadherin expression and SNAI1 immunopositivity (Natsugoe et al., 2007). However, it remains to be addressed the E-cadherin expression in the presence of potent transcription repressors. It has been previously reported that ZEB2 protein sumoylation at Lys391 and Lys866 disrupts the recruitment of the co-repressor CtBP and therefore attenuates repression of the *E-cadherin* promoter (Long et al., 2005). As a consequence, posttranslational modifications may partly explain this phenomenon in benign and malignant melanocytic lesions as well as in normal melanocytes.

4.4.2 ZEB1 regulates VDR expression in MM

In MM and other malignancies, there is evidence that cancer cells become unresponsive to vitamin D and thus evade its anti-proliferative and anti-apoptotic activity (Evans et al., 1996). Unpublished results of immunohistochemistry staining of VDR (Dr. PE Hutchinson, personal communication) in an archive of patient samples revealed that a significant proportion of primary and metastatic melanomas showed decrease in VDR expression with tumour depth, negatively stained cells and highest cytoplasmic localisation in nodal metastases. From the same data was also evident that in the benign melanocytic lesions the VDR staining was confined only to the nuclei and deep lesions showed weaker staining. In addition, a recent study demonstrated that VDR protein reduction was more pronounced in cell nuclei than in cytoplasm with the development of pigmented lesions (Brozyna et al., 2011).

Identical results have been observed in this study, when a small number of independent and paired melanoma biopsies tested for VDR immunoreactivity showed decrease of staining in the deep sites of primaries and nodal metastases and a cytoplasmic location in all metastatic lesions (Figures 4.10 - 4.12-A/B-i, Appendix V-e). A possible explanation for the loss of expression in deep melanocytic lesions is that during early development tumour malignant cells with decreased expression of VDR are more likely to invade deeper into the dermis and metastasise. In the progression of melanocytic lesions, increasing ratios of the receptor expression in the cytoplasm compared with the nucleus indicates that less of this protein translocate to the nucleus. Such augment of the non-functional cytoplasmic protein expression can contribute to the escape of neoplastic cells from growth control and homeostatic surveillance.

As yet, the mechanism for cytoplasmic accumulation of VDR has not been explored extensively. In addition, published evidence demonstrated that constitutive active MAPK signalling-induced RXR α phosphorylation resulted in reduced 1,25(OH) $_2$ D $_3$ -mediated gene transcription in transformed prostate epithelial cells (Zhang et al., 2010). Phosphorylation of RXR at serine 260 also led to a disrupted recruitment of co-activators to the VDR / RXR α complex inducing vitamin D resistance in *RAS*-transformed keratinocytes (Macoritto et al., 2008). In addition, RXR was found to promote VDR nuclear retention (Prufer and Barsony, 2002). Therefore, it is plausible to argue that increased VDR cytoplasmic expression during melanoma progression may be due in part to the RXR posttranscriptional changes at specific amino acid residues.

A study conducted by Reichrath and colleagues demonstrated that only about half of melanoma cell lines respond to 1,25(OH) $_2$ D $_3$, the ligand of the VDR (Reichrath et al., 2007). VDR protein analysis in human malignant melanoma cell lines showed reduced expression of VDR in the metastatic A375M cell line compared to the parental, less aggressive, A375P. In contrast to the MM cell lines, endogenous protein expression of VDR was absent in cultured normal melanocytes, but 1,25(OH) $_2$ D $_3$ induced VDR responsiveness and that was in accordance with previous studies (Ranson et al., 1988) (Appendix VI). This supports a mechanism whereby 1,25(OH) $_2$ D $_3$ autoregulates the expression of its own receptor by the presence of VDR response elements within the *VDR* gene (Pike et al., 2007, Zella et al., 2006). In melanoma cultures this regulation seems to be impaired as two of the MM cell lines derived from metastatic disease, SK-MEL-2 and WM-266-4, were unresponsive to 1,25(OH) $_2$ D $_3$ (Appendix VI). In this example the opposite is the case, as a melanoma cell line derived from a primary melanoma (SK-MEL-28) showed a weak response to 1,25(OH) $_2$ D $_3$. Therefore, decreased VDR nuclear expression in metastatic primary melanomas and nodal

metastases and unresponsiveness to $1,25(\text{OH})_2\text{D}_3$ in most of melanoma cell lines supports its important role controlling differentiation of melanoma cells and suppressing transformation and progression of the disease.

The molecular mechanisms for $1,25(\text{OH})_2\text{D}_3$ ligand insensitivity in malignancies are as yet ambiguous. A possible mechanism regulating VDR signalling in MM could include a direct binding and functional inhibition of the *VDR* gene promoter by different EMT transcriptional repressors. Consistent with the hypothesis that MR-EMT act as transcriptional repressors of VDR with the development of cancer, Mittal *et al* documented that SNAI2 repress directly the *VDR* by binding to its promoter in breast cancer cells (Mittal et al., 2008). In addition, SNAI1 and SNAI2 transcription factors are not only inverse correlated with VDR but also act additively to represses the *VDR* gene promoter in cultured colorectal cells and patient samples (Larriba et al., 2009). As a result, a correlation between the upregulation of SNAI1 and / or SNAI2 and the loss of VDR may be a good indication of a similar resistance mechanism operating in MM.

Unlike to other carcinomas, recent findings of Mikesch *et al* and Shirley *et al* revealed lower protein expression of SNAI1 and SNAI2 in metastatic melanocytic lesions compared to naevi and primary melanomas and in metastatic cell lines (Mikesch et al., 2010, Shirley et al., 2012). These findings indicated that downregulation of VDR is not necessarily related to the repressive activity of the SNAI family members, and might other EMT inducers, such as ZEB1 and ZEB2, contribute to the onset of an invasive and metastatic phenotype during melanoma progression and the loss of VDR.

Although, *ZEB* genes have been classically described as transcriptional repressors, it has been reported an opposite effect of ZEB1 on *VDR* promoter activity in SW620 colon carcinoma cells (Lazarova et al., 2001). This switch of function of ZEB1 can be achieved through differential recruitment of either co-activators (p300 and p300 / CBP-associated factor, PCAF) or co-repressors (C-terminal-binding protein, CtBP) (Postigo et al., 2003). However, the work of Larriba *et al* suggested that ZEB1 and ZEB2 did not repress the *VDR* gene promoter activity in a colorectal cell line SW480-ADH, which is responsive to $1,25(\text{OH})_2\text{D}_3$ (Larriba et al., 2009).

The current study indicated that transient repression of ZEB1 by specific siRNAs increased dramatically the endogenous VDR protein levels in the BRAF mutated A375 melanoma cells (Figure 4.9). In addition, immunohistochemical analysis in a subset of tumour biopsies showed a differential staining pattern between VDR and ZEB1 (Figures 4.10-4.12). Taken together these results provided evidence that ZEB1 is involved in the repression of VDR in melanoma. In addition, the changed ratio of cytoplasmic relative to nuclear VDR may act synergistically with ZEB1 stimulation to reduce or inhibit VDR activity and promote aberrant growth and tumour metastasis.

Another mechanism of downregulation of the VDR in malignancy includes miR inhibition of VDR protein synthesis. In many studies different types of tumours showed a negative correlation between the VDR protein and mRNA levels, indicating that VDR suppression is partially subject to posttranscriptional regulation (Essa et al., 2012, Vuolo et al., 2012). Recently it has been documented for the first time, that VDR is a potential target for miR-125b (Mohri et al., 2009). This study revealed that miR-125b could bind to the 3'UTR region of the mRNA-VDR, resulting in VDR downregulation in MCF-7 breast cancer cells. This inverse relationship was further confirmed in

melanoma cell lines (Essa et al., 2010). Two recent studies from Glud *et al* confirmed that miR-125b expression not only was significantly reduced in non-metastasising melanomas compared to metastases in lymph nodes but also induced senescence in human transformed melanocytes (Glud et al., 2011, Glud et al., 2010). Evidence from this study demonstrated miR-125b is lost with melanoma progression and therefore cannot act to repress VDR. This suggests that expression of this particular miR may be used to identify benign disease rather than a prognostic marker of metastasis (Figure 4.13).

4.4.3 ZEB proteins affect migration in BRAF mutated melanoma cell lines

Activation of ZEB1 transcription by silencing of ZEB2 might have consequences for functionality. There is a large body of evidence indicating that MR-EMT induce migration in various cell types. Due to the E-cadherin reactivation after double silencing of ZEB1 and ZEB2, it has been postulated a migratory-promoting role of these factors. In fact, double knockdown of ZEB1 and ZEB2 by siRNAs resulted in a decreased migration of A375M melanoma cell cultures (Figure 4.15). Of note, individual knockdown for ZEB2 showed increased migration only in high-ZEB2 A375P cells (Figure 4.14) that may be supported by recent findings indicating the tumour suppressive properties of ZEB2 in melanoma (Karreth et al., 2011). Knockdown of ZEB1 activated E-cadherin and suppressed migration only in high-ZEB1 A375M cells (Figure 4.15).

Interestingly, migration assays showed that A375P cells were more motile (higher relative fluorescence) compared to A375M cells. This observation is puzzling as high metastatic variants were expected to have an enhanced migratory potential. However, a

recent study demonstrated that A375P cells are subdivided into two cell populations with different morphology (40%-mesenchymal / elongated phenotype and 60% rounded / amoeboid phenotype) (Sanz-Moreno et al., 2008). Alternatively, the A375M cells, used in this study, were predominantly of an elongated phenotype (>95%).

In the Boyden chamber-based motility assays A375 cells were exposed to a chemoattractant solution and passed through a uniform microporous membrane. In this movement cells must squeeze their cell body through a narrow space. In addition, it has been demonstrated that non-muscle myosin-II activity is a prerequisite for nuclear translocation through narrow pores, which is a vital step for rapid migration (Breckenridge et al., 2010). Thus, it can be postulated that A375P single cells may migrate fast through mechanically restrictive pores due to the presence of less bulky rounded cells and increased activity of the non-muscle myosin-II. Conversely, decreased movement of A375M cells may be indicative of a perturbed non-muscle myosin-II activity and slower mesenchymal-type movement. Perhaps the use of transverse micro-pores that vary in width and length will facilitate fast migration of the relatively bulky A375M cells.

4.4.4 Conclusions

- In ZEB1 immunopositive tumour areas of metastatic melanomas, ZEB2 and E-cadherin protein expressions were either reduced or completely lost. In the same tumour areas, VDR protein expression was either absent or localised exclusively in the cytoplasm of tumour cells.
- Transient knockdown of ZEB1 in melanoma cells demonstrated increased protein expression for VDR and E-cadherin.
- siRNA experiments clearly indicated that ZEB1, but not ZEB2, SNAI2 or TWIST1, represses E-cadherin in melanoma cells. Interestingly, double knockdown of ZEB1 and ZEB2 showed the highest repressive activity in the same cells.
- The previous work in melanoma cell lines showed that miR-125b targets VDR. This was not confirmed in melanoma tissues as miR-125b expression was significantly reduced in primary and metastatic melanoma tissues compared to the naevi.
- Transient depletion of ZEB1 significantly reduced cell motility in A375M cells. In contrast, ZEB2 siRNA-mediated inhibition significantly augmented the migratory ability of A375P cells. Double knockdown of ZEB1 and ZEB2 significantly impaired cell motility in A375M melanoma cells.

5 Distribution of MR-EMT in melanoma tissues and mouse melanoma model

5.1 Introduction

The EMT repressor proteins are required to complete gastrulation and the migration of the neural crest cells during embryonic development. In these tightly regulated processes, different EMT transcription factors, including genes of the *SNAI*, *TWIST* and *ZEB* superfamilies, repress E-cadherin expression, causing epithelial cells and melanoblasts to acquire a fibroblastic phenotype. Notably, the same EMT regulators are found to be reactivated in different types of highly-aggressive tumours. However, the published data on a role of EMT transcription factors in melanocytic lesions is incomplete and comes mostly from cell line and animal model studies. As yet, while *SNAI1* was found to be expressed only in a small number of melanoma tissue samples (4%) (Mikesh et al., 2010), immunohistochemical distribution of other MR-EMT was either assessed in a limited number of cases (*TWIST1*) (Ansieau et al., 2008) or not studied at all (*ZEB1* and *ZEB2*). In this respect, *in vivo* analysis of a subset of EMT repressors will give a greater understanding to their potential role in melanoma progression.

5.2 Aims and Objectives

The aim of this chapter was to investigate the clinical significance of MR-EMT expression in melanoma tissues, in particular ZEB1, ZEB2, SNAI2 and TWIST1.

The specific objectives were as follows:

- To evaluate the specificity of antibodies raised against ZEB1, ZEB2, TWIST1, SNAI1 and SNAI2 by using control paraffin-embedded cell lines and tumour samples.
- To identify the expression pattern of ZEB1 and ZEB2 in a mouse *BRAF*^{V600E} melanoma model.
- To assess the IHC-P staining pattern of ZEB1, ZEB2, SNAI2 and TWIST1 with melanoma progression, by comparing benign naevi with primary melanomas and lymph node metastases using independent and matched tumour samples.
- To evaluate the clinical significance of IHC-P staining for ZEB1, ZEB2 and TWIST1 using tissue from a selected cohort of melanoma patients augmented with extra cases showing lymph node metastases. The association of clinicopathological variables was tested using univariate and multivariate models.

5.3 Results

5.3.1 *Patient demographics and melanocytic tissues*

A total of one hundred forty two MM cases, including thirty one with both primary and metastatic tissue, and twenty one compound naevi, were examined for ZEB1 and ZEB2 immunoreactivity. A total of one hundred and thirty three cases melanoma samples were stained for TWIST1, comprising nineteen CAN, forty nine unpaired non metastatic primary MMs and forty five metastatic primary MMs, of which thirty one were pairs of primary tumours with their matching lymph node metastases. A small cohort of thirty eight cases was analysed for SNAI2 expression by immunohistochemistry, including four intradermal common acquired melanocytic naevi, six unpaired primary melanomas with and without metastases (three each) and fourteen matched pairs. To evaluate SNAI1 protein expression in naevi versus primary melanomas and nodal metastases, expression of SNAI1 was compared in three compound naevi, twelve primary MMs and eleven distant metastases in lymph nodes. For these tumours six cases were matched pairs of primary MMs and their corresponding metastases. In addition, a small number of patient biopsies were immunostained for VDR and E-cadherin (refer to sections 4.3.1 and 4.3.3). Finally, patient demographics for all cases with 5-year follow-up (n=98) data is shown in

Table 5.1 - Clinicopathological characteristics in a subset of MM patients

Variable	Evaluation	n=98
Age (years)	< 60	46
	> 60	52
Gender	Female	57
	Male	41
Breslow	< 1.5 mm	29
	> 1.5 mm < 4.0 mm	43
	> 4.0 mm	26
Ulceration	No ulceration	59
	ulceration	39
Stage	1	24
	2	14
	3	35
	4	25

5.3.2 *MR-EMT immunoreactivity control examples*

To confirm specificity and functionality of both ZEB1 and TWIST1 antibodies formalin-fixed, paraffin-embedded cytoblock preparations of the urinary bladder carcinoma cell line RT-112 and osteosarcoma HOS cells were prepared and served as external negative and positive controls respectively (Figures 5.1 and 5.2-A-i/ii). For the analysis of ZEB1 staining in melanoma samples, blood and lymphatic vessels were served as endogenous positive controls (Figure 5.1-B). Consistent with published data, dermal fibroblasts were reactive for TWIST1 and used as an internal positive control (Figure 5.6-A/B) (Ansieau et al., 2008). A431 cells expressing myc-tagged ZEB2 in DOX-regulated manner (Mejlvang et al., 2007) and intercellular staining of normal melanocytes were served as an external and internal positive control for ZEB2 respectively (Figures 5.1-C-ii, 5.5-D and 5.9-A-ii/C). Inflammatory cells were served as an internal negative control for both ZEB1 and ZEB2 immunostaining (Figures 5.13-B and 5.19). HEK-293 cells expressing Snail under the control of the tetracycline-inducible system was used as a positive control for SNAI1 expression (Figure 5.3-A-ii) (Grotegut et al., 2006). For SNAI2, melanoma cells IPC-298 and SK-MEL-2 were employed as external negative and positive control cell lines with every run of immunohistochemistry, respectively (Figure 5.2-B). RPMI-7951 cells were acted as external positive and negative control cell lines for VDR and E-cadherin expression, respectively (Figure 5.3-B-i/C-ii). A nodal melanoma metastasis specimen was used as a negative control tissue for VDR protein expression (Figure 5.3-C-i), while sections of archival invasive ductal breast carcinoma were served as positive control tissue for E-cadherin protein immunoreactivity (Figure 5.3-B-ii). The specificity of EMT modulators antibodies was additionally confirmed by immunoblotting (Figures 5.1-D, 5.2-C and 5.3-D).

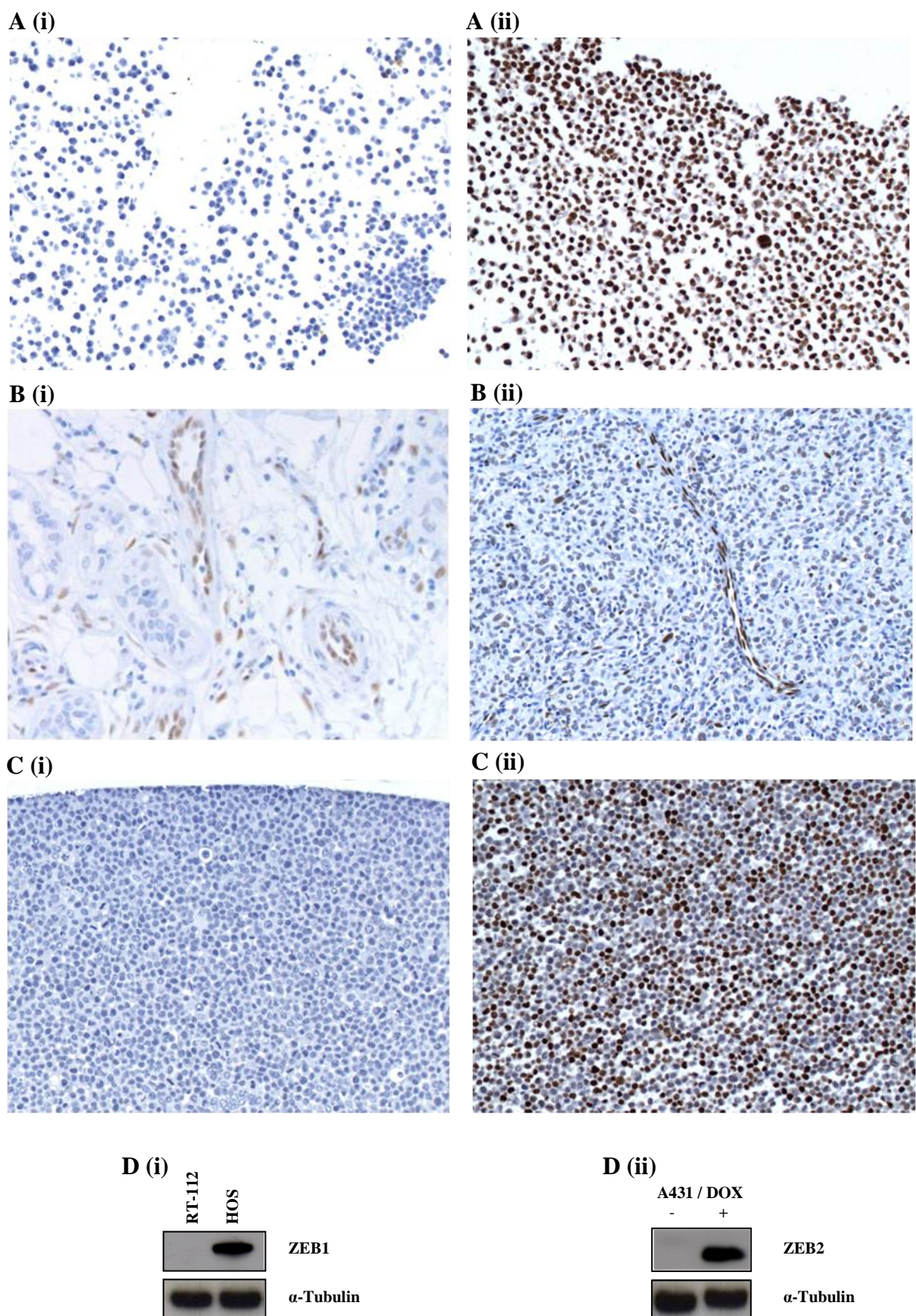


Figure 5.1 - Immunohistochemical and western blot analyses of ZEB1 and ZEB2 expression in control cell lines. (A) Low power view (×20) of paraffin-embedded (i) RT-112 and (ii) HOS cells exhibiting negative and nuclear positive staining for ZEB1 respectively. (B) (i) The endothelium of peritumoural blood vessels / fibroblasts and (ii) lymphatic vessels in melanocytic lesions served as internal positive controls for ZEB1 staining. (C) (i) Low power view (×20) of A431 cells showed negative immunoreactivity for ZEB2. (C) (ii) A431 / ZEB2 / DOX+ induced cells demonstrated strong nuclear positive staining for ZEB2. (D) The specificity of (i) ZEB1 and (ii) ZEB2 antibodies was also confirmed by immunoblotting.

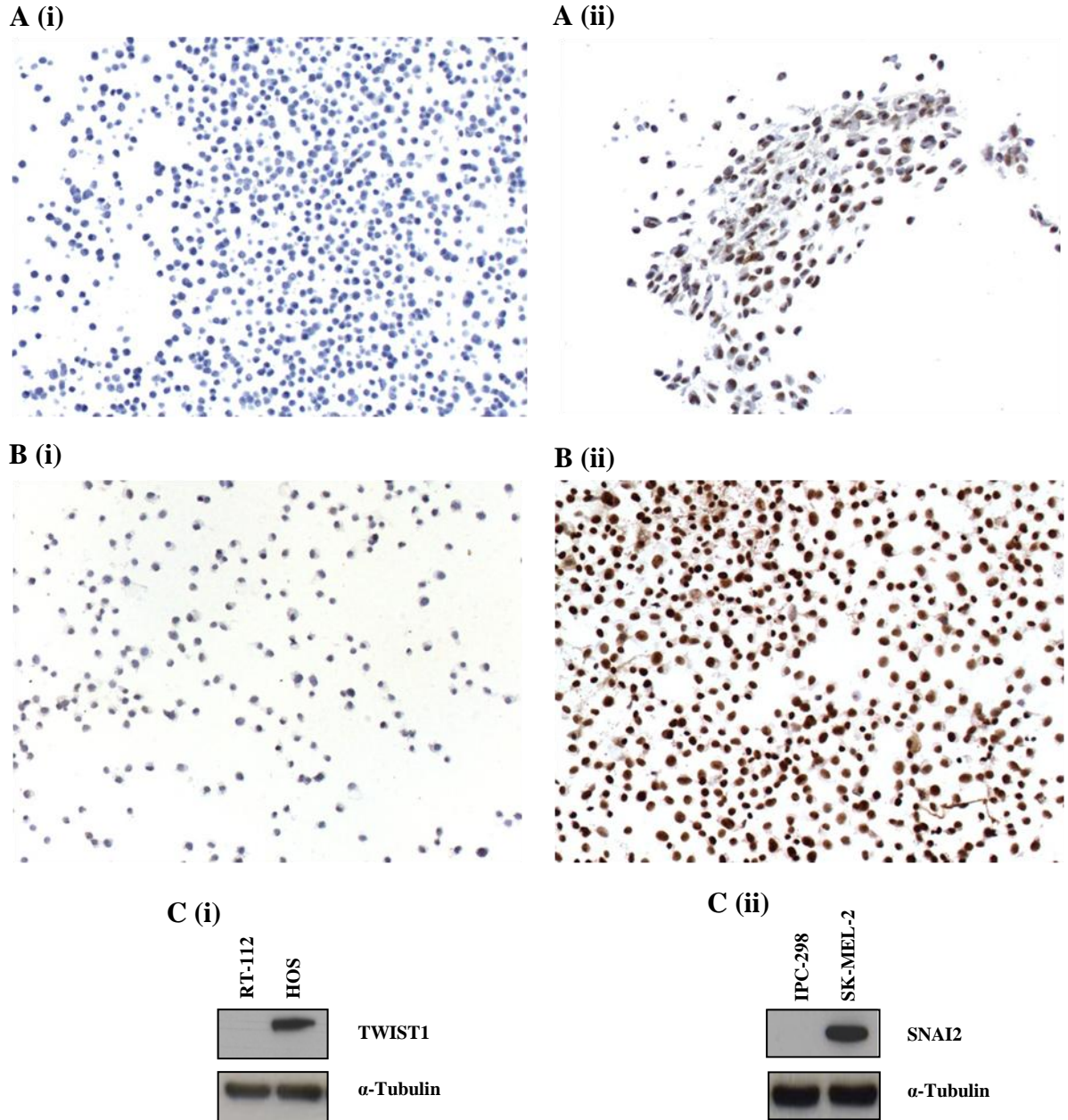


Figure 5.2 - Immunohistochemical and western blot analyses of TWIST1 and SNAI2 expression in control cell lines. (A) Low power view ($\times 20$) of paraffin-embedded (i) RT-112 and (ii) HOS cells showed negative and nuclear positive staining for TWIST1 respectively. (B) Low power view ($\times 20$) of (i) IPC-298 and (ii) SK-MEL-2 melanoma cells exhibiting negative and nuclear positive staining for SNAI2 respectively. (C) The specificity of (i) TWIST1 and (ii) SNAI2 antibodies was also confirmed by western blotting.

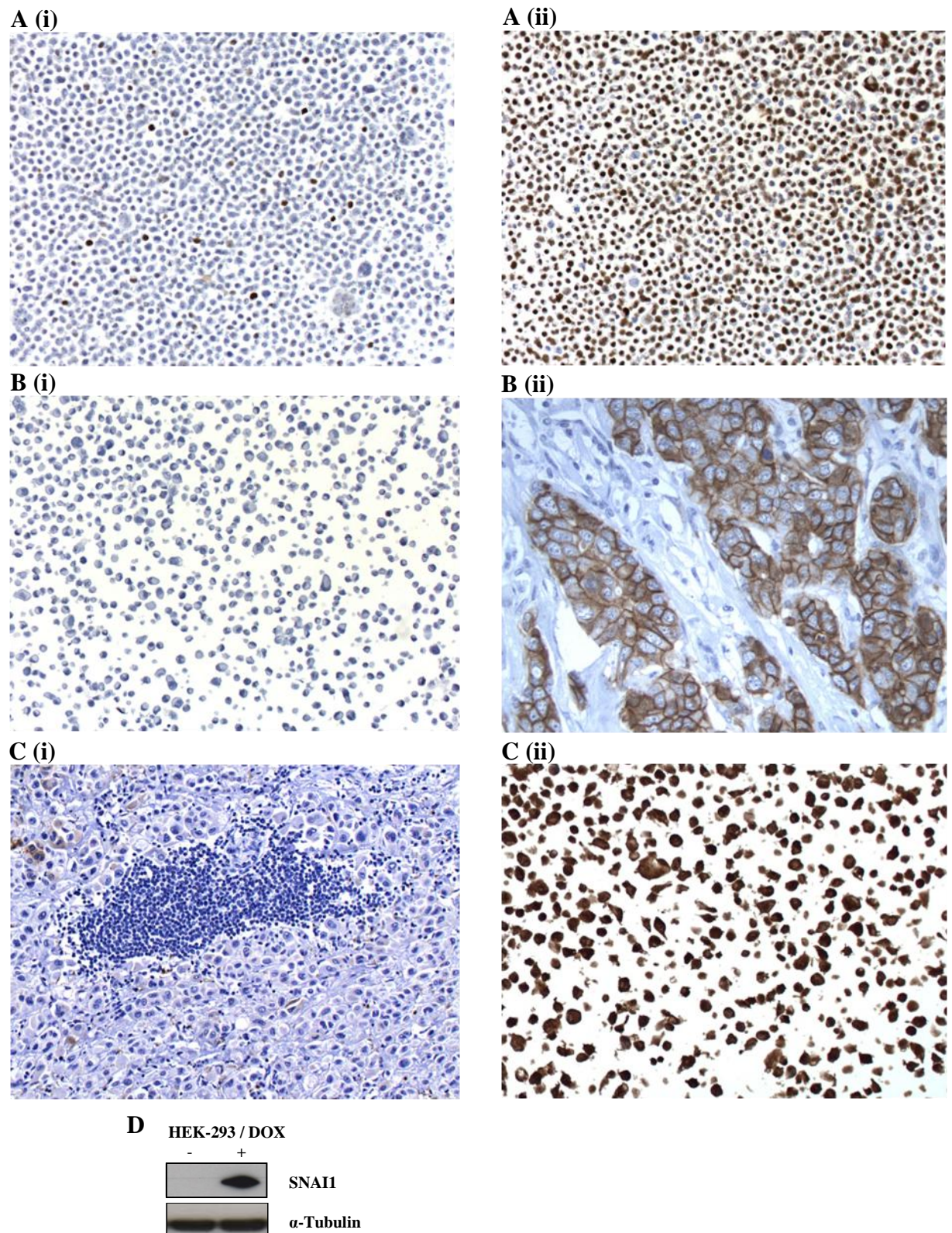


Figure 5.3 - Immunohistochemical and western blot analyses of SNAI1, E-cadherin and VDR expression in control cell lines and tissues. (A) Low power view ($\times 20$) of paraffin-embedded (i) HEK-293 and (ii) HEK-293 / SNAI1 / DOX induced cells exhibited a negative and nuclear positive immunoreactivity for SNAI1 respectively. (B) (i) Low power magnification ($\times 20$) showed no E-cadherin immunoreactivity for RPMI-7951 melanoma cells. (B) (ii) Sections of invasive ductal breast carcinoma tissue showed strong cell membrane staining and were used as a positive control for E-cadherin. (C) (i) Sections of nodal melanoma metastasis tissue (intratumoural area) were used as a negative control for VDR immunoreactivity. (C) (ii) Paraffin-embedded RPMI-7951 melanoma cells showed positive reactivity for VDR. (D) The specificity of SNAI1 antibody was also confirmed by western blotting.

5.3.3 Immunohistochemical evaluation examples

Expression of ZEB1, ZEB2 and TWIST1 was evaluated via a quantitative method based on the H-score by light microscopy (section 2.2.4.7), and representative examples are presented in Figures 5.4-5.6. To determine the reliability of the staining an inter-observer agreement (Dr. JH Pringle and Mr. E Papadogeorgakis) was measured using twenty randomly selected cases and an intra-class correlation coefficient (ICC) indicated high agreement (ICC = 0.92).

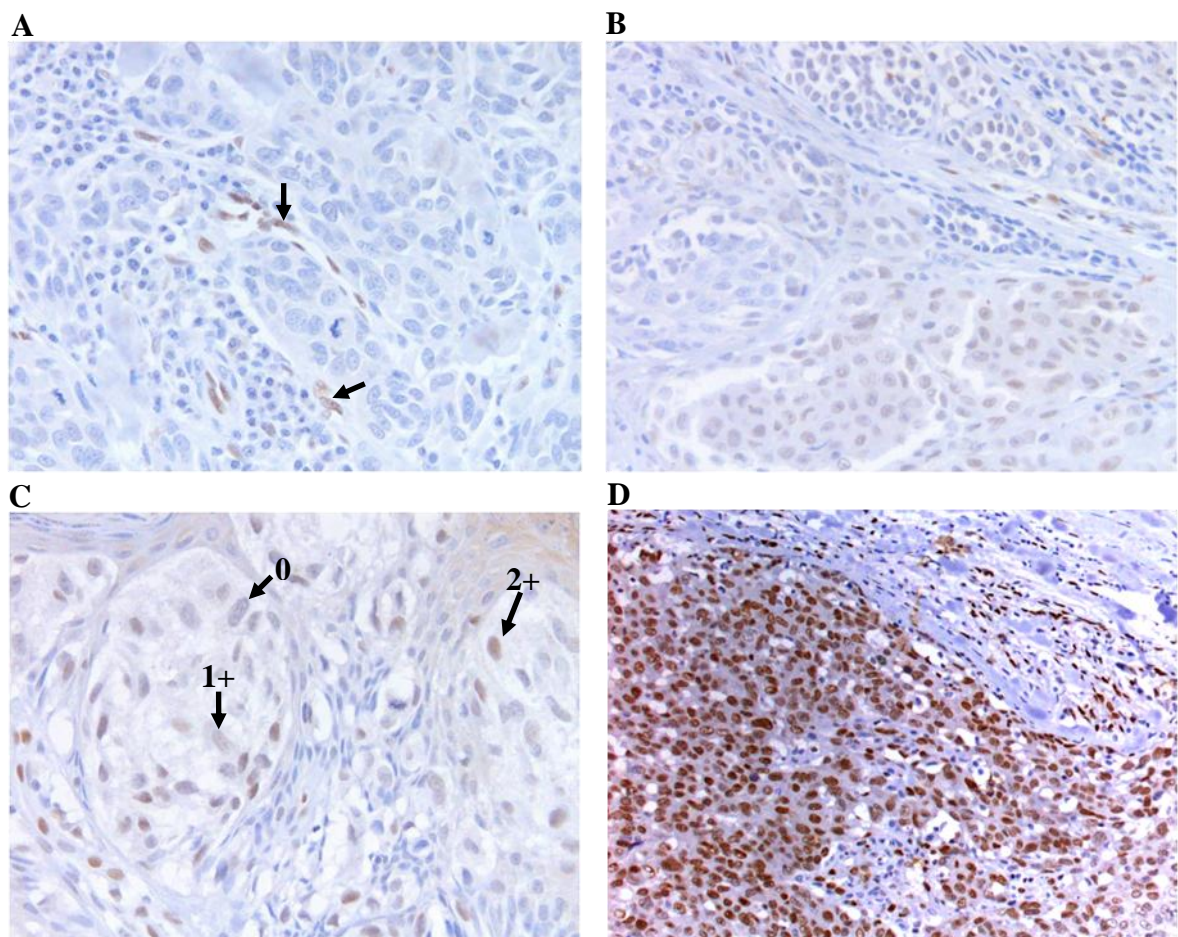


Figure 5.4 - Staining intensity examples for ZEB1. (A) Low power view (×20) of a paraffin-embedded melanoma sample showing no ZEB1 immunoreactivity (0). Stromal cells with fibroblastic morphology were strongly positive for ZEB1 (3+) (arrows). (B) Representative primary melanoma section exhibiting weak (1+) nuclear staining for ZEB1. (C) Primary MM demonstrating a heterogeneous ZEB1 staining from 0 to 2+ (arrows). (D) A paraffin-embedded metastatic melanoma (lymph node, peripheral area) specimen showing strong (3+) ZEB1 immunoreactivity.

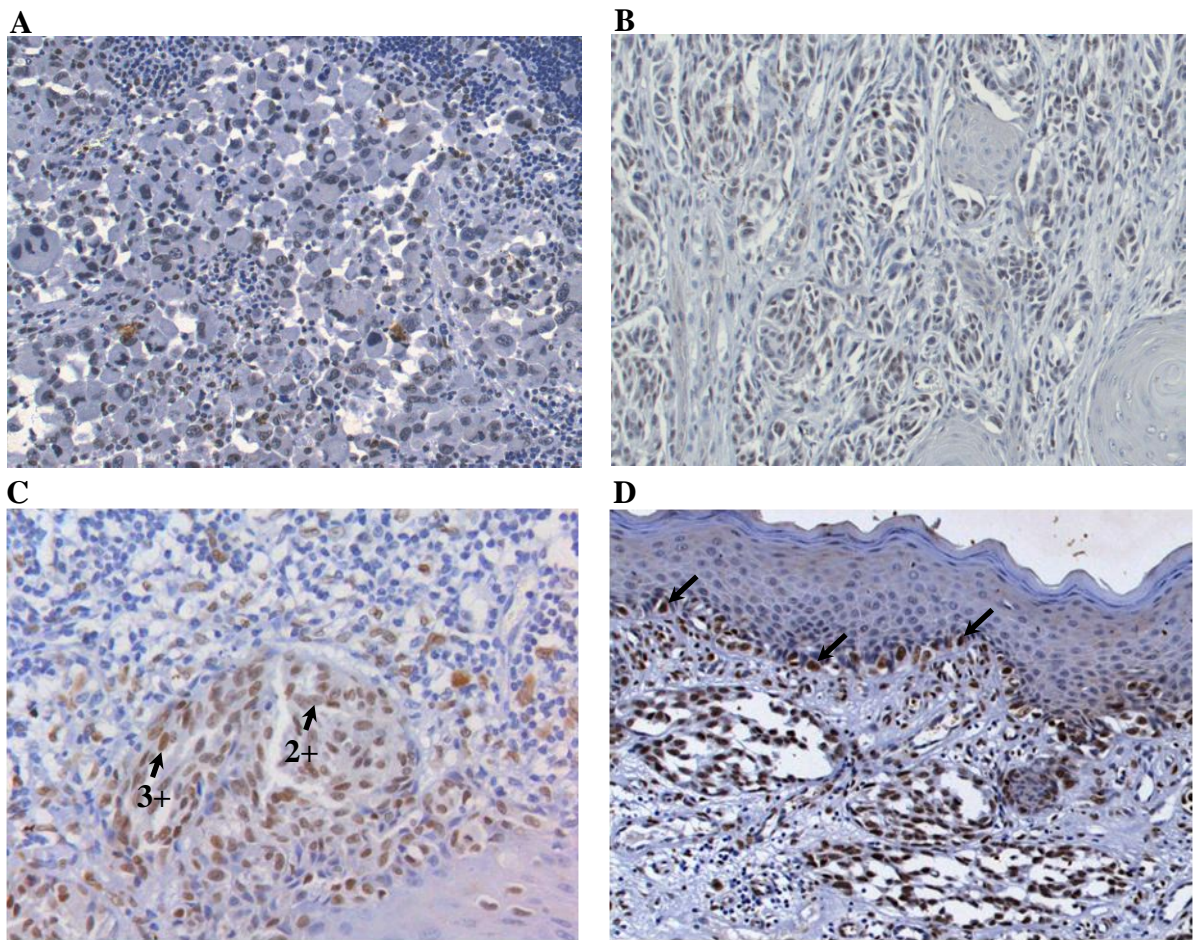


Figure 5.5 - Staining intensity examples for ZEB2. (A) Low power view ($\times 20$) of a paraffin-embedded nodal metastasis sample showing no ZEB2 immunoreactivity (0). (B) Representative primary melanoma section exhibiting weak (1+) nuclear staining for ZEB2. (C) Primary MM demonstrating a heterogeneous ZEB2 staining from 2+ to 3+ (arrows). (D) A paraffin-embedded primary melanoma specimen showing strong (3+) ZEB2 immunoreactivity. Normal melanocytes in the epidermis were positive for ZEB2 (arrows).

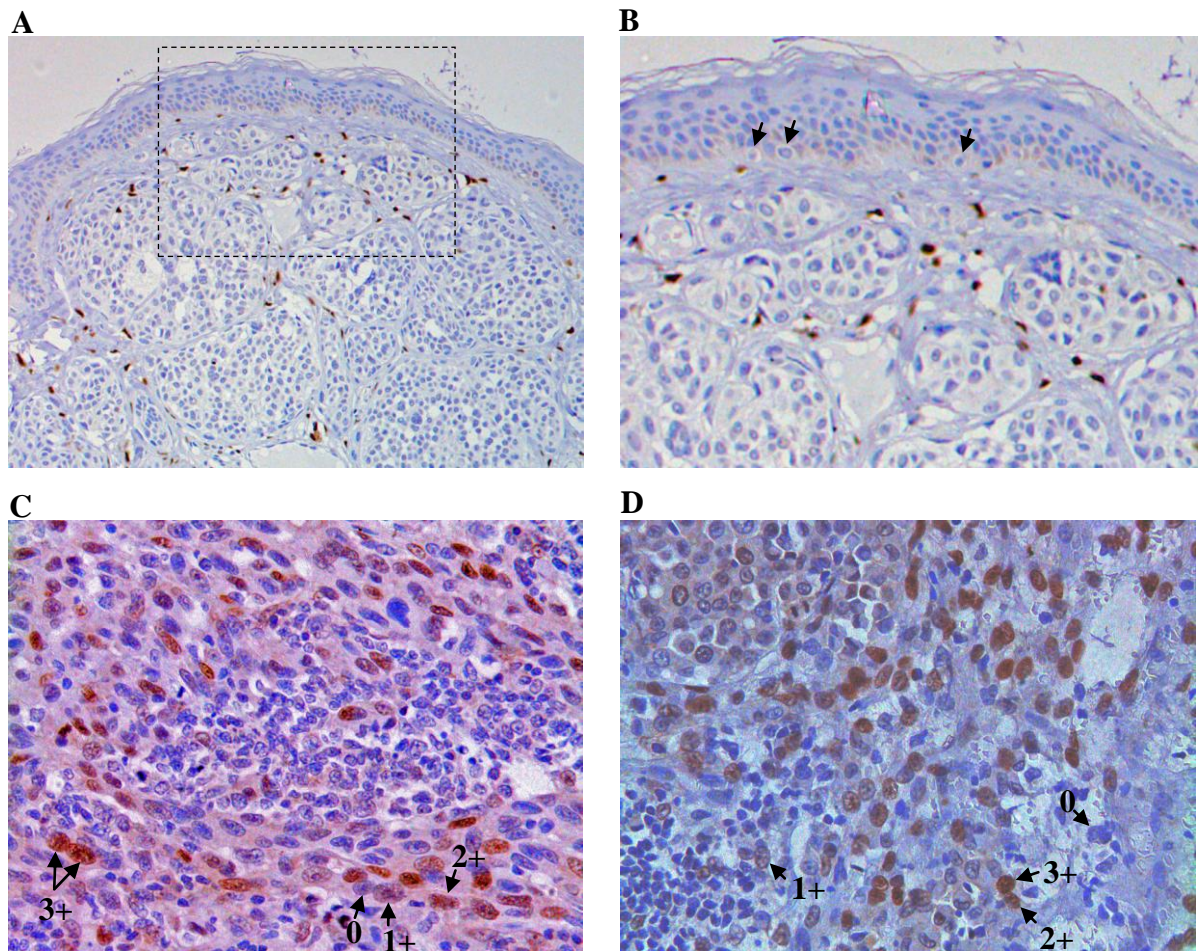


Figure 5.6 - Staining intensity examples for TWIST1. (A) Low power view (×20) of a common acquired naevus exhibiting absent nuclear TWIST1 immunosignals in normal skin and benign intradermal melanocytic nevi. (B) Negative TWIST1 staining is more evident on higher power magnification (×40) of A (rectangle), showing negative nuclear staining of intradermal nests / basal keratinocytes and positivity of stromal cells (dark brown stained cells). Normal melanocytes in the epidermis showed no immunoreactivity for TWIST1 (arrows). (C-D) High power views (×40) of paraffin-embedded nodal metastasis specimens reveal heterogeneous TWIST1 staining (0 to 3+).

5.3.4 Expression of ZEB1 and ZEB2 in a mouse $BRAF^{V600E}$ melanoma model

To assess the importance of ZEB1 and ZEB2 *in vivo*, IHC-P analysis was performed in a model of malignant melanoma based on the conditional expression of the knock-in $BRAF^{V600E}$ mutant allele in mouse melanocytes. Expression of $BRAF^{V600E}$ resulted in different melanocyte-derived lesions including classic and blue naevi in all animals and melanoma in 70% of one-year old mice. No metastases were observed in this model, although, when melanoma cells were cultured and injected into the tail veins of nude mice, colonization in lungs was detected (Andersen et al., 2002). Herein, high ZEB1 and ZEB2 immunoreactivity was detected in 30-50% of tumour cells in mouse melanoma samples (n=4) (Figure 5.7-B-D). No immunoreactivity was seen in normal mouse skin sections (n=2) (Figure 5.7-A).

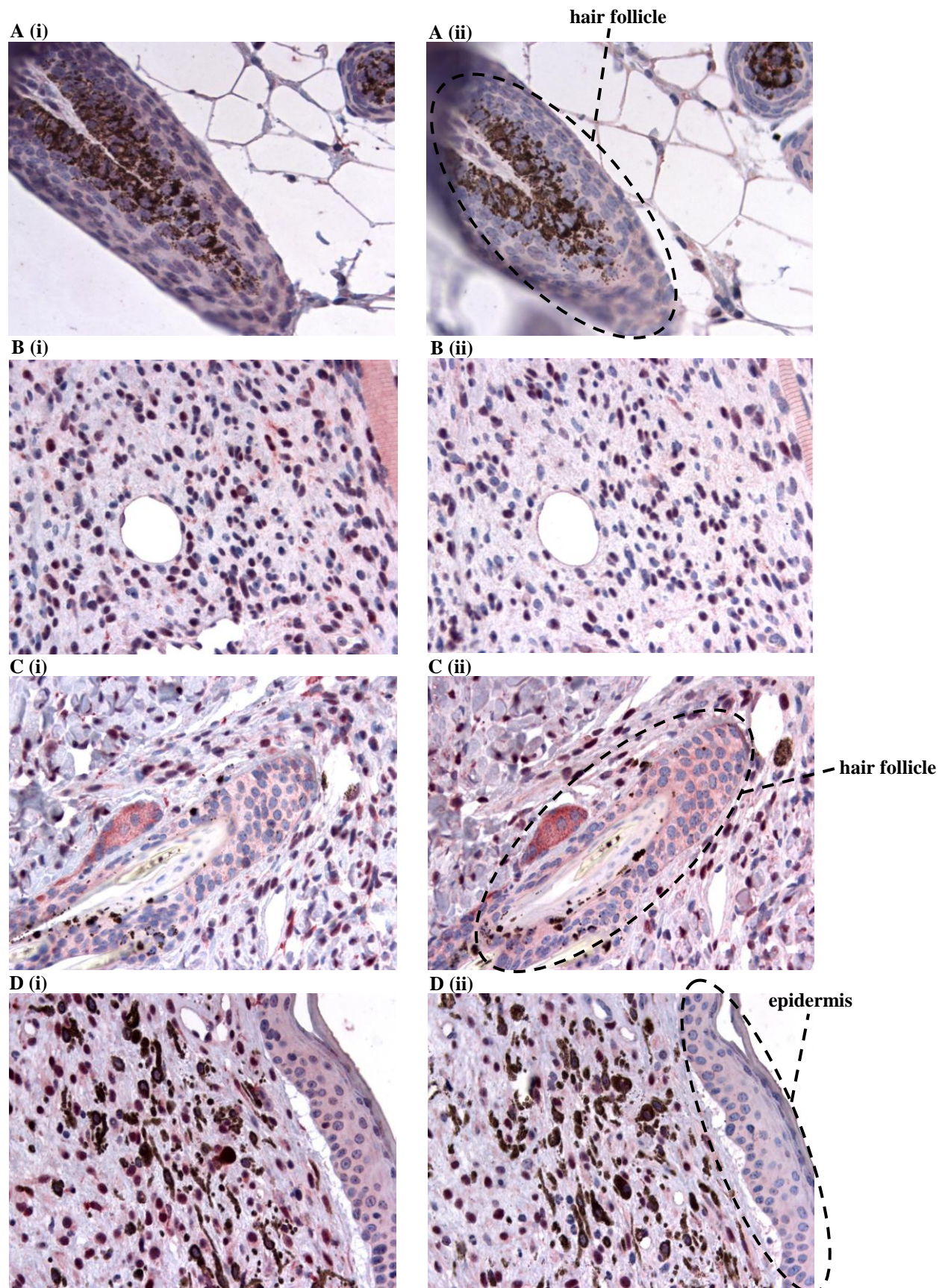


Figure 5.7 - Immunohistochemical analysis of the expression of ZEB1 and ZEB2 in the mouse $BRAF^{V600E}$ model of malignant melanoma. ZEB1 and ZEB2 staining is shown in panels A-D (i) and A-D (ii) respectively. Low power view ($\times 20$) of serial sections of normal mouse skin revealed no immunoreactivity for ZEB1 (A-i) and ZEB2 (A-ii) antibodies. (B-D) In mouse melanoma sections, ZEB1 and ZEB2 are expressed in the majority of tumour cells and in likely overlapping cell populations.

5.3.5 Expression of MR-EMT proteins in benign and MM tumours

5.3.5.1 MR-EMT immunostaining patterns

Immunohistochemical staining of MR-EMT in benign and MM samples displayed an exclusive nuclear reactivity. The strongest immunoreactivity for ZEB1 and TWIST1 antibodies was detected in lymph node metastases. TWIST1 staining demonstrated a clonal distribution with distinct areas of the tumour revealing a heterogeneous staining pattern. Examples of metastatic tumour heterogeneity are shown in Figures 5.6-C/D and 5.13-D. In most of ZEB1-positive cases the staining was confined in small areas of deep primary MMs and nodal metastases (Figures 5.13-B and 5.15-A-ii). In melanocytic naevi SNAI2 and ZEB2 immunoreactivity showed a distinct gradient of staining with stronger staining at superficial sites compared to the deeper sites of the lesions (Figures 5.11 and 5.12). The staining pattern of MR-EMT in melanocytic naevi and epidermal melanocytes is shown in Figures 5.8-5.10. Stratification of ZEB2 staining in relation to the depth of the lesion was additionally observed in primary MMs (Figure 5.14-B). Interestingly, ZEB1 expression in invasive portions of the primary melanomas and intratumoural lymph nodes was inversely correlated with ZEB2 expression (Figures 5.17-5.19). In accordance with recent results, all analysed melanoma cases (n=26) were SNAI1-negative (results not shown) (Mikesh et al., 2010).

5.3.5.2 Expression of EMT modulators during melanoma progression

To further characterise the expression of MR-EMT in melanoma clinical samples, comparison of tumour lesions at different stages of progression was performed. The staining for ZEB1, ZEB2 and TWIST1 was measured at superficial and deep sites for each melanocytic lesion (Figures 5.20-5.23).

5.3.5.2.1 ZEB1

Stromal cells in the naevi and basal keratinocytes in the normal epidermis showed no ZEB1 immunoreactivity. Interestingly, the majority of stromal cells in primary melanomas and lymph node metastases were ZEB1 immunopositive (Figures 5.4-A and 5.13-A/B). In naevi cells ZEB1 staining was generally absent, with only two naevi exhibiting a weak immunoreactivity in a small number of tumour cells at intradermal nests (Figure 5.8-A-C-i and Appendix V-a). In addition, the median ZEB1 H-Score was 0 in both superficial and deep sites of the naevi ($P>0.05$, Wilcoxon signed rank test, Figure 5.12).

Increased expression of ZEB1 protein was observed in independent and matched lymph node metastases compared to primary MMs (Figures 5.13-A/B and 5.15-A). In addition, ZEB1 expression was significantly increased in most deep sites of independent metastatic primary melanomas and peripheral / intratumoural components of lymph nodes compared to naevi ($P=0.001$ and $P=0.003$ / $P=0.014$, respectively, Dunn's post-Kruskal-Wallis test) (Figure 5.20-A/B). Independent primary MMs showed similar levels of ZEB1 staining at both superficial and deep sites, irrespectively to their metastatic potential (median H-Score ≤ 4.0 , Figure 5.20-C-i). Based on the Jonckheere-Terpstra trend analysis ZEB1 expression was significantly correlated with tumour progression at both superficial and deep sites ($P<0.0001$ in both) of independent benign

and malignant melanoma cases (Figure 5.20-C-ii). In cases of primary MMs with matched metastases an increasing trend of staining was observed from superficial to deep sites in the primary tumour and intratumoural areas of the metastases ($P < 0.01$, Page's L Trend, Figure 5.23-A, E).

5.3.5.2.2 ZEB2

Histological examination revealed strong positive nuclear ZEB2 staining in all melanocytic naevi cases (Appendix V-b). The median H-score for ZEB2 in deep sites (111.0) was lower compared to superficial sites (160.0) ($P < 0.0001$, Wilcoxon signed rank test, Figure 5.12). Normal melanocytes residing in the basal layer of the epidermis revealed strong nuclear immunoreactivity for ZEB2. In contrast, stromal cells and basal keratinocytes showed negative and occasional nuclear ZEB2 immunostaining respectively (Figures 5.8-A-C-ii and 5.9-A-ii/C).

Increased expression of ZEB2 protein was observed in independent and matched primary melanomas compared to lymph node metastases (Figures 5.14 and 5.15-B). Statistical analysis demonstrated that ZEB2 protein was significantly downregulated in both peripheral and intratumoural sites of independent lymph nodes compared to melanocytic naevi ($P < 0.0001$ in both, Dunn's post-Kruskal-Wallis test) (Figure 5.21-A/B). Furthermore, deep metastatic and non-metastatic primary MMs showed levels of ZEB2 that were similar to peripheral sites in lymph nodes (median H-Score=45.0, 47.5 and 28.5 respectively, Figure 5.21-C-i) and then further reduced in the central component of the lymph nodes (median H-Score=5.0). It has also been demonstrated a comparable ZEB2 reactivity in superficial areas of primary melanomas with or without metastases (median H-Score=135.0 and 121.5 respectively, Figure 5.21-A/B/C-i). Melanoma tumour cells showed significant different levels of ZEB2 between the

superficial and deep dermal components of metastatic and non-metastatic primary MMs ($P<0.01$ and $P<0.05$ respectively, Dunn's post-Kruskal-Wallis test, Figure 5.21-C-i and Appendix V-b). Based on the Jonckheere-Terpstra trend analysis, ZEB2 expression was significantly correlated with tumour progression at both superficial and deep sites ($P=0.04$ and $P<0.0001$ respectively) of independent melanoma cases (Figure 5.21-C-ii).

In cases of primary MMs with matched metastases, ZEB2 expression was significantly decreased in deep sites of primary MMs and both peripheral and intratumoural areas of the nodal metastases compared with superficial sites in primary MMs ($P<0.001$; $P<0.05$; $P<0.001$ respectively, Dunn's multiple comparison-Friedman test, Figure 5.23-B). In addition, a decreasing trend of positive ZEB2 staining was observed from superficial sites to deep sites in the primary tumour and intratumoural sites of the metastases ($P<0.01$, Page's L Trend, Figure 5.23-E).

5.3.5.2.3 TWIST1

TWIST1 nuclear staining for benign naevi was negative in basilar keratinocytes and normal melanocytes in the epidermis. Most melanocytic naevi showed negative immunoreactivity, with three cases demonstrating positive staining at deep sites (Figures 5.8-A/C-iii and Figure 5.9-D, Appendix V-c). In contrast, dermal fibroblasts displayed strong positivity (Figures 5.6-A and 5.8-A/C-iii). Increased expression of nuclear TWIST1 immunoreactivity was observed in independent and matched lymph node metastases compared to primary MMs (Figures 5.13-C/D and 5.15-C).

Upon acquiring features of invasion, expression of TWIST1 was significantly augmented at superficial sites of independent malignant melanomas, with or without metastasis, and peripheral components of lymph nodes compared to naevi ($P=0.014$, Jonckheere-Terpstra Trend) (Figure 5.22-A/C). In paired cases, the percentage of

TWIST1-positive cells and the intensity of immunoreactivity were found to be increased in the periphery of nodal metastases compared to primary melanomas (Figure 5.23-C). However, no statistically significant trend was established ($P>0.05$, Page's L Trend, Figure 5.23-E). Of note, no staining differences were observed between superficial and deep components of naevi, primary MMs and nodal metastases in both independent and matched melanoma cases (Figures 5.21-C-i and 5.23-E, Appendix V-c). Finally, H-scores for TWIST1 staining at deep sites of matched primary MMs were correlated with ZEB1 scores ($r^2=0.295$, $P=0.005$, Spearman's rho).

5.3.5.2.4 SNAI2

Histological examination of cases with common acquired melanocytic intradermal naevi ($n=4$) revealed positive nuclear SNAI2 staining in intradermal nests of naevi cells, basal keratinocytes and occasional staining in normal melanocytes residing in the basal layer of the epidermis (Figures 5.10 and 5.11). Interestingly, SNAI2 staining in benign naevi suggested decreased SNAI2 expression with depth (Figure 5.11). Apart from one non metastatic primary MM displaying weak superficial SNAI2 staining, the rest of independent primary MMs ($n=6$), with or without metastases, showed no SNAI2 reactivity at both superficial and deep sites (Appendix V-d). Increased expression of nuclear SNAI2 immunoreactivity was observed in matched primary MMs compared to their corresponding lymph node metastases (Figure 5.16). Furthermore, in cases of primary MMs with matched metastases a decreasing trend of positive staining was observed from superficial sites to deep sites in the primary tumour and intratumoural sites of the metastases ($P<0.01$, Page's L Trend, Figure 5.23-D/E-ii). Finally, H-Scores for SNAI2 staining at deep sites of matched primary MMs were correlated with ZEB2 scores ($r^2=0.6744$, $P=0.006$, Spearman's rho).

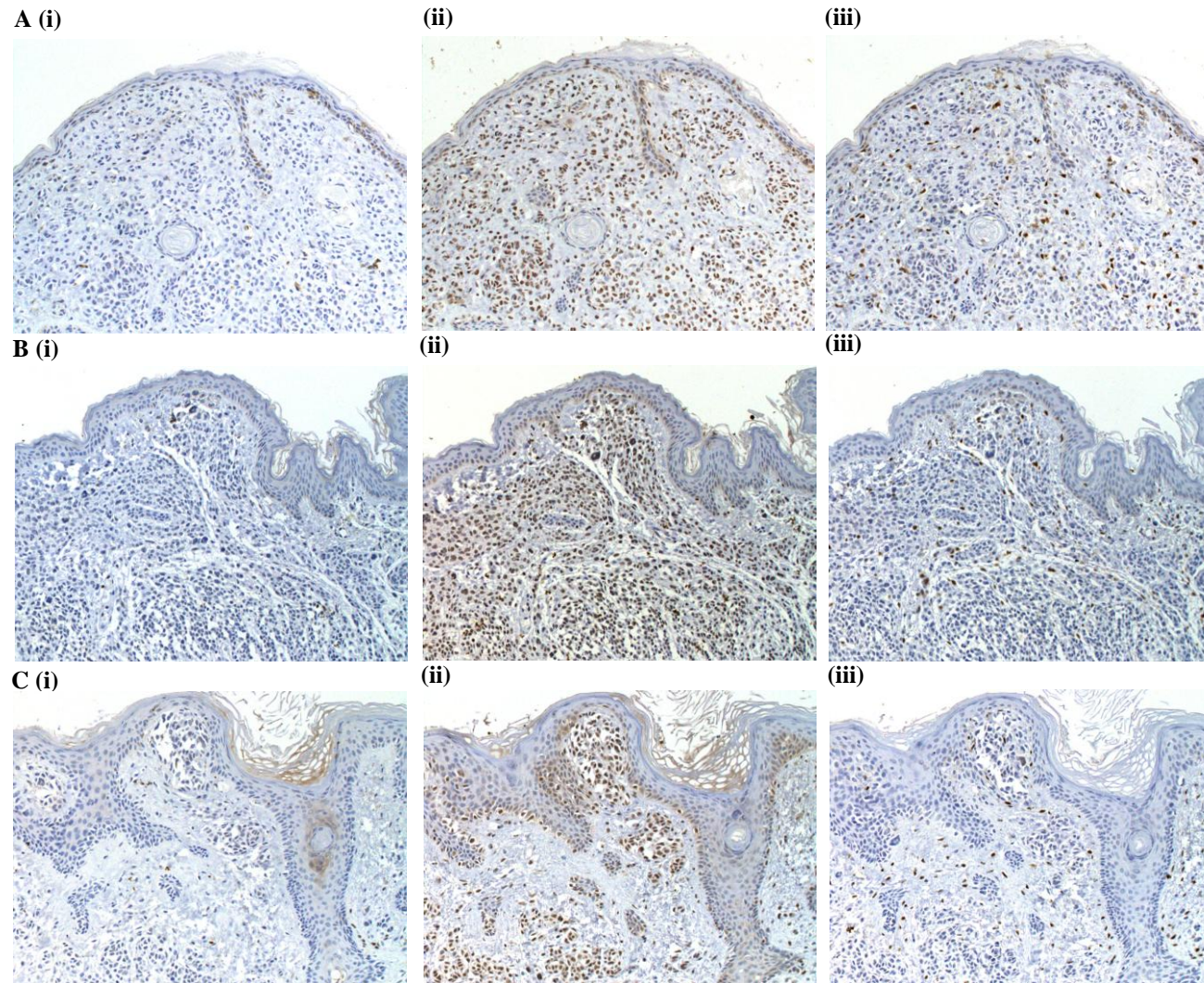


Figure 5.8 - Representative photomicrographs of ZEB1, ZEB2 and TWIST1 expression in common acquired melanocytic naevi. Low power view ($\times 20$) of serial sections of naevi specimens reveals negative protein expression for ZEB1 (A-C-i) and TWIST1 (A-C-iii) antibodies. Fibroblasts were strongly positive for TWIST1 (dark brown stained cells). Melanocytic naevi cells exhibited strong nuclear immunoreactivity for ZEB2 (A-C-ii).

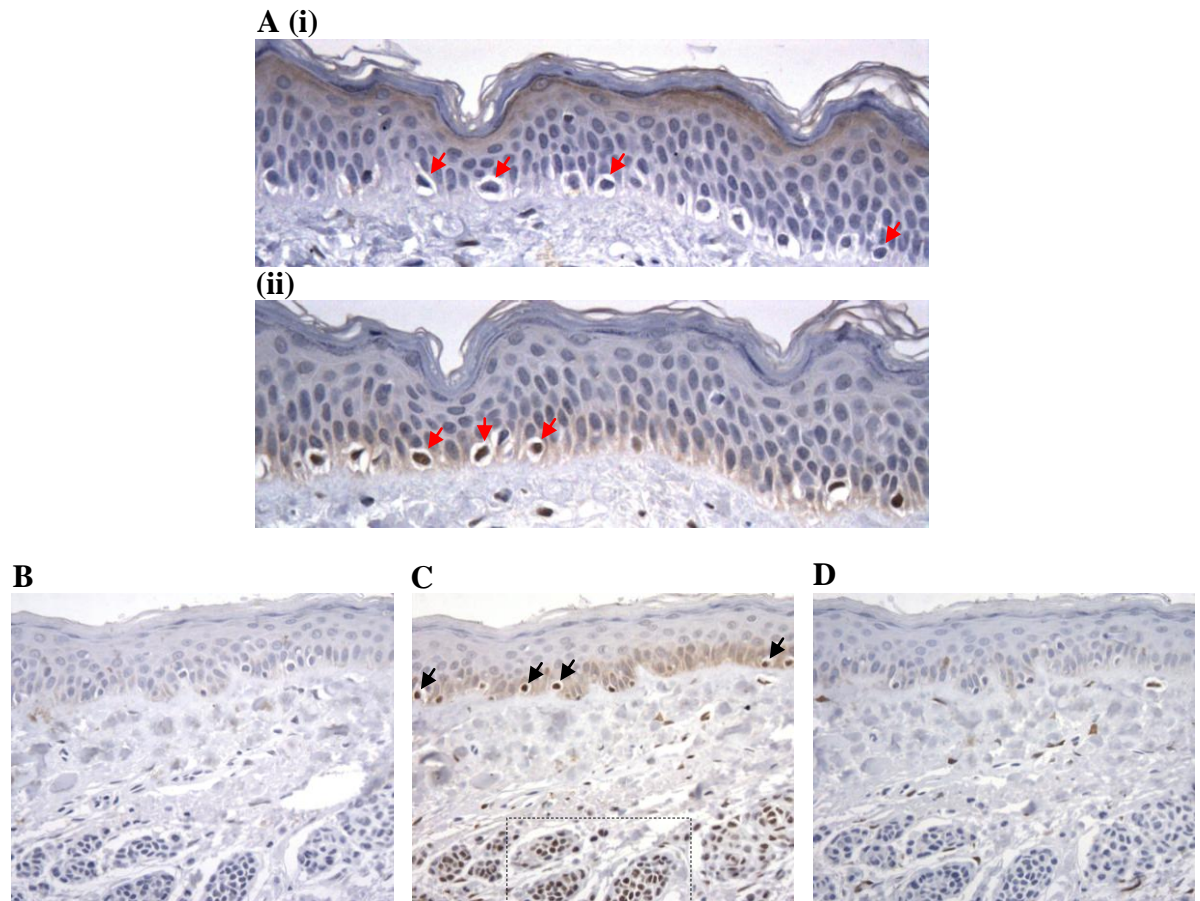


Figure 5.9 - ZEB1, ZEB2 and TWIST1 immunoreactivity in epidermal melanocytes. Immunohistochemical staining of serial sections of common acquired naevi specimens showed negative ZEB1 (A-i-arrows, B) and TWIST1 (D) reactivity of normal melanocytes and intradermal nests of melanocytes (B, D). In contrast, low power view ($\times 20$) revealed positive ZEB2 staining of normal melanocytes (A-ii, C-arrows) and intradermal melanocytic nests (C, rectangle).

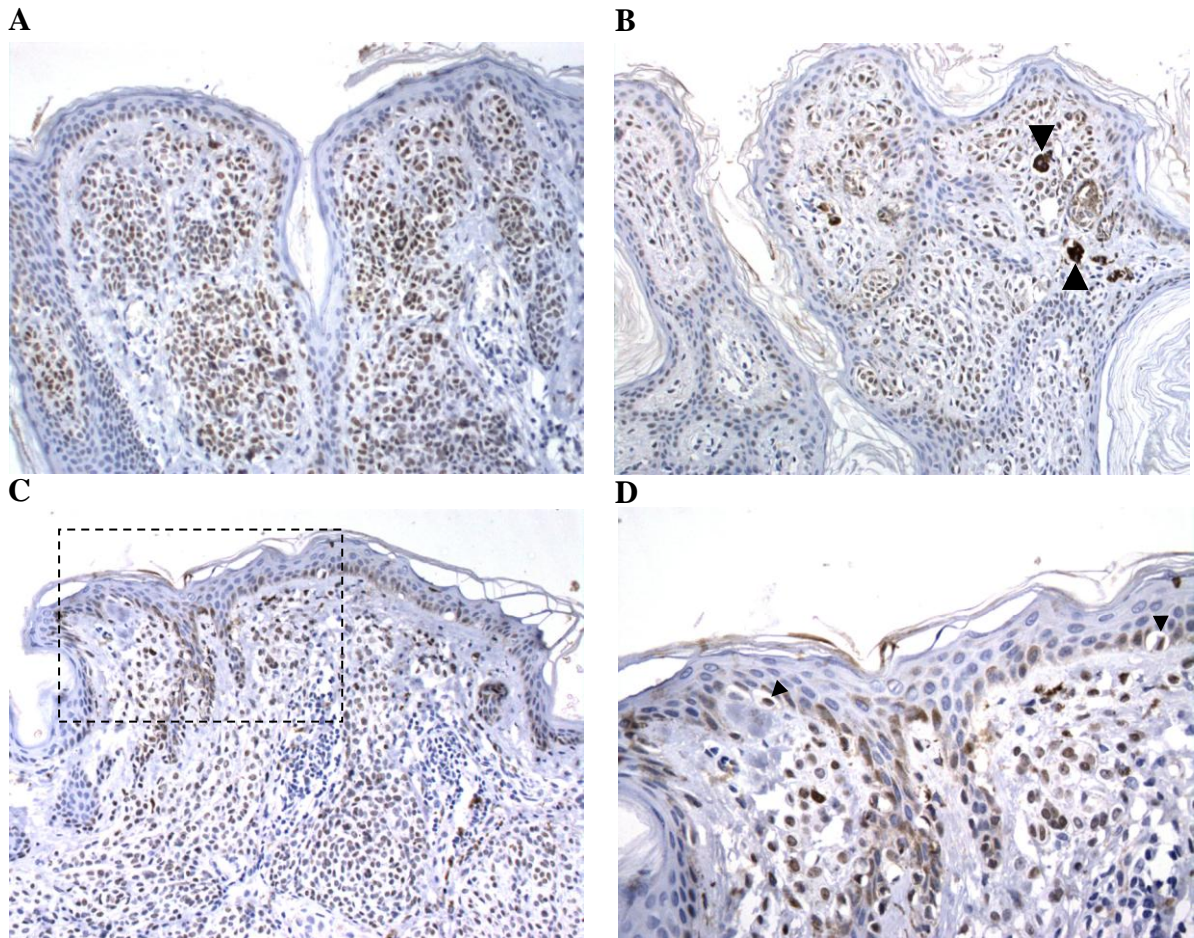
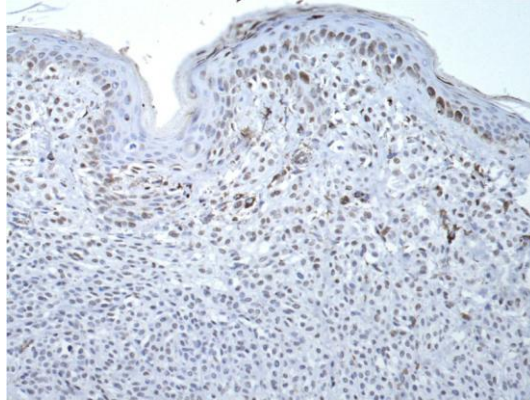


Figure 5.10 - Representative photomicrographs of SNAI2 expression in common acquired melanocytic naevi. Low power view ($\times 20$) revealed strong nuclear SNAI2 immunoreactivity in intradermal melanocytic nests (A-C). Cytoplasmic melanin is also present (arrowheads in panel B). (D) A high power view ($\times 40$) of the area outlined by the rectangle in panel C showing SNAI2-positive melanocytes (arrowheads).

A



B

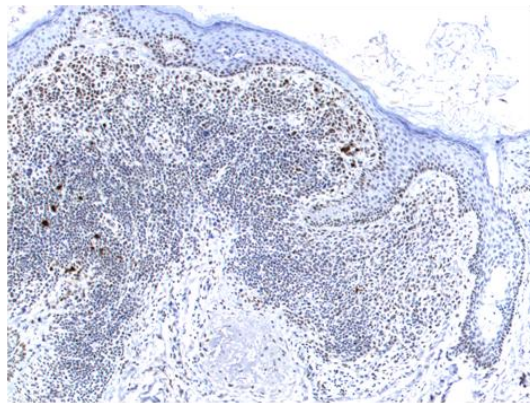


Figure 5.11 - Representative sections of benign naevi showing loss of SNAI2 expression throughout the depth of the tumour. (A-B) Low power views revealed strong nuclear SNAI2 immunoreactivity in the normal epidermis, mainly in the basal layer, and decreased or complete loss of staining in the deeper sites of the tumour. (A) ($\times 20$); (B) ($\times 10$).

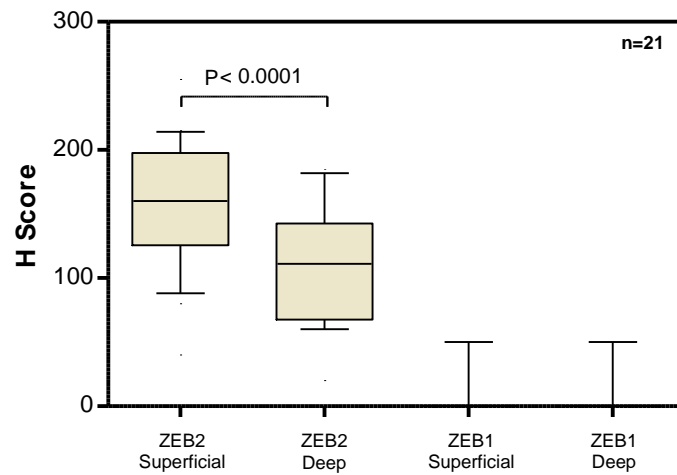


Figure 5.12 - Box and whisker plot showing nuclear ZEB1 and ZEB2 immunostaining in melanocytic naevi. ZEB2 expression was weaker at deep dermal components compared to the superficial sites in the naevi ($P < 0.0001$, Wilcoxon signed rank test). In contrast, ZEB1 immunoreactivity was almost absent ($P > 0.05$, Wilcoxon signed rank test). Error bars represent the 10th and 90th percentiles.

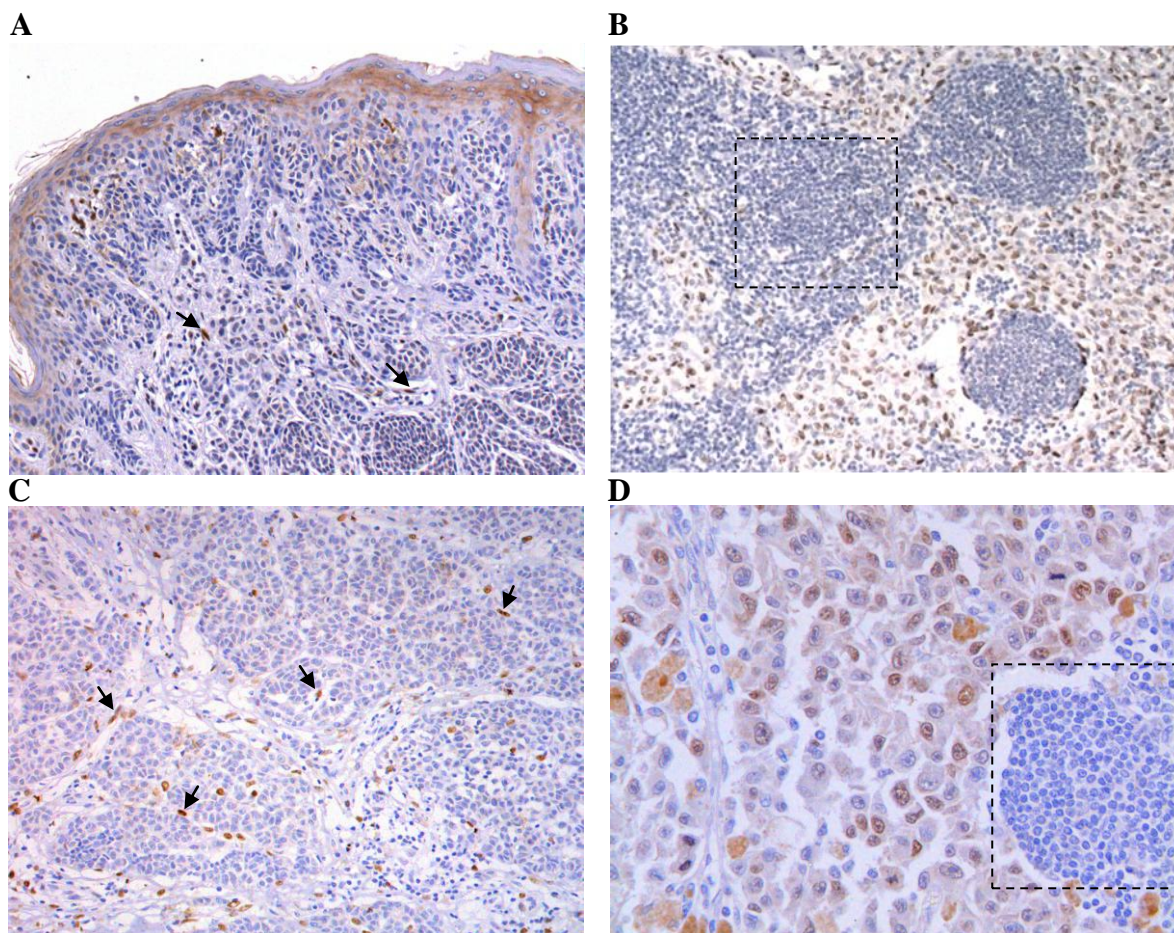


Figure 5.13 - Progression related ZEB1 and TWIST1 expression in independent primary MMs and lymph node metastases. (A-B) Markedly increased expression of ZEB1 protein was observed in lymph node metastasis (B) compared to a primary melanoma (A). (C) Immunohistochemistry showing a negative TWIST1 expression in the deep site of a primary melanoma. (D) A heterogeneous nuclear TWIST1 reactivity of tumour cells at intratumoural site in a nodal metastasis. Note that tumour associated stromal cells (arrows in panels A and C) and inflammatory cells, outlined by the rectangles in panels B and D, served as positive and negative internal controls respectively. (A-C) ($\times 20$); (D) ($\times 40$).

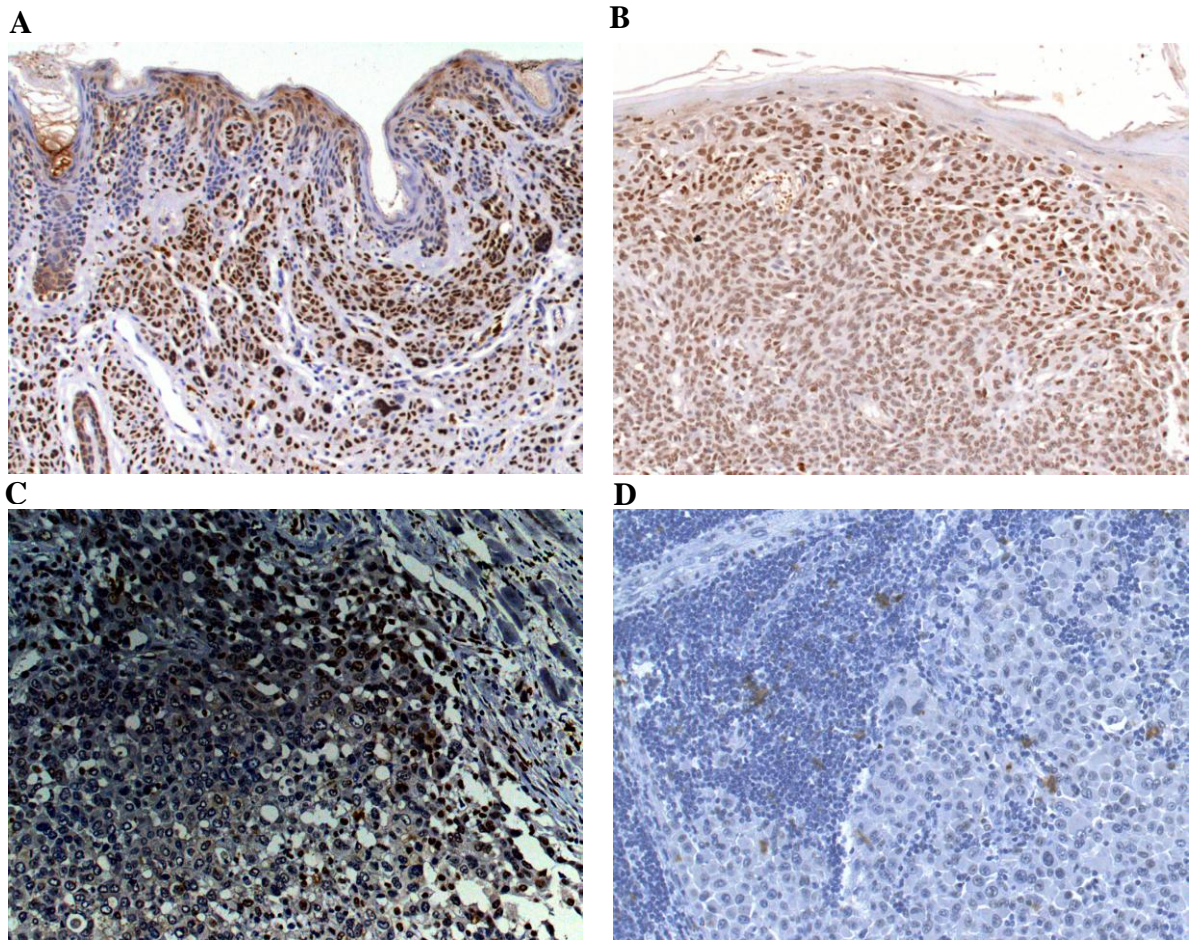


Figure 5.14 - Representative sections of progression related ZEB2 expression in MM. (A-B) Immunostaining of ZEB2 revealed strong nuclear immunosignals in a melanocytic naevus (A) and primary melanoma (B), and reduced or complete loss in nodal metastases (C, D). Of note, ZEB2 immunoreactivity was decreased in the deep sites in both naevus and primary melanoma (A, B). All photomicrographs $\times 20$.

Primary MMs → Paired nodal metastases

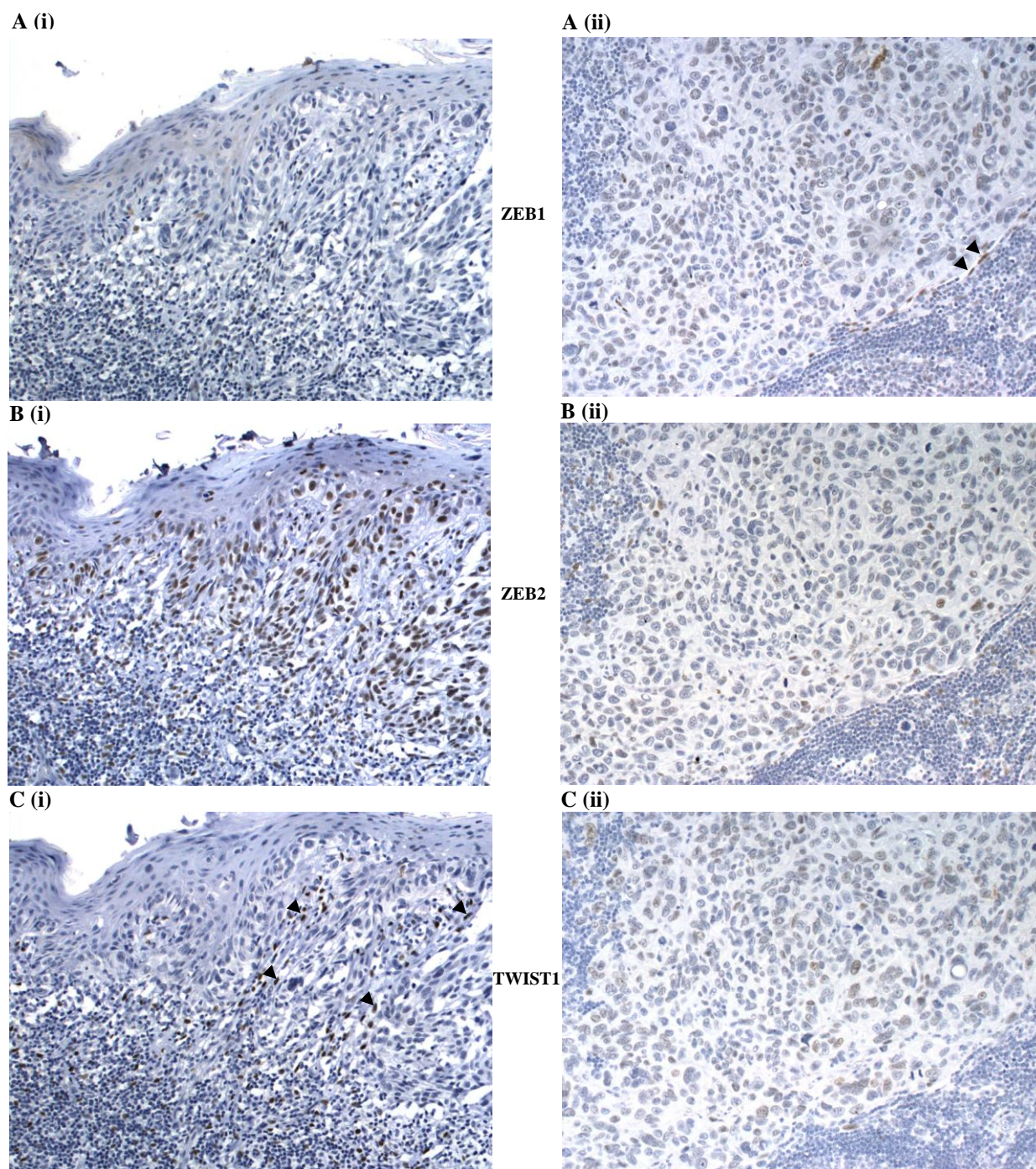


Figure 5.15 - Representative serial sections of progression related ZEB1, ZEB2 and TWIST1 expression in a paired nodal metastasis. (A) Immunostaining of ZEB1 revealed absent immunosignals in a primary melanoma (i), and increased nuclear reactivity of tumour cells in the matching lymph node metastasis (ii). (B) In contrast, ZEB2 expression showed strong immunoreactivity in the primary melanoma and markedly reduced expression in the corresponding metastasis (ii, intratumoural area). (C-i/ii) TWIST1 staining pattern was similar to ZEB1. Dermal fibroblasts were strongly positive for ZEB1 and TWIST1 antibodies (arrowheads in A-ii and C-i respectively). All photomicrographs $\times 20$.

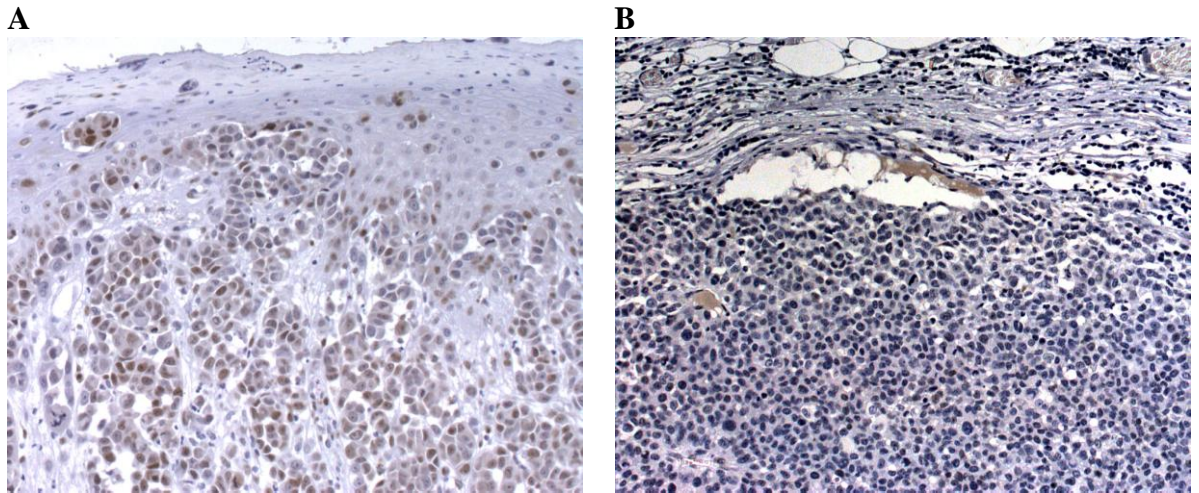


Figure 5.16 - Representative photomicrographs of SNAI2 expression in a paired nodal metastasis. (A) SNAI2-expressing cells are evident in malignant cells in the dermis of a primary melanoma ($\times 20$). (B) Low power view ($\times 20$) showing complete loss of SNAI2 immunoreactivity in the corresponding lymph node metastasis.

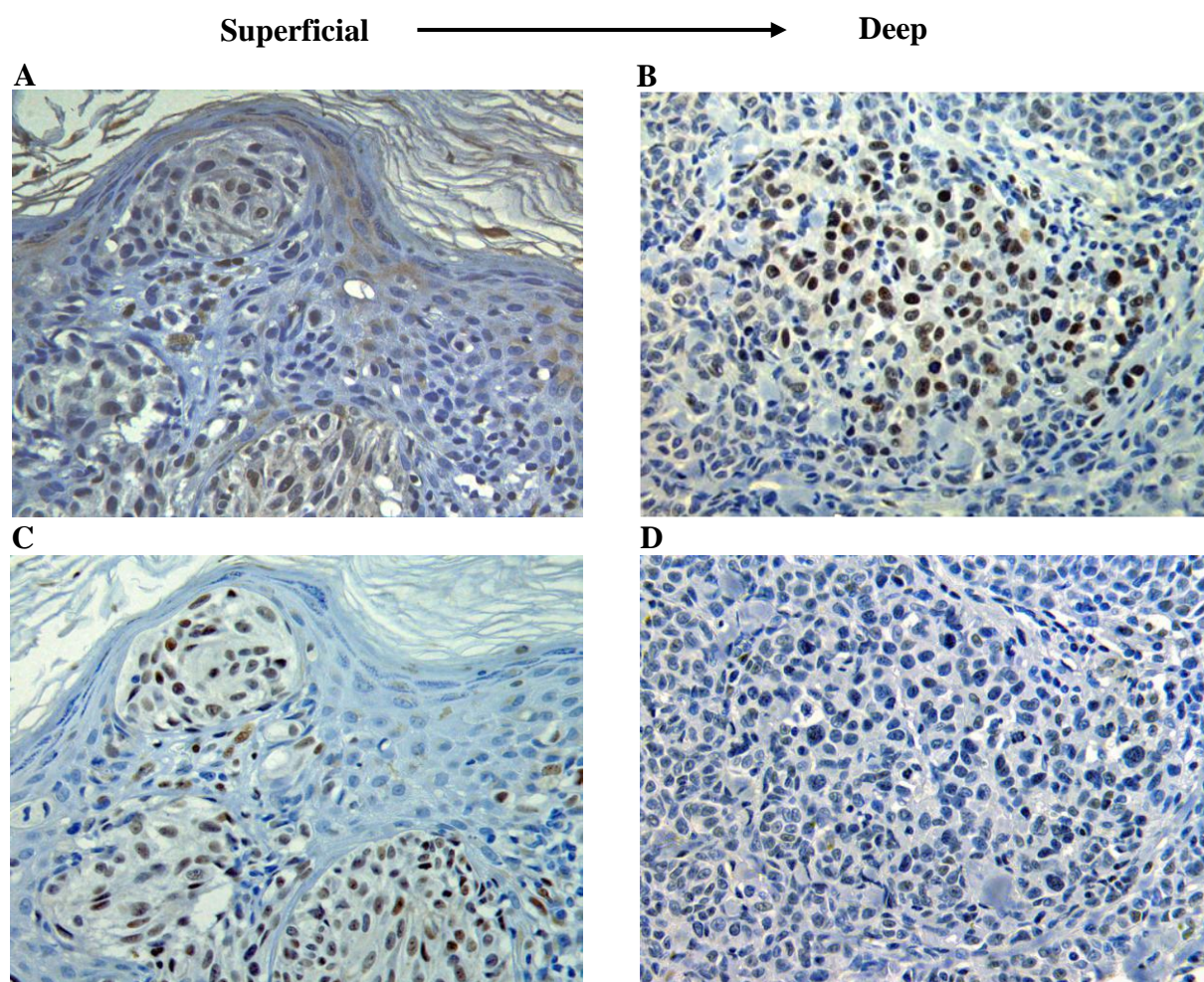
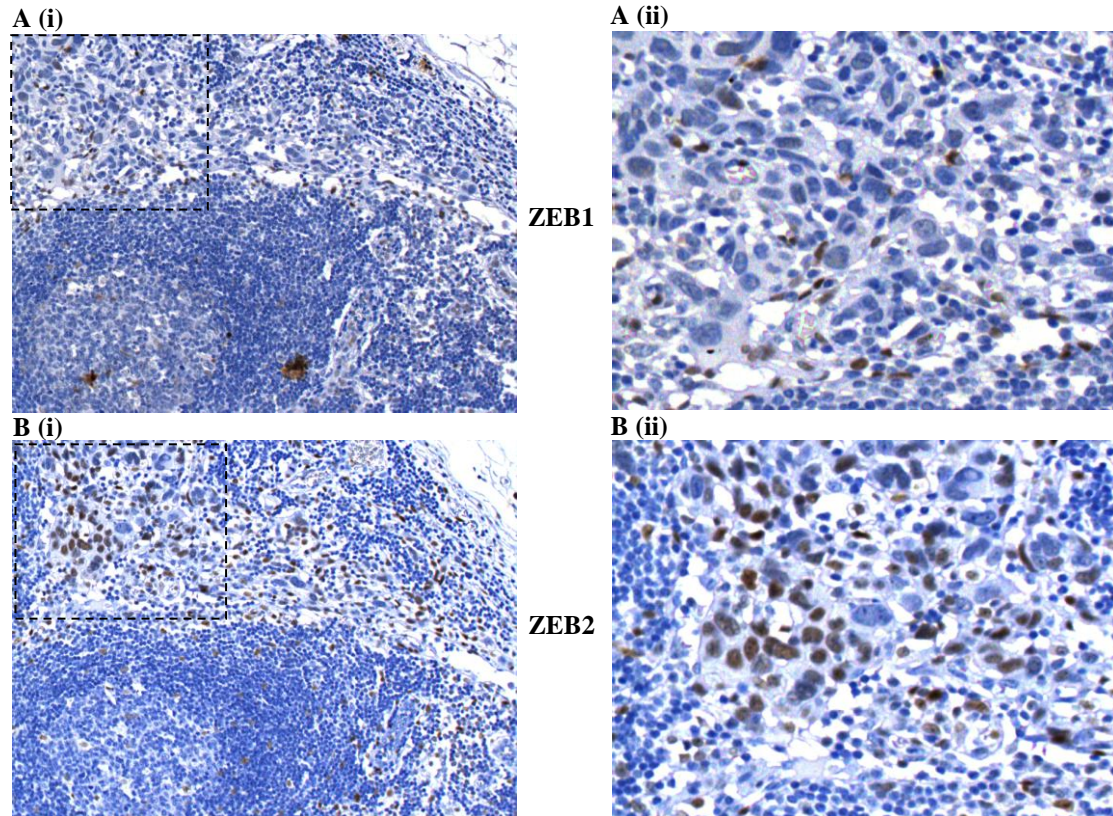


Figure 5.17 - ZEB1 and ZEB2 immunohistochemical staining of serial sections of a primary MM. (A-B) Comparing expression of ZEB1 between the deep and superficial sites, there was increased expression in the deep sites of the melanoma. (C-D) In contrast, ZEB2 immunostaining was decreased in the deep site compared to the superficial tumour area.

Periphery



Intratumoural

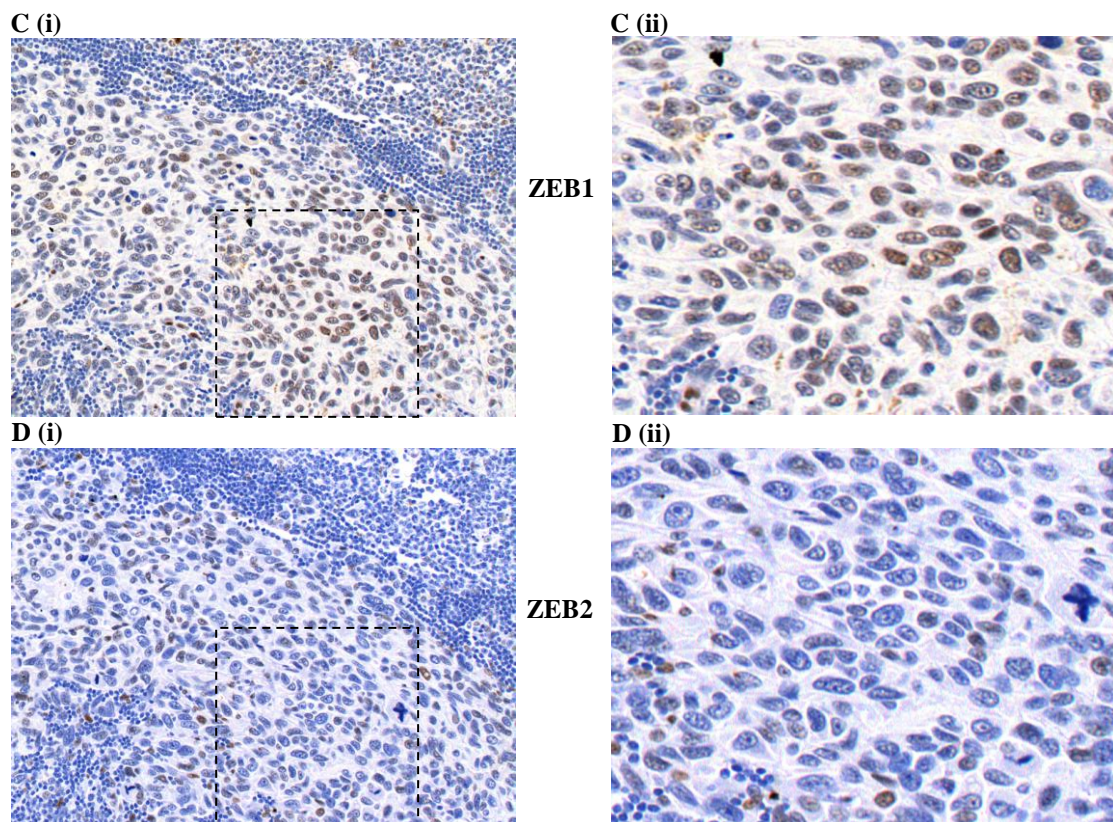


Figure 5.18 - Immunostaining for ZEB1 and ZEB2 in serial sections of a nodal metastasis (1st example). (A-i) Low power magnification (×20) in the periphery of the lymph node showed absent ZEB1 immunoreactivity. (B-i) Same tumour area demonstrated strong nuclear ZEB2 reactivity. (C-D) Inversely, immunostaining of ZEB1 revealed strong nuclear immunosignals (C-i) and complete loss of ZEB2 expression (D-i), in the same intratumoural part of the lymph node. (A-D-ii) High power views of the areas outlined by the rectangles in panels A-D (i).

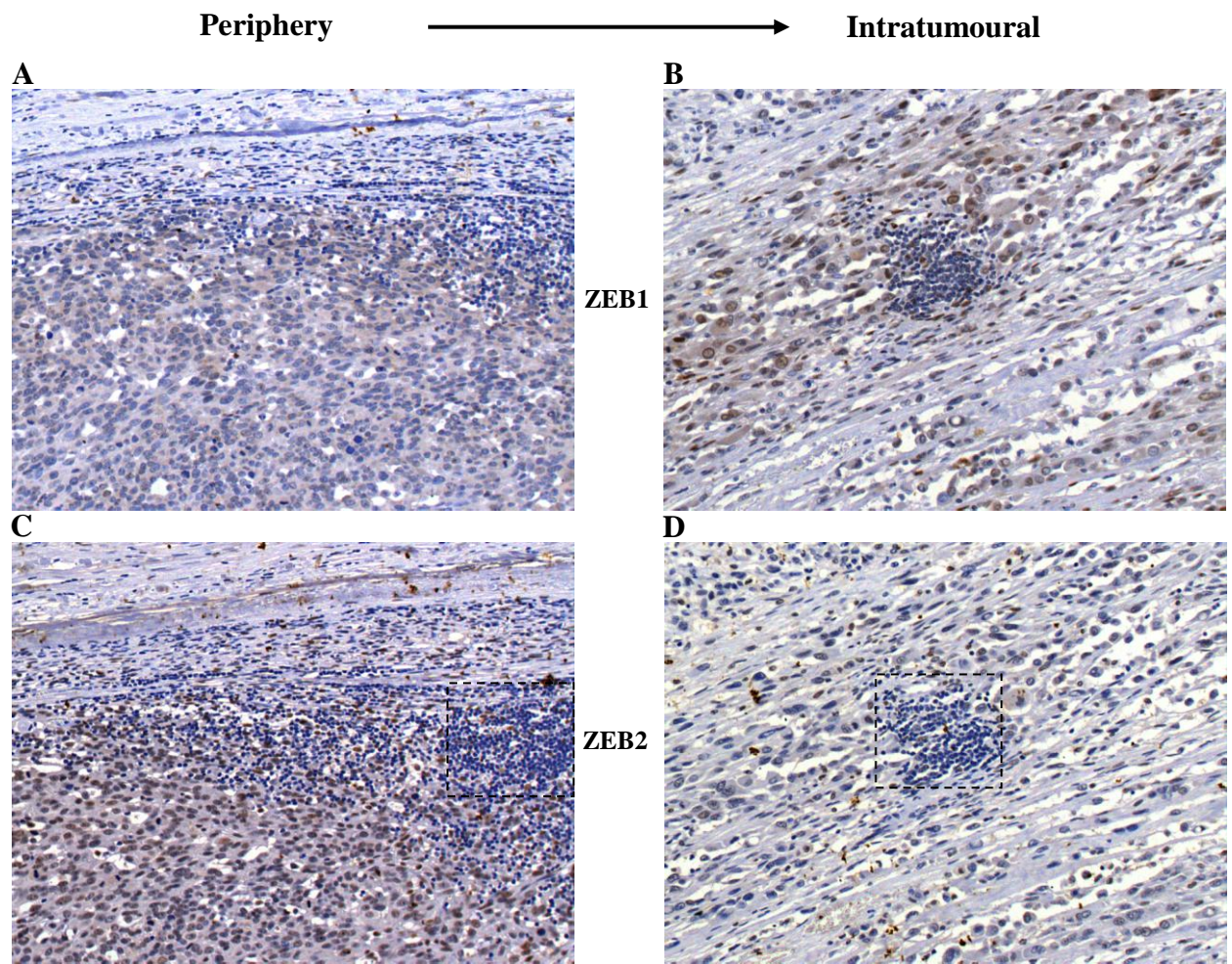


Figure 5.19 - Immunoreactivity for ZEB1 and ZEB2 in serial sections of a lymph node metastasis (2nd example). (A) Low power view (×20) in the periphery of the lymph node showed absent ZEB1 immunoreactivity. (C) Same tumour area demonstrated strong nuclear ZEB2 reactivity. (B, D) In contrast, immunostaining of ZEB1 revealed nuclear staining (B) and complete loss of ZEB2 expression (D) in the same intratumoural part of the lymph node. Lymphocytes are negative for both ZEB proteins (rectangles in panels C and D).

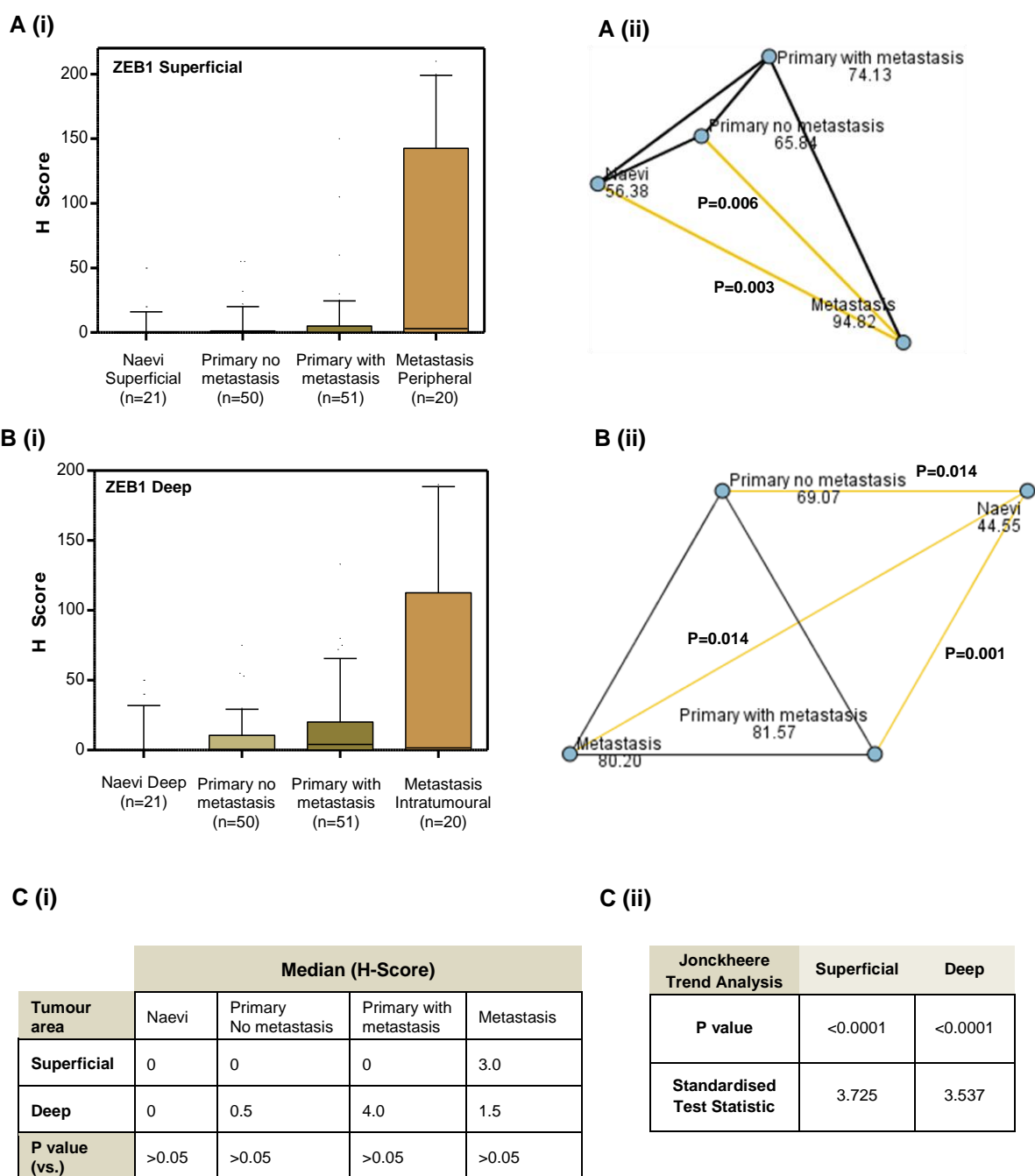


Figure 5.20 - Box and whisker plots of ZEB1 IHC staining (H-Score) for a melanoma independent progression series including naevi, primary melanoma and metastasis. Staining was measured at superficial and deep sites for each melanocytic lesion. (A-B) Expression of ZEB1 was significantly increased with melanoma progression at both superficial (A-i) and deeper lesions (B-i) ($P=0.002$, Kruskal-Wallis). Higher levels of staining were found at deeper tumour sites. (A-B-ii) Schematic representations of pairwise comparisons in which each node represents the sample average rank of tumour type. Yellow lines correspond to a significant difference in staining between tumour types. Error bars represent the 10th and 90th percentiles. (C) (i) Medians and P values between superficial and deep IHC staining (Kruskal-Wallis). (ii) Jonckheere-Terpstra trend analysis showed a significant association of ZEB1 expression with tumour progression.

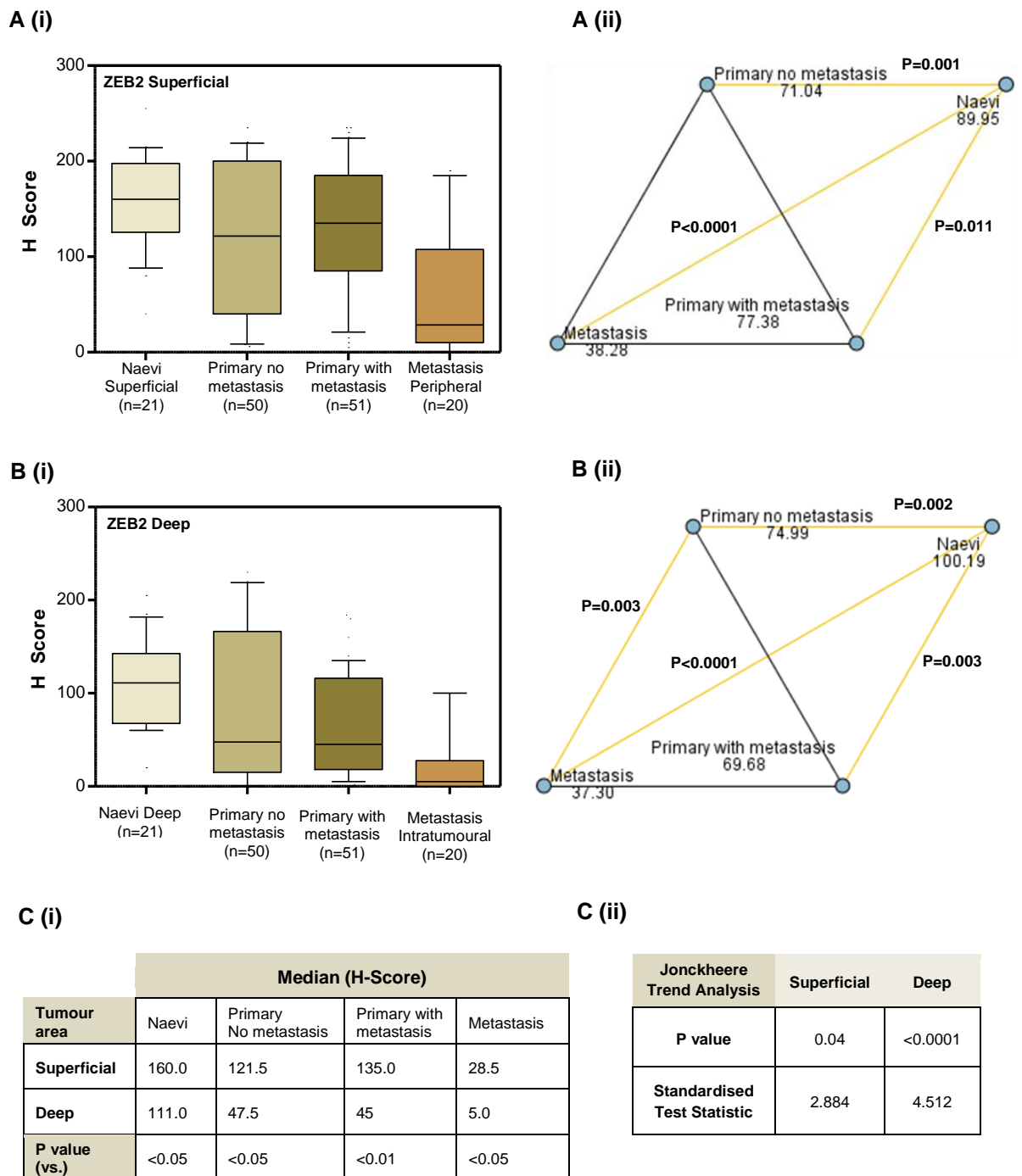


Figure 5.21 - Box and whisker plots of ZEB2 IHC staining (H-Score) for a melanoma independent progression series including naevi, primary melanoma and metastasis. (A-B) Expression of ZEB2 was significantly decreased with melanoma progression at both superficial (A-i) and deeper lesions (B-i) ($P<0.0001$, Kruskal-Wallis). Lower levels of staining were found at deeper tumour sites. (A-B-ii) Schematic representations of pairwise comparisons in which each node represents the sample average rank of tumour type. Yellow lines correspond to a significant difference in staining between tumour types. Error bars represent the 10th and 90th percentiles. (C) (i) Medians and P values between superficial and deep IHC staining (Kruskal-Wallis). (ii) Jonckheere-Terpstra trend analysis showed a significant association of ZEB2 expression with tumour progression.

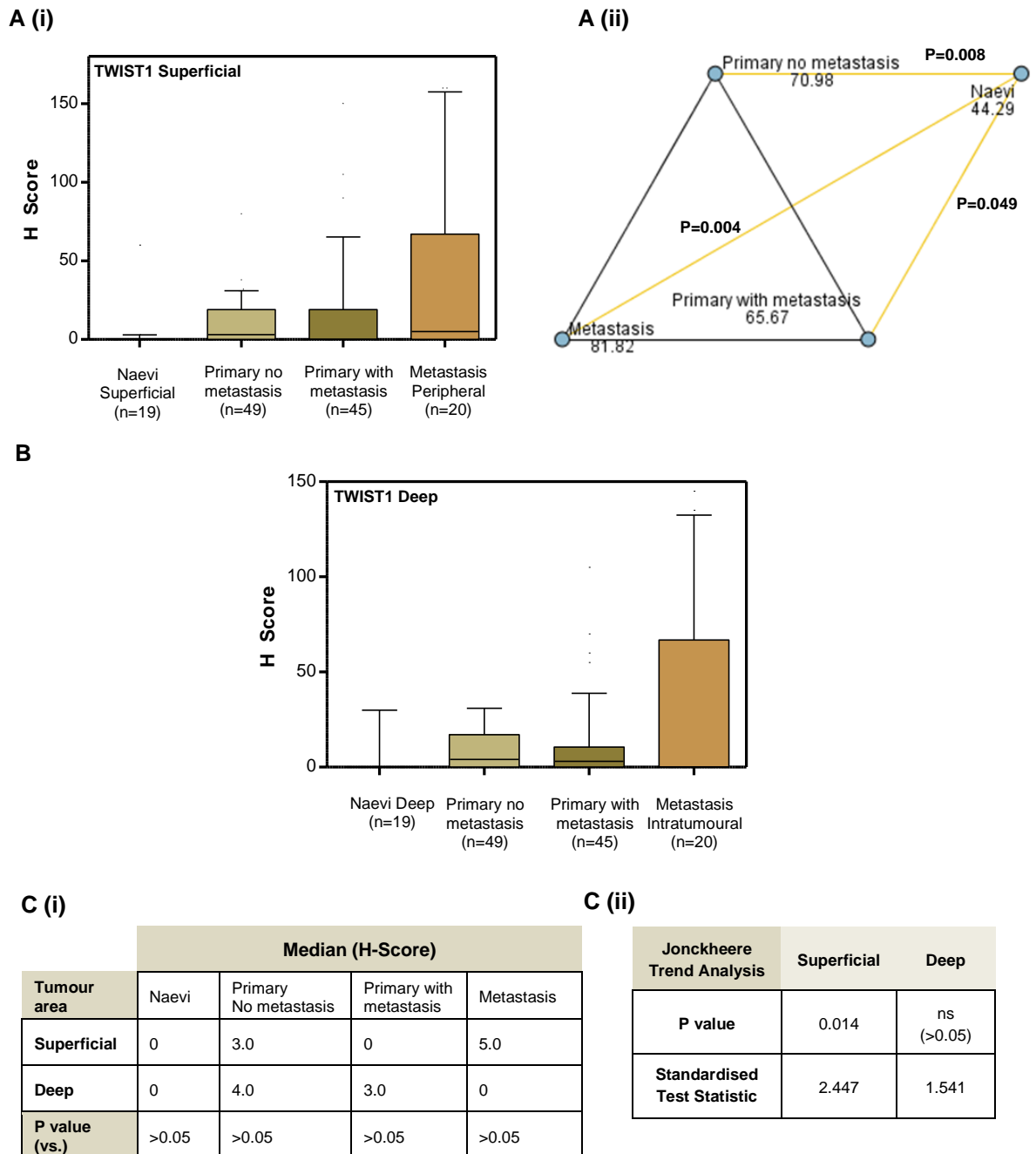
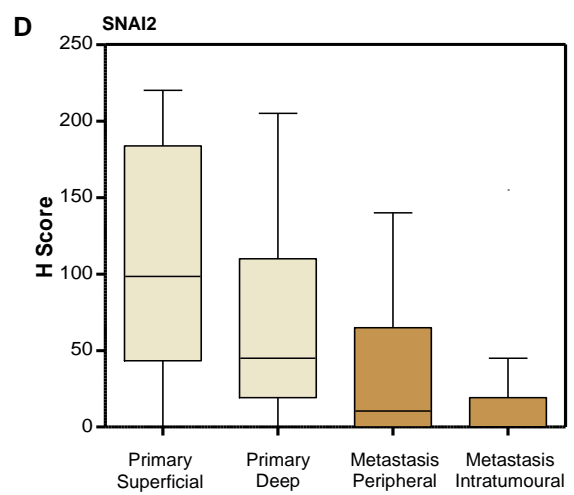
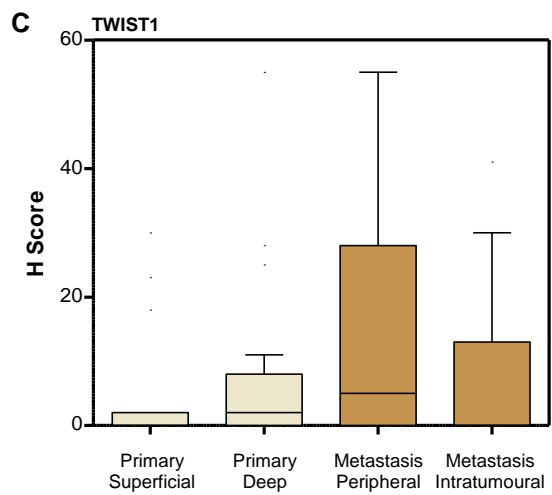
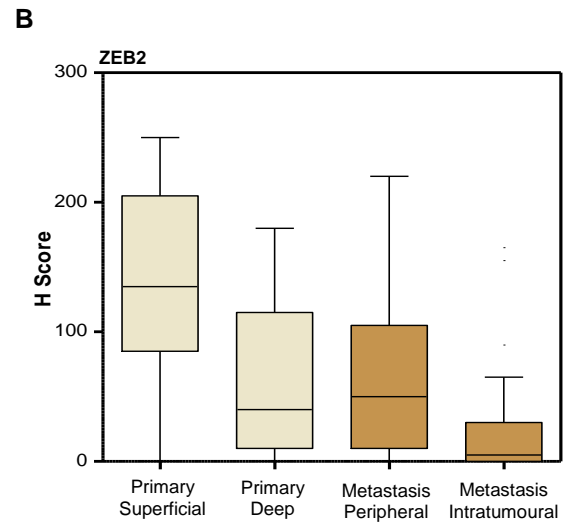
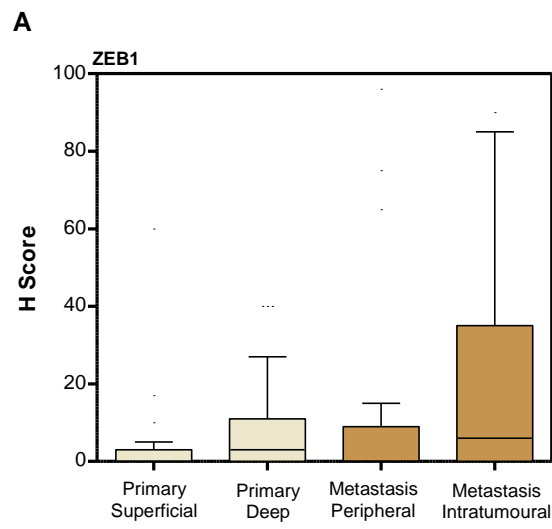


Figure 5.22 - Box and whisker plots of TWIST1 IHC staining (H-Score) for a melanoma independent progression series including naevi, primary melanoma and metastasis. Staining was measured at superficial and deep sites for each melanocytic lesion. (A-B) Expression of TWIST1 was significantly increased with melanoma progression at both superficial (A-i) and deeper lesions (B) ($P=0.007$ and $P=0.034$, respectively-Kruskal-Wallis). (A-ii) A schematic representation of pairwise comparisons, in which each node represents the sample average rank of tumour type. Yellow lines correspond to a significant difference in staining between tumour types. Multiple comparisons were not performed for TWIST1 (deep site) because the overall test did not show significant differences across samples. Error bars represent the 10th and 90th percentiles. (C) (i) Medians and P values between superficial and deep IHC staining (Kruskal-Wallis). (ii) Jonckheere-Terpstra trend analysis showed a non significant association of TWIST1 expression with tumour progression.



E (i)

	Paired Melanomas			
	Primary MMs		Nodal metastases	
	Superficial site H-Score	Deep site H-Score	Peripheral site H-Score	Intratumoural site H-Score
ZEB1				
Median	0	3.0	0	6.0
P value (vs.)	ns (P>0.05)		ns (P>0.05)	
ZEB2				
Median	135.0	40.0	50.0	5.0
P value (vs.)	P<0.001		P<0.001	
TWIST1				
Median	0	2.0	5.0	0
P value (vs.)	ns (P>0.05)		ns (P>0.05)	
SNAI2				
Median	98.5	45.0	10.5	0
P value (vs.)	P<0.01		P<0.01	

(ii)

Page's L Trend Analysis	ZEB1	ZEB2	TWIST1	SNAI2
P value	<0.01	<0.01	ns (>0.05)	<0.01

Figure 5.23 - MR-EMT expression in paired melanoma samples. (A) Expression of ZEB1 was significantly increased in paired cases (P<0.0001, Friedman test). (B, D) Expression of ZEB2 and SNAI2 was significantly downregulated in paired cases (P<0.0001 in both, Friedman test). (C) TWIST1 upregulation was not statistically significant (P=0.6291, Friedman test). Error bars represent the 10th and 90th percentiles. (E) (i) Medians and P values between superficial and deep IHC-P staining (Friedman test). (ii) A decreasing trend of positive staining was observed from superficial sites to deep sites in the primary tumour and intratumoural sites of the metastases for both ZEB2 and SNAI2. ZEB1 and TWIST1 showed an increasing trend, but only ZEB1 was significant. ZEB1, ZEB2 and TWIST1 n=31; SNAI2 n=14.

5.3.6 Correlation of MR-EMT expression with clinical parameters

Previous results (section 5.3.5.2) showed a trend of transition from ZEB2^{high}/SNAI2^{high}/ZEB1^{low}/TWIST1^{low} towards a ZEB2^{low}/SNAI2^{low}/ZEB1^{high}/TWIST1^{high} expression pattern. This transition was evident at deeper sites of the lesions and correlated with the level of malignancy. These findings prompted further to perform survival analyses for all primary melanomas with 5-years follow-up data (n=98). Kaplan Meier survival curves for the expression of different MR-EMT modulators (ZEB1, ZEB2 and TWIST1) and Breslow depth are shown in Figure 5.24. Significant shorter metastasis-free survival were observed for Breslow depth (<1.5mm, <4.0mm, >4.0mm P<0.0001, log-rank test), ZEB1-positive (P<0.01) and ZEB2 low (H-Score <50, P<0.05) at deep sites and TWIST1 high (H-Score >40, P=0.001) at superficial sites (Figure 5.24-A-D). Two step cluster analysis using H-Scores of these MR-EMT identified three distinct natural groups of expression with significant differences in clinical outcome. High ZEB1, low ZEB2 and high TWIST1 had the worse prognosis, whereas those with low ZEB1, high ZEB2 and low TWIST1 had the best disease-free survival rate. The third subgroup of patients with low H-Score staining for these MR-EMT showed an intermediate survival rate (P=0.001, log-rank test) (Figure 5.24-E). In univariate analysis, both superficial and deep staining of ZEB1, deep staining of ZEB2 and superficial staining of TWIST1 are significant with Breslow depth (Table 5.2). In a multivariate analysis, both superficial and deep staining of ZEB1 and superficial TWIST1 combined with Breslow thickness, were all significant independent predictors of time to metastasis (Table 5.2). Loss of ZEB2 staining at deep sites decreased metastasis-free survival but not independent of tumour depth (Table 5.2).

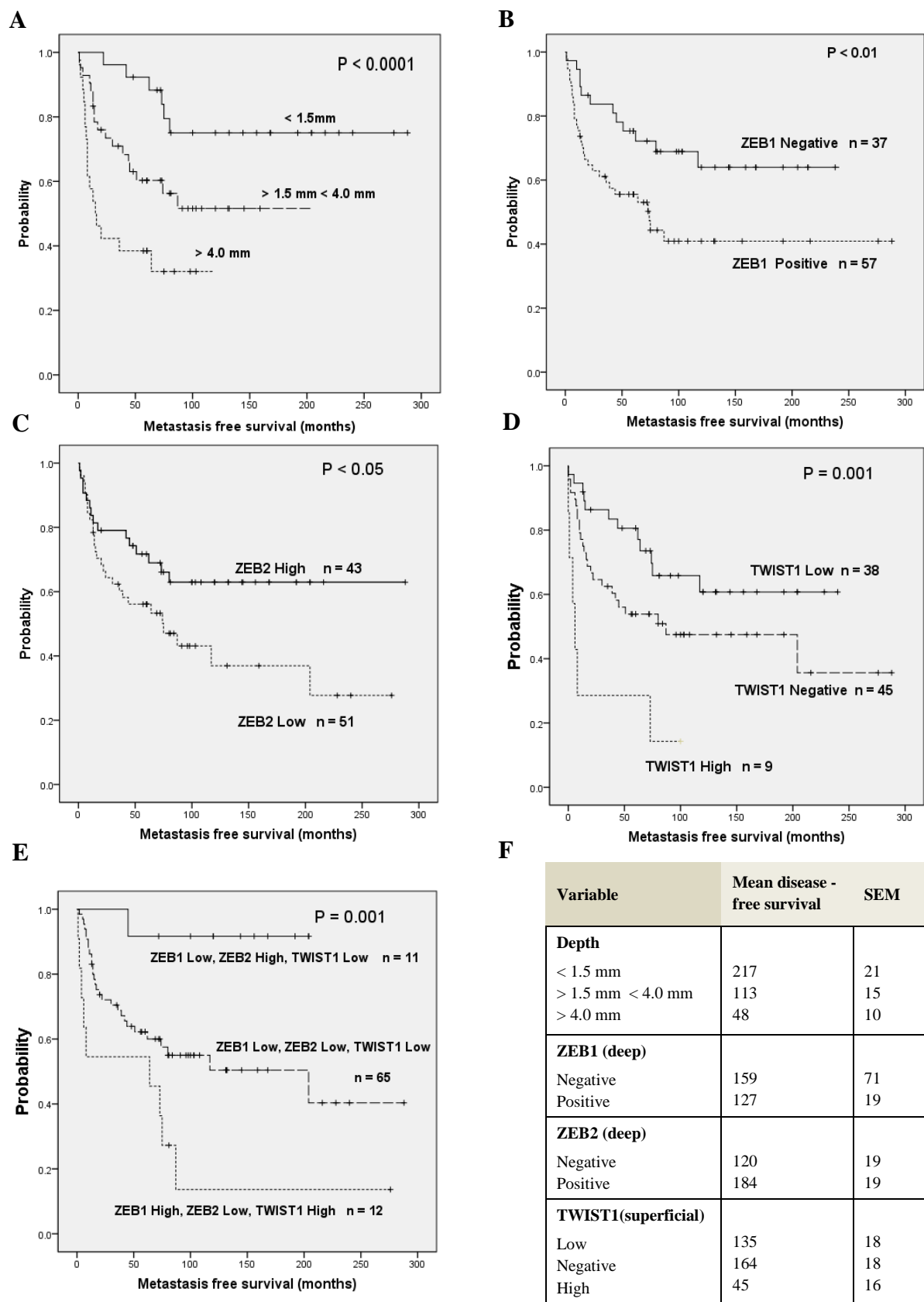


Figure 5.24 - Kaplan Meier survival curves comparing disease free survival in patients with primary cutaneous MM with or without metastases. (A) Breslow depth, (B) ZEB1 deep H-Score (positive ≥ 1), (C) ZEB2 deep H-Score (cut-off >50 for high H-Score), (D) TWIST1 superficial H-Score (cut-off >40 for high H-Score), (E) Two step cluster analysis survival curve, (F) Mean disease-free survival and SEM values for survival curves.

Table 5.2. Univariate and multivariate Cox proportional hazard analysis for clinical prognostic factors, age, gender, tumour Breslow depth, ulceration, stage and MR-EMT expression (H-Score).

			Univariate Cox Proportional hazard analysis Metastasis free survival			Multivariate Cox Proportional hazard analysis Metastasis free survival		
Variable	Evaluation	N*	HR (95% confidence interval)		P value	HR (95% confidence interval)		P value
Age	< 60	46	1			1		
	> 60	52	1.643	0.909-2.969	0.01	0.781	0.404-1.513	0.464
Gender	Female	57	1			1		
	Male	41	1.995	1.119-3.555	0.02	1.760	0.933-3.320	0.081
Breslow	< 1.5 mm	29	1			1		
	> 1.5 mm < 4.0mm	43	2.674	1.159-6.17	0.021	3.088	1.179-8.088	0.0220
	> 4.0mm	26	5.104	2.141-12.17	< 0.001	5.352	1.893-15.12	0.002
Ulceration	No ulceration	59	1			1		
	ulceration	39	1.808	1.008-3.242	0.049	1.178	0.585-2.374	0.646
Stage	1	24	1					
	2	14	2.976	1.774-11.449	0.113			
	3	35	6.222	2.061-8.784	0.001			N/T
	4	25	10.380	3.342-32.241	<0.001			
ZEB1 Superficial	H-Score	98	1.0209	1.009-1.033	<0.001	1.0222	1.009-1.035	<0.001
ZEB1 Deep	H-Score	98	1.0147	1.006-1.023	<0.001	1.0125	1.004-1.021	0.002
ZEB2 Superficial	H-Score	98	0.999	0.996-1.003	0.811	1.0022	0.997-1.007	0.357
ZEB2 Deep	H-Score	98	0.993	0.988-0.998	0.017	0.998	0.992-1.004	0.443
TWIST1 Superficial	H-Score	92	1.014	0.999-1.029	0.064	1.0204	1.004-1.036	0.012
TWIST1 Deep	H-Score	92	1.003	0.989-1.0173	0.664	1.0094	0.995-1.024	0.195

*Cases were excluded where time-to-event was zero (i.e. 4 cases where metastasis was the outcome); N/T not tested

5.4 Discussion

5.4.1 *A subset of MR-EMT has distinct protein expression patterns in melanocytic lesions*

To date most expression studies of MR-EMT genes in different cancer types have used RT-PCR or RNA microarrays in cell lines. Where MR-EMT mRNAs are expressed, the cells invariably have a mesenchymal phenotype and the mRNA expression levels do not necessarily always reflect protein levels. In addition, it is important to take into consideration that extraction of total mRNA from human tissues includes a population of contaminating cells, such as fibroblasts. Recently, it has also been demonstrated that post-transcriptional mechanisms are key players in the regulation of ZEB1 and ZEB2 abundance (Gregory et al., 2008, Park et al., 2008c). Therefore, RT-PCR analyses from various reports need to be interpreted with caution.

In this chapter, the expression of MR-EMT was evaluated in benign naevi and melanoma tissues by immunohistochemistry to provide a more accurate identification of cellular expression of these transcription factors. In addition, to ensure specificity of staining validated commercial or donated antibodies were further evaluated to confirm the specificity of MR-EMT by immunopositivity in nuclei of control cells. Compared to other studies, in this study the immunohistochemical analysis of melanoma biopsies has also benefited from having a proportion of primary melanomas with their corresponding lymph node metastases.

5.4.1.1 ZEB1

Immunohistochemical analysis of ZEB1 in various epithelial tumours supports the hypothesis that ZEB1 contributes to the development and progression of malignancies (reviewed in Sanchez-Tillo et al., 2011, Vandewalle et al., 2009). Elevated ZEB1 expression at the invasive front of different primary human carcinomas, including, breast, colon, prostate, ovarian, endometrium and ovarian, translates into increased aggressiveness and higher metastatic potential (Graham et al., 2010, Spaderna et al., 2008). In most of these studies de-differentiated tumour cells at the tumour-host interface exhibited primarily cytoplasmic ZEB1 staining. In contrast, tumour-associated stromal cells displayed an exclusive nuclear reactivity.

Herein, ZEB1 expression was absent in benign melanocytic naevi and normal melanocytes, but significantly increased with progressive tumour de-differentiation. In contrast to previous reports, ZEB1 showed a nucleus-restricted immunoreactivity in both tumour and reactive stromal cells. Interestingly, highest expression of ZEB1 was observed in deep sites of metastatic primary MMs and intratumoural areas of lymph node metastases, suggesting a potential role of ZEB1 in the invasion and dissemination of tumour cells to metastatic sites via EMT. In addition, ZEB1 transient activation seems to occur in a subset of cells which are confined to restricted areas at deep and intratumoural components of metastatic primary melanomas and nodal metastases respectively. It would be of great interest to investigate whether ZEB1 immunopositivity in these specific tumour regions is associated with vascular invasion that predominantly occurs via lymphatic vessels (Storr et al., 2012). As previously studies have shown, it was not possible to accurately assess ZEB1 staining in relation to lymphatic invasion using double immunolabelling (Massi et al., 2006, Niakosari et al., 2008). Lymphatic vessels were predominantly identified by the specific endothelial

marker D2-40 in the superficial / peripheral components of primary melanomas and nodal metastases which showed fewer or none ZEB1 positive cells compared to melanoma cells at deeper sites.

Noteworthy, the molecular cues that induce ZEB1 expression are still elusive. One attractive hypothesis is that dermal fibroblasts, which are detected at the tumour-host interface and previously shown to produce TGF- β and tumour necrosis factor- α (TNF- α) may induce ZEB1 expression (Chua et al., 2007, Nishimura et al., 2006). Melanoma-associated stromal cells were also ZEB1-positive in metastatic melanomas. Increasing evidence suggests that ongoing alterations of tumour microenvironment exert major effects on neoplastic cells, and that the tumour-associated stromal cells make an important contribution to the process of malignant transformation and / or progression (Orimo et al., 2005).

5.4.1.2 ZEB2

Immunohistochemical data on the expression of ZEB2 in human tumour biopsy samples is limited. Few studies demonstrated that ZEB2 protein can activate tumour cell invasiveness (Alves et al., 2007, Rosivatz et al., 2002). A recent study by Oztas *et al* reported a differential expression of ZEB2 in a series of human carcinomas via tissue microarrays (Oztas et al., 2010). Whilst ZEB2 was found to be downregulated in cancers from stomach, liver, rectum, esophagus and colon tissues, it was overexpressed in tumours of the uterus, breast, lung and kidney compared with their normal tissues. The authors also found cytoplasmic ZEB2 staining in most of the analysed tissues. Cytoplasmic localisation of ZEB2 has also been observed in ovarian and bladder tumours (Sayan et al., 2009, Yoshida et al., 2009). Since ZEB2 is only known as transcriptional factor, its cytoplasmic expression indicates implication of as yet unknown regulatory mechanisms that prevent translocation of ZEB2 into the nucleus.

In the present study all benign and MM samples displayed an exclusive nuclear expression of ZEB2, where it can exert its gene repressive function. In addition, despite the presence of ZEB2 in cultured melanoma cells and its biological ability to protect neoplastic cells from DNA damage-induced apoptosis (Sayan et al., 2009) the assumption that ZEB2 may function as an oncogenic marker in melanoma progression was contradicted by the IHC data.

The current immunohistochemical analysis revealed a heterogeneous loss of ZEB2, with preferential loss of staining at deep / intratumoural sites of benign, malignant tissues and nodal metastases, and a significant trend of decreasing expression from naevi to melanoma. In fact, ZEB2 was found to exert tumour-suppressive properties by direct repression of cyclin D1 (Mejlvang et al., 2007) and induction of replicative senescence (Ozturk et al., 2006). Recently, ZEB2 mRNA was shown to suppress melanomagenesis by enhancing PTEN expression in a miR-dependent manner (Karreth et al., 2011). However, in the lymph node metastases, peripheral staining of ZEB2 and loss at the intratumoural areas may imply that melanoma cells require active ZEB2 to acquire an epithelial phenotype via MET and establish micro or macro / clinical metastases.

Taken together these findings suggest that within melanoma progression, ZEB2 may be something of a paradox, having a protective tumour suppressive role against malignant transformation in benign and primary melanocytic lesions, but promoting acquisition of epithelial phenotype through MET in the periphery of lymph nodes.

5.4.1.3 ZEB1 and ZEB2 expression patterns in paired samples

The majority of the mRNA and protein expression studies of ZEB1 and ZEB2 in several cancer types indicated that both are associated with a mesenchymal phenotype and promote tumour progression and the spread of neoplastic cells to regional lymph nodes (Gemmell et al., 2011, Kurahara et al., 2012).

Analyses of paired melanoma tissues revealed that the transition from a benign into malignant melanoma requires an oncogenic switch in MR-EMT network. In this regard, ZEB1 and ZEB2 demonstrated a unique mutually exclusive pattern during the course of melanoma progression (Figures 5.15 and 5.17-19). In particular, even if ZEB2 was still expressed in the majority of nodal metastases its staining was mainly peripheral. The central part of the node had no or very little ZEB2. Inversely, ZEB1 expression in metastases was primarily expressed at intratumoural sites and ZEB2-negative areas. Increased ZEB1 and reduced ZEB2 protein levels were observed in areas of vertical growth with no or aberrant E-cadherin expression in the invading melanoma cells (section 4.3.1, Figures 4.1-4.7) indicating that the switch from ZEB2 to ZEB1 might be associated with acquisition of an invasive phenotype as part of the EMT.

Interestingly, there was a significant inter-tumoural heterogeneity of ZEB1 and ZEB2 proteins in metastases, with a proportion of nodal metastases exhibiting ZEB2 expression only, others a mutually exclusive pattern and a further group maintained expression of ZEB1 and ZEB2 at both tumour locations. The existence of different regulatory mechanisms may reflect these differing staining patterns of ZEB proteins.

5.4.1.4 TWIST1

Tissue microarray and immunohistochemical staining analyses showed upregulation of TWIST1 reactivity in a wide range of human cancers and tumour-derived cell lines (section 1.4.2.3), and have highlighted its important role in tumour initiation, progression and metastasis (reviewed in Qin et al., 2012). The association of TWIST1 expression with metastatic melanoma lesions, including nodal and distant metastases, has been reported in a previous study (Hoek et al., 2004). However, its exclusive cytoplasmic localisation is likely to be an artefact due to the poor IHC-P specificity of most commercial antibodies raised against TWIST1.

In melanomas activation of TWIST1 has been suggested to cooperate with mitogenic oncoproteins and to play an early role in carcinoma initiation and cell dissemination (Ansieau et al., 2008). The same authors also reported that nuclear TWIST1 staining was strong in the majority of primary melanomas, whereas no TWIST1-expressing cells were detected in a small number of benign lesions. However, they have not investigated TWIST1 in regional or distant metastatic tissue to complete the analysis of the progression series. This current study has extended the range of human melanoma specimens, to include metastatic tissue.

Significant differences in TWIST1 staining were found between benign and malignant melanoma biopsies. In the naevi all tumour cells were negatively stained in contrast to melanocytic lesions where TWIST1 staining was significantly increased in few deep MMs and in the majority of peripheral components of nodal metastases. This may suggest that TWIST1 regulates distinct stages of melanoma progression, such as invasion deeper into the dermis and re-differentiation and settlement at nodal metastases. In addition, TWIST1 was highly expressed in stromal cells in most benign

and malignant melanomas. The nature of these fibroblast-like cells remains unknown but it has been recently postulated that may represent tumour cells that have undergone a TWIST1-dependent EMT *in vivo* (Mink et al., 2010, Rhim et al., 2012).

In the present study it is noteworthy to mention that TWIST1 staining showed a significant clonal phenotypic heterogeneity in metastases. According to the traditional model of linear tumour development, the acquisition of metastatic ability is considered to be the final step in cancer progression. As a result, neoplastic cells found in metastases are considered as direct descendants of clones present in the bulk of primary tumour cells. In addition, this model predicts that anatomically distinct metastases, originated from the same patient, should demonstrate similar clonal relationships among each other. Liu *et al* elegantly illustrated this prediction by analysing different metastatic lesions in prostate tumour patients using high-resolution genome-wide single nucleotide polymorphism and comparative genomic hybridization arrays (Liu et al., 2009a).

However, increasing evidence challenges this model of progression indicating that metastatic tumours have diverged from different clones at earlier stages of tumour evolution. A recent report demonstrated multiple mutations present only in metastatic sites compared to primary tumours in lobular breast malignancies (Shah et al., 2009). Moreover, in esophageal cancers resection of primary lesions did not improve patient survival, underlying the significance of early metastatic dissemination (Bedenne et al., 2007). As only a very small proportion of metastatic primary melanomas showed TWIST1 reactivity, it is plausible that TWIST1-positive clones may derived from neoplastic cells capable of early spread and initiation of secondary tumours at metastatic sites. Nevertheless, the co-existence of distinct clones within a metastatic

tumour not only emphasizes the complex network of interactions between neoplastic cells but also poses challenges for the development of efficient targeted therapy approaches.

5.4.1.5 SNAI2

Few studies to date demonstrated that overexpression of SNAI2 in primary human tumours is associated with tumour grade, distant metastasis and patient poor survival (Alves et al., 2009). In addition, SNAI2 has been associated with melanoma metastasis in a mouse model (Gupta et al., 2005). The current immunohistochemical analysis of a small series of melanoma paired tissues showed a progressive change in SNAI2 expression through the tumour mass with immunopositivity mainly at superficial sites of melanocytic lesions. Similarly to ZEB2, nuclear localised active SNAI2 was found to be less in metastasis than in corresponding primary tumours. Consistent with other studies the immunohistochemical staining of SNAI2 in naevi showed nucleus-restricted immunoreactivity and was expressed predominately in superficial sites, basal proliferating keratinocytes and normal melanocytes in the basal layer of the epidermis (Turner et al., 2006). In contrast, SNAI2 was expressed in all melanoma cultures, indicating a potential contribution of SNAI2 to BRAF / NRAS-driven melanocyte transformation (section 3.3.1, Figure, 3.3).

A potential explanation for this apparent discrepancy between *in vivo* and *in vitro* data might be the presence of additional transcriptional factors in human melanoma specimens that can modulate SNAI2 activity or SNAI2 expression is "exposed" to different levels of transcriptional regulators. Another putative explanation is that total protein expression does not necessarily reflect the amount of functional SNAI2.

Based on the current *in vivo* data and in contrast to *in vitro* findings seems that SNAI2 is likely to be important in *BRAF* oncogene-induced cell-cycle arrested melanocytic naevi conferring resistance to both cell proliferation and acquisition of invasive phenotype. Therefore and in line with recent studies, that also reported higher expression of SNAI2 protein in naevi than in primary and metastatic melanomas, SNAI2 seems to play an essential tumour suppressing role early during melanoma development (Koefinger et al., 2011, Sanchez-Martin et al., 2002, Shirley et al., 2012). Shirley *et al* further demonstrated co-expression of MITF and SNAI2 in melanoma tumours (Shirley et al., 2012). There are several lines of evidence supporting the link between MR-EMT and MITF. A study by Liu *et al* suggested that *ZEB1* knockout downregulates MITF in renal pigment epithelium (Liu et al., 2009b). The neural crest-specific knockout of *ZEB2* reduced MITF-positive cells in mouse embryos (Van de Putte et al., 2003). In addition, mutations in *MITF* and homozygous deletion of *SNAI2* caused the auditory-pigmentary symptoms in at least some individuals with Waardenburg syndrome type 2 (Sanchez-Martin et al., 2002).

Comparison of gene expression profiles of tumor cell lines derived from melanocytes, radial and vertical growth phase melanomas showed loss of differentiation-associated genes, early during melanoma development (Ryu et al., 2007). A recent work postulated that MITF is involved in the induction of the tumour suppressor gene *CDKN2A* and subsequent cell-cycle arrest (Bloethner et al., 2007). However, the role of MITF is not limited to melanoma initiation (Garraway et al., 2005) and currently its function is being intensively discussed in the context of the mechanisms underlying cell plasticity in MM. According to the "phenotypic" plasticity model, the highest MITF expression maintains a differentiated status of cell-cycle arrested melanocytes, while reduction of MITF expression contributes to the transition from a quiescent to a proliferative stage.

Further decrease in MITF expression generates invasive and slow-proliferating cells with tumour-initiating properties (reviewed in Bell and Levy, 2011).

5.4.2 Expression of ZEB proteins in a mouse $BRAF^{V600E}$ model

A powerful approach in investigating the direct pathophysiological role of mutations *in vivo* is the generation of mutant mice model systems. The relevance of such systems to humans is an essential issue in order to assess molecular and histological changes that take place during melanomagenesis. For that reason, ZEB1 and ZEB2 protein expression has also been examined by immunohistochemistry in a $BRAF^{V600E}$ - driven murine melanoma (Dhomen et al., 2009).

The immunostaining of a small number of wild-type mouse skin and melanoma lesions for ZEB1 and ZEB2 revealed high reactivity only in melanocytic lesions. The normal melanocytes in murine skin sections did not display any staining for ZEB2, opposing the findings from human melanocytes residing in the epidermis of normal or lesional skin (Figures 5.7 and 5.9). These contrasting results elucidate certain limitations of using murine melanoma models. At the outset, the complexity of experimental tumours is low in model systems compared with the variability of melanoma biology in humans. Furthermore, the structure of skin in mice is different to humans as for instance there is no a junctional component (epidermal / dermal crossover). Finally, in murine melanomas melanocytes are usually exclusively located in the dermis and do not have metastatic capabilities. In contrast, histological localisation of human melanocytes is epidermal. However, it may be argued that according to recent evidence a significant proportion of mouse melanocytes is located in hair follicles, which is an epidermal appendage and therefore melanomas could be of epidermal origin (Larue, 2012). Thus,

the location of melanocytes in the dermis, from which a subset of mouse melanomas originate, may explain the differential expression of ZEB2 compared to epidermal human melanocytes.

5.4.3 *MR-EMT expression and clinical outcome*

The association of ZEB1, ZEB2 and TWIST1 expression of the primary tumour and metastasis with highly specific antibodies has not been previously investigated in MM. At later stages of melanoma development, ZEB1 high expression and ZEB2 loss at deep sites and TWIST1 high expression at superficial sites of primary MMs were significantly associated with adverse prognosis, predicting shortened tumour-specific survival in melanoma patients. This is compatible with progressive gain of ZEB1/TWIST1 and decrease of ZEB2 predisposing to dermal invasion leading to thicker and more aggressive tumours. This finding is in agreement with the data reported by previous studies showing that increased expression of ZEB1 and TWIST1 is a significant predictor of poor patient survival (Hoek et al., 2004, Kyo et al., 2006, Spaderna et al., 2006, Spoelstra et al., 2006). Although, in the majority of IHC-P studies increased ZEB2 expression contributes to poor patient survival, a recent study by Oztas *et al* demonstrated that ZEB2 expression was reduced in a subset of carcinomas (Oztas et al., 2010), section 5.4.1.2). Even if this observation coincides with the findings from this work, the authors did not investigate associations between ZEB2 and clinical parameters.

In the present study, Breslow thickness was the single most important histological prognostic factor of metastasis-free survival. Multivariate analysis using the Cox model demonstrated that metastasis-free survival was significantly correlated with high ZEB1 expression at both superficial and deep sites and TWIST1 at the superficial sites independently of Breslow thickness. In contrast, the occurrence of metastasis was inversely related to downregulation of the ZEB2 at the deep primary sites but not independently of Breslow depth. As a result, any influence of ZEB2 at this site on metastasis, would be secondary to an effect on tumour thickness. This may indicate that during early development of the tumour, when malignant cells are invading the dermis, tumours composed of malignant cells with lower levels of ZEB2 are more likely to invade deeper into the dermis. Together, these data suggests that a switch from ZEB2 to ZEB1/TWIST1 expression is a risk factor for outcome in MM when controlling for other clinicopathological variables.

The association of MR-EMT (ZEB1, ZEB2 and TWIST1) expression of the primary tumour and metastasis has not been reported previously in systemic cancers. Herein, clustering of primary melanomas on the basis of immunohistochemical H-Score analysis revealed that patients with ZEB1^{high/deep}, TWIST1^{high/superficial} and ZEB2^{low/deep} had the lowest metastasis-free survival. This novel finding suggests that differential expression of these factors at distinct sites (superficial or deep) could predict clinical outcome in melanoma patients.

5.4.4 Conclusions

- The expression of ZEB1, ZEB2, SNAI1, SNAI2 and TWIST1 showed an exclusive nuclear immunoreactivity in melanoma tissues and specificity was confirmed using suitable controls.
- In a murine *BRAF*^{V600E} model ZEB1 and ZEB2 proteins were only detected in malignant tumours but not in the normal skin.
- IHC-P showed that differentiated epidermal human melanocytes were positive for ZEB2 and SNAI2 but negative for ZEB1 and TWIST1.
- The protein expression levels of ZEB2 and SNAI2 were reduced in deep naevi / primary melanomas and intratumoural areas of nodal metastases compared to superficial sites. In contrast, ZEB1 and TWIST1 showed negative immunostaining in naevi but increased expression in deep primary melanomas and central areas of lymph node metastases compared to superficial areas.
- Trend analyses demonstrated a significant gain of ZEB1 and TWIST1 protein expression with tumour progression by comparing benign naevi with primary melanomas and lymph node metastases using independent and matched tumour samples. An opposite trend to ZEB1 and TWIST1 was evident for ZEB2 and SNAI2.
- Kaplan Meier analysis showed an association between decreased metastasis-free survival and high expression of ZEB1 and TWIST1 at deep and superficial sites of primary melanomas respectively. In addition, low ZEB2 expression at deep sites of primary melanoma reduced metastasis-free survival.

- Multivariate analysis suggested that gain of ZEB1 and TWIST1 was directly associated with poor patient survival and independent of breslow thickness. In addition, ZEB2 loss decreased metastasis-free survival but not independent of tumour depth.
- Cluster analysis predicted the lowest disease-free survival rate in patients with ZEB1^{high/deep}, TWIST1^{high/superficial} and ZEB2^{low/deep}.

6 Final discussion

6.1 A network of MR-EMT contributes to the neoplastic transformation of melanocytes

The aberrant reactivation of embryonic inducers of the EMT in carcinomas has previously been shown to generate tumour cells with a high degree of plasticity (Nieto, 2011, Polyak and Weinberg, 2009). In addition, the data obtained in recent years indicate that MR-EMT are often expressed differentially and / or sequentially contributing to the disease progression by generation of motile, drug-resistant cells with stem-like properties (Elloul et al., 2006, Tran et al., 2011). Recently it has been suggested that a subset of MR-EMT can cooperate with mitogenic oncoproteins to play an important role in tumour initiation and early dissemination (Ansieau et al., 2008, Rhim et al., 2012). However, a regulatory link between MR-EMT and mitogenic factors remains to be explored.

In this thesis the experimental evidence has demonstrated that active RAS-RAF-MEK MAPK pathway induces a switch of MR-EMT proteins which may act to promote tumour progression in melanoma. It has also been suggested that reorganisation of the MR-EMT is complex, as a subset of the transcription factors can have distinct and even antagonistic functions, involving transcriptional repression by ZEB2/SNAI2 and activation by ZEB1/TWIST1 (Figure 6.1). Of note, in this network, activation of the RAS-RAF-MEK pathway altered the regulation of ZEB1 and ZEB2 gene expression by a transcriptional mechanism independent of miR-200 family. A recent report by Martello and colleagues suggested that high levels of miR-103/107 reduce Dicer expression, which in turn downregulates members of the miR-200 family promoting upregulation of ZEB1/ZEB2 and EMT in metastatic breast cancer cells (Martello et al.,

2010). In contrast, siRNA knockdown of ZEB1/ZEB2 had no effect on miR-200 family expression in metastatic melanoma cells, therefore it is plausible to suggest that the expression levels of ZEB1/ZEB2 are not controlled directly in a miR103/107-Dicer-miR-200 family dependent manner in melanoma or melanocytes (Stark et al., 2010).

IHC-P analyses indicated that the activation of the MR-EMT switch was predominantly detectable at deep sites of primary melanomas and intratumoural areas of nodal metastases which predicted poor patient survival. However, the MR-EMT switch was not detectable in benign lesions, despite oncogenic activation of the BRAF-MAPK signalling, suggesting that additional somatic mutations are required to override the negative feedback on ERK activity to produce genetic instability and allow reprogramming of these transcription factors (Pratilas et al., 2009). Therefore, most primary melanomas have to reduce ZEB2 and SNAI2 expression before gaining ZEB1 and TWIST1.

Further IHC-P findings, by comparing benign naevi with primary melanomas and lymph node metastases using independent and matched tumour samples, suggested that ZEB2 and SNAI2 might act as differentiation markers, early in the course of melanoma progression. ZEB2 and SNAI2 are strongly expressed in normal melanocytes and naevi and therefore may also be considered as regulators of terminal differentiation and candidate genes regulating replicative senescence in these cells. Noteworthy, reduced immunopositivity of ZEB2/SNAI2 in melanoma cells at deep areas of primary MMs may be indicative of an alternative pathway for melanoma cell proliferation and invasion in the absence of the EMT. In contrast, upregulation of ZEB1 and TWIST1 in secondary tumours could contribute to the induction and maintenance of migratory cell behavior and malignancy. However, initiation of secondary tumours at metastatic sites

requires acquisition of additional genetic changes and specific microenvironmental cues to relieve growth arrest and reactivate tumour outgrowth. Increased protein expression of ZEB1 and TWIST1 in nodal metastases and intratumoural clonal diversity of TWIST1 may further support that melanoma cells of metastatic lesions have been diverged at earlier stages and therefore melanoma development and progression is likely to be non-linear (Ansieau et al., 2008).

Interestingly, reactivation of ZEB2 in the periphery of nodal metastases and co-expression with E-cadherin may indicate its additional role in the establishment of melanoma micrometastases by promoting acquisition of an epithelial phenotype through MET. Nonetheless, the partial loss or downregulation of E-cadherin in focal areas in nodal metastases further suggests that melanoma cells do not follow the "classical" EMT, in which E-cadherin expression is completely lost for the whole tumour. In addition, changes in E-cadherin expression and loss of functional VDR, which is associated with loss of cell differentiation, by a ZEB1-mediated upregulation, may contribute to the development of metastatic outgrowths.

6.2 Fra-1: an appealing target for therapy

Fra-1 is a potential inducer of the BRAF-mediated MR-EMT reprogramming in melanocytic lesions. Previous studies demonstrated that Fra-1 is a key effector of MAPK pathway which regulates cytoskeletal dynamics, tumour cell motility and adhesion (Kustikova et al., 1998, Vial and Marshall, 2003a, Vial et al., 2003b). In mammary epithelial cells, Fra-1 stabilisation contributes to an EMT program downstream of ERK2 or *Ras*-V12 via the upregulation of ZEB1 and ZEB2 (Shin and Blenis, 2010b). Although the mechanism of ZEB1 upregulation is not yet elucidated in these cells the induction of ZEB2 by Fra-1 is likely to be indirect and driven by the

GATA family transcriptional repressor tricho-rhino-phalangeal syndrome type 1 (TRPS1) and miR-221/222 (Stinson et al., 2011).

Further evidence indicated that in melanoma cells the crosstalk between MEK-Fra-1 axis and MR-EMT network has a fundamentally different effect, as Fra-1 does not activate, but directly represses *ZEB2* via interaction with the 4 kb upstream repressor element (personal communication, Dr. E. Tulchinsky) (Figure 6.2). The mechanisms underlying contrasting effects of Fra-1 on *ZEB2* transcription in breast epithelial versus melanoma cells is currently unknown. Notably, MEK1-ERK-mediated posttranslational modifications stabilise the interaction between Fra-1 and negative regulators of gene expression, such as histone deacetylase 1 (HDAC1) (Hoffmann et al., 2005). It is therefore plausible to speculate that melanoma-specific posttranslational modifications of Fra-1 determine its function as a transcriptional repressor. As *ZEB2* is a repressor for *ZEB1* then the effect of Fra-1 on *ZEB1* is at least in part via *ZEB2* repression. However, the mechanism underlying regulation of other MR-EMT by Fra-1 seems more complex and may occur at both transcriptional and posttranslational levels.

Recent clinical trials in patients with *BRAF* mutant melanoma have demonstrated that the acquired resistance to BRAF selective inhibitors is an important clinical challenge. In many cases, the mechanism of the resistance was based on the restoration of MEK activity, which occurred via various mechanisms such as an activating mutation in MEK1 (Emery et al., 2009) or switching among the three RAF isoforms (Villanueva et al., 2010). Therefore, targeting melanoma cells downstream of MEK represents an attractive strategy for treatment. Given that Fra-1 seems to play an important role in MR-EMT reprogramming and is required for melanocyte transformation by BRAF,

molecular pathways regulating Fra-1 activity in melanoma appear as appealing targets for future therapies.

6.3 Limitations of the study

Although in this thesis evidence has been provided for the role of MR-EMT in melanoma, a number of important limitations need to be considered.

- For all *in vitro* analyses only two metastatic melanoma cell lines (A375P and A375M) and HEMN were used. Thus, further experiments using additional cell lines, in particular cells originated from primary melanomas with or without metastases and adult epidermal melanocytes, are required to validate and extend this work.
- In this study the main focus was to investigate the role of selected transcription factors (ZEB1, ZEB2, TWIST1 and SNAI2) in melanoma and EMT. However, this does not exclude a similar role by other EMT-inducing factors that directly repress *E-cadherin* promoter activity, such as TBX2 and TBX3.
- The immunostaining of ZEB1 and TWIST1 in most of tumour samples showed weak intensity in focal areas mainly at deep sites of primary melanomas or nodal metastasis. Therefore, it is plausible to question the significance of these results to tumour metastasis. However, transient expression of ZEB1 and TWIST1 in small numbers of tumour cells may be sufficient to promote metastasis. Knock-in and knock-out of *ZEB1* and *TWIST1* in a mouse melanoma model could be used to assess the mechanisms of controlling development of metastases and the significance of these factors.

- Although, E-cadherin protein expression was reduced in a small number of nodal metastases compared to the naevi and primary melanomas, other cadherins, in particular N- and P-cadherins, were not assessed. It will be of great interest to evaluate the immunostaining pattern of these cadherins and MR-EMT in an additional set of benign and melanoma tumours.
- Another limitation of this work was the small number of functional studies. Further functional experiments are described in section 6.5.
- Apart from E-cadherin and VDR, other downstream target genes of ZEB1 could be important during melanoma development, such as the loss of differentiation-associated marker, MITF. Therefore, IHC-P and functional studies could be used to further evaluate the MR-EMT switch in association with MITF.

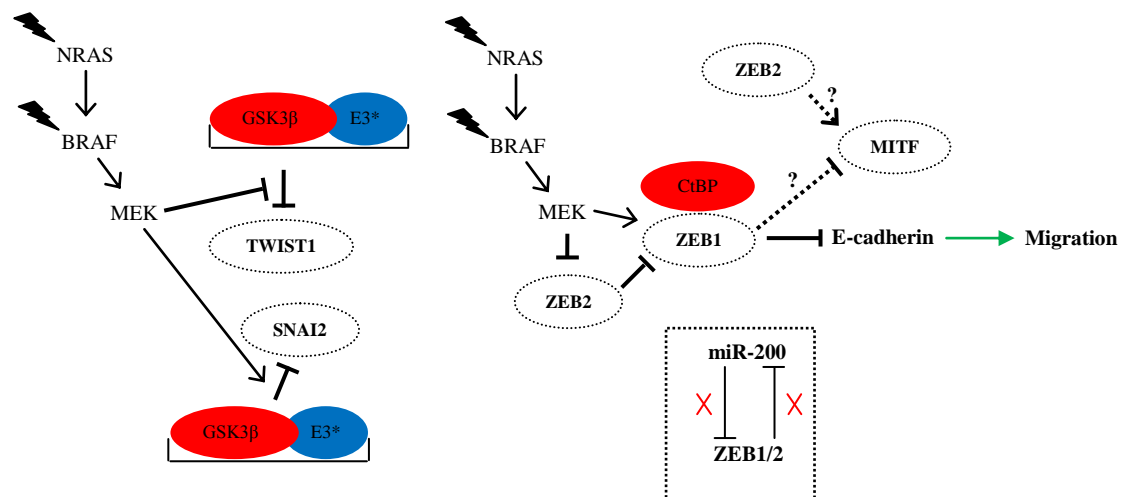


Figure 6.1 - Proposed model illustrating RAS-RAF-MEK dependent regulation of MR-EMT in melanoma cells. In this model, RAS-RAF-MEK inhibits expression of SNAI2 and ZEB2, but activates ZEB1 and TWIST1. Effects of the pathway are either transcriptional (ZEB1 and ZEB2) or involve both transcriptional regulation and control of protein stability (SNAI2 and TWIST1). GSK3- β regulates proteosomal degradation of both SNAI2 and TWIST1. Downregulation of ZEB2 by RAF-MEK MAPK contributes to the upregulation of ZEB1. ZEB1, but not ZEB2, SNAI2 or TWIST1 is an effective transcriptional repressor of E-cadherin in melanoma cells. Loss of E-cadherin further contributes to augmented motility of melanoma cells. Repression is stimulated by active MAPK signalling whose activity is required for the interaction between ZEB proteins and CtBP. ZEB1 and ZEB2 transcriptional regulation was independent of miR-200 family members. In retinal pigment epithelial cells, pigmentation has been shown to be regulated by ZEB1 through MITF downregulation (Liu et al., 2009b). Future work, may then suggest that MR-EMT switch affects MITF expression and activity in melanoma cells.

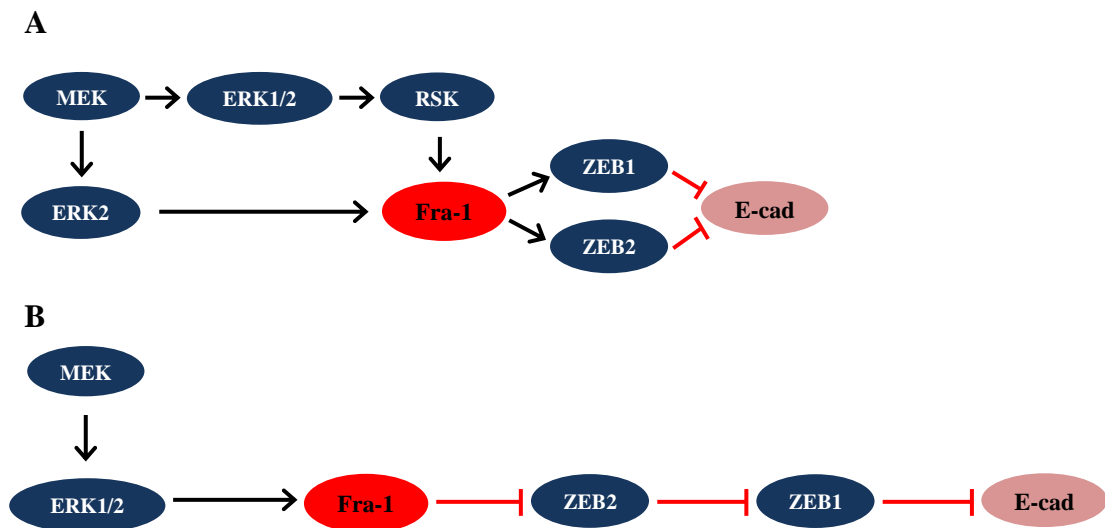


Figure 6.2 - Schematic representation of molecular signalling pathways linking MEK-Fra-1 with MR-EMT in carcinoma and melanoma cells. (A) In carcinomas, ERK2/Fra-1 mediated induction of ZEB1 and ZEB2 contributes to the loss of E-cadherin and EMT (Shin et al., 2010a). In addition, ERK-regulated kinases (or RSKs) act downstream of ERK1/2 and phosphorylate Fra-1 at Ser-252 (Doehn et al., 2009). (B) In contrast, evidence from this study suggested that Fra-1 activation links, at least in part, the BRAF-MAPK pathway with ZEB1 and ZEB2 and acts as a transcriptional repressor of ZEB2. Loss of ZEB2 resulted in ZEB1-mediated E-cadherin downregulation.

6.4 Final conclusions

- Evidence from this study supports a distinct link between a constitutive active oncogenic (*NRAS* / *BRAF*) signalling pathway and MR-EMT reprogramming that may be associated to melanoma development and progression.
- Further evidence supported a melanoma specific interactome of MR-EMT, in which transcriptional repression of ZEB2 by Fra-1 resulted in upregulation of ZEB1 and repression of E-cadherin and VDR, independently of miR-200 family.
- In tissue samples, the shift in the expression pattern of MR-EMT was a late event and demonstrated a novel independent factor of poor prognosis in patients with malignant melanoma.
- The findings from this investigation suggested that MR-EMT in MM and epithelial tumours are regulated by different mechanisms reflecting the embryological origins of each tumour. However, further functional studies and mouse models are required to fully assess all involved mechanisms.

6.5 Future work

6.5.1 ZEB2/SNAI2 - miR-200/E-cadherin co-expression paradox

Further studies are required to address the puzzling phenomenon of miR-200 expression in the presence of potent repressors, ZEB2 and SNAI2, in normal melanocytes and common acquired naevi. Manual microdissection used in this study possibly resulted in acquisition of heterogeneous cell populations, which contain large proportions of non-malignant cells. To avoid poor sample quality and erroneous conclusions, *in situ* hybridisation and laser capture microdissection of areas of interest will allow accurate quantitative and qualitative measures of miR expression and localisation in melanoma biopsies.

In regards to ZEB2/SNAI2 - E-cadherin co-expression in benign and melanoma tissues, it is known that recruitment of CtBP1/2 to *E-cadherin* promoter by ZEB1 and ZEB2 is required for transcriptional repression (Shi et al., 2003). A recent study carried out in mouse NMuMG cells has demonstrated that interaction between ZEB1 and CtBP1 is stimulated by fibroblast growth factor receptors via MEK activation (Shirakihara et al., 2011). Therefore, it appears likely that active MEK is required for the recruitment of CtBP to the *E-cadherin* promoter. Interactions between ZEB proteins and CtBP could be analysed by co-immunoprecipitation and ChIP assays.

Moreover, it could be investigated whether ectopic expression of CtBP1, in CtBP-negative melanoma cell lines, is sufficient to repress E-cadherin via ZEB2 or SNAI2 and whether the MEK-ERK activity regulates suppression of E-cadherin. In case that MEK activity regulates the recruitment of CtBP to *E-cadherin* promoter, it will be of great interest to assess the role of posttranslational modifications (Long et al., 2005) in CtBP/ZEB2 interaction and E-cadherin repression. Finally, previous work

indicated that cysteine-dependent dual-specificity protein phosphatase 5 (DUSP5), and in contrast to other phosphatases of the same family, displays its activity specifically to ERK (Mandl et al., 2005). In addition, growth-arrested common acquired naevi have absent or very low ERK1/2 activity (Saldanha et al., 2004). Therefore, it is worth assessing whether the presence of DUSP5 contributes to the opposing expression of ZEB proteins in these premalignant lesions by ERK1/2 dephosphorylation and for this purpose DUSP5 expression could be initially analysed using tissue microarrays and *in situ* hybridisation.

6.5.2 MR-EMT expression by BRAF activation

To further assess whether the MR-EMT expression is regulated by the BRAF-ERK pathway, immortalized murine melan-a cells could be transduced by a tamoxifen-inducible version of a dominant-active truncated variant of $BRAF^{V600E}$. In addition, HEMN could be infected with a vector expressing a constitutively active $BRAF^{V600E}$ mutant. Expression of MR-EMT and Fra-1 and their importance in naevus formation and melanoma progression could be investigated in a $BRAF^{V600E}$ / tyrosinase-CreERT2 melanoma model (Bosenberg et al., 2006, Damsky and Bosenberg, 2010).

6.5.3 Role of Fra-1 in malignant melanoma

In human embryonic stem cells, ZEB2 transcription is regulated via a composite silencer element interacting with stem cell factors responsible for maintenance of pluripotency, such as NANOG, SOX2 and OCT4. It has been noticed that the silencer element contains a perfect evolutionary conserved AP-1 binding site at the position-3554 relative to the ZEB2 transcription start site. In mammary epithelial cells activation

of the transcription factor Fra-1, an AP-1 family member, is necessary for EMT and increases ZEB1 and ZEB2 proteins in response to *RAS* activation. In addition, Fra-1 is strongly activated by the BRAF-MEK pathway in melanoma cell lines (Packer et al., 2009, Pratilas et al., 2009, Shin and Blenis, 2010b). Therefore, ChIP experiments could be performed to determine the potential *in vivo* binding of Fra-1-containing complexes to the silencer element of ZEB2.

Phosphorylated ERK1/2 is present in malignant melanoma cells with a significantly higher frequency than in naevi (Saldanha et al., 2004). The underlying mechanism is not completely clear but may involve the activation of negative feedback mechanisms suppressing NRAS-BRAF-MEK pathway in benign melanocytic lesion or *BRAF* and *NRAS* gene amplification in advanced cancers. In this study, it has been demonstrated that Fra-1 expression seems to be dependent on ERK activation. Therefore, it will be of great interest to evaluate Fra-1 expression with ZEB proteins and E-cadherin status by using a cohort of benign and malignant melanomas. To further elucidate the Fra-1/MR-EMT and Fra-1/E-cadherin correlations on the single-cell level a selection of melanoma samples could be analysed by double immunofluorescence labelling.

6.5.4 Clinical aspects

To further investigate the prognostic significance of ZEB1, ZEB2, SNAI2 and TWIST1 to melanoma progression and metastases-free survival a larger select or contiguous cohort of tumour samples should be used. In addition, the role of candidate EMT transcription factors in metastasis could be further assessed *in vivo* by performing IHC-P on sentinel nodes, which indicate sites that circulating transformed melanocytes reach first in metastasis.

6.5.5 Migration and invasion of melanoma cells

One final aspect of this study that warrants further investigation is to assess how MR-EMT switch affects migratory and invasive characteristics of melanoma cells. In malignant melanoma migration is characterised by high degree of plasticity and migrating cells utilise two different inter-convertible migration modes, amoeboid and mesenchymal. A recent report has revealed that in a panel of melanoma cell lines, including A375, the mode of migration is regulated by two members of miR-200 family, namely miR-200a and miR-200c, which promote mesenchymal and amoeboid cell motility, respectively (Elson-Schwab et al., 2010). Furthermore, in carcinoma cells miR-200a and miR-200c target ZEB proteins and ZEB1 directly suppress transcription of miR-200c (Brabletz and Brabletz, 2010). Whereas amoeboid mode of cell movement is driven by actomyosin contractility generated by high Rho-ROCK signalling, mesenchymal-type migration is RAC-dependent and involves actin assembly and extracellular matrix proteolysis by MMPs (Friedl and Wolf, 2010, Sanz-Moreno et al., 2008). Therefore, it is worth analysing the morphological effects of ROCK and MMP inhibitors in 2D melanoma cultures and on thick collagen matrices by time-lapse and confocal microscopy.

7 Appendix

7.1 I-Ethics-letter of approval



Health Research Authority

NRES Committee East Midlands - Leicester

The Old Chapel
Royal Standard Place
Nottingham
NG1 6FS

Tel: 0115 8838435
Fax: 0115 8838284

09 May 2012

Dr Gerald Saldanha
University of Leicester
Senior Lecturer/Honorary Consultant Pathologist
University of Leicester
Department of Cancer Studies and Molecular Medicine
Level 3 RK-CSB
Leicester Royal Infirmary
LE2 7LX

Dear Dr Saldanha

Study title: Molecular pathology of malignant melanoma
REC reference: 6791
Amendment number: 3
Amendment date: 07 March 2012

The above amendment was reviewed at the meeting of the Sub-Committee held on 04 May 2012.

Ethical opinion

The members of the Committee taking part in the review gave a favourable ethical opinion of the amendment on the basis described in the notice of amendment form and supporting documentation.

Approved documents

The documents reviewed and approved at the meeting were:

Document	Version	Date
Protocol	4	07 March 2012
Notice of Substantial Amendment (non-CTIMPs)	3	07 March 2012

Membership of the Committee

The members of the Committee who took part in the review are listed on the attached sheet.

R&D approval


All investigators and research collaborators in the NHS should notify the R&D office for the relevant NHS care organisation of this amendment and check whether it affects R&D approval of the research.

Statement of compliance

The Committee is constituted in accordance with the Governance Arrangements for Research Ethics Committees and complies fully with the Standard Operating Procedures for Research Ethics Committees in the UK.

6791:	Please quote this number on all correspondence
--------------	---

Yours sincerely

PP. 

Dr Carl Edwards
Chair

E-mail: georgia.copeland@nottspct.nhs.uk

Enclosures: *List of names and professions of members who took part in the review*

Copy to: *R&D contact - UHL*

7.2 II-Table S1-Summary of primary MMs used in this study

H Number	Gender (1 = M, 2 = F)	Age	Primary site	Breslow Depth (mm)	Ulceration (0 = no, 1 = yes)	Stage
H02/11	1	83	head	4	1	3
H12/08	2	52	trunk	5	1	4
H130/07	2	55	lower leg	2.5	0	3
H139/08	2	36	leg	0.8	0	1
H14/08	1	83	trunk	5.6	1	4
H141/08	2	57	arm	0.98	0	1
H143/08	2	63	leg	0.4	0	1
H144/08	2	43	trunk	0	0	1
H146/08	2	56	arm	0	0	1
H147/08	2	22	trunk	0	0	1
H148/08	2	28	trunk	0	0	1
H150/08	2	51	arm	0.4	0	1
H151/08	1	61	trunk	0.9	0	1
H154/08	1	70	head/neck	1.8	0	1
H156/08	1	24	arm	0.6	0	1
H157/09	2	75	upper leg	7.4	0	4
H158/09	1	88	head/neck	6.3	1	4
H159/08	2	27	leg	3.8	0	3
H160/08	2	25	trunk	0	0	1
H162/08	1	72	trunk	3.3		3
H163/08	1	51	head/neck	0.3	0	1
H164/08	2	56	leg	0.7	0	1
H167/08	2	59	trunk	0	0	1
H170/07	1	77	upper arm	2.3	0	3
H261/07	2	29	trunk	4	1	3
H269/04	1	54	arm	8	1	4
H271/04	2	64	not stated	1.3	0	2
H292/04	2	74	leg	2.8	1	3
H341/07	2	77	toe	4.3	1	4
H373/09	2	56	lower leg	3.6	1	3
H378/09	2	49	trunk	2	1	2
H382/09	1	57	trunk	4.5	0	4
H383/09	1	63	trunk	2.4	1	3
H400/09	2	35	head/neck	2.5	0	3
H401/09	2	67	lower leg	4.2	0	4
H404/09	2	74	lower leg	1.5	1	2
H415/09	2	95	head/neck	5.7	0	4

H416/09	1	56	trunk	2	1	2
H418/09	2	58	upper arm	9	0	4
H421/10	1	46	scalp	2.5	0	3
H454/11	2	67	elbow	1.1	1	2
H456/11	1	60	abdomen	3.3	0	3
H457/11	2	63	R ankle	1.6	1	2
H458/11	2	83	not stated	1.5	1	2
H460/11	1	80	back	1.2	1	2
H461/11	1	58	abdomen	2.2	0	3
H484/02	1	55	forehead	4.8	0	4
H487/02	2	49	abdomen	3	1	3
H488/02	1	51	head	5	1	4
H520/04	2	63	head/neck	10	0	4
H539/04	2	61	leg	2.5	1	3
H549/04	2	82	leg	3.5	0	3
H591/04	1	73	trunk	10	0	4
H609/04	1	25	trunk	3	0	3
H627/10	1	54	abdomen	0.4	0	1
H629/10	1	76	abdomen	0.8	0	1
H631/10	1	64	shoulder	1.2	0	2
H633/10	2	42	back	1.3	0	2
H635/10	1	61	head	1.9	0	2
H637/10	2	68	arm	2.5	0	3
H639/10	2	69	back	4	0	3
H647/04	1	58	trunk	3	0	3
H651/10	2	57	heel	2.3	1	3
H656/10	2	50	ankle	0.8	0	1
H669/04	2	76	sole	8	1	4
H678/04	1	41	arm	0.7	0	1
H681/04	2	44	trunk	0.7	0	1
H732/04	2	45	trunk	0.7	0	1
H74/09	2	74	trunk	3.6	0	3
H746/04	2	61	leg	0.6	0	1
H75/09	2	68	arm	3	1	3
H752/04	1	55	head/neck	4.5	1	4
H757/04	1	51	trunk	0.5	0	1
H758/04	2	48	trunk	0.5	0	1
H759/04	1	53	trunk	2.7	1	3
H761/04	2	88	arm	3	0	3
H765/04	2	62	trunk	1.7	0	2

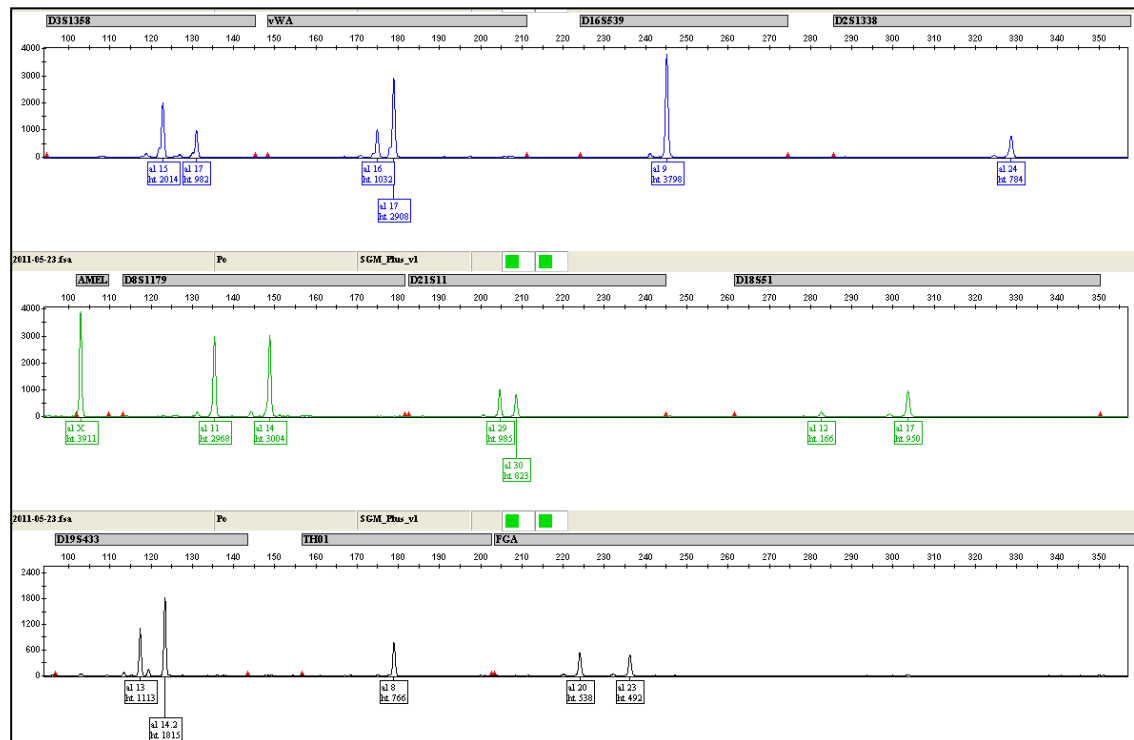
H768/04	2	50	leg	3	1	3
H769/04	1	75	abdomen	5	1	4
H770/04	1	54	trunk	1.8	0	2
H773/04	2	38	trunk	1.7	0	2
H8/08	1	51	upper arm	4.9	1	4
H81/09	2	68	upper leg	2.5	1	3
H870/10	2	74	lower leg	3.3		3
H874/10	1	65	head/neck	3.3		3
H875/10	1	76	trunk	7	1	3
H876/10	2	74	head/neck	7	1	4
H880/10	1	66	trunk	4.6	1	4
H883/10	1	61	thigh	8	1	4
H889/10	2	67	head/neck	2.5	1	3
H890/10	1	72	head/neck	5.7	0	4
H891/10	2	72	thigh	3.5	1	3
H892/10	1	61	upper arm	2.8	1	3
H898/10	1	76	arm	2.6	0	3
H900/10	2	76	back	9	1	4
H904/10	2	70	arm	4.1	0	4
H909/10	2	72	foot	3.8	1	3
H910/10	1	86	back	5	1	4

n=101, however it was not possible to retrieve clinical data for 3 cases

7.3 III - STR Profiling for A375 melanoma cells

The probability (random match probability) of two cell lines selected randomly having the same DNA profile with A375P and A375M cell lines is $6.23e^{-16}$ and $3.1e^{-17}$, respectively. This strongly suggests that the different batches of A375P and A375M cell lines were originated from the same individual (Figure S1 and S2). The different genotype observed in locus D2S1338 (A375P 24, 24 → A375M 16, 24 - allele drop in) could be due to different metastatic potential between A375P and A375M cells (Table S2).

A375P batch #1



A375P batch #2

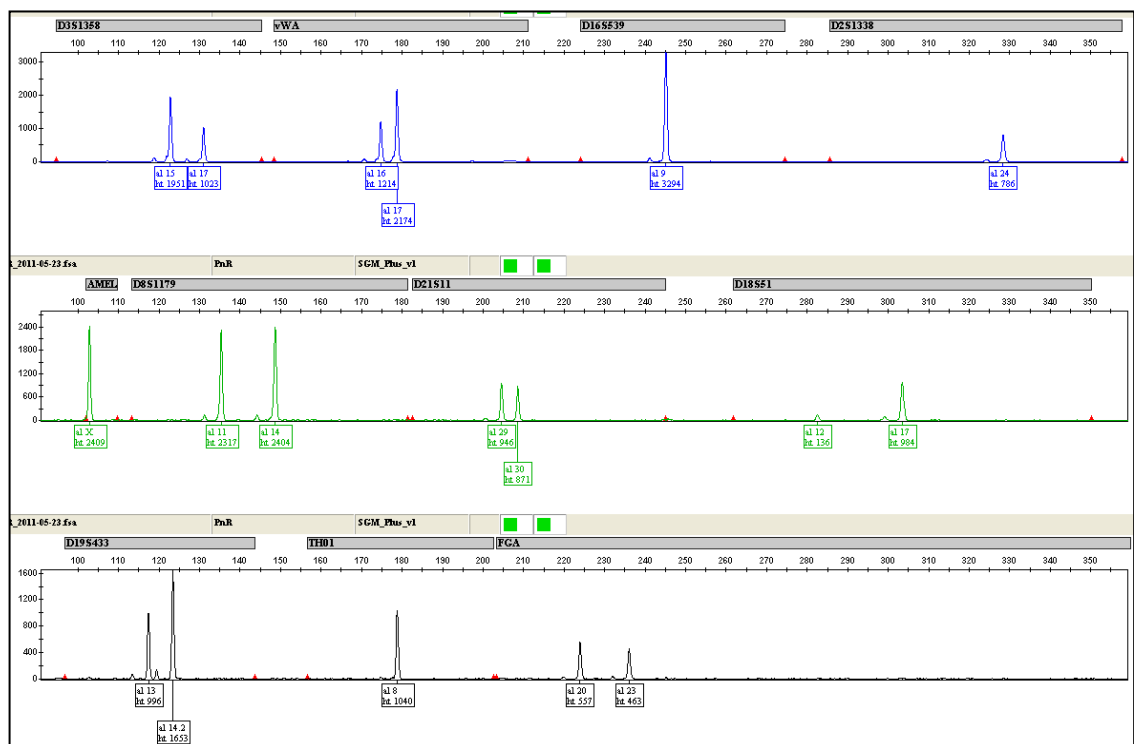
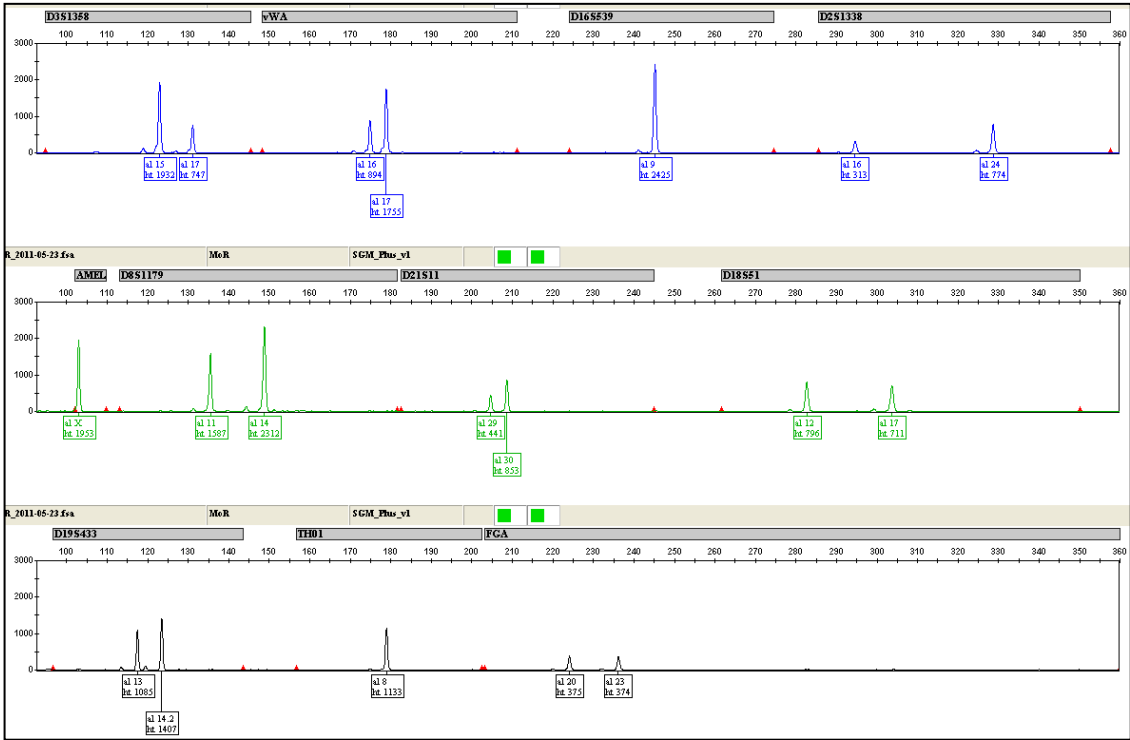


Figure S1 - Electropherograms showing the STR profiling results of A375P cells.

A375M batch #1



A375M batch #2

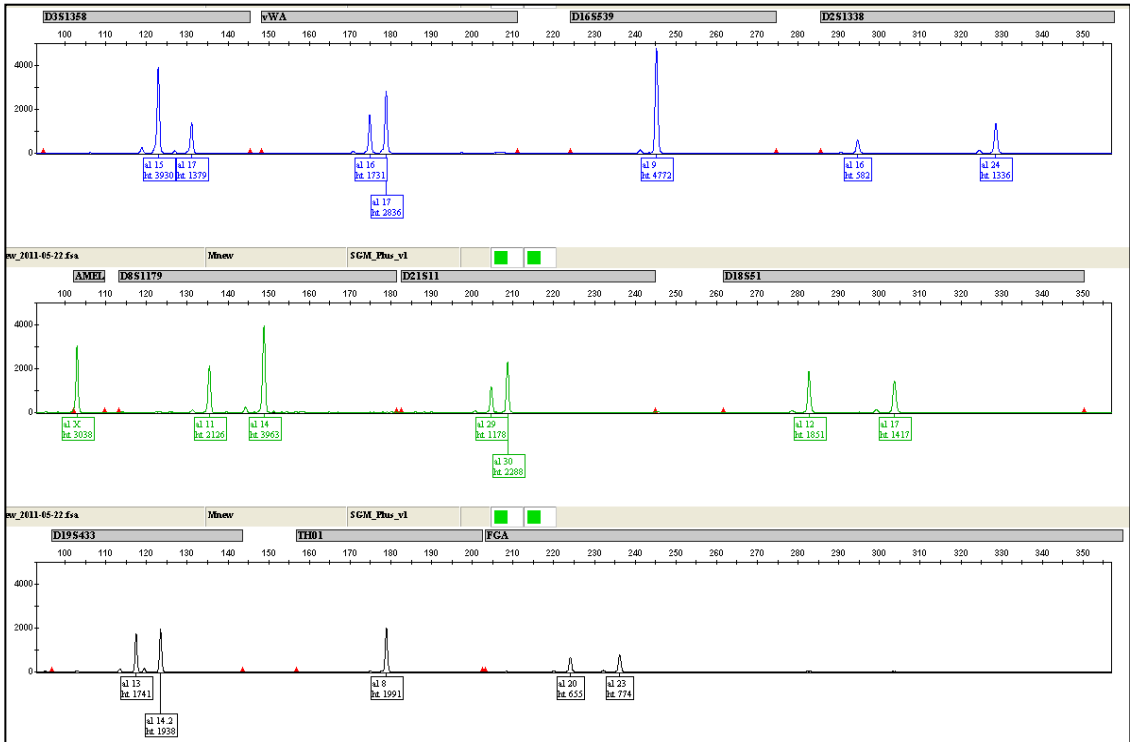


Figure S2 - Electropherograms showing the STR profiling results of A375M cells.

Table S2 - The SGM plus profile of A375 cell lines

STR Locus Designation	Chromosome Location	A375P #1 (allele values)	A375P #2 (allele values)	A375M #1 (allele values)	A375M #2 (allele values)
FGA	4q28	20,23	20,23	20,23	20,23
THO1	11p15.5	8,8	8,8	8,8	8,8
vWA	12p12-pter	16,17	16,17	16,17	16,17
D2S1338	2q35–37.1	24,24	24,24	16,24	16,24
D3S1358	3p	15,17	15,17	15,17	15,17
D8S1179	8	11,14	11,14	11,14	11,14
D16S539	16q24-qter	9,9	9,9	9,9	9,9
D18S51	18q21.3	12,17	12,17	12,17	12,17
D19S433	19q12–13.1	13,14.2	13,14.2	13,14.2	13,14.2
D21S11	21q11.2–q21	29,30	29,30	29,30	29,30
Amelogenin	X: p22.1–22.3 Y: p11.2	X,X	X,X	X,X	X,X

7.4 IV-Post-endogenous control array analysis / Expression stability of candidate endogenous genes

In order to validate the most stable candidate endogenous control genes (ECGs), the expression of sixteen ECGs was measured across seven different melanoma cell lines and cultured normal melanocytes by qRT-PCR using a TaqMan endogenous control array. GAPDH was excluded from the analysis due to significant variability in expression among the melanoma samples. The gene expression stability of ECGs was assessed using two programs, geNorm and NormFinder, which both rank candidate ECGs based on their stable gene expression in a given sample set. Using the geNorm software, fourteen out of the fifteen ECGs displayed high expression stability with low stability M values, which were below the stability cut-off value of 1.5 (result not shown). UBC (average M = 0.160), PPIA (average M = 0.162) and RPLP0 (average M = 0.202) were identified as the best stably expressed ECGs and 18S rRNA was the least stable gene (average M = 1.65) (Figure S3). The most stable pair of ECGs was PPIA and RPLP0 (Figure S3). Similar to the results from geNorm, NormFinder selected PPIA as the most stable single ECG (stability value = 0.207), followed by UBC (stability value = 0.209) and RPLP0 (stability value = 0.286) (Figure S4). Of note, the choice of the most stable gene pair was identical to that determined using the geNorm program (PPIA and RPLP0). Finally, the NormFinder ranking of all fifteen ECGs was almost identical to that generated using the geNorm program (Figures S3 and S4).

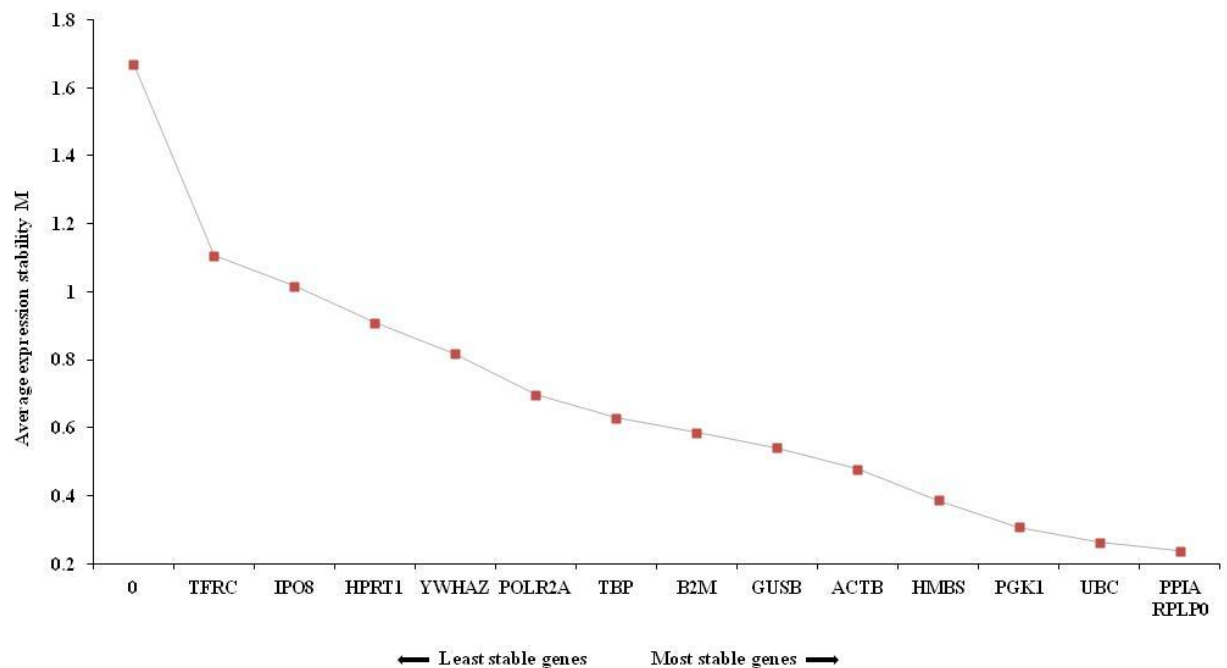


Figure S3 - Candidate endogenous genes for normalization listed according to their expression stability M value calculated by the geNorm software. The chart illustrates the stepwise exclusion of the least stable expressed candidate endogenous gene by measuring the average stability M value of each gene. Starting from the least stable gene with the highest stability M value (on the left), the different endogenous genes are ranked in order of increasing expression stability in melanoma cell lines and cultured normal melanocytes (HEMN) (on the right). In this experiment, ubiquitin C (UBC), peptidylprolyl isomerase A (PPIA) and ribosomal protein-large (RPLP0) are the three most stable genes. Note that 0 on the x-axis indicates the least stable endogenous gene, which is the 18S rRNA.

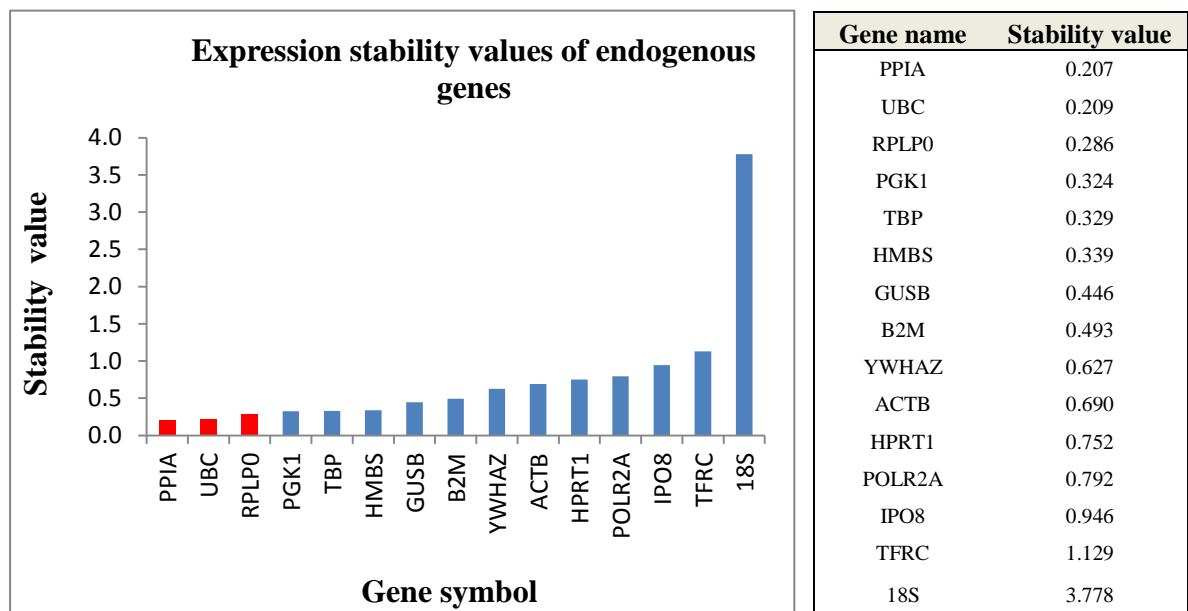


Figure S4 - NormFinder analysis of the 15 candidate endogenous genes using melanoma cell lines and normal melanocytes. The most stable genes with the lowest stability values are presented on the left (red colour) of the chart and are calculated by the NormFinder software. The table on the right shows the stability values of each candidate endogenous gene according to the output file of the NormFinder program. The three most stable genes are PPIA, UBC and RPLP0 and the most stable gene pair is PPIA and RPLP0.

7.5 V-Distribution of the MR-EMT/VDR/E-cadherin staining intensity and pattern (total H-Score)

a)

			INDEPENDENT SAMPLES			PAIRED SAMPLES		
			CAN	Primary MMs		Nodal Metastases	Primary MMs	Nodal Metastases
				Non Metastatic	Metastatic			
ZEB1	Superficial	Negative (0)	21/21 (100%)	41/50 (82%)	8/19 (42%)	8/20 (40%)	23/31(74%)	23/31(74%)
		Positive (1+, 2+, 3+)	0/21 (0%)	9/50 (18%)	11/19 (58%)	12/20 (60%)	8/31 (26%)	8/31 (26%)
	Deep	Negative (0)	19/21 (90%)	26/50 (52%)	6/19 (32%)	10/20 (50%)	10/31 (32%)	9/31 (29%)
		Positive (1+, 2+, 3+)	2/21(10%)	24/50 (48%)	13/19 (68%)	10/20 (50%)	21/31 (68%)	22/31 (71%)

b)

			INDEPENDENT SAMPLES			PAIRED SAMPLES		
			CAN	Primary MMs		Nodal Metastases	Primary MMs	Nodal Metastases
				Non Metastatic	Metastatic			
ZEB2	Superficial	Negative (0, 1+)	2/21 (10%)	19/50 (38%)	4/19 (21%)	14/20 (70%)	10/31 (32%)	23/31 (74%)
		Positive (2+, 3+)	19/21 (90%)	31/50 (62%)	15/19 (79%)	6/20 (30%)	21/31 (68%)	8/31 (26%)
	Deep	Negative (0, 1+)	9/21 (43%)	36/50 (72%)	13/19 (68%)	17/20 (85%)	22/31 (71%)	29/31 (94%)
		Positive (2+, 3+)	12/21 (57%)	14/50 (28%)	6/19 (32%)	3/20 (15%)	9/31 (29%)	2/31 (6%)

c)

			INDEPENDENT SAMPLES			PAIRED SAMPLES		
			CAN	Primary MMs		Nodal Metastases	Primary MMs	Nodal Metastases
				Non Metastatic	Metastatic			
TWIST1	Superficial	Negative (0)	17/19 (89%)	23/49 (47%)	4/13 (31%)	8/20 (40%)	21/31 (68%)	15/31 (48%)
		Positive (1+, 2+, 3+)	2/19 (11%)	26/49 (53%)	9/13 (69%)	12/20 (60%)	10/31 (32%)	16/31 (52%)
	Deep	Negative (0)	16/19 (84%)	20/49 (41%)	4/13 (31%)	10/20 (50%)	13/31 (42%)	16/31 (52%)
		Positive (1+, 2+, 3+)	3/19 (16%)	29/49 (59%)	9/13 (69%)	10/20 (50%)	18/31 (58%)	15/31 (48%)

d)

			INDEPENDENT SAMPLES			PAIRED SAMPLES		
			CAN	Primary MMs		Nodal Metastases	Primary MMs	Nodal Metastases
				Non Metastatic	Metastatic			
SNAI2	Superficial	Negative (0, 1+)	0/4 (0%)	2/3 (67%)	3/3 (100%)	-	7/14 (50%)	13/14 (93%)
		Positive (2+, 3+)	4/4 (100%)	1/3 (33%)	0/3 (0%)	-	7/14 (50%)	1/14 (7%)
	Deep	Negative (0, 1+)	1/4 (25%)	3/3 (100%)	3/3 (100%)	-	11/14 (79%)	13/14 (93%)
		Positive (2+, 3+)	3/4 (75%)	0/3 (0%)	0/3 (0%)	-	3/14 (21%)	1/14 (7%)

e)

				INDEPENDENT SAMPLES		PAIRED SAMPLES		
				Primary MMs		Nodal Metastases	Primary MMs	Nodal Metastases
				Non Metastatic	Metastatic			
VDR	Localisation	Tumour area	Measure (positive)					
	Nuclear	Superficial	(+1)	5/5 (100%)	5/5 (100%)	0/10 (0%)	10/10 (100%)	0/10 (0%)
		Deep	(+1)	3/5 (60%)	3/5 (60%)	0/10 (0%)	6/10 (60%)	0/10 (0%)
	Cytoplasmic	Superficial	(+1)	1/5 (20%)	1/5 (20%)	8/10 (80%)	1/10 (10%)	9/10 (90%)
		Deep	(+1)	2/5 (40%)	3/5 (60%)	5/10 (50%)	3/10 (30%)	6/10 (60%)

7.6 VI-Cell lines and VDR ligand treatments

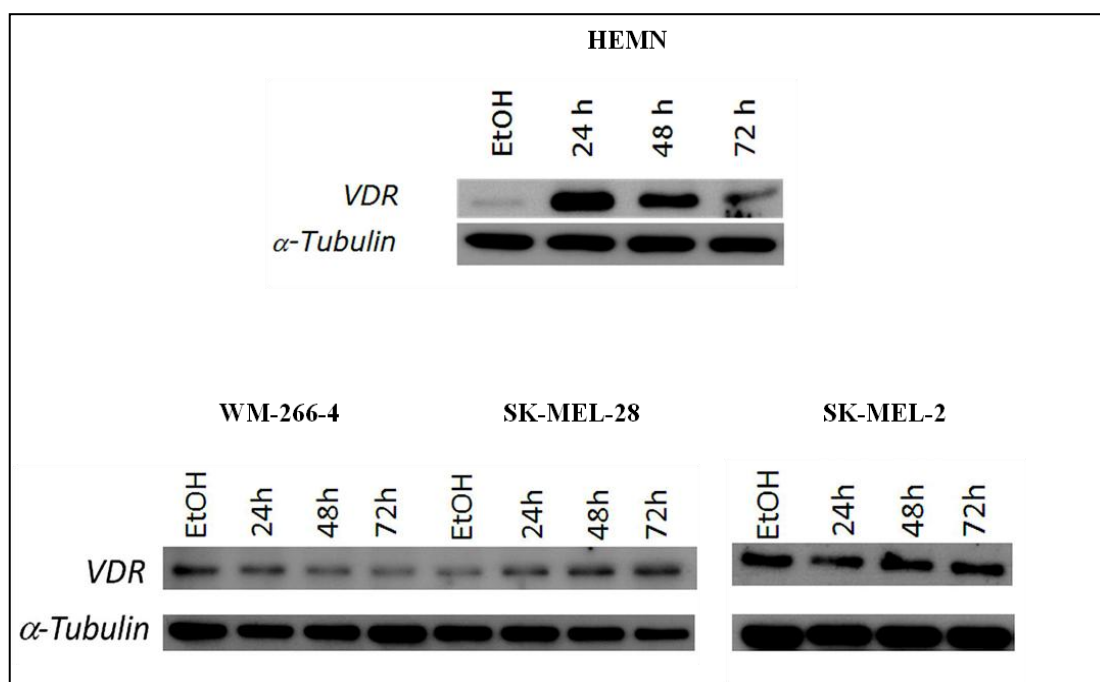


Figure S5 - VDR expression of normal neonatal melanocytes (HEMN) and melanoma cell lines in response to 1,25(OH)₂D₃. Western blot analyses of cell lysates from SK-MEL-2, SK-MEL-28, WM266-4 and HEMN 24, 48 and 72 hrs after treatment with 1,25(OH)₂D₃ at the physiological concentration of 10⁻⁹ M. Melanocytes and melanoma cells incubated with culture medium and ethanol (EtOH) served as controls (untreated cells).

Publications

SALDANHA, G., POTTER, L., SHENDGE P., OSBORNE J., NICHOLSON S., YIL, N., VARMA, S., ASLAM, M. I., ELSHAW S., PAPADOGEORGAKIS, E., & PRINGLE, J. H. 2013. **Plasma MicroRNA-21 Is Associated with Tumor Burden in Cutaneous Melanoma.** *J Invest Dermatol*, 133, 1381-84.

Currently under consideration at *Cancer Cell*:

CARMEL, J^{*}, PAPADOGEORGAKIS, E^{*}, HILL, L., BROWNE, G. J., RICHARD, G., WIERINCKX, A., SALDANHA, G., HUTCHINSON, P., PUISIEUX, A., PRINGLE, J. H., ANSIEAU, S., TULCHINSKY, E. 2013. **A switch in the expression of embryonic EMT-inducers drives the development of malignant melanoma.**

**These authors contributed equally to this work*

References

- ACKERMAN, A. B. 1980. Malignant melanoma. A unifying concept. *Am J Dermatopathol*, 2, 309-13.
- AIGNER, K., DAMPIER, B., DESCOVICH, L., MIKULA, M., SULTAN, A., SCHREIBER, M., MIKULITS, W., BRABLETZ, T., STRAND, D., OBRIST, P., SOMMERGRUBER, W., SCHWEIFER, N., WERNITZNIG, A., BEUG, H., FOISNER, R. & EGER, A. 2007. The transcription factor ZEB1 (deltaEF1) promotes tumour cell dedifferentiation by repressing master regulators of epithelial polarity. *Oncogene*, 26, 6979-88.
- ALVES, C. C., CARNEIRO, F., HOEFLER, H. & BECKER, K. F. 2009. Role of the epithelial-mesenchymal transition regulator Slug in primary human cancers. *Front Biosci*, 14, 3035-50.
- ALVES, C. C., ROSIVATZ, E., SCHOTT, C., HOLLWECK, R., BECKER, I., SARBIA, M., CARNEIRO, F. & BECKER, K. F. 2007. Slug is overexpressed in gastric carcinomas and may act synergistically with SIP1 and Snail in the down-regulation of E-cadherin. *The Journal of Pathology*, 211, 507-515.
- ANDERSEN, C. L., JENSEN, J. L. & ORNTOF, T. F. 2004. Normalization of real-time quantitative reverse transcription-PCR data: a model-based variance estimation approach to identify genes suited for normalization, applied to bladder and colon cancer data sets. *Cancer Res*, 64, 5245-50.
- ANDERSEN, T. E., FINSEN, B., GOFFINET, A. M., ISSINGER, O. G. & BOLDYREFF, B. 2002. A reeler mutant mouse with a new, spontaneous mutation in the reelin gene. *Brain Res Mol Brain Res*, 105, 153-6.
- ANSIEAU, S., BASTID, J., DOREAU, A., MOREL, A. P., BOUCHET, B. P., THOMAS, C., FAUVET, F., PUISIEUX, I., DOGLIONI, C., PICCININ, S., MAESTRO, R., VOELTZEL, T., SELMI, A., VALSESIA-WITTMANN, S., CARON DE FROMENTEL, C. & PUISIEUX, A. 2008. Induction of EMT by twist proteins as a collateral effect of tumor-promoting inactivation of premature senescence. *Cancer Cell*, 14, 79-89.
- AUBERT, C., ROUGE, F., REILLAUDOU, M. & METGE, P. 1993. Establishment and characterization of human ocular melanoma cell lines. *Int J Cancer*, 54, 784-92.
- AYBAR, M. J., NIETO, M. A. & MAYOR, R. 2003. Snail precedes slug in the genetic cascade required for the specification and migration of the Xenopus neural crest. *Development*, 130, 483-94.
- BARKAN, D., KLEINMAN, H., SIMMONS, J. L., ASMUSSEN, H., KAMARAJU, A. K., HOENORHOFF, M. J., LIU, Z. Y., COSTES, S. V., CHO, E. H., LOCKETT, S., KHANNA, C., CHAMBERS, A. F. & GREEN, J. E. 2008. Inhibition of metastatic outgrowth from single dormant tumor cells by targeting the cytoskeleton. *Cancer Res*, 68, 6241-50.
- BARRALLO-GIMENO, A. & NIETO, M. A. 2005. The Snail genes as inducers of cell movement and survival: implications in development and cancer. *Development*, 132, 3151-61.

- BARTH, A., WANER, L. A. & MORTON, D. L. 1995. Prognostic factors in 1,521 melanoma patients with distant metastases. *J Am Coll Surg*, 181, 193-201.
- BASTIAN, B. C., KASHANI-SABET, M., HAMM, H., GODFREY, T., MOORE, D. H., 2ND, BROCKER, E. B., LEBOIT, P. E. & PINKEL, D. 2000. Gene amplifications characterize acral melanoma and permit the detection of occult tumor cells in the surrounding skin. *Cancer Res*, 60, 1968-73.
- BATLLE, E., SANCHO, E., FRANCI, C., DOMINGUEZ, D., MONFAR, M., BAULIDA, J. & GARCIA DE HERREROS, A. 2000. The transcription factor snail is a repressor of E-cadherin gene expression in epithelial tumour cells. *Nat Cell Biol*, 2, 84-9.
- BEDENNE, L., MICHEL, P., BOUCHE, O., MILAN, C., MARIETTE, C., CONROY, T., PEZET, D., ROULLET, B., SEITZ, J. F., HERR, J. P., PAILLOT, B., ARVEUX, P., BONNETAIN, F. & BINQUET, C. 2007. Chemoradiation followed by surgery compared with chemoradiation alone in squamous cancer of the esophagus: FFCD 9102. *J Clin Oncol*, 25, 1160-8.
- BEHRENS, J., VON KRIES, J. P., KUHL, M., BRUHN, L., WEDLICH, D., GROSSCHEDL, R. & BIRCHMEIER, W. 1996. Functional interaction of beta-catenin with the transcription factor LEF-1. *Nature*, 382, 638-42.
- BELL, R. E. & LEVY, C. 2011. The three M's: melanoma, microphthalmia-associated transcription factor and microRNA. *Pigment Cell Melanoma Res*, 24, 1088-106.
- BELLOWS, C. F., BELAFSKY, P., FORTGANG, I. S. & BEECH, D. J. 2001. Melanoma in African-Americans: trends in biological behavior and clinical characteristics over two decades. *J Surg Oncol*, 78, 10-6.
- BERGER, R., FEBBO, P. G., MAJUMDER, P. K., ZHAO, J. J., MUKHERJEE, S., SIGNORETTI, S., CAMPBELL, K. T., SELLERS, W. R., ROBERTS, T. M., LODA, M., GOLUB, T. R. & HAHN, W. C. 2004. Androgen-induced differentiation and tumorigenicity of human prostate epithelial cells. *Cancer Res*, 64, 8867-75.
- BERWICK, M., ORLOW, I., HUMMER, A. J., ARMSTRONG, B. K., KRICKER, A., MARRETT, L. D., MILLIKAN, R. C., GRUBER, S. B., ANTON-CULVER, H., ZANETTI, R., GALLAGHER, R. P., DWYER, T., REBBECK, T. R., KANETSKY, P. A., BUSAM, K., FROM, L., MUJUMDAR, U., WILCOX, H., BEGG, C. B. & GROUP, G. E. M. S. 2006. The prevalence of CDKN2A germ-line mutations and relative risk for cutaneous malignant melanoma: an international population-based study. *Cancer Epidemiol Biomarkers Prev*, 15, 1520-5.
- BETANCUR, P., BRONNER-FRASER, M. & SAUKA-SPENGLER, T. 2010. Assembling neural crest regulatory circuits into a gene regulatory network. *Annu Rev Cell Dev Biol*, 26, 581-603.
- BHARTI, K. & ARNHEITER, H. 2005. When pigment cells turn into neurons. *J Invest Dermatol*, 125, x-xi.

- BINNI, F., ANTIGONI, I., DE SIMONE, P., MAJORE, S., SILIPO, V., CRISI, A., AMANTEA, A., PACCHIARINI, D., CASTORI, M., DE BERNARDO, C., CATRICALA, C. & GRAMMATICO, P. 2010. Novel and recurrent p14 mutations in Italian familial melanoma. *Clin Genet*, 77, 581-6.
- BIRCK, A., AHRENKIEL, V., ZEUTHEN, J., HOU-JENSEN, K. & GULDBERG, P. 2000. Mutation and allelic loss of the PTEN/MMAC1 gene in primary and metastatic melanoma biopsies. *J Invest Dermatol*, 114, 277-80.
- BISHOP, D. T., DEMENAI, F., ILES, M. M., HARLAND, M., TAYLOR, J. C., CORDA, E., RANDERSON-MOOR, J., AITKEN, J. F., AVRIL, M. F., AZIZI, E., BAKKER, B., BIANCHI-SCARRA, G., BRESSAC-DE PAILLERETS, B., CALISTA, D., CANNON-ALBRIGHT, L. A., CHIN, A. W. T., DEBNAK, T., GALORE-HASKEL, G., GHIORZO, P., GUT, I., HANSSON, J., HOCEVAR, M., HOIOM, V., HOPPER, J. L., INGVAR, C., KANETSKY, P. A., KEFFORD, R. F., LANDI, M. T., LANG, J., LUBINSKI, J., MACKIE, R., MALVEHY, J., MANN, G. J., MARTIN, N. G., MONTGOMERY, G. W., VAN NIEUWPOORT, F. A., NOVAKOVIC, S., OLSSON, H., PUIG, S., WEISS, M., VAN WORKUM, W., ZELENIKA, D., BROWN, K. M., GOLDSTEIN, A. M., GILLANDERS, E. M., BOLAND, A., GALAN, P., ELDER, D. E., GRUIS, N. A., HAYWARD, N. K., LATHROP, G. M., BARRETT, J. H. & BISHOP, J. A. 2009. Genome-wide association study identifies three loci associated with melanoma risk. *Nat Genet*, 41, 920-5.
- BISSIG, H., RICHTER, J., DESPER, R., MEIER, V., SCHRAML, P., SCHAFFER, A. A., SAUTER, G., MIHATSCH, M. J. & MOCH, H. 1999. Evaluation of the clonal relationship between primary and metastatic renal cell carcinoma by comparative genomic hybridization. *Am J Pathol*, 155, 267-74.
- BITON, S. & ASHKENAZI, A. 2011. NEMO and RIP1 Control Cell Fate in Response to Extensive DNA Damage via TNF- α Feedforward Signaling. *Cell*, 145, 92-103.
- BLANCO, M. J., MORENO-BUENO, G., SARRIO, D., LOCASCIO, A., CANO, A., PALACIOS, J. & NIETO, M. A. 2002. Correlation of Snail expression with histological grade and lymph node status in breast carcinomas. *Oncogene*, 21, 3241-6.
- BLEYER, A., VINY, A. & BARR, R. 2006. Cancer in 15- to 29-year-olds by primary site. *Oncologist*, 11, 590-601.
- BLOETHNER, S., SNELLMAN, E., BERMEJO, J. L., HIRIPI, E., GAST, A., THIRUMARAN, R. K., WELLENREUTHER, R., HEMMINKI, K. & KUMAR, R. 2007. Differential gene expression in melanocytic nevi with the V600E BRAF mutation. *Genes Chromosomes Cancer*, 46, 1019-27.
- BOLOS, V., PEINADO, H., PEREZ-MORENO, M. A., FRAGA, M. F., ESTELLER, M. & CANO, A. 2003. The transcription factor Slug represses E-cadherin expression and induces epithelial to mesenchymal transitions: a comparison with Snail and E47 repressors. *J Cell Sci*, 116, 499-511.
- BONITSIS, N., BATISTATOU, A., KARANTIMA, S. & CHARALABOPOULOS, K. 2006. The role of cadherin/catenin complex in malignant melanoma. *Exp Oncol*, 28, 187-93.
- BOSENBERG, M., MUTHUSAMY, V., CURLEY, D. P., WANG, Z., HOBBS, C., NELSON, B., NOGUEIRA, C., HORNER, J. W., 2ND, DEPINHO, R. & CHIN, L. 2006. Characterization of melanocyte-specific inducible Cre recombinase transgenic mice. *Genesis*, 44, 262-7.

- BOSSERHOFF, A. K., ELLMANN, L. & KUPHAL, S. 2011. Melanoblasts in culture as an in vitro system to determine molecular changes in melanoma. *Exp Dermatol*, 20, 435-40.
- BOX, N. F., DUFFY, D. L., CHEN, W., STARK, M., MARTIN, N. G., STURM, R. A. & HAYWARD, N. K. 2001. MC1R genotype modifies risk of melanoma in families segregating CDKN2A mutations. *Am J Hum Genet*, 69, 765-73.
- BRABLETZ, S. & BRABLETZ, T. 2010. The ZEB/miR-200 feedback loop--a motor of cellular plasticity in development and cancer? *EMBO Rep*, 11, 670-7.
- BRASEL, K., ESCOBAR, S., ANDERBERG, R., DE VRIES, P., GRUSS, H. J. & LYMAN, S. D. 1995. Expression of the flt3 receptor and its ligand on hematopoietic cells. *Leukemia*, 9, 1212-8.
- BRAY, F., REN, J. S., MASUYER, E. & FERLAY, J. 2012. Global estimates of cancer prevalence for 27 sites in the adult population in 2008. *Int J Cancer*.
- BRECKENRIDGE, M. T., EGELHOFF, T. T. & BASKARAN, H. 2010. A microfluidic imaging chamber for the direct observation of chemotactic transmigration. *Biomed Microdevices*, 12, 543-53.
- BRITO, F. C. & KOS, L. 2008. Timeline and distribution of melanocyte precursors in the mouse heart. *Pigment Cell Melanoma Res*, 21, 464-70.
- BRONNER-FRASER, M. & FRASER, S. E. 1988. Cell lineage analysis reveals multipotency of some avian neural crest cells. *Nature*, 335, 161-4.
- BROWN, A. J., DUSSO, A. & SLATOPOLSKY, E. 1999. Vitamin D. *Am J Physiol*, 277, F157-75.
- BROWN, K. M., MACGREGOR, S., MONTGOMERY, G. W., CRAIG, D. W., ZHAO, Z. Z., IYADURAI, K., HENDERS, A. K., HOMER, N., CAMPBELL, M. J., STARK, M., THOMAS, S., SCHMID, H., HOLLAND, E. A., GILLANDERS, E. M., DUFFY, D. L., MASKIELL, J. A., JETANN, J., FERGUSON, M., STEPHAN, D. A., CUST, A. E., WHITEMAN, D., GREEN, A., OLSSON, H., PUIG, S., GHIORZO, P., HANSSON, J., DEMENAI, F., GOLDSTEIN, A. M., GRUIS, N. A., ELDER, D. E., BISHOP, J. N., KEFFORD, R. F., GILES, G. G., ARMSTRONG, B. K., AITKEN, J. F., HOPPER, J. L., MARTIN, N. G., TRENT, J. M., MANN, G. J. & HAYWARD, N. K. 2008. Common sequence variants on 20q11.22 confer melanoma susceptibility. *Nat Genet*, 40, 838-40.
- BROWNE, G., SAYAN, A. E. & TULCHINSKY, E. 2010. ZEB proteins link cell motility with cell cycle control and cell survival in cancer. *Cell Cycle*, 9, 886-91.
- BROZYNA, A. A., JOZWICKI, W., JANJETOVIC, Z. & SLOMINSKI, A. T. 2011. Expression of vitamin D receptor decreases during progression of pigmented skin lesions. *Hum Pathol*, 42, 618-31.
- BRUGGEN, J., SORG, C. & MACHER, E. 1978. Membrane-Associated Antigens of Human Malignant Melanoma-V - Serological Typing of Cell Lines Using Antisera from Nonhuman-Primates. *Cancer Immunology Immunotherapy*, 5, 53-62.

- BURK, U., SCHUBERT, J., WELLNER, U., SCHMALHOFFER, O., VINCAN, E., SPADERNA, S. & BRABLETZ, T. 2008. A reciprocal repression between ZEB1 and members of the miR-200 family promotes EMT and invasion in cancer cells. *EMBO Rep*, 9, 582-9.
- BYRD, K. M., WILSON, D. C., HOYLER, S. S. & PECK, G. L. 2004. Advanced presentation of melanoma in African Americans. *J Am Acad Dermatol*, 50, 21-4; discussion 142-3.
- CALIN, G. A. & CROCE, C. M. 2006. MicroRNA-cancer connection: the beginning of a new tale. *Cancer Res*, 66, 7390-4.
- CALIN, G. A., SEVIGNANI, C., DUMITRU, C. D., HYSLOP, T., NOCH, E., YENDAMURI, S., SHIMIZU, M., RATTAN, S., BULLRICH, F., NEGRINI, M. & CROCE, C. M. 2004. Human microRNA genes are frequently located at fragile sites and genomic regions involved in cancers. *Proc Natl Acad Sci U S A*, 101, 2999-3004.
- CANO, A., PEREZ-MORENO, M. A., RODRIGO, I., LOCASCIO, A., BLANCO, M. J., DEL BARRIO, M. G., PORTILLO, F. & NIETO, M. A. 2000. The transcription factor snail controls epithelial-mesenchymal transitions by repressing E-cadherin expression. *Nat Cell Biol*, 2, 76-83.
- CAREY, T. E., TAKAHASHI, T., RESNICK, L. A., OETTGEN, H. F. & OLD, L. J. 1976. Cell surface antigens of human malignant melanoma: mixed hemadsorption assays for humoral immunity to cultured autologous melanoma cells. *Proc Natl Acad Sci U S A*, 73, 3278-82.
- CARL, T. F., DUFTON, C., HANKEN, J. & KLYMKOWSKY, M. W. 1999. Inhibition of neural crest migration in *Xenopus* using antisense slug RNA. *Dev Biol*, 213, 101-15.
- CARREIRA, S., DEXTER, T. J., YAVUZER, U., EASTY, D. J. & GODING, C. R. 1998. Brachyury-related transcription factor Tbx2 and repression of the melanocyte-specific TRP-1 promoter. *Mol Cell Biol*, 18, 5099-108.
- CARRIO, M., ARDERIU, G., MYERS, C. & BOUDREAU, N. J. 2005. Homeobox D10 induces phenotypic reversion of breast tumor cells in a three-dimensional culture model. *Cancer Res*, 65, 7177-85.
- CARROZZINO, F., PUGNALE, P., FERAILLE, E. & MONTESANO, R. 2009. Inhibition of basal p38 or JNK activity enhances epithelial barrier function through differential modulation of claudin expression. *Am J Physiol Cell Physiol*, 297, C775-87.
- CASALINO, L., DE CESARE, D. & VERDE, P. 2003. Accumulation of Fra-1 in ras-transformed cells depends on both transcriptional autoregulation and MEK-dependent posttranslational stabilization. *Mol. Cell. Biol*, 23, 4401-15.
- CASAS, E., KIM, J., BENDESKY, A., OHNO-MACHADO, L., WOLFE, C. J. & YANG, J. 2011. Snail2 is an essential mediator of Twist1-induced epithelial mesenchymal transition and metastasis. *Cancer Res*, 71, 245-54.

- CASORZO, L., LUZZI, C., NARDACCHIONE, A., PICCIOTTO, F., PISACANE, A. & RISIO, M. 2005. Fluorescence in situ hybridization (FISH) evaluation of chromosomes 6, 7, 9 and 10 throughout human melanocytic tumorigenesis. *Melanoma Res*, 15, 155-60.
- CASTILLA, M. A., MORENO-BUENO, G., ROMERO-PEREZ, L., VAN DE VIJVER, K., BISCUOLA, M., LOPEZ-GARCIA, M. A., PRAT, J., MATIAS-GUIU, X., CANO, A., OLIVA, E. & PALACIOS, J. 2011. Micro-RNA signature of the epithelial-mesenchymal transition in endometrial carcinosarcoma. *J Pathol*, 223, 72-80.
- CHATZINASIIOU, F., LILL, C. M., KYPREOU, K., STEFANAKI, I., NICOLAOU, V., SPYROU, G., EVANGELOU, E., ROEHR, J. T., KODELA, E., KATSAMBAS, A., TSAO, H., IOANNIDIS, J. P., BERTRAM, L. & STRATIGOS, A. J. 2011. Comprehensive field synopsis and systematic meta-analyses of genetic association studies in cutaneous melanoma. *J Natl Cancer Inst*, 103, 1227-35.
- CHEN, H., ZHU, G., LI, Y., PADIA, R. N., DONG, Z., PAN, Z. K., LIU, K. & HUANG, S. 2009. Extracellular signal-regulated kinase signaling pathway regulates breast cancer cell migration by maintaining slug expression. *Cancer Res*, 69, 9228-35.
- CHEN, Z. F. & BEHRINGER, R. R. 1995. twist is required in head mesenchyme for cranial neural tube morphogenesis. *Genes Dev*, 9, 686-99.
- CHEUNG, M., CHABOISSIER, M. C., MYNETT, A., HIRST, E., SCHEDL, A. & BRISCOE, J. 2005. The transcriptional control of trunk neural crest induction, survival, and delamination. *Dev Cell*, 8, 179-92.
- CHIN, L. 2003. The genetics of malignant melanoma: lessons from mouse and man. *Nat Rev Cancer*, 3, 559-70.
- CHUA, H. L., BHAT-NAKSHATRI, P., CLARE, S. E., MORIMIYA, A., BADVE, S. & NAKSHATRI, H. 2007. NF-kappaB represses E-cadherin expression and enhances epithelial to mesenchymal transition of mammary epithelial cells: potential involvement of ZEB-1 and ZEB-2. *Oncogene*, 26, 711-24.
- COHEN, Y., ROSENBAUM, E., BEGUM, S., GOLDENBERG, D., ESCHE, C., LAVIE, O., SIDRANSKY, D. & WESTRA, W. H. 2004. Exon 15 BRAF mutations are uncommon in melanomas arising in nonsun-exposed sites. *Clin Cancer Res*, 10, 3444-7.
- COLLISSON, E. A., DE, A., SUZUKI, H., GAMBHIR, S. S. & KOLODNEY, M. S. 2003. Treatment of metastatic melanoma with an orally available inhibitor of the Ras-Raf-MAPK cascade. *Cancer Res*, 63, 5669-73.
- COLOMBINO, M., CAPONE, M., LISSIA, A., COSSU, A., RUBINO, C., DE GIORGI, V., MASSI, D., FONSATTI, E., STAIBANO, S., NAPPI, O., PAGANI, E., CASULA, M., MANCA, A., SINI, M., FRANCO, R., BOTTI, G., CARACO, C., MOZZILLO, N., ASCIERTO, P. A. & PALMIERI, G. 2012. BRAF/NRAS Mutation Frequencies Among Primary Tumors and Metastases in Patients With Melanoma. *J Clin Oncol*, 30, 2522-9.

- COME, C., ARNOUX, V., BIBEAU, F. & SAVAGNER, P. 2004. Roles of the transcription factors snail and slug during mammary morphogenesis and breast carcinoma progression. *J Mammary Gland Biol Neoplasia*, 9, 183-93.
- COME, C., MAGNINO, F., BIBEAU, F., DE SANTA BARBARA, P., BECKER, K. F., THEILLET, C. & SAVAGNER, P. 2006. Snail and slug play distinct roles during breast carcinoma progression. *Clin Cancer Res*, 12, 5395-402.
- COMIJN, J., BERX, G., VERMASSEN, P., VERSCHUEREN, K., VAN GRUNSVEN, L., BRUYNEEL, E., MAREEL, M., HUYLEBROECK, D. & VAN ROY, F. 2001. The two-handed E box binding zinc finger protein SIP1 downregulates E-cadherin and induces invasion. *Mol Cell*, 7, 1267-78.
- CONACCI-SORRELL, M., SIMCHA, I., BEN-YEDIDIA, T., BLECHMAN, J., SAVAGNER, P. & BEN-ZE'EV, A. 2003. Autoregulation of E-cadherin expression by cadherin-cadherin interactions: the roles of beta-catenin signaling, Slug, and MAPK. *J Cell Biol*, 163, 847-57.
- COOK, A. L., DONATIEN, P. D., SMITH, A. G., MURPHY, M., JONES, M. K., HERLYN, M., BENNETT, D. C., LEONARD, J. H. & STURM, R. A. 2003. Human melanoblasts in culture: expression of BRN2 and synergistic regulation by fibroblast growth factor-2, stem cell factor, and endothelin-3. *J Invest Dermatol*, 121, 1150-9.
- COORY, M., BAADE, P., AITKEN, J., SMITHERS, M., MCLEOD, G. & RING, I. 2006. Trends for in situ and Invasive Melanoma in Queensland, Australia, 1982-2002. *Cancer Causes and Control*, 17, 21-27.
- CORREIA, A. C., COSTA, M., MORAES, F., BOM, J., NOVOA, A. & MALLO, M. 2007. Bmp2 is required for migration but not for induction of neural crest cells in the mouse. *Dev Dyn*, 236, 2493-501.
- CRESS, R. D. & HOLLY, E. A. 1997. Incidence of cutaneous melanoma among non-Hispanic whites, Hispanics, Asians, and blacks: an analysis of california cancer registry data, 1988-93. *Cancer Causes Control*, 8, 246-52.
- CRUK. 2010a. *CancerStats Report, Incidence Malignant Melanoma UK, Cancer Research UK* [Online]. Available: <http://info.cancerresearchuk.org/cancerstats/types/skin/incidence/#country> [Accessed August 2012].
- CRUK. 2010b. *CancerStats Report, Mortality Malignant Melanoma UK, Cancer Research UK* [Online]. Available: <http://info.cancerresearchuk.org/cancerstats/types/skin/mortality/> [Accessed August 2012].
- CRUK. 2010c. *CancerStats Report, Cancer Mortality for common cancers UK, Cancer Research UK* [Online]. Available: <http://info.cancerresearchuk.org/cancerstats/mortality/cancerdeaths/> [Accessed August 2012].
- CURTIN, J. A., BUSAM, K., PINKEL, D. & BASTIAN, B. C. 2006b. Somatic activation of KIT in distinct subtypes of melanoma. *J Clin Oncol*, 24, 4340-6.

- CURTIN, J. A., FRIDLYAND, J., KAGESHITA, T., PATEL, H. N., BUSAM, K. J., KUTZNER, H., CHO, K. H., AIBA, S., BROCKER, E. B., LEBOIT, P. E., PINKEL, D. & BASTIAN, B. C. 2005. Distinct sets of genetic alterations in melanoma. *N Engl J Med*, 353, 2135-47.
- CURTIN, J. A., STARK, M. S., PINKEL, D., HAYWARD, N. K. & BASTIAN, B. C. 2006a. PI3-kinase subunits are infrequent somatic targets in melanoma. *J Invest Dermatol*, 126, 1660-3.
- DAHL, C. & GULDBERG, P. 2007. The genome and epigenome of malignant melanoma. *APMIS*, 115, 1161-76.
- DAI, Y. H., TANG, Y. P., ZHU, H. Y., LV, L., CHU, Y., ZHOU, Y. Q. & HUO, J. R. 2012. ZEB2 promotes the metastasis of gastric cancer and modulates epithelial mesenchymal transition of gastric cancer cells. *Dig Dis Sci*, 57, 1253-60.
- DAMSKY, W. E., JR. & BOSENBERG, M. 2010. Mouse melanoma models and cell lines. *Pigment Cell Melanoma Res*, 23, 853-9.
- DANKORT, D., CURLEY, D. P., CARTLIDGE, R. A., NELSON, B., KARNEZIS, A. N., DAMSKY, W. E., JR., YOU, M. J., DEPINHO, R. A., MCMAHON, M. & BOSENBERG, M. 2009. Braf(V600E) cooperates with Pten loss to induce metastatic melanoma. *Nat Genet*, 41, 544-52.
- DARKEN, R. S. & WILSON, P. A. 2001. Axis induction by wnt signaling: Target promoter responsiveness regulates competence. *Dev Biol*, 234, 42-54.
- DAVALOS, V., MOUTINHO, C., VILLANUEVA, A., BOQUE, R., SILVA, P., CARNEIRO, F. & ESTELLER, M. 2012. Dynamic epigenetic regulation of the microRNA-200 family mediates epithelial and mesenchymal transitions in human tumorigenesis. *Oncogene*, 31, 2062-74.
- DAVIES, H., BIGNELL, G. R., COX, C., STEPHENS, P., EDKINS, S., CLEGG, S., TEAGUE, J., WOFFENDIN, H., GARNETT, M. J., BOTTOMLEY, W., DAVIS, N., DICKS, E., EWING, R., FLOYD, Y., GRAY, K., HALL, S., HAWES, R., HUGHES, J., KOSMIDOU, V., MENZIES, A., MOULD, C., PARKER, A., STEVENS, C., WATT, S., HOOPER, S., WILSON, R., JAYATILAKE, H., GUSTERSON, B. A., COOPER, C., SHIPLEY, J., HARGRAVE, D., PRITCHARD-JONES, K., MAITLAND, N., CHENEVIX-TRENCH, G., RIGGINS, G. J., BIGNER, D. D., PALMIERI, G., COSSU, A., FLANAGAN, A., NICHOLSON, A., HO, J. W., LEUNG, S. Y., YUEN, S. T., WEBER, B. L., SEIGLER, H. F., DARROW, T. L., PATERSON, H., MARAIS, R., MARSHALL, C. J., WOOSTER, R., STRATTON, M. R. & FUTREAL, P. A. 2002. Mutations of the BRAF gene in human cancer. *Nature*, 417, 949-54.
- DEMENAIS, F., MOHAMDI, H., CHAUDRU, V., GOLDSTEIN, A. M., NEWTON BISHOP, J. A., BISHOP, D. T., KANETSKY, P. A., HAYWARD, N. K., GILLANDERS, E., ELDER, D. E., AVRIL, M. F., AZIZI, E., VAN BELLE, P., BERGMAN, W., BIANCHI-SCARRA, G., BRESSAC-DE PAILLERETS, B., CALISTA, D., CARRERA, C., HANSSON, J., HARLAND, M., HOGG, D., HOIOM, V., HOLLAND, E. A., INGVAR, C., LANDI, M. T., LANG, J. M., MACKIE, R. M., MANN, G. J., MING, M. E., NJAUW, C. J., OLSSON, H., PALMER, J., PASTORINO, L., PUIG, S., RANDERSON-MOOR, J., STARK, M., TSAO, H., TUCKER, M. A., VAN DER VELDEN, P., YANG, X. R., GRUIS, N. & MELANOMA GENETICS, C. 2010. Association of MC1R variants and host phenotypes with melanoma risk in CDKN2A mutation carriers: a GenoMEL study. *J Natl Cancer Inst*, 102, 1568-83.

- DEMIRKAN, N. C., KESEN, Z., AKDAG, B., LARUE, L. & DELMAS, V. 2007. The effect of the sun on expression of beta-catenin, p16 and cyclin d1 proteins in melanocytic lesions. *Clin Exp Dermatol*, 32, 733-9.
- DEMUNTER, A., STAS, M., DEGREEF, H., DE WOLF-PEETERS, C. & VAN DEN OORD, J. J. 2001. Analysis of N- and K-ras mutations in the distinctive tumor progression phases of melanoma. *J Invest Dermatol*, 117, 1483-9.
- DESSARS, B., DE RAEVE, L. E., MORANDINI, R., LEFORT, A., EL HOUSNI, H., GHANEM, G. E., VAN DEN EYNDE, B. J., MA, W., ROSEEUW, D., VASSART, G., LIBERT, F. & HEIMANN, P. 2009. Genotypic and gene expression studies in congenital melanocytic nevi: insight into initial steps of melanotumorigenesis. *J Invest Dermatol*, 129, 139-47.
- DHOMEN, N., REIS-FILHO, J. S., DA ROCHA DIAS, S., HAYWARD, R., SAVAGE, K., DELMAS, V., LARUE, L., PRITCHARD, C. & MARAIS, R. 2009. Oncogenic Braf induces melanocyte senescence and melanoma in mice. *Cancer Cell*, 15, 294-303.
- DO, N. Y., PARK, S. Y. & LIM, S. C. 2004. The role of E-cadherin/beta-catenin complex and cyclin D1 in head and neck squamous cell carcinoma. *Cancer Res Treat*, 36, 72-8.
- DOEHN, U., HAUGE, C., FRANK, S. R., JENSEN, C. J., DUDA, K., NIELSEN, J. V., COHEN, M. S., JOHANSEN, J. V., WINTHER, B. R., LUND, L. R., WINTHER, O., TAUNTON, J., HANSEN, S. H. & FRODIN, M. 2009. RSK is a principal effector of the RAS-ERK pathway for eliciting a coordinate promotile/invasive gene program and phenotype in epithelial cells. *Mol Cell*, 35, 511-22.
- DO VALE, A., COSTA-RAMOS, C., SILVA, D. S., MACEDO, P. M., FERNANDES, R., SAMPAIO, P., DOS SANTOS, N. M. & SILVA, M. T. 2007. Cytochemical and ultrastructural study of anoikis and secondary necrosis in enterocytes detached in vivo. *Apoptosis*, 12, 1069-83.
- DORSKY, R. I., MOON, R. T. & RAIBLE, D. W. 1998. Control of neural crest cell fate by the Wnt signalling pathway. *Nature*, 396, 370-3.
- DUPIN, E., GLAVIEUX, C., VAIGOT, P. & LE DOUARIN, N. M. 2000. Endothelin 3 induces the reversion of melanocytes to glia through a neural crest-derived glial-melanocytic progenitor. *Proc Natl Acad Sci U S A*, 97, 7882-7.
- DUPIN, E. & LE DOUARIN, N. M. 2003. Development of melanocyte precursors from the vertebrate neural crest. *Oncogene*, 22, 3016-23.
- DUVAL, M. 1879. *Atlas d'embryologie* (Masson, Paris).
- EDLUNDH-ROSE, E., EGYHAZI, S., OMHOLT, K., MANSSON-BRAHME, E., PLATZ, A., HANSSON, J. & LUNDEBERG, J. 2006. NRAS and BRAF mutations in melanoma tumours in relation to clinical characteristics: a study based on mutation screening by pyrosequencing. *Melanoma Res*, 16, 471-8.

- EDWARDS, R. H., WARD, M. R., WU, H., MEDINA, C. A., BROSE, M. S., VOLPE, P., NUSSEN-LEE, S., HAUPT, H. M., MARTIN, A. M., HERLYN, M., LESSIN, S. R. & WEBER, B. L. 2004. Absence of BRAF mutations in UV-protected mucosal melanomas. *J Med Genet*, 41, 270-2.
- EGER, A., AIGNER, K., SONDEREGGER, S., DAMPIER, B., OEHLER, S., SCHREIBER, M., BERX, G., CANO, A., BEUG, H. & FOISNER, R. 2005. DeltaEF1 is a transcriptional repressor of E-cadherin and regulates epithelial plasticity in breast cancer cells. *Oncogene*, 24, 2375-85.
- ELLOUL, S., ELSTRAND, M. B., NESLAND, J. M., TROPE, C. G., KVALHEIM, G., GOLDBERG, I., REICH, R. & DAVIDSON, B. 2005. Snail, Slug, and Smad-interacting protein 1 as novel parameters of disease aggressiveness in metastatic ovarian and breast carcinoma. *Cancer*, 103, 1631-43.
- ELLOUL, S., SILINS, I., TROPE, C. G., BENSHUSHAN, A., DAVIDSON, B. & REICH, R. 2006. Expression of E-cadherin transcriptional regulators in ovarian carcinoma. *Virchows Arch*, 449, 520-8.
- ELSON-SCHWAB, I., LORENTZEN, A. & MARSHALL, C. J. 2010. MicroRNA-200 family members differentially regulate morphological plasticity and mode of melanoma cell invasion. *PLoS One*, 5.
- ELWARY, S. M., CHAVAN, B. & SCHALLREUTER, K. U. 2006. The vesicular acetylcholine transporter is present in melanocytes and keratinocytes in the human epidermis. *J Invest Dermatol*, 126, 1879-84.
- EMERY, C. M., VIJAYENDRAN, K. G., ZIPSER, M. C., SAWYER, A. M., NIU, L., KIM, J. J., HATTON, C., CHOPRA, R., OBERHOLZER, P. A., KARPOVA, M. B., MACCONAILL, L. E., ZHANG, J., GRAY, N. S., SELLERS, W. R., DUMMER, R. & GARRAWAY, L. A. 2009. MEK1 mutations confer resistance to MEK and B-Raf inhibition. *Proc Natl Acad Sci U S A*, 106, 20411-6.
- ERNFORS, P. 2010. Cellular origin and developmental mechanisms during the formation of skin melanocytes. *Exp Cell Res*, 316, 1397-407.
- ESQUELA-KERSCHER, A. & SLACK, F. J. 2006. Oncomirs - microRNAs with a role in cancer. *Nat Rev Cancer*, 6, 259-69.
- ESSA, S., DENZER, N., MAHLKNECHT, U., KLEIN, R., COLLNOT, E. M., TILGEN, W. & REICHRATH, J. 2010. VDR microRNA expression and epigenetic silencing of vitamin D signaling in melanoma cells. *J Steroid Biochem Mol Biol*, 121, 110-3.
- ESSA, S., REICHRATH, S., MAHLKNECHT, U., MONTENARH, M., VOGT, T. & REICHRATH, J. 2012. Signature of VDR miRNAs and epigenetic modulation of vitamin D signaling in melanoma cell lines. *Anticancer Res*, 32, 383-9.
- ESTRADA, Y., DONG, J. & OSSOWSKI, L. 2009. Positive crosstalk between ERK and p38 in melanoma stimulates migration and in vivo proliferation. *Pigment Cell Melanoma Res*, 22, 66-76.

- EVANS, S. R., HOUGHTON, A. M., SCHUMAKER, L., BRENNER, R. V., BURAS, R. R., DAVOODI, F., NAUTA, R. J. & SHABAHANG, M. 1996. Vitamin D receptor and growth inhibition by 1,25-dihydroxyvitamin D3 in human malignant melanoma cell lines. *J Surg Res*, 61, 127-33.
- FANG, X., CAI, Y., LIU, J., WANG, Z., WU, Q., ZHANG, Z., YANG, C. J., YUAN, L. & OUYANG, G. 2011. Twist2 contributes to breast cancer progression by promoting an epithelial-mesenchymal transition and cancer stem-like cell self-renewal. *Oncogene*, 30, 4707-20.
- FARACH-CARSON, M. C. & RIDALL, A. L. 1998. Dual 1,25-dihydroxyvitamin D3 signal response pathways in osteoblasts: cross-talk between genomic and membrane-initiated pathways. *Am J Kidney Dis*, 31, 729-42.
- FECHER, L. A., AMARAVADI, R. K. & FLAHERTY, K. T. 2008. The MAPK pathway in melanoma. *Curr Opin Oncol*, 20, 183-9.
- FEHRENBACHER, N., BASTHOLM, L., KIRKEGAARD-SORENSEN, T., RAFN, B., BOTTZAUW, T., NIELSEN, C., WEBER, E., SHIRASAWA, S., KALLUNKI, T. & JAATTELA, M. 2008. Sensitization to the lysosomal cell death pathway by oncogene-induced down-regulation of lysosome-associated membrane proteins 1 and 2. *Cancer Res*, 68, 6623-33.
- FERLAY, J., SHIN, H. R., BRAY, F., FORMAN, D., MATHERS, C. & PARKIN, D. M. 2010. Estimates of worldwide burden of cancer in 2008: GLOBOCAN 2008. *Int J Cancer*, 127, 2893-917.
- FLAHERTY, K. T., INFANTE, J. R., DAUD, A., GONZALEZ, R., KEFFORD, R. F., SOSMAN, J., HAMID, O., SCHUCHTER, L., CEBON, J., IBRAHIM, N., KUDCHADKAR, R., BURRIS, H. A., FALCHOOK, G., ALGAZI, A., LEWIS, K., LONG, G. V., PUZANOV, I., LEBOWITZ, P., SINGH, A., LITTLE, S., SUN, P., ALLRED, A., OUELLET, D., KIM, K. B., PATEL, K. & WEBER, J. 2012. Combined BRAF and MEK Inhibition in Melanoma with BRAF V600 Mutations. *N Engl J Med*, 367, 1694-703.
- FOGH, J., FOGH, J. M. & ORFEO, T. 1977. One hundred and twenty-seven cultured human tumor cell lines producing tumors in nude mice. *J Natl Cancer Inst*, 59, 221-6.
- FORBES, S. A., BHAMRA, G., BAMFORD, S., DAWSON, E., KOK, C., CLEMENTS, J., MENZIES, A., TEAGUE, J. W., FUTREAL, P. A. & STRATTON, M. R. 2008. The Catalogue of Somatic Mutations in Cancer (COSMIC). *Curr Protoc Hum Genet*, Chapter 10, Unit 10 11.
- FORBES, S. A., TANG, G., BINDAL, N., BAMFORD, S., DAWSON, E., COLE, C., KOK, C. Y., JIA, M., EWING, R., MENZIES, A., TEAGUE, J. W., STRATTON, M. R. & FUTREAL, P. A. 2010. COSMIC (the Catalogue of Somatic Mutations in Cancer): a resource to investigate acquired mutations in human cancer. *Nucleic Acids Res*, 38, D652-7.
- FRANCI, C., TAKKUNEN, M., DAVE, N., ALAMEDA, F., GOMEZ, S., RODRIGUEZ, R., ESCRIVA, M., MONTSERRAT-SENTIS, B., BARO, T., GARRIDO, M., BONILLA, F., VIRTANEN, I. & GARCIA DE HERREROS, A. 2006. Expression of Snail protein in tumor-stroma interface. *Oncogene*, 25, 5134-44.

- FRIEDL, P. & WOLF, K. 2010. Plasticity of cell migration: a multiscale tuning model. *J Cell Biol*, 188, 11-9.
- FRISCH, S. M. & FRANCIS, H. 1994. Disruption of epithelial cell-matrix interactions induces apoptosis. *J Cell Biol*, 124, 619-26.
- FUNAHASHI, J., SEKIDO, R., MURAI, K., KAMACHI, Y. & KONDOH, H. 1993. Delta-crystallin enhancer binding protein delta EF1 is a zinc finger-homeodomain protein implicated in postgastrulation embryogenesis. *Development*, 119, 433-46.
- GAGGIOLI, C. & SAHAI, E. 2007. Melanoma invasion - current knowledge and future directions. *Pigment Cell Res*, 20, 161-72.
- GARRAWAY, L. A. & SELLERS, W. R. 2006. Lineage dependency and lineage-survival oncogenes in human cancer. *Nat Rev Cancer*, 6, 593-602.
- GARRAWAY, L. A., WIDLUND, H. R., RUBIN, M. A., GETZ, G., BERGER, A. J., RAMASWAMY, S., BEROUKHIM, R., MILNER, D. A., GRANTER, S. R., DU, J., LEE, C., WAGNER, S. N., LI, C., GOLUB, T. R., RIMM, D. L., MEYERSON, M. L., FISHER, D. E. & SELLERS, W. R. 2005. Integrative genomic analyses identify MITF as a lineage survival oncogene amplified in malignant melanoma. *Nature*, 436, 117-22.
- GASPAROTTO, D., POESEL, J., MARZOTTO, A., COLLADEL, R., PICCININ, S., MODENA, P., GRIZZO, A., SULFARO, S., SERRAINO, D., BARZAN, L., DOGLIONI, C. & MAESTRO, R. 2011. Overexpression of TWIST2 correlates with poor prognosis in head and neck squamous cell carcinomas. *Oncotarget*, 2, 1165-75.
- GEIGER, T. R. & PEEPER, D. S. 2009. Metastasis mechanisms. *Biochim Biophys Acta*, 1796, 293-308.
- GEMMILL, R. M., ROCHE, J., POTIRON, V. A., NASARRE, P., MITAS, M., COLDREN, C. D., HELFRICH, B. A., GARRETT-MAYER, E., BUNN, P. A. & DRABKIN, H. A. 2011. ZEB1-responsive genes in non-small cell lung cancer. *Cancer Lett*, 300, 66-78.
- GIARD, D. J., AARONSON, S. A., TODARO, G. J., ARNSTEIN, P., KERSEY, J. H., DOSIK, H. & PARKS, W. P. 1973. In vitro cultivation of human tumors: establishment of cell lines derived from a series of solid tumors. *J Natl Cancer Inst*, 51, 1417-23.
- GLUD, M., MANFE, V., BISKUP, E., HOLST, L., DIRKSEN, A. M., HASTRUP, N., NIELSEN, F. C., DRZEWIECKI, K. T. & GNIADCKI, R. 2011. MicroRNA miR-125b induces senescence in human melanoma cells. *Melanoma Res*, 21, 253-6.
- GLUD, M., ROSSING, M., HOTHER, C., HOLST, L., HASTRUP, N., NIELSEN, F. C., GNIADCKI, R. & DRZEWIECKI, K. T. 2010. Downregulation of miR-125b in metastatic cutaneous malignant melanoma. *Melanoma Res*, 20, 479-84.

- GODAR, D. E. 2011. Worldwide increasing incidences of cutaneous malignant melanoma. *J Skin Cancer*, 2011, 858425.
- GODING, C. R. 2000. Mitf from neural crest to melanoma: signal transduction and transcription in the melanocyte lineage. *Genes & Development*, 14, 1712-1728.
- GOEL, V. K., LAZAR, A. J., WARNEKE, C. L., REDSTON, M. S. & HALUSKA, F. G. 2006. Examination of mutations in BRAF, NRAS, and PTEN in primary cutaneous melanoma. *J Invest Dermatol*, 126, 154-60.
- GOLDSTEIN, A. M., CHAN, M., HARLAND, M., GILLANDERS, E. M., HAYWARD, N. K., AVRIL, M. F., AZIZI, E., BIANCHI-SCARRA, G., BISHOP, D. T., BRESSAC-DE PAILLERETS, B., BRUNO, W., CALISTA, D., CANNON ALBRIGHT, L. A., DEMENAI, F., ELDER, D. E., GHIORZO, P., GRUIS, N. A., HANSSON, J., HOGG, D., HOLLAND, E. A., KANETSKY, P. A., KEFFORD, R. F., LANDI, M. T., LANG, J., LEACHMAN, S. A., MACKIE, R. M., MAGNUSSON, V., MANN, G. J., NIENDORF, K., NEWTON BISHOP, J., PALMER, J. M., PUIG, S., PUIG-BUTILLE, J. A., DE SNOO, F. A., STARK, M., TSAO, H., TUCKER, M. A., WHITAKER, L., YAKOBSON, E. & MELANOMA GENETICS, C. 2006. High-risk melanoma susceptibility genes and pancreatic cancer, neural system tumors, and uveal melanoma across GenoMEL. *Cancer Res*, 66, 9818-28.
- GORDEN, A., OSMAN, I., GAI, W., HE, D., HUANG, W., DAVIDSON, A., HOUGHTON, A. N., BUSAM, K. & POLSKY, D. 2003. Analysis of BRAF and N-RAS mutations in metastatic melanoma tissues. *Cancer Res*, 63, 3955-7.
- GOYDOS, J. S., MANN, B., KIM, H. J., GABRIEL, E. M., ALSINA, J., GERMINO, F. J., SHIH, W. & GORSKI, D. H. 2005. Detection of B-RAF and N-RAS mutations in human melanoma. *J Am Coll Surg*, 200, 362-70.
- GRAHAM, T. R., YACIOUB, R., TALIAFERRO-SMITH, L., OSUNKOYA, A. O., ODERO-MARAH, V. A., LIU, T., KIMBRO, K. S., SHARMA, D. & O'REGAN, R. M. 2010. Reciprocal regulation of ZEB1 and AR in triple negative breast cancer cells. *Breast Cancer Res Treat*, 123, 139-47.
- GRAU, Y., CARTERET, C. & SIMPSON, P. 1984. Mutations and Chromosomal Rearrangements Affecting the Expression of Snail, a Gene Involved in Embryonic Patterning in DROSOPHILA MELANOGASTER. *Genetics*, 108, 347-60.
- GRAY-SCHOPFER, V. C., CHEONG, S. C., CHONG, H., CHOW, J., MOSS, T., ABDEL-MALEK, Z. A., MARAIS, R., WYNFORD-THOMAS, D. & BENNETT, D. C. 2006. Cellular senescence in naevi and immortalisation in melanoma: a role for p16? *Br J Cancer*, 95, 496-505.
- GREENBURG, G. & HAY, E. D. 1982. Epithelia suspended in collagen gels can lose polarity and express characteristics of migrating mesenchymal cells. *The Journal of Cell Biology*, 95, 333-339.
- GREGORY, P. A., BERT, A. G., PATERSON, E. L., BARRY, S. C., TSYKIN, A., FARSHID, G., VADAS, M. A., KHEW-GOODALL, Y. & GOODALL, G. J. 2008. The miR-200 family and miR-205 regulate epithelial to mesenchymal transition by targeting ZEB1 and SIP1. *Nat Cell Biol*, 10, 593-601.

- GROOTECLAES, M. L. & FRISCH, S. M. 2000. Evidence for a function of CtBP in epithelial gene regulation and anoikis. *Oncogene*, 19, 3823-8.
- GROS, J., MANCEAU, M., THOME, V. & MARCELLE, C. 2005. A common somitic origin for embryonic muscle progenitors and satellite cells. *Nature*, 435, 954-8.
- GROSS, J. C., SCHREINER, A., ENGELS, K. & STARZINSKI-POWITZ, A. 2009. E-cadherin surface levels in epithelial growth factor-stimulated cells depend on adherens junction protein shrew-1. *Mol Biol Cell*, 20, 3598-607.
- GROSSMANN, J., WALTHER, K., ARTINGER, M., KIESSLING, S. & SCHOLMERICH, J. 2001. Apoptotic signaling during initiation of detachment-induced apoptosis ("anoikis") of primary human intestinal epithelial cells. *Cell Growth Differ*, 12, 147-55.
- GROTEGUT, S., VON SCHWEINITZ, D., CHRISTOFORI, G. & LEHEMBRE, F. 2006. Hepatocyte growth factor induces cell scattering through MAPK/Egr-1-mediated upregulation of Snail. *EMBO J*, 25, 3534-45.
- GUAITA, S., PUIG, I., FRANCI, C., GARRIDO, M., DOMINGUEZ, D., BATLLE, E., SANCHO, E., DEDHAR, S., DE HERREROS, A. G. & BAULIDA, J. 2002. Snail induction of epithelial to mesenchymal transition in tumor cells is accompanied by MUC1 repression and ZEB1 expression. *J Biol Chem*, 277, 39209-16.
- GUDBJARTSSON, D. F., SULEM, P., STACEY, S. N., GOLDSTEIN, A. M., RAFNAR, T., SIGURGEIRSSON, B., BENEDIKTSDOTTIR, K. R., THORISDOTTIR, K., RAGNARSSON, R., SVEINSDOTTIR, S. G., MAGNUSSON, V., LINDBLOM, A., KOSTULAS, K., BOTELLA-ESTRADA, R., SORIANO, V., JUBERIAS, P., GRASA, M., SAEZ, B., ANDRES, R., SCHERER, D., RUDNAI, P., GURZAU, E., KOPPOVA, K., KIEMENEY, L. A., JAKOBSDOTTIR, M., STEINBERG, S., HELGASON, A., GRETARSDOTTIR, S., TUCKER, M. A., MAYORDOMO, J. I., NAGORE, E., KUMAR, R., HANSSON, J., OLAFSSON, J. H., GULCHER, J., KONG, A., THORSTEINSDOTTIR, U. & STEFANSSON, K. 2008. ASIP and TYR pigmentation variants associate with cutaneous melanoma and basal cell carcinoma. *Nat Genet*, 40, 886-91.
- GUERTIN, D. A., STEVENS, D. M., SAITOH, M., KINKEL, S., CROSBY, K., SHEEN, J.-H., MULLHOLLAND, D. J., MAGNUSON, M. A., WU, H. & SABATINI, D. M. 2009. mTOR Complex 2 Is Required for the Development of Prostate Cancer Induced by Pten Loss in Mice. *Cancer Cell*, 15, 148-159.
- GUPTA, P. B., KUPERWASSER, C., BRUNET, J. P., RAMASWAMY, S., KUO, W. L., GRAY, J. W., NABER, S. P. & WEINBERG, R. A. 2005. The melanocyte differentiation program predisposes to metastasis after neoplastic transformation. *Nat Genet*, 37, 1047-54.
- HAASS, N. K., SMALLEY, K. S. & HERLYN, M. 2004. The role of altered cell-cell communication in melanoma progression. *J Mol Histol*, 35, 309-18.
- HAFNER, C., VAN OERS, J. M., VOGT, T., LANDTHALER, M., STOEHR, R., BLASZYK, H., HOFSTAEDTER, F., ZWARTHOFF, E. C. & HARTMANN, A. 2006. Mosaicism of activating FGFR3 mutations in human skin causes epidermal nevi. *J Clin Invest*, 116, 2201-2207.

- HALL, P. A., COATES, P. J., ANSARI, B. & HOPWOOD, D. 1994. Regulation of cell number in the mammalian gastrointestinal tract: the importance of apoptosis. *J Cell Sci*, 107 (Pt 12), 3569-77.
- HAO, L., HA, J. R., KUZEL, P., GARCIA, E. & PERSAD, S. 2012. Cadherin switch from E- to N-cadherin in melanoma progression is regulated by the PI3K/PTEN pathway through Twist and Snail. *British Journal of Dermatology*, 166, 1184-1197.
- HAUSSLER, M. R., HAUSSLER, C. A., JURUTKA, P. W., THOMPSON, P. D., HSIEH, J. C., REMUS, L. S., SELZNICK, S. H. & WHITFIELD, G. K. 1997. The vitamin D hormone and its nuclear receptor: molecular actions and disease states. *J Endocrinol*, 154 Suppl, S57-73.
- HAUSSLER, M. R. & NORMAN, A. W. 1969. Chromosomal receptor for a vitamin D metabolite. *PNAS*, 62, 155-62.
- HAYASHI, H., SONE, M., SCHACHERN, P. A., WAKAMATSU, K., PAPARELLA, M. M. & NAKASHIMA, T. 2007. Comparison of the quantity of cochlear melanin in young and old C57BL/6 mice. *Arch Otolaryngol Head Neck Surg*, 133, 151-4.
- HAYWARD, N. K. 2003. Genetics of melanoma predisposition. *Oncogene*, 22, 3053-62.
- HE, L. & HANNON, G. J. 2004. MicroRNAs: small RNAs with a big role in gene regulation. *Nat Rev Genet*, 5, 522-31.
- HEIDORN, S. J., MILAGRE, C., WHITTAKER, S., NOURRY, A., NICULESCU-DUVAS, I., DHOMEN, N., HUSSAIN, J., REIS-FILHO, J. S., SPRINGER, C. J., PRITCHARD, C. & MARAIS, R. 2010. Kinase-dead BRAF and oncogenic RAS cooperate to drive tumor progression through CRAF. *Cell*, 140, 209-21.
- HEINLEIN, C. A. & CHANG, C. 2004. Androgen receptor in prostate cancer. *Endocr Rev*, 25, 276-308.
- HELSING, P., NYMOEN, D. A., ARIANSEN, S., STEINE, S. J., MAEHLE, L., AAMDAL, S., LANGMARK, F., LOEB, M., AKSLEN, L. A., MOLVEN, A. & ANDRESEN, P. A. 2008. Population-based prevalence of CDKN2A and CDK4 mutations in patients with multiple primary melanomas. *Genes Chromosomes Cancer*, 47, 175-84.
- HENDRICKSON, W. K., FLAVIN, R., KASPERZYK, J. L., FIORENTINO, M., FANG, F., LIS, R., FIORE, C., PENNEY, K. L., MA, J., KANTOFF, P. W., STAMPFER, M. J., LODA, M., MUCCI, L. A. & GIOVANNUCCI, E. 2011. Vitamin D receptor protein expression in tumor tissue and prostate cancer progression. *J Clin Oncol*, 29, 2378-85.
- HERSHKO, A. & CIECHANOVER, A. 1998. The ubiquitin system. *Annu Rev Biochem*, 67, 425-79.
- HOCKER, T. L., SINGH, M. K. & TSAO, H. 2008. Melanoma genetics and therapeutic approaches in the 21st century: moving from the benchside to the bedside. *J Invest Dermatol*, 128, 2575-95.

- HODIS, E., WATSON, I. R., KRYUKOV, G. V., AROLD, S. T., IMIELINSKI, M., THEURILLAT, J. P., NICKERSON, E., AUCLAIR, D., LI, L., PLACE, C., DICARA, D., RAMOS, A. H., LAWRENCE, M. S., CIBULSKIS, K., SIVACHENKO, A., VOET, D., SAKSENA, G., STRANSKY, N., ONOFRIO, R. C., WINCKLER, W., ARDLIE, K., WAGLE, N., WARGO, J., CHONG, K., MORTON, D. L., STEMKE-HALE, K., CHEN, G., NOBLE, M., MEYERSON, M., LADBURY, J. E., DAVIES, M. A., GERSHENWALD, J. E., WAGNER, S. N., HOON, D. S., SCHADENDORF, D., LANDER, E. S., GABRIEL, S. B., GETZ, G., GARRAWAY, L. A. & CHIN, L. 2012. A landscape of driver mutations in melanoma. *Cell*, 150, 251-63.
- HOEK, K., RIMM, D. L., WILLIAMS, K. R., ZHAO, H., ARIYAN, S., LIN, A., KLUGER, H. M., BERGER, A. J., CHENG, E., TROMBETTA, E. S., WU, T., NIINOBE, M., YOSHIKAWA, K., HANNIGAN, G. E. & HALABAN, R. 2004. Expression profiling reveals novel pathways in the transformation of melanocytes to melanomas. *Cancer Res*, 64, 5270-82.
- HOFFMANN, E., THIEFES, A., BUHROW, D., DITTRICH-BREIHL, O., SCHNEIDER, H., RESCH, K. & KRACHT, M. 2005. MEK1-dependent delayed expression of Fos-related antigen-1 counteracts c-Fos and p65 NF-kappaB-mediated interleukin-8 transcription in response to cytokines or growth factors. *J Biol Chem*, 280, 9706-18.
- HOLICK, M. F. 2007. Vitamin D deficiency. *N Engl J Med*, 357, 266-81.
- HORIKAWA, T., NORRIS, D. A., JOHNSON, T. W., ZEKMAN, T., DUNSCOMB, N., BENNION, S. D., JACKSON, R. L. & MORELLI, J. G. 1996. DOPA-negative melanocytes in the outer root sheath of human hair follicles express premelanosomal antigens but not a melanosomal antigen or the melanosome-associated glycoproteins tyrosinase, TRP-1, and TRP-2. *J Invest Dermatol*, 106, 28-35.
- HOWLANDER N, N. A., KRAPCHO M, NEYMAN N, AMINOU R, ALTEKRUSE SF, KOSARY CL, RUHL J, TATALOVICH Z, CHO H, MARIOTTO A, EISNER MP, LEWIS DR, CHEN HS, FEUER EJ, CRONIN KA 2011. SEER Cancer Statistics Review, 1975-2009 (Vintage 2009 Populations). April 2012 ed.: National Cancer Institute.
- HSU, M. Y., MEIER, F. E., NESBIT, M., HSU, J. Y., VAN BELLE, P., ELDER, D. E. & HERLYN, M. 2000. E-cadherin expression in melanoma cells restores keratinocyte-mediated growth control and down-regulates expression of invasion-related adhesion receptors. *Am J Pathol*, 156, 1515-25.
- HU, D. N., SIMON, J. D. & SARNA, T. 2008. Role of ocular melanin in ophthalmic physiology and pathology. *Photochem Photobiol*, 84, 639-44.
- HUBER, M. A., KRAUT, N. & BEUG, H. 2005. Molecular requirements for epithelial-mesenchymal transition during tumor progression. *Curr Opin Cell Biol*, 17, 548-58.
- HUGO, H., ACKLAND, M. L., BLICK, T., LAWRENCE, M. G., CLEMENTS, J. A., WILLIAMS, E. D. & THOMPSON, E. W. 2007. Epithelial-mesenchymal and mesenchymal-epithelial transitions in carcinoma progression. *J Cell Physiol*, 213, 374-83.

- HUI, L., LIU, B., ZHAO, L., ZHANG, S., ZHOU, B., QIU, X. & CUI, Z. 2009. High expression of twist is positively correlated with the differentiation of lung cancer. *Zhongguo Fei Ai Za Zhi*, 12, 294-9.
- HUSEMANN, Y., GEIGL, J. B., SCHUBERT, F., MUSIANI, P., MEYER, M., BURGHART, E., FORNI, G., EILS, R., FEHM, T., RIETHMULLER, G. & KLEIN, C. A. 2008. Systemic spread is an early step in breast cancer. *Cancer Cell*, 13, 58-68.
- IBRAHIM, N. & HALUSKA, F. G. 2009. Molecular pathogenesis of cutaneous melanocytic neoplasms. *Annu Rev Pathol*, 4, 551-79.
- IMAMICHI, Y., KONIG, A., GRESS, T. & MENKE, A. 2007. Collagen type I-induced Smad-interacting protein 1 expression downregulates E-cadherin in pancreatic cancer. *Oncogene*, 26, 2381-5.
- ISHIHARA, K., SAIDA, T., YAMAMOTO, A., JAPANESE SKIN CANCER SOCIETY, P. & STATISTICAL INVESTIGATION, C. 2001. Updated statistical data for malignant melanoma in Japan. *Int J Clin Oncol*, 6, 109-16.
- JAISWAL, B. S., JANAKIRAMAN, V., KLJAVIN, N. M., EASTHAM-ANDERSON, J., CUPP, J. E., LIANG, Y., DAVIS, D. P., HOEFELICH, K. P. & SESHAGIRI, S. 2009. Combined targeting of BRAF and CRAF or BRAF and PI3K effector pathways is required for efficacy in NRAS mutant tumours. *PLoS One*, 4, e5717.
- JOHANNESSEN, C. M., BOEHM, J. S., KIM, S. Y., THOMAS, S. R., WARDWELL, L., JOHNSON, L. A., EMERY, C. M., STRANSKY, N., COGDILL, A., BARRETINA, J., CAPONIGRO, G., HIERONYMUS, H., MURRAY, R. R., SALEHI-ASHTIANI, K., HILL, D. E., VIDAL, M., ZHAO, J. J., YANG, X., ALKAN, O., KIM, S., HARRIS, J. L., WILSON, C. J., MYER, V. E., FINAN, P. M., ROOT, D. E., ROBERTS, T. M., GOLUB, T., FLAHERTY, K. T., DUMMER, R., WEBER, B. L., SELLERS, W. R., SCHLEGEL, R., WARGO, J. A., HAHN, W. C. & GARRAWAY, L. A. 2010. COT drives resistance to RAF inhibition through MAP kinase pathway reactivation. *Nature*, 468, 968-72.
- JONES, N. C. & TRAINOR, P. A. 2005. Role of morphogens in neural crest cell determination. *J Neurobiol*, 64, 388-404.
- JONES, W. O., HARMAN, C. R., NG, A. K. T. & SHAW, J. H. F. 1999. Incidence of Malignant Melanoma in Auckland, New Zealand: Highest Rates in the World. *World Journal of Surgery*, 23, 732-735.
- JOOST, S., ALMADA, L. L., ROHNALTER, V., HOLZ, P. S., VRABEL, A. M., FERNANDEZ-BARRENA, M. G., MCWILLIAMS, R. R., KRAUSE, M., FERNANDEZ-ZAPICO, M. E. & LAUTH, M. 2012. GLI1 inhibition promotes epithelial-to-mesenchymal transition in pancreatic cancer cells. *Cancer Res*, 72, 88-99.
- KABIGTING, F. D., NELSON, F. P., KAUFFMAN, C. L., POPOVENIUC, G., DASANU, C. A. & ALEXANDRESCU, D. T. 2009. Malignant melanoma in African-Americans. *Dermatol Online J*, 15, 3.
- KALLURI, R. & NEILSON, E. G. 2003. Epithelial-mesenchymal transition and its implications for fibrosis. *The Journal of Clinical Investigation*, 112, 1776-1784.

- KARBOWNICZEK, M., SPITTLE, C. S., MORRISON, T., WU, H. & HENSKE, E. P. 2008. mTOR is activated in the majority of malignant melanomas. *J Invest Dermatol*, 128, 980-7.
- KARRETH, F. A., TAY, Y., PERNA, D., ALA, U., TAN, S. M., RUST, A. G., DENICOLA, G., WEBSTER, K. A., WEISS, D., PEREZ-MANCERA, P. A., KRAUTHAMMER, M., HALABAN, R., PROVERO, P., ADAMS, D. J., TUVESON, D. A. & PANDOLFI, P. P. 2011. In vivo identification of tumor- suppressive PTEN ceRNAs in an oncogenic BRAF-induced mouse model of melanoma. *Cell*, 147, 382-95.
- KATAOKA, H., MURAYAMA, T., YOKODE, M., MORI, S., SANO, H., OZAKI, H., YOKOTA, Y., NISHIKAWA, S. & KITA, T. 2000. A novel snail-related transcription factor Smuc regulates basic helix-loop-helix transcription factor activities via specific E-box motifs. *Nucleic Acids Res*, 28, 626-33.
- KINSEL, L. B., SZABO, E., GREENE, G. L., KONRATH, J., LEIGHT, G. S. & MCCARTY, K. S., JR. 1989. Immunocytochemical analysis of estrogen receptors as a predictor of prognosis in breast cancer patients: comparison with quantitative biochemical methods. *Cancer Res*, 49, 1052-6.
- KIRIAKIDOU, M., NELSON, P. T., KOURANOV, A., FITZIEV, P., BOUYIOUKOS, C., MOURELATOS, Z. & HATZIGEORGIOU, A. 2004. A combined computational-experimental approach predicts human microRNA targets. *Genes Dev*, 18, 1165-78.
- KLEIN, C. A. 2009. Parallel progression of primary tumours and metastases. *Nat Rev Cancer*, 9, 302-12.
- KLEIN, C. A., BLANKENSTEIN, T. J., SCHMIDT-KITTLER, O., PETRONIO, M., POLZER, B., STOECKLEIN, N. H. & RIETHMULLER, G. 2002. Genetic heterogeneity of single disseminated tumour cells in minimal residual cancer. *Lancet*, 360, 683-9.
- KOEFINGER, P., WELS, C., JOSHI, S., DAMM, S., STEINBAUER, E., BEHAM-SCHMID, C., FRANK, S., BERGLER, H. & SCHAUER, H. 2011. The cadherin switch in melanoma instigated by HGF is mediated through epithelial-mesenchymal transition regulators. *Pigment Cell Melanoma Res*, 24, 382-5.
- KOKKINOS, M. I., MURTHI, P., WAFAI, R., THOMPSON, E. W. & NEWGREEN, D. F. 2010. Cadherins in the human placenta--epithelial-mesenchymal transition (EMT) and placental development. *Placenta*, 31, 747-55.
- KORPAL, M., LEE, E. S., HU, G. & KANG, Y. 2008. The miR-200 family inhibits epithelial-mesenchymal transition and cancer cell migration by direct targeting of E-cadherin transcriptional repressors ZEB1 and ZEB2. *J Biol Chem*, 283, 14910-4.
- KOZLOWSKI, J. M., HART, I. R., FIDLER, I. J. & HANNA, N. 1984. A human melanoma line heterogeneous with respect to metastatic capacity in athymic nude mice. *J Natl Cancer Inst*, 72, 913-7.
- KURAHARA, H., TAKAO, S., MAEMURA, K., MATAKI, Y., KUWAHATA, T., MAEDA, K., DING, Q., SAKODA, M., IINO, S., ISHIGAMI, S., UENO, S., SHINCHI, H. & NATSUGOE, S. 2012. Epithelial-mesenchymal transition and mesenchymal-epithelial transition via regulation of ZEB-1 and ZEB-2 expression in pancreatic cancer. *J Surg Oncol*, 105, 655-61.

- KURIYAMA, S. & MAYOR, R. 2008. Molecular analysis of neural crest migration. *Philos Trans R Soc Lond B Biol Sci*, 363, 1349-62.
- KUSTIKOVA, O., KRAMEROV, D., GRIGORIAN, M., BEREZIN, V., BOCK, E., LUKANIDIN, E. & TULCHINSKY, E. 1998. Fra-1 induces morphological transformation and increases in vitro invasiveness and motility of epithelioid adenocarcinoma cells. *Mol Cell Biol*, 18, 7095-105.
- KWOK, W. K., LING, M. T., LEE, T. W., LAU, T. C., ZHOU, C., ZHANG, X., CHUA, C. W., CHAN, K. W., CHAN, F. L., GLACKIN, C., WONG, Y. C. & WANG, X. 2005. Up-regulation of TWIST in prostate cancer and its implication as a therapeutic target. *Cancer Res*, 65, 5153-62.
- KYO, S., SAKAGUCHI, J., OHNO, S., MIZUMOTO, Y., MAIDA, Y., HASHIMOTO, M., NAKAMURA, M., TAKAKURA, M., NAKAJIMA, M., MASUTOMI, K. & INOUE, M. 2006. High Twist expression is involved in infiltrative endometrial cancer and affects patient survival. *Hum Pathol*, 37, 431-8.
- LABONNE, C. & BRONNER-FRASER, M. 2000. Snail-related transcriptional repressors are required in *Xenopus* for both the induction of the neural crest and its subsequent migration. *Dev Biol*, 221, 195-205.
- LAMOLET, B., PULICHINO, A. M., LAMONERIE, T., GAUTHIER, Y., BRUE, T., ENJALBERT, A. & DROUIN, J. 2001. A pituitary cell-restricted T box factor, Tpit, activates POMC transcription in cooperation with Pitx homeoproteins. *Cell*, 104, 849-59.
- LAN, R., GENG, H., POLICHNOWSKI, A. J., SINGHA, P. K., SAIKUMAR, P., MCEWEN, D. G., GRIFFIN, K. A., KOESTERS, R., WEINBERG, J. M., BIDANI, A. K., KRIZ, W. & VENKATACHALAM, M. A. 2012. PTEN loss defines a TGF- β -induced tubule phenotype of failed differentiation and JNK signaling during renal fibrosis. *American Journal of Physiology - Renal Physiology*, 302, F1210-F1223.
- LANDER, R., NORDIN, K. & LABONNE, C. 2011. The F-box protein Ppa is a common regulator of core EMT factors Twist, Snail, Slug, and Sip1. *J Cell Biol*, 194, 17-25.
- LARRIBA, M. J., MARTIN-VILLAR, E., GARCIA, J. M., PEREIRA, F., PENA, C., DE HERREROS, A. G., BONILLA, F. & MUNOZ, A. 2009. Snail2 cooperates with Snail1 in the repression of vitamin D receptor in colon cancer. *Carcinogenesis*, 30, 1459-68.
- LARUE, L. 2012. Origin of mouse melanomas. *J Invest Dermatol*, 132, 2135-6.
- LAZAROVA, D. L., BORDONARO, M. & SARTORELLI, A. C. 2001. Transcriptional regulation of the vitamin D(3) receptor gene by ZEB. *Cell Growth Differ*, 12, 319-26.
- LE POOLE, I. C., MUTIS, T., VAN DEN WIJNGAARD, R. M., WESTERHOF, W., OTTENHOFF, T., DE VRIES, R. R. & DAS, P. K. 1993a. A novel, antigen-presenting function of melanocytes and its possible relationship to hypopigmentary disorders. *J Immunol*, 151, 7284-92.

- LE POOLE, I. C., VAN DEN WIJNGAARD, R. M., WESTERHOF, W., VERKRUISEN, R. P., DUTRIEUX, R. P., DINGEMANS, K. P. & DAS, P. K. 1993b. Phagocytosis by normal human melanocytes in vitro. *Exp Cell Res*, 205, 388-95.
- LEE, H. Y., KLEBER, M., HARI, L., BRAULT, V., SUTER, U., TAKETO, M. M., KEMLER, R. & SOMMER, L. 2004. Instructive role of Wnt/beta-catenin in sensory fate specification in neural crest stem cells. *Science*, 303, 1020-3.
- LEE, J. M., DEDHAR, S., KALLURI, R. & THOMPSON, E. W. 2006a. The epithelial-mesenchymal transition: new insights in signaling, development, and disease. *J Cell Biol*, 172, 973-81.
- LEE, R. C., FEINBAUM, R. L. & AMBROS, V. 1993. The *C. elegans* heterochronic gene *lin-4* encodes small RNAs with antisense complementarity to *lin-14*. *Cell*, 75, 843-54.
- LEE, T. K., POON, R. T., YUEN, A. P., LING, M. T., KWOK, W. K., WANG, X. H., WONG, Y. C., GUAN, X. Y., MAN, K., CHAU, K. L. & FAN, S. T. 2006b. Twist overexpression correlates with hepatocellular carcinoma metastasis through induction of epithelial-mesenchymal transition. *Clin Cancer Res*, 12, 5369-76.
- LEMIEUX, E., BERGERON, S., DURAND, V., ASSELIN, C., SAUCIER, C. & RIVARD, N. 2009. Constitutively active MEK1 is sufficient to induce epithelial-to-mesenchymal transition in intestinal epithelial cells and to promote tumor invasion and metastasis. *Int J Cancer*, 125, 1575-86.
- LEVIN, M. D., LU, M. M., PETRENKO, N. B., HAWKINS, B. J., GUPTA, T. H., LANG, D., BUCKLEY, P. T., JOCHEMS, J., LIU, F., SPURNEY, C. F., YUAN, L. J., JACOBSON, J. T., BROWN, C. B., HUANG, L., BEERMANN, F., MARGULIES, K. B., MADESH, M., EBERWINE, J. H., EPSTEIN, J. A. & PATEL, V. V. 2009. Melanocyte-like cells in the heart and pulmonary veins contribute to atrial arrhythmia triggers. *J Clin Invest*, 119, 3420-36.
- LEWIS, B. P., SHIH, I. H., JONES-RHOADES, M. W., BARTEL, D. P. & BURGE, C. B. 2003. Prediction of mammalian microRNA targets. *Cell*, 115, 787-98.
- LI, L., FUKUNAGA-KALABIS, M., YU, H., XU, X., KONG, J., LEE, J. T. & HERLYN, M. 2010. Human dermal stem cells differentiate into functional epidermal melanocytes. *J Cell Sci*, 123, 853-60.
- LI, Y., WANG, W., WANG, W., YANG, R., WANG, T., SU, T., WENG, D., TAO, T., LI, W., MA, D. & WANG, S. 2012. Correlation of TWIST2 up-regulation and epithelial-mesenchymal transition during tumorigenesis and progression of cervical carcinoma. *Gynecol Oncol*, 124, 112-8.
- LINKER, C., BRONNER-FRASER, M. & MAYOR, R. 2000. Relationship between gene expression domains of Xsnail, Xslug, and Xtwist and cell movement in the prospective neural crest of *Xenopus*. *Dev Biol*, 224, 215-25.
- LIU, J. & BROWN, R. E. 2010. Immunohistochemical detection of epithelial-mesenchymal transition associated with stemness phenotype in anaplastic thyroid carcinoma. *Int J Clin Exp Pathol*, 3, 755-62.

- LIU, S., KUMAR, S. M., LU, H., LIU, A., YANG, R., PUSHPARAJAN, A., GUO, W. & XU, X. 2012a. MicroRNA-9 up-regulates E-cadherin through inhibition of NF-kappaB1-Snail1 pathway in melanoma. *J Pathol*, 226, 61-72.
- LIU, S., TETZLAFF, M. T., LIU, A., LIEGL-ATZWANGER, B., GUO, J. & XU, X. 2012b. Loss of microRNA-205 expression is associated with melanoma progression. *Lab Invest*, 92, 1084-96.
- LIU, W., LAITINEN, S., KHAN, S., VIHINEN, M., KOWALSKI, J., YU, G., CHEN, L., EWING, C. M., EISENBERGER, M. A., CARDUCCI, M. A., NELSON, W. G., YEGNASUBRAMANIAN, S., LUO, J., WANG, Y., XU, J., ISAACS, W. B., VISAKORPI, T. & BOVA, G. S. 2009a. Copy number analysis indicates monoclonal origin of lethal metastatic prostate cancer. *Nat Med*, 15, 559-65.
- LIU, Y., YE, F., LI, Q., TAMIYA, S., DARLING, D. S., KAPLAN, H. J. & DEAN, D. C. 2009b. Zeb1 represses Mitf and regulates pigment synthesis, cell proliferation, and epithelial morphology. *Invest Ophthalmol Vis Sci*, 50, 5080-8.
- LIVAK, K. J. & SCHMITTGEN, T. D. 2001. Analysis of relative gene expression data using real-time quantitative PCR and the 2(-Delta Delta C(T)) Method. *Methods*, 25, 402-8.
- LONG, J., ZUO, D. & PARK, M. 2005. Pc2-mediated sumoylation of Smad-interacting protein 1 attenuates transcriptional repression of E-cadherin. *J Biol Chem*, 280, 35477-89.
- LOPES, N., SOUSA, B., MARTINS, D., GOMES, M., VIEIRA, D., VERONESE, L. A., MILANEZI, F., PAREDES, J., COSTA, J. L. & SCHMITT, F. 2010. Alterations in Vitamin D signalling and metabolic pathways in breast cancer progression: a study of VDR, CYP27B1 and CYP24A1 expression in benign and malignant breast lesions. *BMC Cancer*, 10, 483.
- LOPEZ-BERGAMI, P. 2011. The role of mitogen- and stress-activated protein kinase pathways in melanoma. *Pigment Cell Melanoma Res*, 24, 902-21.
- LOPEZ-BERGAMI, P., HUANG, C., GOYDOS, J. S., YIP, D., BAR-ELI, M., HERLYN, M., SMALLEY, K. S., MAHALE, A., EROSHKIN, A., AARONSON, S. & RONAI, Z. 2007. Rewired ERK-JNK signaling pathways in melanoma. *Cancer Cell*, 11, 447-60.
- LUZZI, K. J., MACDONALD, I. C., SCHMIDT, E. E., KERKVLIT, N., MORRIS, V. L., CHAMBERS, A. F. & GROOM, A. C. 1998. Multistep nature of metastatic inefficiency: dormancy of solitary cells after successful extravasation and limited survival of early micrometastases. *Am J Pathol*, 153, 865-73.
- MA, L., TERUYA-FELDSTEIN, J. & WEINBERG, R. A. 2007. Tumour invasion and metastasis initiated by microRNA-10b in breast cancer. *Nature*, 449, 682-8.
- MACKIE, R. M. 2000. Malignant melanoma: clinical variants and prognostic indicators. *Clin Exp Dermatol*, 25, 471-5.

- MACKINTOSH, J. A. 2001. The antimicrobial properties of melanocytes, melanosomes and melanin and the evolution of black skin. *J Theor Biol*, 211, 101-13.
- MACORITTO, M., NGUYEN-YAMAMOTO, L., HUANG, D. C., SAMUEL, S., YANG, X. F., WANG, T. T., WHITE, J. H. & KREMER, R. 2008. Phosphorylation of the human retinoid X receptor alpha at serine 260 impairs coactivator(s) recruitment and induces hormone resistance to multiple ligands. *J Biol Chem*, 283, 4943-56.
- MAEDA, G., CHIBA, T., OKAZAKI, M., SATOH, T., TAYA, Y., AOBA, T., KATO, K., KAWASHIRI, S. & IMAI, K. 2005. Expression of SIP1 in oral squamous cell carcinomas: implications for E-cadherin expression and tumor progression. *Int J Oncol*, 27, 1535-41.
- MALDONADO, J. L., FRIDLYAND, J., PATEL, H., JAIN, A. N., BUSAM, K., KAGESHITA, T., ONO, T., ALBERTSON, D. G., PINKEL, D. & BASTIAN, B. C. 2003. Determinants of BRAF mutations in primary melanomas. *J Natl Cancer Inst*, 95, 1878-90.
- MANDL, M., SLACK, D. N. & KEYSE, S. M. 2005. Specific inactivation and nuclear anchoring of extracellular signal-regulated kinase 2 by the inducible dual-specificity protein phosphatase DUSP5. *Mol Cell Biol*, 25, 1830-45.
- MARTELLO, G., ROSATO, A., FERRARI, F., MANFRIN, A., CORDENONSI, M., DUPONT, S., ENZO, E., GUZZARDO, V., RONDINA, M., SPRUCE, T., PARENTI, A. R., DAIDONE, M. G., BICCIATO, S. & PICCOLO, S. 2010. A MicroRNA targeting dicer for metastasis control. *Cell*, 141, 1195-207.
- MARTIN, T. A., GOYAL, A., WATKINS, G. & JIANG, W. G. 2005. Expression of the transcription factors snail, slug, and twist and their clinical significance in human breast cancer. *Ann Surg Oncol*, 12, 488-96.
- MASSI, D., PUIG, S., FRANCHI, A., MALVEHY, J., VIDAL-SICART, S., GONZALEZ-CAO, M., BARONI, G., KETABCHI, S., PALOU, J. & SANTUCCI, M. 2006. Tumour lymphangiogenesis is a possible predictor of sentinel lymph node status in cutaneous melanoma: a case-control study. *J Clin Pathol*, 59, 166-73.
- MASSOUMI, R., KUPHAL, S., HELLERBRAND, C., HAAS, B., WILD, P., SPRUSS, T., PFEIFER, A., FASSLER, R. & BOSSERHOFF, A. K. 2009. Down-regulation of CYLD expression by Snail promotes tumor progression in malignant melanoma. *J Exp Med*, 206, 221-32.
- MAYHEW, T. M., MYKLEBUST, R., WHYBROW, A. & JENKINS, R. 1999. Epithelial integrity, cell death and cell loss in mammalian small intestine. *Histol Histopathol*, 14, 257-67.
- MEJLVANG, J., KRIAJEVSKA, M., VANDEWALLE, C., CHERNOVA, T., SAYAN, A. E., BERX, G., MELLON, J. K. & TULCHINSKY, E. 2007. Direct repression of cyclin D1 by SIP1 attenuates cell cycle progression in cells undergoing an epithelial mesenchymal transition. *Mol Biol Cell*, 18, 4615-24.
- MEYLE, K. D. & GULDBERG, P. 2009. Genetic risk factors for melanoma. *Hum Genet*, 126, 499-510.

- MICHALOGLU, C., VREDEVELD, L. C., SOENGAS, M. S., DENOYELLE, C., KUILMAN, T., VAN DER HORST, C. M., MAJOOR, D. M., SHAY, J. W., MOOI, W. J. & PEEPER, D. S. 2005. BRAFE600-associated senescence-like cell cycle arrest of human naevi. *Nature*, 436, 720-4.
- MIKESH, L. M., KUMAR, M., ERDAG, G., HOGAN, K. T., MOLHOEK, K. R., MAYO, M. W. & SLINGLUFF, C. L., JR. 2010. Evaluation of molecular markers of mesenchymal phenotype in melanoma. *Melanoma Res*, 20, 485-95.
- MINK, S. R., VASHISTHA, S., ZHANG, W., HODGE, A., AGUS, D. B. & JAIN, A. 2010. Cancer-associated fibroblasts derived from EGFR-TKI-resistant tumors reverse EGFR pathway inhibition by EGFR-TKIs. *Mol Cancer Res*, 8, 809-20.
- MITTAL, M. K., MYERS, J. N., MISRA, S., BAILEY, C. K. & CHAUDHURI, G. 2008. In vivo binding to and functional repression of the VDR gene promoter by SLUG in human breast cells. *Biochem Biophys Res Commun*, 372, 30-4.
- MIYAJI, M., KORTUM, R. L., SURANA, R., LI, W., WOOLARD, K. D., SIMPSON, R. M., SAMELSON, L. E. & SOMMERS, C. L. 2009. Genetic evidence for the role of Erk activation in a lymphoproliferative disease of mice. *Proc Natl Acad Sci U S A*, 106, 14502-7.
- MIYOSHI, A., KITAJIMA, Y., KIDO, S., SHIMONISHI, T., MATSUYAMA, S., KITAHARA, K. & MIYAZAKI, K. 2005. Snail accelerates cancer invasion by upregulating MMP expression and is associated with poor prognosis of hepatocellular carcinoma. *Br J Cancer*, 92, 252-8.
- MIYOSHI, A., KITAJIMA, Y., SUMI, K., SATO, K., HAGIWARA, A., KOGA, Y. & MIYAZAKI, K. 2004. Snail and SIP1 increase cancer invasion by upregulating MMP family in hepatocellular carcinoma cells. *Br J Cancer*, 90, 1265-1273.
- MIYOSHI, T., MARUHASHI, M., VAN DE PUTTE, T., KONDOH, H., HUYLEBROECK, D. & HIGASHI, Y. 2006. Complementary expression pattern of Zfhx1 genes Sip1 and deltaEF1 in the mouse embryo and their genetic interaction revealed by compound mutants. *Dev Dyn*, 235, 1941-52.
- MOHRI, T., NAKAJIMA, M., TAKAGI, S., KOMAGATA, S. & YOKOI, T. 2009. MicroRNA regulates human vitamin D receptor. *Int J Cancer*, 125, 1328-33.
- MONSORO-BURQ, A. H., FLETCHER, R. B. & HARLAND, R. M. 2003. Neural crest induction by paraxial mesoderm in *Xenopus* embryos requires FGF signals. *Development*, 130, 3111-24.
- MORRIS, V. L., SCHMIDT, E. E., MACDONALD, I. C., GROOM, A. C. & CHAMBERS, A. F. 1997. Sequential steps in hematogenous metastasis of cancer cells studied by in vivo videomicroscopy. *Invasion Metastasis*, 17, 281-96.
- MUELLER, D. W., REHLI, M. & BOSSERHOFF, A. K. 2009. miRNA expression profiling in melanocytes and melanoma cell lines reveals miRNAs associated with formation and progression of malignant melanoma. *J Invest Dermatol*, 129, 1740-51.

- MULLIS, K., FALOONA, F., SCHARF, S., SAIKI, R., HORN, G. & ERLICH, H. 1986. Specific enzymatic amplification of DNA in vitro: the polymerase chain reaction. *Cold Spring Harb Symp Quant Biol*, 51 Pt 1, 263-73.
- MURILLO-CUESTA, S., CONTRERAS, J., ZURITA, E., CEDIEL, R., CANTERO, M., VARELA-NIETO, I. & MONTOLIU, L. 2010. Melanin precursors prevent premature age-related and noise-induced hearing loss in albino mice. *Pigment Cell Melanoma Res*, 23, 72-83.
- NAKAYA, Y. & SHENG, G. 2008. Epithelial to mesenchymal transition during gastrulation: an embryological view. *Dev Growth Differ*, 50, 755-66.
- NAN, H., KRAFT, P., HUNTER, D. J. & HAN, J. 2009. Genetic variants in pigmentation genes, pigmentary phenotypes, and risk of skin cancer in Caucasians. *Int J Cancer*, 125, 909-17.
- NARISAWA, Y., KOHDA, H. & TANAKA, T. 1997. Three-dimensional demonstration of melanocyte distribution of human hair follicles: special reference to the bulge area. *Acta Derm Venereol*, 77, 97-101.
- NATSUGOE, S., UCHIKADO, Y., OKUMURA, H., MATSUMOTO, M., SETOYAMA, T., TAMOTSU, K., KITA, Y., SAKAMOTO, A., OWAKI, T., ISHIGAMI, S. & AIKOU, T. 2007. Snail plays a key role in E-cadherin-preserved esophageal squamous cell carcinoma. *Oncol Rep*, 17, 517-23.
- NAZARIAN, R., SHI, H., WANG, Q., KONG, X., KOYA, R. C., LEE, H., CHEN, Z., LEE, M. K., ATTAR, N., SAZEGAR, H., CHODON, T., NELSON, S. F., MCARTHUR, G., SOSMAN, J. A., RIBAS, A. & LO, R. S. 2010b. Melanomas acquire resistance to B-RAF(V600E) inhibition by RTK or N-RAS upregulation. *Nature*, 468, 973-7.
- NAZARIAN, R. M., PRIETO, V. G., ELDER, D. E. & DUNCAN, L. M. 2010a. Melanoma biomarker expression in melanocytic tumor progression: a tissue microarray study. *J Cutan Pathol*, 37 Suppl 1, 41-7.
- NELSON, P. T., BALDWIN, D. A., SCEARCE, L. M., OBERHOLTZER, J. C., TOBIAS, J. W. & MOURELATOS, Z. 2004. Microarray-based, high-throughput gene expression profiling of microRNAs. *Nat Methods*, 1, 155-61.
- NIAKOSARI, F., KAHN, H. J., MCCREADY, D., GHAZARIAN, D., ROTSTEIN, L. E., MARKS, A., KISS, A. & FROM, L. 2008. Lymphatic invasion identified by monoclonal antibody D2-40, younger age, and ulceration: predictors of sentinel lymph node involvement in primary cutaneous melanoma. *Arch Dermatol*, 144, 462-7.
- NIETO, M. A. 2002. The snail superfamily of zinc-finger transcription factors. *Nat Rev Mol Cell Biol*, 3, 155-166.
- NIETO, M. A. 2009. Epithelial-Mesenchymal Transitions in development and disease: old views and new perspectives. *Int J Dev Biol*, 53, 1541-7.

- NIETO, M. A. 2011. The ins and outs of the epithelial to mesenchymal transition in health and disease. *Annu Rev Cell Dev Biol*, 27, 347-76.
- NIETO, M. A., SARGENT, M. G., WILKINSON, D. G. & COOKE, J. 1994. Control of cell behavior during vertebrate development by Slug, a zinc finger gene. *Science*, 264, 835-9.
- NISHIMURA, E. K., JORDAN, S. A., OSHIMA, H., YOSHIDA, H., OSAWA, M., MORIYAMA, M., JACKSON, I. J., BARRANDON, Y., MIYACHI, Y. & NISHIKAWA, S. 2002. Dominant role of the niche in melanocyte stem-cell fate determination. *Nature*, 416, 854-60.
- NISHIMURA, G., MANABE, I., TSUSHIMA, K., FUJII, K., OISHI, Y., IMAI, Y., MAEMURA, K., MIYAGISHI, M., HIGASHI, Y., KONDOH, H. & NAGAI, R. 2006. DeltaEF1 mediates TGF-beta signaling in vascular smooth muscle cell differentiation. *Dev Cell*, 11, 93-104.
- O'ROURKE, M. P. & TAM, P. P. 2002. Twist functions in mouse development. *Int J Dev Biol*, 46, 401-13.
- OBA, J., NAKAHARA, T., ABE, T., HAGIHARA, A., MOROI, Y. & FURUE, M. 2011. Expression of c-Kit, p-ERK and cyclin D1 in malignant melanoma: an immunohistochemical study and analysis of prognostic value. *J Dermatol Sci*, 62, 116-23.
- OHIRA, T., GEMMILL, R. M., FERGUSON, K., KUSY, S., ROCHE, J., BRAMBILLA, E., ZENG, C., BARON, A., BEMIS, L., ERICKSON, P., WILDER, E., RUSTGI, A., KITAJEWSKI, J., GABRIELSON, E., BREMNES, R., FRANKLIN, W. & DRABKIN, H. A. 2003. WNT7a induces E-cadherin in lung cancer cells. *Proc Natl Acad Sci U S A*, 100, 10429-34.
- OLMEDA, D., MONTES, A., MORENO-BUENO, G., FLORES, J. M., PORTILLO, F. & CANO, A. 2008. Snai1 and Snai2 collaborate on tumor growth and metastasis properties of mouse skin carcinoma cell lines. *Oncogene*, 27, 4690-4701.
- OMHOLT, K., PLATZ, A., KANTER, L., RINGBORG, U. & HANSSON, J. 2003. NRAS and BRAF mutations arise early during melanoma pathogenesis and are preserved throughout tumor progression. *Clin Cancer Res*, 9, 6483-8.
- OMHOLT, K., PLATZ, A., RINGBORG, U. & HANSSON, J. 2001. Cytoplasmic and nuclear accumulation of beta-catenin is rarely caused by CTNNB1 exon 3 mutations in cutaneous malignant melanoma. *Int J Cancer*, 92, 839-42.
- ONDER, T. T., GUPTA, P. B., MANI, S. A., YANG, J., LANDER, E. S. & WEINBERG, R. A. 2008. Loss of E-cadherin promotes metastasis via multiple downstream transcriptional pathways. *Cancer Res*, 68, 3645-54.
- ORIMO, A., GUPTA, P. B., SGROI, D. C., ARENZANA-SEISDEDOS, F., DELAUNAY, T., NAEEM, R., CAREY, V. J., RICHARDSON, A. L. & WEINBERG, R. A. 2005. Stromal fibroblasts present in invasive human breast carcinomas promote tumor growth and angiogenesis through elevated SDF-1/CXCL12 secretion. *Cell*, 121, 335-48.

- OZTAS, E., AVCI, M. E., OZCAN, A., SAYAN, A. E., TULCHINSKY, E. & YAGCI, T. 2010. Novel monoclonal antibodies detect Smad-interacting protein 1 (SIP1) in the cytoplasm of human cells from multiple tumor tissue arrays. *Exp Mol Pathol*, 89, 182-9.
- OZTURK, N., ERDAL, E., MUMCUOGLU, M., AKCALI, K. C., YALCIN, O., SENTURK, S., ARSLAN-ERGUL, A., GUR, B., YULUG, I., CETIN-ATALAY, R., YAKICIER, C., YAGCI, T., TEZ, M. & OZTURK, M. 2006. Reprogramming of replicative senescence in hepatocellular carcinoma-derived cells. *Proc Natl Acad Sci U S A*, 103, 2178-83.
- PACKER, L. M., EAST, P., REIS-FILHO, J. S. & MARAIS, R. 2009. Identification of direct transcriptional targets of (V600E)BRAF/MEK signalling in melanoma. *Pigment Cell Melanoma Res*, 22, 785-98.
- PAEZ, D., LABONTE, M. J., BOHANES, P., ZHANG, W., BENHANIM, L., NING, Y., WAKATSUKI, T., LOUPAKIS, F. & LENZ, H. J. 2012. Cancer dormancy: a model of early dissemination and late cancer recurrence. *Clin Cancer Res*, 18, 645-53.
- PALMER, H. G., GONZALEZ-SANCHO, J. M., ESPADA, J., BERCIANO, M. T., PUIG, I., BAULIDA, J., QUINTANILLA, M., CANO, A., DE HERREROS, A. G., LAFARGA, M. & MUNOZ, A. 2001. Vitamin D(3) promotes the differentiation of colon carcinoma cells by the induction of E-cadherin and the inhibition of beta-catenin signaling. *J Cell Biol*, 154, 369-87.
- PAPP, T., PEMSEL, H., ROLLWITZ, I., SCHIPPER, H., WEISS, D. G., SCHIFFMANN, D. & ZIMMERMANN, R. 2003. Mutational analysis of N-ras, p53, CDKN2A (p16(INK4a)), p14(ARF), CDK4, and MC1R genes in human dysplastic melanocytic naevi. *J Med Genet*, 40, E14.
- PAPP, T., PEMSEL, H., ZIMMERMANN, R., BASTROP, R., WEISS, D. G. & SCHIFFMANN, D. 1999. Mutational analysis of the N-ras, p53, p16INK4a, CDK4, and MC1R genes in human congenital melanocytic naevi. *J Med Genet*, 36, 610-4.
- PARAISO, K. H., FEDORENKO, I. V., CANTINI, L. P., MUNKO, A. C., HALL, M., SONDAK, V. K., MESSINA, J. L., FLAHERTY, K. T. & SMALLEY, K. S. 2010. Recovery of phospho-ERK activity allows melanoma cells to escape from BRAF inhibitor therapy. *Br J Cancer*, 102, 1724-30.
- PARK, S. M., GAUR, A. B., LENGUEL, E. & PETER, M. E. 2008a. The miR-200 family determines the epithelial phenotype of cancer cells by targeting the E-cadherin repressors ZEB1 and ZEB2. *Genes & Development*, 22, 894-907.
- PARK, S. H., CHEUNG, L. W., WONG, A. S. & LEUNG, P. C. 2008b. Estrogen regulates Snail and Slug in the down-regulation of E-cadherin and induces metastatic potential of ovarian cancer cells through estrogen receptor alpha. *Mol Endocrinol*, 22, 2085-98.
- PARK, S. M., GAUR, A. B., LENGUEL, E. & PETER, M. E. 2008c. The miR-200 family determines the epithelial phenotype of cancer cells by targeting the E-cadherin repressors ZEB1 and ZEB2. *Genes Dev*, 22, 894-907.

- PATTON, E. E., WIDLUND, H. R., KUTOK, J. L., KOPANI, K. R., AMATRUDA, J. F., MURPHEY, R. D., BERGHMANS, S., MAYHALL, E. A., TRAVER, D., FLETCHER, C. D., ASTER, J. C., GRANTER, S. R., LOOK, A. T., LEE, C., FISHER, D. E. & ZON, L. I. 2005. BRAF mutations are sufficient to promote nevi formation and cooperate with p53 in the genesis of melanoma. *Curr Biol*, 15, 249-54.
- PEINADO, H., OLMEDA, D. & CANO, A. 2007. Snail, Zeb and bHLH factors in tumour progression: an alliance against the epithelial phenotype? *Nat Rev Cancer*, 7, 415-28.
- PEINADO, H., PORTILLO, F. & CANO, A. 2004. Transcriptional regulation of cadherins during development and carcinogenesis. *Int J Dev Biol*, 48, 365-75.
- PERSON, A. D., KLEWER, S. E. & RUNYAN, R. B. 2005. Cell biology of cardiac cushion development. *Int Rev Cytol*, 243, 287-335.
- PHAN, A., TOUZET, S., DALLE, S., RONGER-SAVLE, S., BALME, B. & THOMAS, L. 2006. Acral lentiginous melanoma: a clinicoprognostic study of 126 cases. *Br J Dermatol*, 155, 561-9.
- PHILIPPIDOU, D., SCHMITT, M., MOSER, D., MARGUE, C., NAZAROV, P. V., MULLER, A., VALLAR, L., NASHAN, D., BEHRMANN, I. & KREIS, S. 2010. Signatures of microRNAs and selected microRNA target genes in human melanoma. *Cancer Res*, 70, 4163-73.
- PIKE, J. W., MEYER, M. B., WATANUKI, M., KIM, S., ZELLA, L. A., FRETZ, J. A., YAMAZAKI, M. & SHEVDE, N. K. 2007. Perspectives on mechanisms of gene regulation by 1,25-dihydroxyvitamin D3 and its receptor. *J Steroid Biochem Mol Biol*, 103, 389-95.
- PLA, P., MOORE, R., MORALI, O. G., GRILLE, S., MARTINOZZI, S., DELMAS, V. & LARUE, L. 2001. Cadherins in neural crest cell development and transformation. *J Cell Physiol*, 189, 121-32.
- PLATZ, A., EGYHAZI, S., RINGBORG, U. & HANSSON, J. 2008. Human cutaneous melanoma; a review of NRAS and BRAF mutation frequencies in relation to histogenetic subclass and body site. *Mol Oncol*, 1, 395-405.
- PLONKA, P. M., PASSERON, T., BRENNER, M., TOBIN, D. J., SHIBAHARA, S., THOMAS, A., SLOMINSKI, A., KADEKARO, A. L., HERSHKOVITZ, D., PETERS, E., NORDLUND, J. J., ABDEL-MALEK, Z., TAKEDA, K., PAUS, R., ORTONNE, J. P., HEARING, V. J. & SCHALLREUTER, K. U. 2009. What are melanocytes really doing all day long...? *Exp Dermatol*, 18, 799-819.
- PLUM, L. A. & DELUCA, H. F. 2010. Vitamin D, disease and therapeutic opportunities. *Nat Rev Drug Discov*, 9, 941-55.
- POLLOCK, P. M., HARPER, U. L., HANSEN, K. S., YUDT, L. M., STARK, M., ROBBINS, C. M., MOSES, T. Y., HOSTETTER, G., WAGNER, U., KAKAREKA, J., SALEM, G., POHIDA, T., HEENAN, P., DURAY, P., KALLIONIEMI, O., HAYWARD, N. K., TRENT, J. M. & MELTZER, P. S. 2003. High frequency of BRAF mutations in nevi. *Nat Genet*, 33, 19-20.

- POLLOCK, P. M., WELCH, J. & HAYWARD, N. K. 2001. Evidence for three tumor suppressor loci on chromosome 9p involved in melanoma development. *Cancer Res*, 61, 1154-61.
- POLYAK, K. & WEINBERG, R. A. 2009. Transitions between epithelial and mesenchymal states: acquisition of malignant and stem cell traits. *Nat Rev Cancer*, 9, 265-73.
- POPULO, H., SOARES, P., FAUSTINO, A., ROCHA, A. S., SILVA, P., AZEVEDO, F. & LOPES, J. M. 2011. mTOR pathway activation in cutaneous melanoma is associated with poorer prognosis characteristics. *Pigment Cell Melanoma Res*, 24, 254-7.
- PORRAS, B. H. & COCKERELL, C. J. 1997. Cutaneous malignant melanoma: classification and clinical diagnosis. *Semin Cutan Med Surg*, 16, 88-96.
- POSTIGO, A. A., DEPP, J. L., TAYLOR, J. J. & KROLL, K. L. 2003. Regulation of Smad signaling through a differential recruitment of coactivators and corepressors by ZEB proteins. *EMBO J*, 22, 2453-62.
- POWLEDGE, T. M. 2004. The polymerase chain reaction. *Adv Physiol Educ*, 28, 44-50.
- POYNTER, J. N., ELDER, J. T., FULLEN, D. R., NAIR, R. P., SOENGAS, M. S., JOHNSON, T. M., REDMAN, B., THOMAS, N. E. & GRUBER, S. B. 2006. BRAF and NRAS mutations in melanoma and melanocytic nevi. *Melanoma Res*, 16, 267-73.
- PRATILAS, C. A., TAYLOR, B. S., YE, Q., VIALE, A., SANDER, C., SOLIT, D. B. & ROSEN, N. 2009. (V600E)BRAF is associated with disabled feedback inhibition of RAF-MEK signaling and elevated transcriptional output of the pathway. *Proc Natl Acad Sci U S A*, 106, 4519-24.
- PRUFER, K. & BARSONY, J. 2002. Retinoid X receptor dominates the nuclear import and export of the unliganded vitamin D receptor. *Mol Endocrinol*, 16, 1738-51.
- QIN, Q., XU, Y., HE, T., QIN, C. & XU, J. 2012. Normal and disease-related biological functions of Twist1 and underlying molecular mechanisms. *Cell Res*, 22, 90-106.
- RAGNARSSON-OLDING, B. K., KARSBERG, S., PLATZ, A. & RINGBORG, U. K. 2002. Mutations in the TP53 gene in human malignant melanomas derived from sun-exposed skin and unexposed mucosal membranes. *Melanoma Res*, 12, 453-63.
- RAJEWSKY, N. 2006. microRNA target predictions in animals. *Nat Genet*, 38 Suppl, S8-13.
- RAKOSY, Z., VIZKELETI, L., ECSEDI, S., BEGANY, A., EMRI, G., ADANY, R. & BALAZS, M. 2008. Characterization of 9p21 copy number alterations in human melanoma by fluorescence in situ hybridization. *Cancer Genet Cytogenet*, 182, 116-21.
- RAMAGOPALAN, S. V., HEGER, A., BERLANGA, A. J., MAUGERI, N. J., LINCOLN, M. R., BURRELL, A., HANDUNNETHI, L., HANDEL, A. E., DISANTO, G., ORTON, S. M., WATSON, C. T., MORAHAN, J.

- M., GIOVANNONI, G., PONTING, C. P., EBERS, G. C. & KNIGHT, J. C. 2010. A ChIP-seq defined genome-wide map of vitamin D receptor binding: associations with disease and evolution. *Genome Res*, 20, 1352-60.
- RAMOS-NINO, M. E., TIMBLIN, C. R. & MOSSMAN, B. T. 2002. Mesothelial cell transformation requires increased AP-1 binding activity and ERK-dependent Fra-1 expression. *Cancer Res*, 62, 6065-9.
- RANDHAWA, M., HUFF, T., VALENCIA, J. C., YOUNOSSI, Z., CHANDHOKE, V., HEARING, V. J. & BARANOVA, A. 2009. Evidence for the ectopic synthesis of melanin in human adipose tissue. *FASEB J*, 23, 835-43.
- RANSON, M., POSEN, S. & MASON, R. S. 1988. Human melanocytes as a target tissue for hormones: in vitro studies with 1 alpha-25, dihydroxyvitamin D3, alpha-melanocyte stimulating hormone, and beta-estradiol. *J Invest Dermatol*, 91, 593-8.
- REICHRATH, J., RECH, M., MOEINI, M., MEESE, E., TILGEN, W. & SEIFERT, M. 2007. In vitro comparison of the vitamin D endocrine system in 1,25(OH)2D3-responsive and -resistant melanoma cells. *Cancer Biol Ther*, 6, 48-55.
- REIFENBERGER, J., KNOBBE, C. B., WOLTER, M., BLASCHKE, B., SCHULTE, K. W., PIETSCH, T., RUZICKA, T. & REIFENBERGER, G. 2002. Molecular genetic analysis of malignant melanomas for aberrations of the WNT signaling pathway genes CTNNB1, APC, ICAT and BTRC. *Int J Cancer*, 100, 549-56.
- REINHART, B. J., SLACK, F. J., BASSON, M., PASQUINELLI, A. E., BETTINGER, J. C., ROUGVIE, A. E., HORVITZ, H. R. & RUVKUN, G. 2000. The 21-nucleotide let-7 RNA regulates developmental timing in *Caenorhabditis elegans*. *Nature*, 403, 901-6.
- REMACLE, J. E., KRAFT, H., LERCHNER, W., WUYTENS, G., COLLART, C., VERSCHUEREN, K., SMITH, J. C. & HUYLEBROECK, D. 1999. New mode of DNA binding of multi-zinc finger transcription factors: deltaEF1 family members bind with two hands to two target sites. *EMBO J*, 18, 5073-84.
- RHIM, A. D., MIREK, E. T., AIELLO, N. M., MAITRA, A., BAILEY, J. M., MCALLISTER, F., REICHERT, M., BEATTY, G. L., RUSTGI, A. K., VONDERHEIDE, R. H., LEACH, S. D. & STANGER, B. Z. 2012. EMT and dissemination precede pancreatic tumor formation. *Cell*, 148, 349-61.
- RIGEL, D. S., ROBINSON, J. K., ROSS, M. I., FRIEDMAN, R., COCKERELL, C. J., LIM, H. & STOCKFLETH, E. 2011. *Cancer of the skin*, Elsevier Saunders.
- RODRIGUEZ, M., ALADOWICZ, E., LANFRANCONE, L. & GODING, C. R. 2008. Tbx3 represses E-cadherin expression and enhances melanoma invasiveness. *Cancer Res*, 68, 7872-81.
- ROSIVATZ, E., BECKER, I., SPECHT, K., FRICKE, E., LUBER, B., BUSCH, R., HOFER, H. & BECKER, K. F. 2002. Differential expression of the epithelial-mesenchymal transition regulators snail, SIP1, and twist in gastric cancer. *Am J Pathol*, 161, 1881-91.

- ROY, H. K., SMYRK, T. C., KOETSIER, J., VICTOR, T. A. & WALI, R. K. 2005. The transcriptional repressor SNAIL is overexpressed in human colon cancer. *Dig Dis Sci*, 50, 42-6.
- RUBINFELD, B., ROBBINS, P., EL-GAMIL, M., ALBERT, I., PORFIRI, E. & POLAKIS, P. 1997. Stabilization of beta-catenin by genetic defects in melanoma cell lines. *Science*, 275, 1790-2.
- RYU, B., KIM, D. S., DELUCA, A. M. & ALANI, R. M. 2007. Comprehensive expression profiling of tumor cell lines identifies molecular signatures of melanoma progression. *PLoS One*, 2, e594.
- S RAIMONDI, F SERA, SARA, G., SIMONA, I., SAVERIO, C., PATRICK, M. & MARIA CONCETTA, F. 2008. MC1R variants, melanoma and red hair color phenotype: A meta-analysis. *International Journal of Cancer*, 122, 2753-2760.
- SAITO, H., YASUMOTO, K., TAKEDA, K., TAKAHASHI, K., YAMAMOTO, H. & SHIBAHARA, S. 2003. Microphthalmia-associated transcription factor in the Wnt signaling pathway. *Pigment Cell Res*, 16, 261-5.
- SAITO, T., ODA, Y., KAWAGUCHI, K., SUGIMACHI, K., YAMAMOTO, H., TATEISHI, N., TANAKA, K., MATSUDA, S., IWAMOTO, Y., LADANYI, M. & TSUNEOYOSHI, M. 2004. E-cadherin mutation and Snail overexpression as alternative mechanisms of E-cadherin inactivation in synovial sarcoma. *Oncogene*, 23, 8629-38.
- SALDANHA, G., PURNELL, D., FLETCHER, A., POTTER, L., GILLIES, A. & PRINGLE, J. H. 2004. High BRAF mutation frequency does not characterize all melanocytic tumor types. *Int J Cancer*, 111, 705-10.
- SANCHEZ-MARTIN, M., RODRIGUEZ-GARCIA, A., PEREZ-LOSADA, J., SAGRERA, A., READ, A. P. & SANCHEZ-GARCIA, I. 2002. SLUG (SNAI2) deletions in patients with Waardenburg disease. *Hum Mol Genet*, 11, 3231-6.
- SANCHEZ-TILLO, E., SILES, L., DE BARRIOS, O., CUATRECASAS, M., VAQUERO, E. C., CASTELLS, A. & POSTIGO, A. 2011. Expanding roles of ZEB factors in tumorigenesis and tumor progression. *Am J Cancer Res*, 1, 897-912.
- SANZ-MORENO, V., GADEA, G., AHN, J., PATERSON, H., MARRA, P., PINNER, S., SAHAI, E. & MARSHALL, C. J. 2008. Rac activation and inactivation control plasticity of tumor cell movement. *Cell*, 135, 510-23.
- SAUKA-SPENGLER, T. & BRONNER-FRASER, M. 2008. A gene regulatory network orchestrates neural crest formation. *Nat Rev Mol Cell Biol*, 9, 557-68.
- SAUTER, E. R., YEO, U. C., VON STEMM, A., ZHU, W., LITWIN, S., TICHANSKY, D. S., PISTRITTO, G., NESBIT, M., PINKEL, D., HERLYN, M. & BASTIAN, B. C. 2002. Cyclin D1 is a candidate oncogene in cutaneous melanoma. *Cancer Res*, 62, 3200-6.

- SAVAGNER, P., KUSEWITT, D. F., CARVER, E. A., MAGNINO, F., CHOI, C., GRIDLEY, T. & HUDSON, L. G. 2005. Developmental transcription factor slug is required for effective re-epithelialization by adult keratinocytes. *J Cell Physiol*, 202, 858-66.
- SAYAN, A. E., GRIFFITHS, T. R., PAL, R., BROWNE, G. J., RUDDICK, A., YAGCI, T., EDWARDS, R., MAYER, N. J., QAZI, H., GOYAL, S., FERNANDEZ, S., STRAATMAN, K., JONES, G. D., BOWMAN, K. J., COLQUHOUN, A., MELLON, J. K., KRIAJEVSKA, M. & TULCHINSKY, E. 2009. SIP1 protein protects cells from DNA damage-induced apoptosis and has independent prognostic value in bladder cancer. *Proc Natl Acad Sci U S A*, 106, 14884-9.
- SAYAN, A. E., STANFORD, R., VICKERY, R., GRIGORENKO, E., DIESCH, J., KULBICKI, K., EDWARDS, R., PAL, R., GREAVES, P., JARIEL-ENCONTRE, I., PIECHACZYK, M., KRIAJEVSKA, M., MELLON, J. K., DHILLON, A. S. & TULCHINSKY, E. 2012. Fra-1 controls motility of bladder cancer cells via transcriptional upregulation of the receptor tyrosine kinase AXL. *Oncogene*, 31, 1493-503.
- SCHMALHOFER, O., BRABLETZ, S. & BRABLETZ, T. 2009. E-cadherin, beta-catenin, and ZEB1 in malignant progression of cancer. *Cancer Metastasis Rev*, 28, 151-66.
- SEIJI, M., SHIMAO, K., BIRBECK, M. S. & FITZPATRICK, T. B. 1963. Subcellular localization of melanin biosynthesis. *Ann N Y Acad Sci*, 100, 497-533.
- SEKULIC, A., HALUSKA, P., JR., MILLER, A. J., GENEVRIERA DE LAMO, J., EJADI, S., PULIDO, J. S., SALOMAO, D. R., THORLAND, E. C., VILE, R. G., SWANSON, D. L., POCKAJ, B. A., LAMAN, S. D., PITTELKOW, M. R., MARKOVIC, S. N. & MELANOMA STUDY GROUP OF MAYO CLINIC CANCER, C. 2008. Malignant melanoma in the 21st century: the emerging molecular landscape. *Mayo Clin Proc*, 83, 825-46.
- SERRANO, M., LIN, A. W., MCCURRACH, M. E., BEACH, D. & LOWE, S. W. 1997. Oncogenic ras provokes premature cell senescence associated with accumulation of p53 and p16INK4a. *Cell*, 88, 593-602.
- SHAH, S. P., MORIN, R. D., KHATTRA, J., PRENTICE, L., PUGH, T., BURLEIGH, A., DELANEY, A., GELMON, K., GULIANY, R., SENZ, J., STEIDL, C., HOLT, R. A., JONES, S., SUN, M., LEUNG, G., MOORE, R., SEVERSON, T., TAYLOR, G. A., TESCHENDORFF, A. E., TSE, K., TURASHVILI, G., VARHOL, R., WARREN, R. L., WATSON, P., ZHAO, Y., CALDAS, C., HUNTSMAN, D., HIRST, M., MARRA, M. A. & APARICIO, S. 2009. Mutational evolution in a lobular breast tumour profiled at single nucleotide resolution. *Nature*, 461, 809-13.
- SHARMA, A., YEOW, W. S., ERTEL, A., COLEMAN, I., CLEGG, N., THANGAVEL, C., MORRISSEY, C., ZHANG, X., COMSTOCK, C. E., WITKIEWICZ, A. K., GOMELLA, L., KNUDSEN, E. S., NELSON, P. S. & KNUDSEN, K. E. 2010. The retinoblastoma tumor suppressor controls androgen signaling and human prostate cancer progression. *J Clin Invest*, 120, 4478-92.
- SHI, Y., SAWADA, J., SUI, G., AFFAR EL, B., WHETSTINE, J. R., LAN, F., OGAWA, H., LUKE, M. P., NAKATANI, Y. & SHI, Y. 2003. Coordinated histone modifications mediated by a CtBP co-repressor complex. *Nature*, 422, 735-8.

- SHIN, S. & BLENIS, J. 2010b. ERK2/Fra1/ZEB pathway induces epithelial-to-mesenchymal transition. *Cell Cycle*, 9, 2483-4.
- SHIN, S., DIMITRI, C. A., YOON, S. O., DOWDLE, W. & BLENIS, J. 2010a. ERK2 but not ERK1 induces epithelial-to-mesenchymal transformation via DEF motif-dependent signaling events. *Mol Cell*, 38, 114-27.
- SHIOIRI, M., SHIDA, T., KODA, K., ODA, K., SEIKE, K., NISHIMURA, M., TAKANO, S. & MIYAZAKI, M. 2006. Slug expression is an independent prognostic parameter for poor survival in colorectal carcinoma patients. *Br J Cancer*, 94, 1816-22.
- SHIRAKIHARA, T., HORIGUCHI, K., MIYAZAWA, K., EHATA, S., SHIBATA, T., MORITA, I., MIYAZONO, K. & SAITOH, M. 2011. TGF-beta regulates isoform switching of FGF receptors and epithelial-mesenchymal transition. *EMBO J*, 30, 783-95.
- SHIRLEY, S. H., GREENE, V. R., DUNCAN, L. M., TORRES CABALA, C. A., GRIMM, E. A. & KUSEWITT, D. F. 2012. Slug expression during melanoma progression. *Am J Pathol*, 180, 2479-89.
- Si, S. P., TSOU, H. C., LEE, X. & PEACOCKE, M. 1993. Cultured Human Melanocytes Express the Intermediate Filament Vimentin. *J Invest Dermatol*, 101, 383-86.
- SICINSKI, P., DONAHER, J. L., PARKER, S. B., LI, T., FAZELI, A., GARDNER, H., HASLAM, S. Z., BRONSON, R. T., ELLEDGE, S. J. & WEINBERG, R. A. 1995. Cyclin D1 provides a link between development and oncogenesis in the retina and breast. *Cell*, 82, 621-30.
- SINGH, M., SPOELSTRA, N. S., JEAN, A., HOWE, E., TORKKO, K. C., CLARK, H. R., DARLING, D. S., SHROYER, K. R., HORWITZ, K. B., BROADDUS, R. R. & RICHER, J. K. 2008. ZEB1 expression in type I vs type II endometrial cancers: a marker of aggressive disease. *Mod Pathol*, 21, 912-23.
- SINI, M. C., MANCA, A., COSSU, A., BUDRONI, M., BOTTI, G., ASCIERTO, P. A., CREMONA, F., MUGGIANO, A., D'ATRI, S., CASULA, M., BALDINU, P., PALOMBA, G., LISSIA, A., TANDA, F. & PALMIERI, G. 2008. Molecular alterations at chromosome 9p21 in melanocytic naevi and melanoma. *Br J Dermatol*, 158, 243-50.
- SIVERTSEN, S., HADAR, R., ELLOUL, S., VINTMAN, L., BEDROSSIAN, C., REICH, R. & DAVIDSON, B. 2006. Expression of Snail, Slug and Sip1 in malignant mesothelioma effusions is associated with matrix metalloproteinase, but not with cadherin expression. *Lung Cancer*, 54, 309-17.
- SLIPICEVIC, A., HOLM, R., NGUYEN, M. T., BOHLER, P. J., DAVIDSON, B. & FLORENES, V. A. 2005. Expression of activated Akt and PTEN in malignant melanomas: relationship with clinical outcome. *Am J Clin Pathol*, 124, 528-36.
- SMALLEY, K. S., HAASS, N. K., BRAFFORD, P. A., LIONI, M., FLAHERTY, K. T. & HERLYN, M. 2006. Multiple signaling pathways must be targeted to overcome drug resistance in cell lines derived from melanoma metastases. *Mol Cancer Ther*, 5, 1136-44.

- SOO, K., O'ROURKE, M. P., KHOO, P. L., STEINER, K. A., WONG, N., BEHRINGER, R. R. & TAM, P. P. 2002. Twist function is required for the morphogenesis of the cephalic neural tube and the differentiation of the cranial neural crest cells in the mouse embryo. *Dev Biol*, 247, 251-70.
- SOSIC, D., RICHARDSON, J. A., YU, K., ORNITZ, D. M. & OLSON, E. N. 2003. Twist regulates cytokine gene expression through a negative feedback loop that represses NF-kappaB activity. *Cell*, 112, 169-80.
- SPADERNA, S., SCHMALHOFER, O., HLUBEK, F., BERX, G., EGER, A., MERKEL, S., JUNG, A., KIRCHNER, T. & BRABLETZ, T. 2006. A transient, EMT-linked loss of basement membranes indicates metastasis and poor survival in colorectal cancer. *Gastroenterology*, 131, 830-40.
- SPADERNA, S., SCHMALHOFER, O., WAHLBUHL, M., DIMMLER, A., BAUER, K., SULTAN, A., HLUBEK, F., JUNG, A., STRAND, D., EGER, A., KIRCHNER, T., BEHRENS, J. & BRABLETZ, T. 2008. The transcriptional repressor ZEB1 promotes metastasis and loss of cell polarity in cancer. *Cancer Res*, 68, 537-44.
- SPOELSTRA, N. S., MANNING, N. G., HIGASHI, Y., DARLING, D., SINGH, M., SHROYER, K. R., BROADDUS, R. R., HORWITZ, K. B. & RICHER, J. K. 2006. The transcription factor ZEB1 is aberrantly expressed in aggressive uterine cancers. *Cancer Res*, 66, 3893-902.
- STAHL, J. M., SHARMA, A., CHEUNG, M., ZIMMERMAN, M., CHENG, J. Q., BOSENBERG, M. W., KESTER, M., SANDIRASEGARANE, L. & ROBERTSON, G. P. 2004. Deregulated Akt3 activity promotes development of malignant melanoma. *Cancer Res*, 64, 7002-10.
- STAHL, S., BAR-MEIR, E., FRIEDMAN, E., REGEV, E., ORENSTEIN, A. & WINKLER, E. 2004a. Genetics in melanoma. *Isr Med Assoc J*, 6, 774-7.
- STARK, M. S., TYAGI, S., NANCARROW, D. J., BOYLE, G. M., COOK, A. L., WHITEMAN, D. C., PARSONS, P. G., SCHMIDT, C., STURM, R. A. & HAYWARD, N. K. 2010. Characterization of the Melanoma miRNAome by Deep Sequencing. *PLoS One*, 5, e9685.
- STEFANO, D., BATISTATOU, A., ZIOGA, A., ARKOUMANI, E., PAPACHRISTOU, D. J. & AGNANTIS, N. J. 2004. Immunohistochemical expression of vascular endothelial growth factor (VEGF) and C-KIT in cutaneous melanocytic lesions. *Int J Surg Pathol*, 12, 133-8.
- STEVENTON, B., CARMONA-FONTAINE, C. & MAYOR, R. 2005. Genetic network during neural crest induction: from cell specification to cell survival. *Semin Cell Dev Biol*, 16, 647-54.
- STINSON, S., LACKNER, M. R., ADAI, A. T., YU, N., KIM, H. J., O'BRIEN, C., SPOERKE, J., JHUNJHUNWALA, S., BOYD, Z., JANUARIO, T., NEWMAN, R. J., YUE, P., BOURGON, R., MODRUSAN, Z., STERN, H. M., WARMING, S., DE SAUVAGE, F. J., AMLER, L., YEH, R. F. & DORNAN, D. 2011. TRPS1 targeting by miR-221/222 promotes the epithelial-to-mesenchymal transition in breast cancer. *Sci Signal*, 4, ra41.

- STORR, S. J., SAFUAN, S., MITRA, A., ELLIOTT, F., WALKER, C., VASKO, M. J., HO, B., COOK, M., MOHAMMED, R. A., PATEL, P. M., ELLIS, I. O., NEWTON-BISHOP, J. A. & MARTIN, S. G. 2012. Objective assessment of blood and lymphatic vessel invasion and association with macrophage infiltration in cutaneous melanoma. *Mod Pathol*, 25, 493-504.
- SU, F., BRADLEY, W. D., WANG, Q., YANG, H., XU, L., HIGGINS, B., KOLINSKY, K., PACKMAN, K., KIM, M. J., TRUNZER, K., LEE, R. J., SCHOSTACK, K., CARTER, J., ALBERT, T., GERMER, S., ROSINSKI, J., MARTIN, M., SIMCOX, M. E., LESTINI, B., HEIMBROOK, D. & BOLLAG, G. 2012. Resistance to selective BRAF inhibition can be mediated by modest upstream pathway activation. *Cancer Res*, 72, 969-78.
- SULEM, P., GUDBJARTSSON, D. F., STACEY, S. N., HELGASON, A., RAFNAR, T., JAKOBSDOTTIR, M., STEINBERG, S., GUDJONSSON, S. A., PALSSON, A., THORLEIFSSON, G., PALSSON, S., SIGURGEIRSSON, B., THORISDOTTIR, K., RAGNARSSON, R., BENEDIKTSDOTTIR, K. R., ABEN, K. K., VERMEULEN, S. H., GOLDSTEIN, A. M., TUCKER, M. A., KIEMENEY, L. A., OLAFSSON, J. H., GULCHER, J., KONG, A., THORSTEINSDOTTIR, U. & STEFANSSON, K. 2008. Two newly identified genetic determinants of pigmentation in Europeans. *Nat Genet*, 40, 835-7.
- SZETO, D. P., GRIFFIN, K. J. & KIMELMAN, D. 2002. HrT is required for cardiovascular development in zebrafish. *Development*, 129, 5093-101.
- TACHIBANA, M. 2001. Cochlear melanocytes and MITF signaling. *J Invest Dermatol Symp Proc*, 6, 95-8.
- TAKAGI, T., MORIBE, H., KONDOH, H. & HIGASHI, Y. 1998. DeltaEF1, a zinc finger and homeodomain transcription factor, is required for skeleton patterning in multiple lineages. *Development*, 125, 21-31.
- TAKATA, M., GOTO, Y., ICHII, N., YAMAURA, M., MURATA, H., KOGA, H., FUJIMOTO, A. & SAIDA, T. 2005. Constitutive activation of the mitogen-activated protein kinase signaling pathway in acral melanomas. *J Invest Dermatol*, 125, 318-22.
- TAKEDA, K., TAKAHASHI, N. H. & SHIBAHARA, S. 2007. Neuroendocrine functions of melanocytes: beyond the skin-deep melanin maker. *Tohoku J Exp Med*, 211, 201-21.
- TANAMI, H., IMOTO, I., HIRASAWA, A., YUKI, Y., SONODA, I., INOUE, J., YASUI, K., MISAWA-FURIHATA, A., KAWAKAMI, Y. & INAZAWA, J. 2004. Involvement of overexpressed wild-type BRAF in the growth of malignant melanoma cell lines. *Oncogene*, 23, 8796-804.
- TANEYHILL, L. A. 2008. To adhere or not to adhere: the role of Cadherins in neural crest development. *Cell Adh Migr*, 2, 223-30.
- TAUBE, J. H., HERSCHKOWITZ, J. I., KOMUROV, K., ZHOU, A. Y., GUPTA, S., YANG, J., HARTWELL, K., ONDER, T. T., GUPTA, P. B., EVANS, K. W., HOLLIER, B. G., RAM, P. T., LANDER, E. S., ROSEN, J. M., WEINBERG, R. A. & MANI, S. A. 2010. Core epithelial-to-mesenchymal transition interactome gene-expression signature is associated with claudin-low and metaplastic breast cancer subtypes. *Proc Natl Acad Sci U S A*, 107, 15449-54.

- THEVENEAU, E. & MAYOR, R. 2012. Neural crest delamination and migration: from epithelium-to-mesenchyme transition to collective cell migration. *Dev Biol*, 366, 34-54.
- THIEDE, C., STEUDEL, C., MOHR, B., SCHAICH, M., SCHAKEL, U., PLATZBECKER, U., WERMKE, M., BORNHAUSER, M., RITTER, M., NEUBAUER, A., EHNINGER, G. & ILLMER, T. 2002. Analysis of FLT3-activating mutations in 979 patients with acute myelogenous leukemia: association with FAB subtypes and identification of subgroups with poor prognosis. *Blood*, 99, 4326-35.
- THIERY, J. P. 2002. Epithelial-mesenchymal transitions in tumour progression. *Nat Rev Cancer*, 2, 442-454.
- THIERY, J. P. 2003. Epithelial-mesenchymal transitions in development and pathologies. *Curr Opin Cell Biol*, 15, 740-6.
- THIERY, J. P., ACLOQUE, H., HUANG, R. Y. & NIETO, M. A. 2009. Epithelial-mesenchymal transitions in development and disease. *Cell*, 139, 871-90.
- THIERY, J. P. & SLEEMAN, J. P. 2006. Complex networks orchestrate epithelial-mesenchymal transitions. *Nat Rev Mol Cell Biol*, 7, 131-42.
- THILL, M., FISCHER, D., KELLING, K., HOELLEN, F., DITTMER, C., HORNEMANN, A., SALEHIN, D., DIEDRICH, K., FRIEDRICH, M. & BECKER, S. 2010. Expression of vitamin D receptor (VDR), cyclooxygenase-2 (COX-2) and 15-hydroxyprostaglandin dehydrogenase (15-PGDH) in benign and malignant ovarian tissue and 25-hydroxycholecalciferol (25(OH)D3) and prostaglandin E2 (PGE2) serum level in ovarian cancer patients. *J Steroid Biochem Mol Biol*, 121, 387-90.
- THOMAS, A. J. & ERICKSON, C. A. 2008. The making of a melanocyte: the specification of melanoblasts from the neural crest. *Pigment Cell Melanoma Res*, 21, 598-610.
- THOMAS, A. J. & ERICKSON, C. A. 2009. FOXD3 regulates the lineage switch between neural crest-derived glial cells and pigment cells by repressing MITF through a non-canonical mechanism. *Development*, 136, 1849-58.
- TOPCZEWSKA, J. M., POSTOVIT, L. M., MARGARYAN, N. V., SAM, A., HESS, A. R., WHEATON, W. W., NICKOLOFF, B. J., TOPCZEWSKI, J. & HENDRIX, M. J. 2006. Embryonic and tumorigenic pathways converge via Nodal signaling: role in melanoma aggressiveness. *Nat Med*, 12, 925-32.
- TORRES, L., RIBEIRO, F. R., PANDIS, N., ANDERSEN, J. A., HEIM, S. & TEIXEIRA, M. R. 2007. Intratumor genomic heterogeneity in breast cancer with clonal divergence between primary carcinomas and lymph node metastases. *Breast Cancer Res Treat*, 102, 143-55.
- TOWBIN, H., STAHELIN, T. & GORDON, J. 1979. Electrophoretic transfer of proteins from polyacrylamide gels to nitrocellulose sheets: procedure and some applications. *Proc Natl Acad Sci U S A*, 76, 4350-4.

- TRAN, D. D., CORSA, C. A., BISWAS, H., AFT, R. L. & LONGMORE, G. D. 2011. Temporal and spatial cooperation of Snail1 and Twist1 during epithelial-mesenchymal transition predicts for human breast cancer recurrence. *Mol Cancer Res*, 9, 1644-57.
- TRIBULO, C., AYBAR, M. J., SANCHEZ, S. S. & MAYOR, R. 2004. A balance between the anti-apoptotic activity of Slug and the apoptotic activity of msx1 is required for the proper development of the neural crest. *Dev Biol*, 275, 325-42.
- TRIPATHI, M. K., MISRA, S., KHEDKAR, S. V., HAMILTON, N., IRVIN-WILSON, C., SHARAN, C., SEALY, L. & CHAUDHURI, G. 2005. Regulation of BRCA2 gene expression by the SLUG repressor protein in human breast cells. *J Biol Chem*, 280, 17163-71.
- TRYNDYAK, V. P., BELAND, F. A. & POGRIBNY, I. P. 2010. E-cadherin transcriptional down-regulation by epigenetic and microRNA-200 family alterations is related to mesenchymal and drug-resistant phenotypes in human breast cancer cells. *Int J Cancer*, 126, 2575-83.
- TSAO, H., MIHM, M. C., JR. & SHEEHAN, C. 2003. PTEN expression in normal skin, acquired melanocytic nevi, and cutaneous melanoma. *J Am Acad Dermatol*, 49, 865-72.
- TULCHINSKY, E. 2000. Fos family members: regulation, structure and role in oncogenic transformation. *Histology and Histopathology*, 15, 921-8.
- TURNER, F. E., BROAD, S., KHANIM, F. L., JEANES, A., TALMA, S., HUGHES, S., TSELEPIS, C. & HOTCHIN, N. A. 2006. Slug regulates integrin expression and cell proliferation in human epidermal keratinocytes. *J Biol Chem*, 281, 21321-31.
- UCHIKADO, Y., NATSUGOE, S., OKUMURA, H., SETOYAMA, T., MATSUMOTO, M., ISHIGAMI, S. & AIKOU, T. 2005. Slug Expression in the E-cadherin preserved tumors is related to prognosis in patients with esophageal squamous cell carcinoma. *Clin Cancer Res*, 11, 1174-80.
- UGUREL, S., HOUBEN, R., SCHRAMA, D., VOIGT, H., ZAPATKA, M., SCHADENDORF, D., BROCKER, E. B. & BECKER, J. C. 2007b. Microphthalmia-associated transcription factor gene amplification in metastatic melanoma is a prognostic marker for patient survival, but not a predictive marker for chemosensitivity and chemotherapy response. *Clin Cancer Res*, 13, 6344-50.
- UGUREL, S., THIRUMARAN, R. K., BLOETHNER, S., GAST, A., SUCKER, A., MUELLER-BERGHHAUS, J., RITTGEN, W., HEMMINKI, K., BECKER, J. C., KUMAR, R. & SCHADENDORF, D. 2007a. B-RAF and N-RAS mutations are preserved during short time in vitro propagation and differentially impact prognosis. *PLoS One*, 2, e236.
- VAN DE PUTTE, T., MARUHASHI, M., FRANCIS, A., NELLES, L., KONDOH, H., HUYLEBROECK, D. & HIGASHI, Y. 2003. Mice Lacking Zfhx1b, the Gene That Codes for Smad-Interacting Protein-1, Reveal a Role for Multiple Neural Crest Cell Defects in the Etiology of Hirschsprung Disease Mental Retardation Syndrome. *American journal of human genetics*, 72, 465-470.

- VAN GRUNSVEN, L. A., MICHIELS, C., VAN DE PUTTE, T., NELLES, L., WUYTENS, G., VERSCHUEREN, K. & HUYLEBROECK, D. 2003. Interaction between Smad-interacting protein-1 and the corepressor C-terminal binding protein is dispensable for transcriptional repression of E-cadherin. *J Biol Chem*, 278, 26135-45.
- VAN GRUNSVEN, L. A., PAPIN, C., AVALOSSE, B., OPDECAMP, K., HUYLEBROECK, D., SMITH, J. C. & BELLEFROID, E. J. 2000. XSIP1, a *Xenopus* zinc finger/homeodomain encoding gene highly expressed during early neural development. *Mech Dev*, 94, 189-93.
- VANDESOMPELE, J., DE PRETER, K., PATTYN, F., POPPE, B., VAN ROY, N., DE PAEPE, A. & SPELEMAN, F. 2002. Accurate normalization of real-time quantitative RT-PCR data by geometric averaging of multiple internal control genes. *Genome Biol*, 3, RESEARCH0034.
- VANDEWALLE, C., VAN ROY, F. & BERX, G. 2009. The role of the ZEB family of transcription factors in development and disease. *Cell Mol Life Sci*, 66, 773-87.
- VEGA, S., MORALES, A. V., OCANA, O. H., VALDES, F., FABREGAT, I. & NIETO, M. A. 2004. Snail blocks the cell cycle and confers resistance to cell death. *Genes Dev*, 18, 1131-43.
- VERGARA, D., VALENTE, C. M., TINELLI, A., SICILIANO, C., LORUSSO, V., ACIERNO, R., GIOVINAZZO, G., SANTINO, A., STORELLI, C. & MAFFIA, M. 2011. Resveratrol inhibits the epidermal growth factor-induced epithelial mesenchymal transition in MCF-7 cells. *Cancer Lett*, 310, 1-8.
- VERSCHUEREN, K., REMACLE, J. E., COLLART, C., KRAFT, H., BAKER, B. S., TYLZANOWSKI, P., NELLES, L., WUYTENS, G., SU, M. T., BODMER, R., SMITH, J. C. & HUYLEBROECK, D. 1999. SIP1, a novel zinc finger/homeodomain repressor, interacts with Smad proteins and binds to 5'-CACCT sequences in candidate target genes. *J Biol Chem*, 274, 20489-98.
- VIAL, E. & MARSHALL, C. J. 2003a. Elevated ERK-MAP kinase activity protects the FOS family member FRA-1 against proteasomal degradation in colon carcinoma cells. *J Cell Sci*, 116, 4957-63.
- VIAL, E., SAHAI, E. & MARSHALL, C. J. 2003b. ERK-MAPK signaling coordinately regulates activity of Rac1 and RhoA for tumor cell motility. *Cancer Cell*, 4, 67-79.
- VILLANUEVA, J., VULTUR, A., LEE, J. T., SOMASUNDARAM, R., FUKUNAGA-KALABIS, M., CIPOLLA, A. K., WUBBENHORST, B., XU, X., GIMOTTY, P. A., KEE, D., SANTIAGO-WALKER, A. E., LETRERO, R., D'ANDREA, K., PUSHPARAJAN, A., HAYDEN, J. E., BROWN, K. D., LAQUERRE, S., MCARTHUR, G. A., SOSMAN, J. A., NATHANSON, K. L. & HERLYN, M. 2010. Acquired resistance to BRAF inhibitors mediated by a RAF kinase switch in melanoma can be overcome by cotargeting MEK and IGF-1R/PI3K. *Cancer Cell*, 18, 683-95.
- VOLINIA, S., CALIN, G. A., LIU, C. G., AMBS, S., CIMMINO, A., PETROCCA, F., VISIONE, R., IORIO, M., ROLDO, C., FERRACIN, M., PRUEITT, R. L., YANAIHARA, N., LANZA, G., SCARPA, A., VECCHIONE, A., NEGRINI, M., HARRIS, C. C. & CROCE, C. M. 2006. A microRNA expression signature of human solid tumors defines cancer gene targets. *Proc Natl Acad Sci U S A*, 103, 2257-61.

- VREDEVELD, L. C., POSSIK, P. A., SMIT, M. A., MEISL, K., MICHALOGLOU, C., HORLINGS, H. M., AJOUAOU, A., KORTMAN, P. C., DANKORT, D., MCMAHON, M., MOOI, W. J. & PEEPER, D. S. 2012. Abrogation of BRAFV600E-induced senescence by PI3K pathway activation contributes to melanomagenesis. *Genes Dev*, 26, 1055-69.
- VUOLO, L., DI SOMMA, C., FAGGIANO, A. & COLAO, A. 2012. Vitamin D and cancer. *Front Endocrinol (Lausanne)*, 3, 58.
- WANG, B., LINDLEY, L. E., FERNANDEZ-VEGA, V., RIEGER, M. E., SIMS, A. H. & BRIEGEL, K. J. 2012. The T Box Transcription Factor TBX2 Promotes Epithelial-Mesenchymal Transition and Invasion of Normal and Malignant Breast Epithelial Cells. *PLoS One*, 7, e41355.
- WANG, T. J., PENCINA, M. J., BOOTH, S. L., JACQUES, P. F., INGELSSON, E., LANIER, K., BENJAMIN, E. J., D'AGOSTINO, R. B., WOLF, M. & VASAN, R. S. 2008. Vitamin D deficiency and risk of cardiovascular disease. *Circulation*, 117, 503-11.
- WANG, Y., BECKLUND, B. R. & DELUCA, H. F. 2010. Identification of a highly specific and versatile vitamin D receptor antibody. *Arch Biochem Biophys*, 494, 166-77.
- WARD, K. A., LAZOVICH, D. & HORDINSKY, M. K. 2012. Germline melanoma susceptibility and prognostic genes: A review of the literature. *J Am Acad Dermatol*.
- WELLBROCK, C., RANA, S., PATERSON, H., PICKERSGILL, H., BRUMMELKAMP, T. & MARAIS, R. 2008. Oncogenic BRAF regulates melanoma proliferation through the lineage specific factor MITF. *PLoS One*, 3, e2734.
- WELS, C., JOSHI, S., KOEFINGER, P., BERGLER, H. & SCHAUER, H. 2011. Transcriptional Activation of ZEB1 by Slug Leads to Cooperative Regulation of the Epithelial-Mesenchymal Transition-Like Phenotype in Melanoma. *J Invest Dermatol*, 131, 1877-85.
- WHITEMAN, D. C., ZHOU, X. P., CUMMINGS, M. C., PAVEY, S., HAYWARD, N. K. & ENG, C. 2002. Nuclear PTEN expression and clinicopathologic features in a population-based series of primary cutaneous melanoma. *Int J Cancer*, 99, 63-7.
- WIDLUND, H. R. & FISHER, D. E. 2003. Microphthalmia-associated transcription factor: a critical regulator of pigment cell development and survival. *Oncogene*, 22, 3035-3041.
- WIKLUND, E. D., BRAMSEN, J. B., HULF, T., DYRSKJOT, L., RAMANATHAN, R., HANSEN, T. B., VILLADSEN, S. B., GAO, S., OSTENFELD, M. S., BORRE, M., PETER, M. E., ORNTOF, T. F., KJEMS, J. & CLARK, S. J. 2011. Coordinated epigenetic repression of the miR-200 family and miR-205 in invasive bladder cancer. *Int J Cancer*, 128, 1327-34.
- WILLMORE-PAYNE, C., HOLDEN, J. A., TRIPP, S. & LAYFIELD, L. J. 2005. Human malignant melanoma: detection of BRAF- and c-kit-activating mutations by high-resolution amplicon melting analysis. *Hum Pathol*, 36, 486-93.

- WOENCKHAUS, C., GIEBEL, J., FAILING, K., FENIC, I., DITTBERNER, T. & POETSCH, M. 2003. Expression of AP-2alpha, c-kit, and cleaved caspase-6 and -3 in naevi and malignant melanomas of the skin. A possible role for caspases in melanoma progression? *J Pathol*, 201, 278-87.
- WORM, J., CHRISTENSEN, C., GRONBAEK, K., TULCHINSKY, E. & GULDBERG, P. 2004. Genetic and epigenetic alterations of the APC gene in malignant melanoma. *Oncogene*, 23, 5215-26.
- WU, J., ROSENBAUM, E., BEGUM, S. & WESTRA, W. H. 2007. Distribution of BRAF T1799A(V600E) mutations across various types of benign nevi: implications for melanocytic tumorigenesis. *Am J Dermatopathol*, 29, 534-7.
- WU, Y., EVERS, B. M. & ZHOU, B. P. 2009. Small C-terminal domain phosphatase enhances snail activity through dephosphorylation. *J Biol Chem*, 284, 640-8.
- XU, Y., BRENN, T., BROWN, E. R., DOHERTY, V. & MELTON, D. W. 2012. Differential expression of microRNAs during melanoma progression: miR-200c, miR-205 and miR-211 are downregulated in melanoma and act as tumour suppressors. *Br J Cancer*, 106, 553-61.
- XUE, C., PLIETH, D., VENKOV, C., XU, C. & NEILSON, E. G. 2003. The gatekeeper effect of epithelial-mesenchymal transition regulates the frequency of breast cancer metastasis. *Cancer Res*, 63, 3386-94.
- YANG, J., MANI, S. A., DONAHER, J. L., RAMASWAMY, S., ITZYKSON, R. A., COME, C., SAVAGNER, P., GITELMAN, I., RICHARDSON, A. & WEINBERG, R. A. 2004. Twist, a master regulator of morphogenesis, plays an essential role in tumor metastasis. *Cell*, 117, 927-39.
- YANG, J. & WEINBERG, R. A. 2008. Epithelial-mesenchymal transition: at the crossroads of development and tumor metastasis. *Dev Cell*, 14, 818-29.
- YANG, M. H., CHANG, S. Y., CHIOU, S. H., LIU, C. J., CHI, C. W., CHEN, P. M., TENG, S. C. & WU, K. J. 2007. Overexpression of NBS1 induces epithelial-mesenchymal transition and co-expression of NBS1 and Snail predicts metastasis of head and neck cancer. *Oncogene*, 26, 1459-67.
- YANG, M. H., CHEN, C. L., CHAU, G. Y., CHIOU, S. H., SU, C. W., CHOU, T. Y., PENG, W. L. & WU, J. C. 2009. Comprehensive analysis of the independent effect of twist and snail in promoting metastasis of hepatocellular carcinoma. *Hepatology*, 50, 1464-74.
- YANG, M. H., HSU, D. S., WANG, H. W., WANG, H. J., LAN, H. Y., YANG, W. H., HUANG, C. H., KAO, S. Y., TZENG, C. H., TAI, S. K., CHANG, S. Y., LEE, O. K. & WU, K. J. 2010. Bmi1 is essential in Twist1-induced epithelial-mesenchymal transition. *Nat Cell Biol*, 12, 982-92.
- YEH, I. & BASTIAN, B. C. 2009. Genome-wide associations studies for melanoma and nevi. *Pigment Cell Melanoma Res*, 22, 527-8.

- YOKOYAMA, K., KAMATA, N., FUJIMOTO, R., TSUTSUMI, S., TOMONARI, M., TAKI, M., HOSOKAWA, H. & NAGAYAMA, M. 2003. Increased invasion and matrix metalloproteinase-2 expression by Snail-induced mesenchymal transition in squamous cell carcinomas. *Int J Oncol*, 22, 891-8.
- YOSHIDA, J., HORIUCHI, A., KIKUCHI, N., HAYASHI, A., OSADA, R., OHIRA, S., SHIOZAWA, T. & KONISHI, I. 2009. Changes in the expression of E-cadherin repressors, Snail, Slug, SIP1, and Twist, in the development and progression of ovarian carcinoma: the important role of Snail in ovarian tumorigenesis and progression. *Med Mol Morphol*, 42, 82-91.
- YOUNG, M. R. & COLBURN, N. H. 2006. Fra-1 a target for cancer prevention or intervention. *Gene*, 379, 1-11.
- YUEN, H. F., CHAN, Y. P., WONG, M. L., KWOK, W. K., CHAN, K. K., LEE, P. Y., SRIVASTAVA, G., LAW, S. Y., WONG, Y. C., WANG, X. & CHAN, K. W. 2007. Upregulation of Twist in oesophageal squamous cell carcinoma is associated with neoplastic transformation and distant metastasis. *J Clin Pathol*, 60, 510-4.
- ZECCA, L., BELLEI, C., COSTI, P., ALBERTINI, A., MONZANI, E., CASELLA, L., GALLORINI, M., BERGAMASCHI, L., MOSCATELLI, A., TURRO, N. J., EISNER, M., CRIPPA, P. R., ITO, S., WAKAMATSU, K., BUSH, W. D., WARD, W. C., SIMON, J. D. & ZUCCA, F. A. 2008. New melanic pigments in the human brain that accumulate in aging and block environmental toxic metals. *Proc Natl Acad Sci U S A*, 105, 17567-72.
- ZELLA, L. A., KIM, S., SHEVDE, N. K. & PIKE, J. W. 2006. Enhancers located within two located introns of the vitamin D receptor gene mediate transcriptional autoregulation by 1,25-dihydroxyvitamin D3. *Mol. Endocrinol*, 20, 1231-47.
- ZERP, S. F., VAN ELSAS, A., PELTENBURG, L. T. & SCHRIER, P. I. 1999. p53 mutations in human cutaneous melanoma correlate with sun exposure but are not always involved in melanomagenesis. *Br J Cancer*, 79, 921-6.
- ZHAN, Y., FUJINO, A., MACLAUGHLIN, D. T., MANGANARO, T. F., SZOTEK, P. P., ARANGO, N. A., TEIXEIRA, J. & DONAHOE, P. K. 2006. Mullerian inhibiting substance regulates its receptor/SMAD signaling and causes mesenchymal transition of the coelomic epithelial cells early in Mullerian duct regression. *Development*, 133, 2359-69.
- ZHANG, B., PAN, X., COBB, G. P. & ANDERSON, T. A. 2007. microRNAs as oncogenes and tumor suppressors. *Dev Biol*, 302, 1-12.
- ZHANG, Y., WEI, J., WANG, H., XUE, X., AN, Y., TANG, D., YUAN, Z., WANG, F., WU, J., ZHANG, J. & MIAO, Y. 2012. Epithelial mesenchymal transition correlates with CD24+CD44+ and CD133+ cells in pancreatic cancer. *Oncol Rep*, 27, 1599-605.
- ZHANG, Z., KOVALENKO, P., CUI, M., DESMET, M., CLINTON, S. K. & FLEET, J. C. 2010. Constitutive activation of the mitogen-activated protein kinase pathway impairs vitamin D signaling in human prostate epithelial cells. *J Cell Physiol*, 224, 433-42.

- ZHANG, Z., ZHANG, B., LI, W., FU, L., FU, L., ZHU, Z. & DONG, J. T. 2011. Epigenetic Silencing of miR-203 Upregulates SNAI2 and Contributes to the Invasiveness of Malignant Breast Cancer Cells. *Genes Cancer*, 2, 782-91.
- ZHOU, B. P., DENG, J., XIA, W., XU, J., LI, Y. M., GUNDUZ, M. & HUNG, M. C. 2004. Dual regulation of Snail by GSK-3 β -mediated phosphorylation in control of epithelial-mesenchymal transition. *Nat Cell Biol*, 6, 931-40.
- ZHUANG, L., LEE, C. S., SCOLYER, R. A., MCCARTHY, S. W., ZHANG, X. D., THOMPSON, J. F. & HERSEY, P. 2007. Mcl-1, Bcl-XL and Stat3 expression are associated with progression of melanoma whereas Bcl-2, AP-2 and MITF levels decrease during progression of melanoma. *Mod Pathol*, 20, 416-26.
- ZIDAR, N., BOSTJANCIC, E., GALE, N., KOJC, N., POLJAK, M., GLAVAC, D. & CARDESA, A. 2011. Down-regulation of microRNAs of the miR-200 family and miR-205, and an altered expression of classic and desmosomal cadherins in spindle cell carcinoma of the head and neck--hallmark of epithelial-mesenchymal transition. *Hum Pathol*, 42, 482-8.
- ZIPITIS, C. S. & AKOBENG, A. K. 2008. Vitamin D supplementation in early childhood and risk of type 1 diabetes: a systematic review and meta-analysis. *Arch Dis Child*, 93, 512-7.
- ZOHN, I. E., LI, Y., SKOLNIK, E. Y., ANDERSON, K. V., HAN, J. & NISWANDER, L. 2006. p38 and a p38-interacting protein are critical for downregulation of E-cadherin during mouse gastrulation. *Cell*, 125, 957-69.